ANALYSIS OF CONDUCTION HEAT TRANSFER IN SEMI-INFINITE SLABS AND INFINITE QUADRANTS WITH DISCRETE HEAT GENERATION SOURCES USING GREEN'S FUNCTION INTEGRAL METHODS

By

Omar Enrique Meza Castillo

A thesis submitted in partial fulfillment of the requirements for the degree of

MASTER OF SCIENCE

in

MECHANICAL ENGINEERING

UNIVERSITY OF PUERTO RICO
MAYAGUEZ CAMPUS
2003

Approved by:

Sandra Coutín Rodicio, Ph.D. Member, Graduate Committee	Date
Jorge E. González Cruz, Ph.D. Member, Graduate Committee	Date
Nellore S. Venkataraman, Ph.D. President, Graduate Committee	Date
Carlos M. Rinaldi Ramos, Ph.D. Representative of Graduate Studies	Date
Jorge E. González Cruz, Ph.D. Chairperson of the Department	Date

ABSTRACT

The problem of steady state heat conduction in semi-infinite plates and infinite quadrants of constant thermal conductivity, with discrete heat generating sources and Dirichlet boundary conditions (temperature specified on the boundary) was solved using the method of Green's functions using the integral techniques. The Green's functions for the geometries were found by the method of images. These functions were then employed for the solution of five cases for semi-infinite slabs with heat generation sources of different geometry. These were: a thin plate heating source, a hollow box heating source, a square prismatic heating source, finite line heating source and a thin cylindrical heating source. For infinite quadrants a heat generation source of the form of a thin current carrying wire in the form a square was considered. The heat sources were idealized as internal thermal energy generation. Solutions found with this method always yield closed form algebraic expressions or analytical solutions or "almost analytical" solutions (in the form of an integral). Results found in this work were validated and compared with the numerical method of finite elements in Ansys 6.0. It was concluded that, for the cases considered here, the method used in the present work is elegant and is superior in terms of computational requirements.

RESUMEN

En el presente trabajo se resolvió el problema de conducción de calor en estado estable en placas semi-infinitas y cuadrantes infinitos de conductividad térmica constante, con fuentes discretas de generación de calor y condiciones de frontera tipo Dirichlet (temperatura especificada en la frontera), utilizando el método de las funciones de Green usando las técnicas integrales. Las funciones de Green para las geometrías fueron obtenidas mediante el método de imágenes. Estas funciones fueron luego empleadas para la solución de cinco casos para placas semi-infinitas con fuentes de generación de calor de diferente geometría. Estas fueron: una placa lineal, una caja hueca, un prisma de base cuadrada, una linea finita y un cilindro de parede delgadas. Para el caso de los cuadrantes infinitos se resolvió un caso con generación de calor cuya forma fue: un alambre fino colocado a lo largo del perímetro de un cuadrado. Las fuentes de generación de calor se idealizaron como generación interna de calor. Las soluciones obtenidas con este método siempre resultan expresiones algebraicas sencillas o soluciones "analíticas" y "cuasi-analíticas" (en la forma de una integral). Los resultados obtenidos en el presente trabajo fueron comparados con el método numérico de elementos finitos, el software utilizado fue Ansys 6.0. Se concluyó que, para los casos considerados aquí, el método empleado en la presente investigación es superior en terminos de elegancia y tiempo computacional.

A:

Mi esposa Marlene por su comprensión y paciencia en estos años de larga lucha, mi chiquita quien me apoyo en todo, gracias mi Amor, te amo.

Mi hijo Adrián Omar, su llegada.... mi mayor ilusión, ahora estimulo constante.

Mis padres Elizabeth y Alberto por su amor y consejos, los amo y respeto.

Mi madrina Delfina y mi hermanita Betty a quienes quiero mucho.

ACKNOWLEDGMENT

I would like to express my thankfulness to Dr. Venkataraman, my academic advisor, thanks to his instruction and advice this work has been finished.

To my friend and college Eduardo Gustavo Perez Diaz for his support and ideas.

To the Department of Mechanical Engineering for giving me the opportunity to pursue my graduate studies.

Thanks.

TABLE OF CONTENTS

LIST OF FIGURES

LIST OF APPENDICES

I. INTRODUCTION

The method of Green's functions is an important technique for solving boundary value and initial value problems. In engineering and applied sciences the steady state and transient heat conduction equation is one of this type of problems that is used to model and study physical phenomenon arising in the real world. It is not at all surprising that their solution has been the major concern of many engineers and scientists.

The thermal control subsystem (TCS) is an integral part of every spacecraft. Its purpose is to maintain all the components of a spacecraft within their respective temperature limits. There are several different sources of thermal energy acting on a spacecraft; solar radiation, albedo, earth emitted infrared, and heat generated by on board equipment. Therefore, the thermal control subsystem is different for every spacecraft. In general, there are two types of TCS, passive and active. A passive system relies on conductive and radiative heat paths and special coatings and has no moving parts or electrical power input. An active system is used in addition to the passive system when passive system is not adequate, for example, on manned missions. Active systems rely on pumps, thermostats, and heaters, use moving parts, and require electrical power.

Many factors influence the design and development of the thermal control system. Figure 1.1 illustrates several possible inputs and outputs, but each spacecraft TCS will have it's own unique set. Mission constraints, mission objectives, and the physical design of a spacecraft determine the inputs and outputs of the TCS interface.

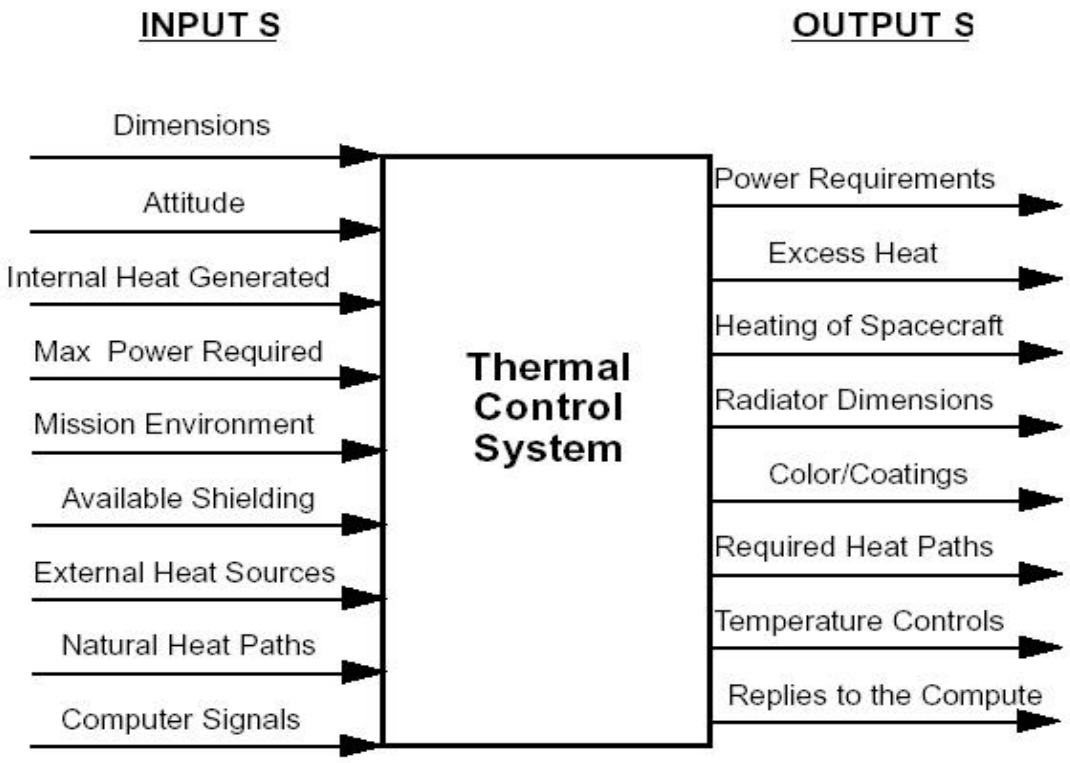

Figura 1.1. TCS Interfase.

There are different types of components for both active and passive systems, one active thermal control component is an electrical heater that is a device that is controlled by a thermostat and used to heat cold regions of the spacecraft. They generate heat by running electrical current through a resistor.

Electrical heaters are used for fine temperature control, usually when the spacecraft is in the shadow of the earth. Often these electrical heaters are thin current carrying wires. When this occurs, the principal mechanism of heat transfer for thermal control subsystem in the spacecraft is conduction heat transfer.

In the preliminary thermal analysis, the spacecraft is divided into a large number of isothermal nodes. The analysis is done by specifying the thermal resistance between the nodes. Often the thermal resistance is guessed by intuition and experience. Attempts are being made to tabulate, thermal resistance in mounting plates with heat generation sources. For this knowledge of the temperature field is required. This work provides preliminary results for temperature distribution, which hopefully will help in evaluation of thermal resistance. Besides the problem of temperature determination due to conduction of heat in solids is a fundamental problem that has numerous applications in various branches of science and engineering. There is considerable interest in the solution of heat conduction problems with the ultimate objective of obtaining useful and practical information.

A variety of methods, exact, approximate, and purely numerical, are available for the solution of these problems. In this work, it is proposed to investigate the conduction heat transfer problem with discrete heat generation sources, with temperature specified on boundaries in a semi-infinite slabs and infinite quadrants using the Green's Functions Integral Method.

About the physical significance of Green's Function, it can be said Green's function is a cause-effect two point function. $G(\vec{x}, \vec{x}')$ is the effect at the field point $\vec{x}$ due to a unit source applied at the source point $\vec{x}'$. It is important to note that the principle of reciprocity holds for Green's functions (i.e., source and field points can be interchanged). Green's function can be applied to many fields of engineering and

sciences. The following figures illustrate these ideas with an example applied to elasticity.

Elasticity:

P = source point

Q= field point

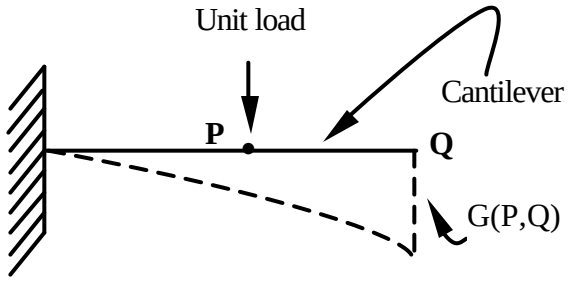

Green's function G(P,Q) = deflection at Q ("effect") due to unit load at P ("cause")

Figure 1.2. (a) Deflection at Q due to unit load P applied to a cantilever.

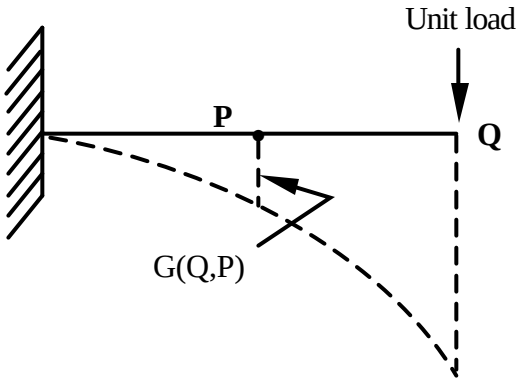

Q = source point

P = field point

Green's function G(Q,P) = deflection at P ("effect") due to unit load at Q ("cause")

Figure 1.2. (b) Deflection at P due to unit load Q applied to a cantilever;
Principle of reciprocity.

It is shown in the theory of elasticity that the reciprocity relation G (P, Q) = G (Q, P) is valid in this case.

The solution of simple cases with Green's Function can be used as building blocks for much more complex solutions. For heat conduction, the Green's Function is proportional to the temperature caused by a concentrated energy source. The exact form of the Green's Function depends on the differential equation, the body shape, and the type of boundary conditions present. Green's Functions are named in honor of English mathematician and physicist George Green (1793-1841) [22]., who in 1828 published an essay entitled "On the Application of Mathematical Analysis to the Theories of Electricity and Magnetism". In this essay he derived the integral identities and used them to obtain integral representations for the solution of problems involving the Laplacian operator.

The use of Green's Functions is a very powerful technique for the analytical solution, numerical solution and mathematical analysis of heat conduction problems. The application of Green's Functions as a means of solving and analyzing initial and boundary value problems is not confined to the study of heat conduction but occurs in almost all branches of mathematical physics, and have been used for many decades for obtaining solutions in electromagnetic theory, elasticity, wave mechanics, fluid mechanics, etc. However, their uses in heat transfer have not been very common especially among engineers. Beck [2, 3 and 4] presents some exact solutions of linear transient heat conduction problems using Green's functions evolved from eigenfunction expansions. Solutions involving eigenfunction expansions in terms of infinite series usually present convergence problems.

The Green's functions integral method was selected because the solution is always in the form of an integral and can be viewed as a recasting of a boundary value problem into integral form. For some cases the integral can be evaluated to yield a closed form solution. The Green's Functions method is useful if the Green's Function is known, and if the integral expressions can be evaluated. If these two limitations can be overcome, the Green's Functions method offers several advantages for the solution of linear heat conduction problems. Even when the integral has to be evaluated numerically this is generally more accurate than numerical methods solutions such as finite differences especially for discrete sources. The advantages of the Green's Functions method are the following:

1. The Green's Functions method is flexible and powerful. The same Green's Functions for a given geometry (including type of boundary conditions) can be used as a building block to the temperature resulting from: space-variable initial conditions; time- and space-variable boundary conditions; and, time- and space-variable energy generation.

2. The solution procedure is systematic. For a given geometry the Green's Function for a particular type of boundary condition has to be determined only once. This then can be used for any type of source, and the solution for the temperature can be written immediately in the form of integrals. The systematic procedure saves time and reduces the possibility of error, which is particularly important for two- and three- dimensional geometries. For complicated problems in which the heat

conduction is caused by several non-homogeneous terms, and the effect of each term can be considered separately.

3. The Green's Functions method gives "almost analytical" solutions in the form of integrals for some specified geometries such as cylinders, sphere and infinite half spaces or quadrants. The solution takes the form of a sum (superposition) of several integrals, one for each non-homogeneous term in the problem. The analytical expressions for temperature can be evaluated with high accuracy; evaluated only where needed for great computer usage efficiency; differentiated to find heat flux or sensitivity coefficients; or, integrated to find average temperature. The integrals can always be evaluated numerically (quadratures) if they cannot be found in closed form. The computational labor involved is minimal when compared to purely numerical finite difference or finite element methods. In general this has much better accuracy than finite difference techniques especially with discrete sources.

4. Two- and three-dimensional transient Green's Functions can be found by simple multiplication of one-dimensional transient Green's Function. This is true for the rectangular coordinate system for most boundary conditions (type 0-No physical boundary, type 1-Dirichlet, prescribed temperature on the boundary, type 2-Neumann, prescribed heat flux and type 3-Robin, convective condition) and for certain cases involving cylindrical coordinates, but it does not work for the spherical coordinates system.

5. Alternative form of the solution can improve series convergence. For heat conduction in finite bodies, infinite series solutions for heat conduction problems driven by non-homogeneous boundary conditions sometimes exhibit slow convergence, requiring a very large number of terms to obtain accurate numerical values. For some of these problems an alternative formulation of the Green's Function Solution Equation reduces the number of required series terms.

1.1 Objectives

The purpose of this work is find the temperature distribution for some two, and three dimensional specific cases in rectangular coordinates of semi-infinite slabs and infinite quadrants with discrete heat generation sources and temperature specified on boundary (Dirichlet problem) using the Green's Functions Integral Method. The specific steps involved are the following:

1. Determine a general Green's Function Solution Equation applicable to the solution of conduction heat transfer with Dirichlet boundary conditions of semi-infinite slabs and infinite quadrants.

2. Find Green's Functions for the specific geometries semi infinite-slabs and infinite quadrants as shown in pages 9-10, using the method of images, the temperature is specified on the boundary.

3. Apply the Green's Function Solution Equation for the geometries considered with various types of heat generation source and determine the temperature profile. The emphasis will be a getting a closed form analytical solution or in the form of an integral ("almost analytical solution"), for the temperature profile.

4. For a typical case compare the results obtained with a numerical technique (finite elements and/or finite differences) to illustrate the advantages of this method.

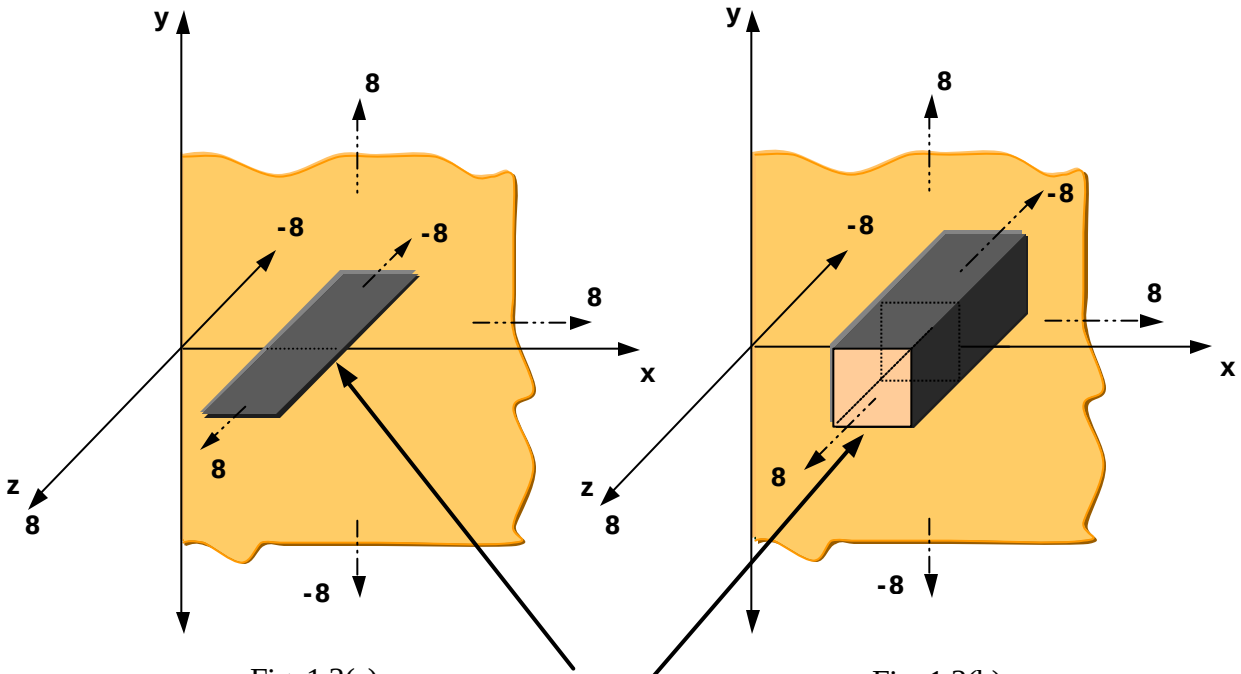

Fig. 1.3(a)
Semi-infinite slab with a
Thin plate heating source
(Two-dimensional problem)

Heat generating elements

Fig. 1.3(b)
Semi-infinite slab with a
Hollow box heating source
(Two-dimensional problem)

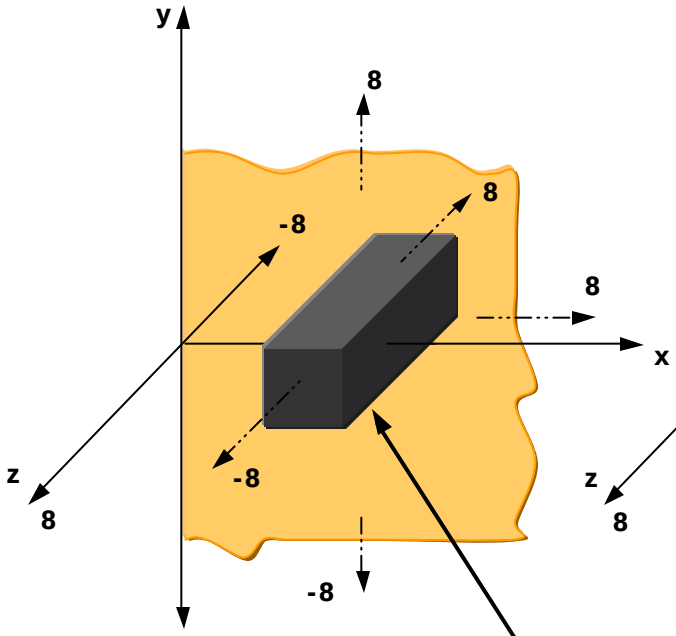

Fig. 1.3(c)
Semi-infinite slab with a
Square prismatic heating source
(Two-dimensional problem)

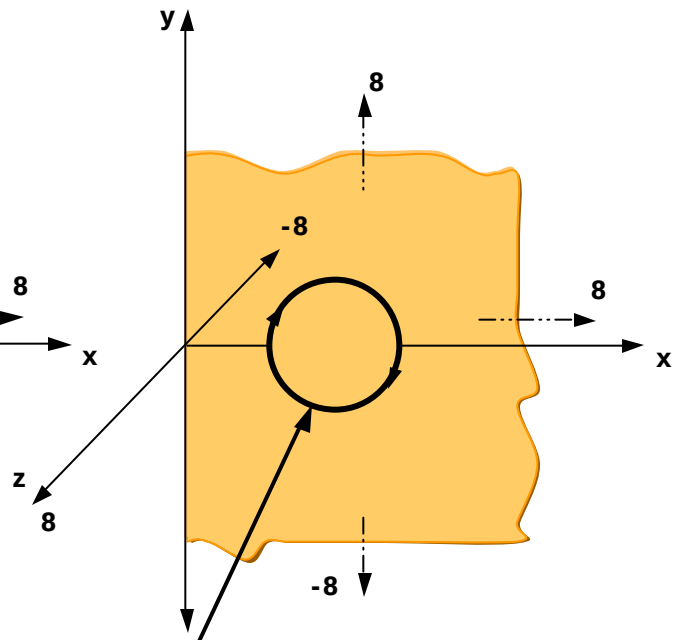

Fig. 1.3(d)
Semi-infinite slab with a
Thin cylindrical heating source
(Two-dimensional problem)

Heat generating elements

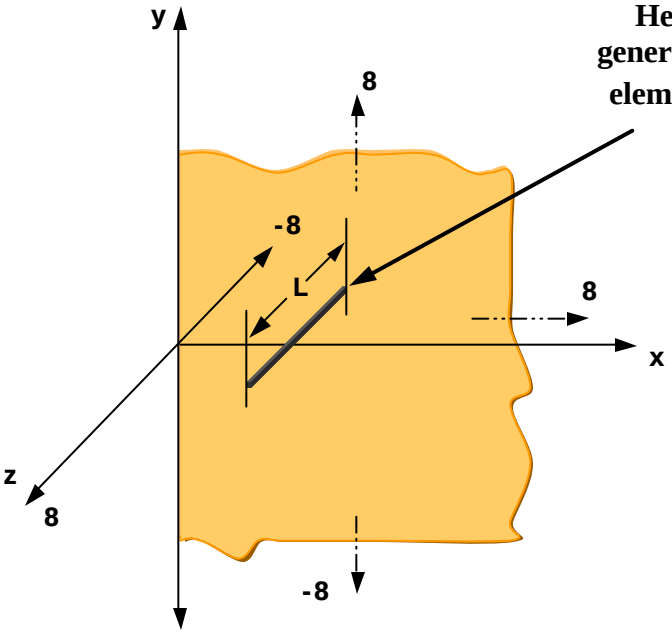

Fig. 1.3(e)
Semi-infinite slab with a
Finite line heating source
(Three-dimensional problem)

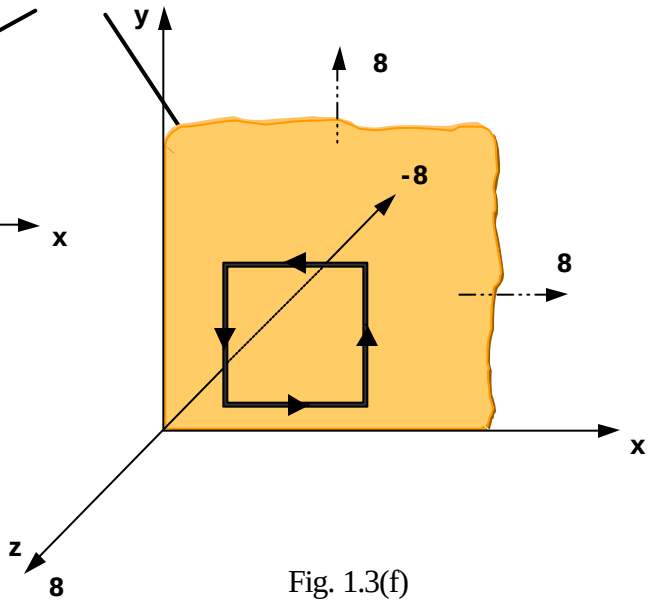

Fig. 1.3(f)
Infinite quadrant with a
Square line heating source
(Two-dimensional problem)

II. PREVIOUS WORKS

Boundary value problems associated with either ordinary or partial differential equations are almost inescapable these days in engineering and many of the applied sciences. The purpose of the mathematicians for decades was to provide an independent, systematic and analytical method to solve such problems. The method in question consists of determining the Green's function, which is associated with most boundary value problems. An integral equation representation of a boundary value problem is often much more amenable to numerical analysis than a differential equation with associated boundary conditions. This method is by no means a new concept, for such functions were first introduced by George Green as early as 1828, and have been used in electromagnetic theory, potential theory and elasticity. However in heat transfer applications the use of Green's function has been more recent.

Green's function integral method applied to diffusion problems have been studied for decades. However just few works have been reported by researchers in the heat transfer area, the main reason being the unfamiliarity of many engineers with this technique.

Morse and Feshbach [21] in "Methods of Theoretical Physics" describe the Green's Function for the Wave Equation, solutions for a generalized inhomogeneous partial differential equation with boundary conditions applied to steady waves. Carslaw and Jaeger [6] in their book "Conduction of Heats in Solids" describe the known exact solutions of problems of heat flow, with detailed discussion of all the most important

boundary value problems. Jackson [17] in his book “Classical Electrodynamics” applied the Green’s Theorem to solve the Kirchhoff’s integral for diffraction problem and also for the wave equation using the concept of retarded potentials.

Carrier and Pearson [8] “Partial Differential Equations – Theory and Technique” discusses the diffusion equation with Dirichlet boundary conditions using the Green’s function orthogonal expansions. Greenberg [12] in his book “Application of Green’s Functions in Science and Engineering” discuss some applications of the Green’s function to solve conduction heat transfer, acoustic, gravitational potential and vibrations problems.

James and Jeffrey [18] in “Heat Conduction” applied Green’s Function to solve heat conduction equation in three dimensions obtaining an integral equation for temperature in terms of the initial and boundaries values of the temperature and heat flux. V.K. Tewary [30] in his paper “Elastic Green’s Functions for Anisotropic Solids” applied the Green’s function method for solution of the Christoffel equation for elastic equilibrium with prescribed boundary conditions.

Beck et al. [4] in their book “Heat Conduction Using Green’s Function” obtained the Green’s Functions and temperature solutions to different boundary conditions for the transient heat conduction equation in Cartesian, cylindrical, and spherical coordinates. The solutions of the different cases are tabulated obtaining the solution of many transient heat conduction problems in a straightforward and efficient manner. This book contains three derivations of Green’s Function Solution Equations, the first for one-dimensional cases, the second for general multidimensional coordinates, and the third is an

alternative form which can aid in obtaining solutions having better convergence properties for some problems having nonhomogeneous boundary conditions. In addition the book discusses the use of these Green's Function for the solution of heat conduction problems in Cartesian coordinates for one-, two-, and three-dimensional cases, in these cases the Green's Functions have been obtained from the eigenfunction expansion. Others sections covers radial heat flow, two-and three-dimensional cases in cylindrical coordinates and some temperature solutions in radial spherical coordinates. This work also discusses the method of images for infinite plane walls and gives the solution in terms of power series. This hardly has any advantages over the classical method of separation of variables.

Ozisik [22] "Heat Conduction" discusses the physical significance of Green's Function and presents general expressions for the solution of inhomogeneous transient heat conduction problems with energy generation, inhomogeneous boundary conditions, and a given initial condition, in terms of Green's condition, for one, two, and three dimensional problems of finite, semi-infinite, and finite regions with representatives examples in the rectangular, cylindrical, and spherical coordinate systems. In addition this book applied this technique to the solution of one-dimensional composite medium.

The books and papers cited cover different applications of Green's Functions. Historically the use of a Green's Function to solve differential equations grew out of a study of a special partial differential equation and boundary condition called the Dirichlet problem. Later it was discovered that similar function could also be used in the analysis of ordinary differential equations featuring nonhomogeneities. Although some

of these functions were originally given different names for different problems, today we collectively refer to them all as " Green's Functions".

In the paper "Initial Value Problem for Boundary Values of the Green's Functions" Edmond Ghandour [13] formulated the equations that govern boundary values of the Green's functions. Then a particular second order differential equation with mixed boundary conditions that is commonly encountered in one-dimensional wave propagation problems and also some applications to the one-dimensional stochastic wave propagations are examined.

Y.P. Chang and R. C. H. Tsou [9] in their work entitled "Heat Conduction in Anisotropic Medium Homogeneous in Cylindrical Regions-Unsteady State" talk about the analytical solution for heat conduction in an anisotropic medium that is homogeneous in circular cylindrical coordinates. They considered boundary conditions of Dirichlet, Newmann and mixed (or convective) types for solid cylinder and hollow cylinder in infinite and finite lengths. The principal subject of their paper is the determination of the Green's functions, using eigenfunctions.

A very important work in this field has been reported by J. Beck [2], where a derivation of the Green's function solution for the linear, transient heat conduction equation in a form that includes five kind of boundary conditions is given, and also demonstrates the conditions under which it is permissible to use the product property of one-dimensional Green's functions.

In 1986, James Beck [3] in the work titled “Green’s Functions and Numbering System for Transient Heat Conduction”, provides a table of Green’s functions that enable us to derive transient conduction solutions for rectangular coordinates system and also provided a numbering system that enables efficient cataloging and locating of Green’s functions. The Green’s functions were obtained using eigenfunction expansions

Haji-Sheikh and J. Beck [15] reported a work for the heat conduction problem in thin films at low temperature where the classical theory of heat conduction breaks down. They report the solution for the temperature distribution for finite bodies.

Kevin D. Cole [10] in his paper “Steady Heat Conduction in Cartesian coordinates and a Library of Green's Functions”, expresses general Green's functions for direct solution of the steady heat equation in finite geometries. In particular, the many combinations of possible boundary conditions lead to hundreds of different functions. Like the transient heat transfer Green's functions described by Beck, these accurate functions serve an important role in the verification of software using other numerical methods and furthermore, these steady-state functions can be used to verify the independently-developed transient Green's functions. They are organized into a systematic taxonomy based on the types of boundary conditions on the faces of the parallelepiped.

John R. Berger [5] in his paper “Green's Functions and Applications for Steady-State Heat Transfer in Functionally Graded Materials”, discusses that the Functionally graded materials (FGMs) are designed with spatial variations in elastic, thermal, magnetic, or optical properties for optimal performance. Some examples of FGMs are

thermal barrier coatings, bone implants, piezoelectric sensors, and graded optical index components. In this paper Green's functions for the steady state heat transfer problem in FGMs were developed. Both isotropic and anisotropic thermal conductivities were considered. The developed Green's functions were used in numerical simulations with the Method of Fundamental Solutions. Results for problems with Dirichlet and Neumann boundary conditions and results on an inverse problem in a graded material were presented.

Sheledeleva M.L. et al. [28], in their paper “Modeling of interfacial temperature effects due to an impulsive line heat source”, discussed the temperature fields generated by an instantaneous line heat source in the medium consisting of two half spaces of different thermal properties are modeled. The analytical calculations employed the Green functions for an impulsive line source derived previously using the Cagniard–de Hoop technique. The analytical model predicts the change of sign of the reflected temperature field along the interface for a certain range of parameters. It has also been found that for the heat source located in the less conductive medium the temperature peak arrival can occur before the peak from the source temperature field. The analytical results are found to be in excellent agreement with numerical modeling using the finite difference method.

All these previous works provide general and exact solutions for homogeneous heat conduction problems but only some few general solutions for simple geometries are found for inhomogeneous cases. In all the works, the Green’s Functions is obtained by using eigenfunction, which of course is applicable to many types of boundary

conditions. None of these works obtain the Green's functions by the physical approach. Venkataraman N.S., Pérez E. and Delgado I. [33] in their paper "Temperature Distribution in Spacecraft Mounting Plates with Discrete Heat Generation Sources due to Conductive Heat Transfer" have used the physical approach of the method of images to obtain Green's functions for cylinders and spheres. They found the temperature distribution in plates, infinite cylinders and spheres with different types discrete heat generation sources such as ring and spiral sources and showed that for discrete sources Green's function determination by method of images yields analytical or "almost analytical" solutions.

The literature review indicates that most authors have used Green's function obtained from eigenfunction expansion for the solution of problems with various boundary conditions. This method though powerful in many cases presents the same complexities and problems as classical methods. In our work it is proposed to obtain the Green's function using a physical approach through the method of images for semi-infinite slabs and infinite quadrants. One of the objectives is to get the Green's function for the region by using analogous concepts used in electrostatics by using heat sources and heat sinks. After obtaining the Green's function we will attempt to solve some two, and three dimensional specific cases in rectangular coordinates of a semi-infinite slabs and infinite quadrant body with discrete heat generation sources and Dirichlet boundary conditions. It should be emphasized that the Green's functions method is specially suited for discrete sources, where classical methods such as separation of variables fail, in many cases.

III. MATHEMATICAL FORMULATION OF THE PROBLEM

3.1. Statement of the Problem

The following chapter explains and develops the solution of problems of heat conduction in steady state and temperature profile for some semi-infinite slabs and infinite quadrants in two and three dimensions with discrete heat generation sources and temperature specified on boundary (Dirichlet problem) using the method of Green's function developed through the method of images. The materials are assumed to be isotropic with constant thermal conductivity k.

3.2. Fundamentals Concepts

A general solution equation will be determined and then it will be limited to the specific boundary conditions of the cases we are focused on. For a better understanding of the development of the Green's function solution equation, it is necessary to introduce the following mathematical concepts:

3.2.1 Dirac-Delta Function

The Dirac Delta function (sometimes called the unit impulse function) is important in the study of phenomena of an impulsive nature, such as the action of heat flow over a very short time interval or over a very small region. This situation occurs in mechanics, for example, when a force concentrated at a point causes deformation on solid surface, impulsive forces in rigid body dynamics, point masses in gravitational field

theory, point charges and multipoles in electrostatics, and point heat sources and pulses in the theory of heat conduction. The Green's function is the impulse response of a differential equation, and the Dirac Delta function describes the impulse.

The Dirac Delta Function $\delta(x)$ is defined to be zero when $x \neq 0$, and infinite at $x = 0$ in such a way that the area under the function is unity.

Dirac Delta function (special case)

$$\left.\begin{aligned} \delta(x) &= 0 \quad \text{if} \quad x \neq 0 \\ \delta(x) &\to \infty \quad \text{if} \quad x \to 0 \end{aligned}\right\} \qquad \ldots\ldots\ldots\ldots\ldots\ldots (3.1)$$

$$\int_{-\infty}^{\infty} \delta(x)dx = 1$$

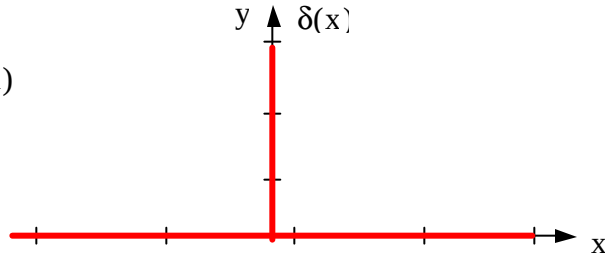

Fig. 3.1. Dirac Delta Function

Generalizing:

General form of Dirac Delta function

$$\delta(x-a) = 0 \quad \text{if} \quad x \neq a$$
$$\delta(x-a) \to \infty \quad \text{if} \quad x \to a$$

$$\int_{-\infty}^{\infty} \delta(x-a)dx = 1$$

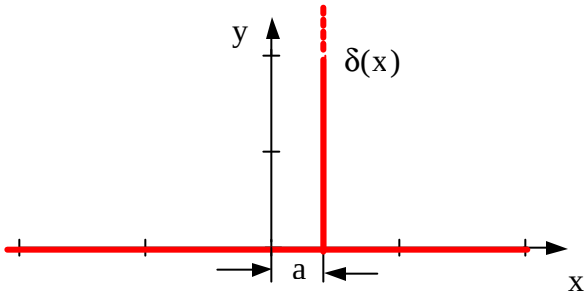

Fig. 3.2. Dirac Delta Function, General Form

x

Equation (3.1) can be seen as a limit of Gaussian

$$\delta(x) = \lim_{\sigma \to 0}\left[\frac{1}{\sqrt{4.\pi.\sigma}}.e^{-x^2/4\sigma}\right]$$

Or Lorentzian

$$\delta(x) = \lim_{\varepsilon \to 0}\left[\frac{1}{\pi}.\frac{\varepsilon}{x^2+\varepsilon^2}\right]$$

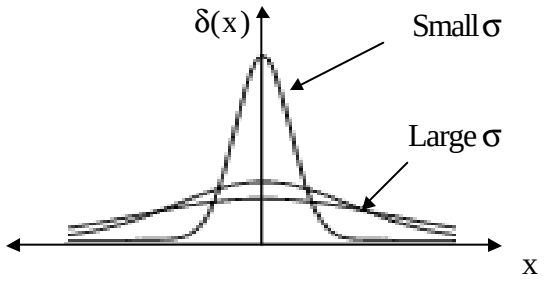

Fig. 3.3. Dirac Delta Function as limit of Gaussian

The important properties of the delta function are the following:

a) $\int_b^c f(x)\delta(x-a)dx = f(a)$ $\qquad b < a < c$

b) $\int_{-\infty}^{\infty}\delta(x-a)dx = \int_{\alpha}^{\beta}\delta(x-a)dx = 1$ $\qquad \alpha < a < \beta$

c) $\int_b^c f(x)\delta'(x-a)dx = -f'(a)$ $\qquad b < a < c$

d) $\frac{\delta(x-a)}{(x-a)} = -\delta'(x-a)$

3.2.2 Heaviside Function

This function is named for the electrical engineer Oliver Heaviside. The Heaviside function (or unit step function) is defined as:

$$H(x-a)=\begin{cases}0 & \text{if } x<a\\ 1 & \text{if } x>a\end{cases}\Bigg\}\ldots\ldots(3.2)$$

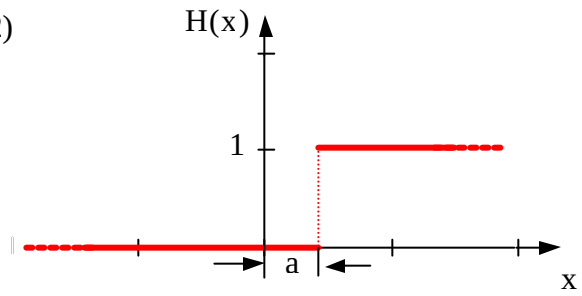

Fig. 3.4. Heaviside Function.

The property that relates the Heaviside function and Dirac-Delta function is:

$$\frac{dH(x)}{dx}=\delta(x)$$

3.2.3 The Divergence Theorem.

One of the most important theorems of vectorial calculus is the divergence theorem; sometimes it is called the Gauss Theorem. The divergence theorem is just going to be mentioned since it can be found in any basic Calculus book as reference [6].

Let S be a surface that encloses a region V in R^3. If A is a continuous vector field whose components have continuous partial derivatives in V, then:

$$\iint_S A.\hat{n}dS = \iiint_V \nabla.AdV$$

Where $\hat{n}$ is an outward unit vector normal to S.

3.2.4 Green's Identities.

If $A = \phi\nabla\psi$, where ϕ and ψ are arbitrary scalar fields, defined in V. Then:

$$\nabla.\vec{A}=\phi\nabla^2\psi+\nabla\phi.\nabla\psi \quad \text{(3.3)}$$

$$\vec{A}.\hat{n}=\phi\nabla\psi.\hat{n}=\phi\frac{\partial\psi}{\partial n} \quad \text{(3.4)}$$

These equations when substituted into divergence theorem, results in ***Green's first identity***:

$$\iiint_V\left(\psi\nabla^2\phi+\nabla\phi.\nabla\psi\right)dV=\iint_S\psi\frac{\partial\phi}{\partial n}dS \quad \text{(3.5)}$$

Instead, If $A = \psi\nabla\phi$ and substitute again in Divergence Theorem obtained:

$$\iiint_V\left(\phi\nabla^2\psi+\nabla\psi.\nabla\phi\right)dV=\iint_S\phi\frac{\partial\psi}{\partial n}dS \quad \text{(3.6)}$$

Subtracting equations (3.6)-(3.5) results the corollary of divergence theorem knows as ***Green's second identity or Green's Theorem***:

$$\iiint_V\left(\phi\nabla^2\psi-\psi\nabla^2\phi\right)dV=\iint_S\left(\phi\frac{\partial\psi}{\partial n}-\psi\frac{\partial\phi}{\partial n}\right)dS \quad \text{(3.7)}$$

3.2.5 Heat Conduction in steady state.

Consider a heated solid body with constant thermal conductivity k, with internal heat generation in steady state (strictly thermal energy generation).

But the term heat generation is commonly acepted in the heat transfer to mean thermal energy generation.

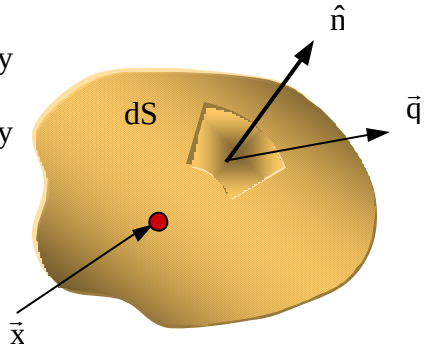

Fig. 3.5. Solid body with internal heat generation

Let:

$T(\vec{x})$ = Temperature at any point $\vec{x}$

$\vec{q} \equiv$ Heat flux vector at surface dS (W/m^2)

$Q(\vec{x}) \equiv$ Heat generation intensity per unit volume at $\vec{x}$ (W/m^3)

Applying conservation of energy the heat flux from the surface must be equal to the thermal energy generation inside the volume; mathematically this can be expressed as:

$$\iint_S \vec{q}(\vec{x}).\hat{n}dS = \iiint_V Q(\vec{x})dV \quad \ldots\ldots\ldots\ldots\ldots\ldots\ldots\ldots\ldots\ldots\ldots\ldots\ldots\ldots \quad (3.8)$$

The divergence theorem applied to the left hand side term:

$$\iint_S \vec{q}(\vec{x}).\hat{n}dS = \iiint_V \nabla.\vec{q}(\vec{x})dV \quad \ldots\ldots\ldots\ldots\ldots\ldots\ldots\ldots\ldots\ldots\ldots\ldots\ldots\ldots \quad (3.9)$$

The right hand sides in equations (3.8) and (3.9) are equivalent:

$$\iiint_V \nabla.\vec{q}(\vec{x})dV = \iiint_V Q(\vec{x})dV \quad \text{Or} \quad \iiint_V \left(\nabla.\vec{q}(\vec{x}) - Q(\vec{x})\right)dV = 0$$

Since no restrictions have been imposed to derive the last expression, this is valid for any size and shape therefore integrand must be zero. Mathematically this can be expressed as follows:

$$\nabla.\vec{q}(\vec{x}) = Q(\vec{x}) \quad \ldots\ldots\ldots\ldots\ldots\ldots\ldots\ldots\ldots\ldots\ldots\ldots\ldots\ldots\ldots\ldots \quad (3.10)$$

The Fourier's law is expressed in the following form:

$$\vec{q}(\vec{x}) = -k\nabla T(\vec{x}) \quad \ldots\ldots\ldots\ldots\ldots\ldots\ldots\ldots\ldots\ldots\ldots\ldots\ldots\ldots\ldots\ldots \quad (3.11)$$

Where $T(\vec{x})$ is temperature

Substituting the equation (3.11) in (3.10) to obtain:

$$\nabla^2 T(\vec{x}) = -\frac{Q(\vec{x})}{k} \quad \ldots\ldots\ldots\ldots\ldots\ldots\ldots\ldots\ldots\ldots\ldots\ldots\ldots\ldots\ldots\ldots \quad (3.12)$$

The equation (3.12) is the heat equation with heat generation for steady state with constant thermal conductivity k.

3.3. Steady State Green's Functions

In steady state conditions the heat conduction equation reduces to the Poisson equation. The Poisson equation has many applications in the fields of electrostatics, elasticity, diffusion, and heat transfer. Morse and Feshbach [21] present the solution methods to the Poisson equation and its special case, the Laplace equation. The method of Green's function is only one of many solutions methods.

In this part of the work we will explain the process of deriving Green's Functions in steady state using the method of images. For this purpose some concepts about point and line heat sources and heat sinks in an infinite medium are needed. These heat sources are expressed in a mathematical form and a relationship between Green's function and the heat conduction equation is also found.

3.3.1 Auxiliary Equation: The Source Solutions

3.3.1.1 Point Heat Source (Three-Dimensional)

Consider a sphere of radius "a", with constant heat generation per unit volume Q (W/m^3) inside the sphere in steady state as shown in figure 3.6.

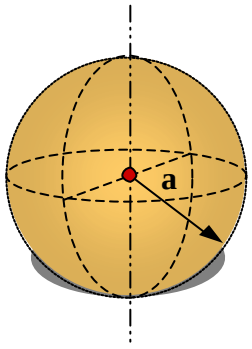

Figure 3.6 Sphere with constant heat generation.

The total heat generation inside the sphere Q_T is given by $Q_T = \frac{4}{3}\pi a^3 Q$.

In the limit as $a \to 0$ and $Q \to \infty$, such that Q_T remains constant, the sphere becomes a point heat source. As a consequence of symmetry, constant temperature spherical surfaces are found around the point heat source (figure 3.7) and the heat flux lines are radial.

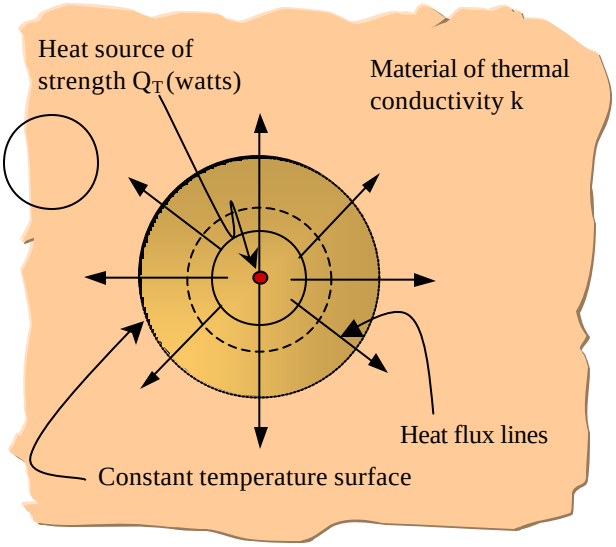

Figure 3.7. Point heat source and constant temperature surface.

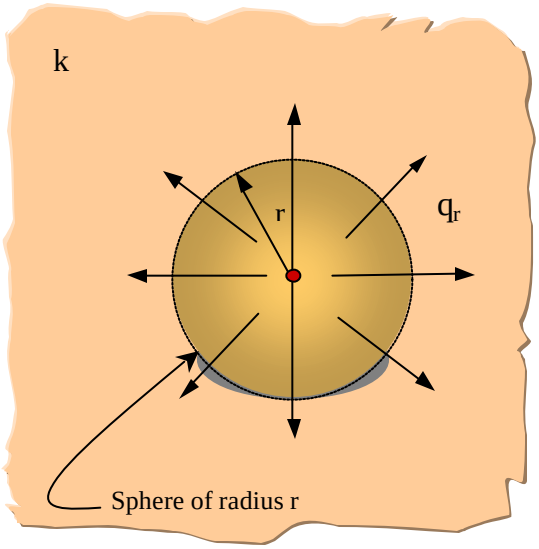

Figure 3.8. Heat flux lines due to a point heat source in an infinite medium with constant thermal conductivity.

In figure 3.8, q represents the radial heat flux at r due to a heat source of strength Q_T in an infinite medium with constant thermal conductivity. Since Q_T is the strength of the source, which is constant then the heat flux (q_r) at the boundary of the sphere of radius r is a function of r only (by symmetry).

An energy balance in the sphere gives:

$$\iint_S \vec{q} \cdot \hat{n} dS = \iiint_V Q d^3x$$

Since q is constant, then:

$$q_r (4\pi r^2) = Q_T$$

Recalling Fourier's law: $q_r = -k\frac{dT(r)}{dr}$ and substituting in the previous equation:

$$-k\frac{dT(r)}{dr} = \frac{Q_T}{4\pi r^2}$$

Integrating and solving for T(r), the following expression is found:

$$T(r) = \frac{Q_T}{4\pi kr} \quad \ldots\ldots\ldots\ldots\ldots\ldots\ldots\ldots\ldots\ldots\ldots\ldots\ldots\ldots\ldots\ldots\ldots\ldots \quad (3.13)$$

This is the equation for the temperature at r due to a three-dimensional heat source Q_T in an infinite medium of thermal conductivity k.

For a heat sink (Figure 3.9) the temperature distribution can be found in the same fashion than for a heat source; the result is the same differing just in sign.

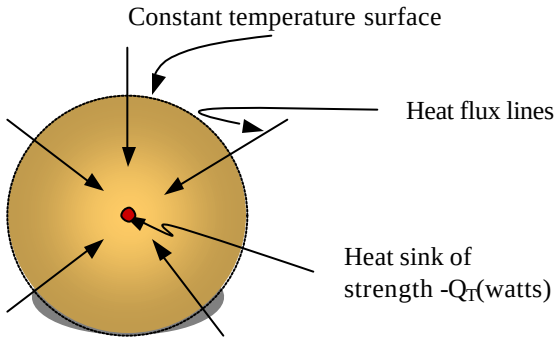

Figure 3.9. Point heat sink and constant temperature surface.

3.3.1.2 Line Heat Source (Two-Dimensional)

Suppose we have an infinite two-dimensional medium with constant thermal conductivity similar to the as previous case; consider a line heat source of strength Λ per unit depth (W/m) along z-axis as shown in figures 3.10 (a) and (b).

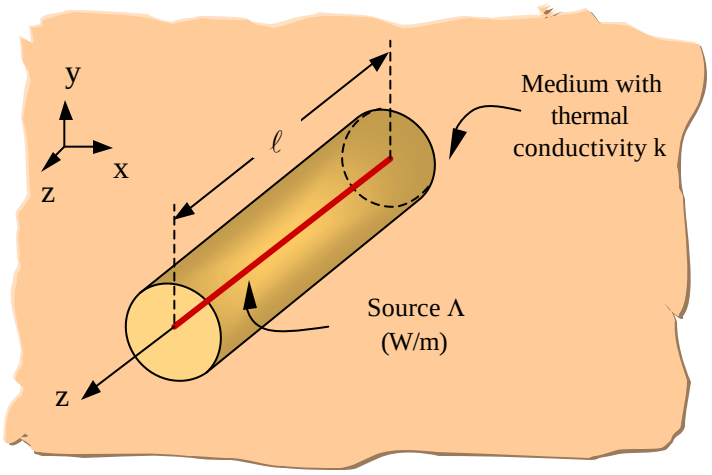

Figure 3.10. (a) Line source in an infinite medium of constant conductivity k.

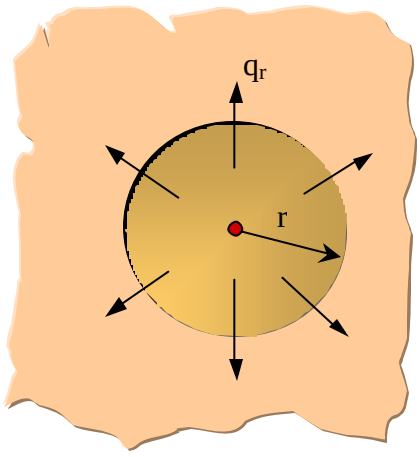

Figure 3.10. (b) Heat flux from surface.

Since the medium is infinite, then there is no variation along z-axis, the temperature profile is a function of radial distance "r" only, then:

$T = T(r)$

$\frac{\partial(\,)}{\partial z} = 0$ and

Total heat generation: $Q_T = \Lambda \,.\, \ell$ (W)

Consider a cylindrical surface of radius r with the line source on the axis. By an energy balance:

Energy flux from the cylindrical surface = heat generation inside volume

$q_r\,(2.\pi.r.\ell) = \Lambda \,.\, \ell$

Once again using Fourier's law and solving for the temperature, the following expression is found:

$$T(r) = \frac{-\Lambda}{2\pi k} \ln r \quad \ldots\ldots\ldots\ldots\ldots\ldots\ldots\ldots\ldots\ldots\ldots\ldots\ldots\ldots\ldots\ldots \quad (3.14)$$

Or

$$T(r) = \frac{-Q_T}{2\pi k \ell} \ln r \quad \ldots\ldots\ldots\ldots\ldots\ldots\ldots\ldots\ldots\ldots\ldots\ldots\ldots\ldots\ldots\ldots \quad (3.15)$$

This is the equation for the temperature at r due to a two-dimensional heat source Q_T in an infinite medium of thermal conductivity k.

3.3.2 Mathematical Representation of a Heat Source

A heat source of strength Q_T (Watts) located at x′ (Figure 3.11) can be represented by:

$$Q(\vec{x}') = Q_T \delta(\vec{x} - \vec{x}') \quad \ldots\ldots\ldots\ldots\ldots\ldots\ldots\ldots\ldots\ldots\ldots\ldots\ldots\ldots\ldots\ldots \quad (3.16)$$

Where $Q(\vec{x}')$ is the heat generation intensity per unit volume (w/m^3).

When $Q(\vec{x}')$ is integrated over the volume the full strength Q_T is obtained, i.e.

$$\iiint_V Q(\vec{x}') d^3 x' = Q_T$$

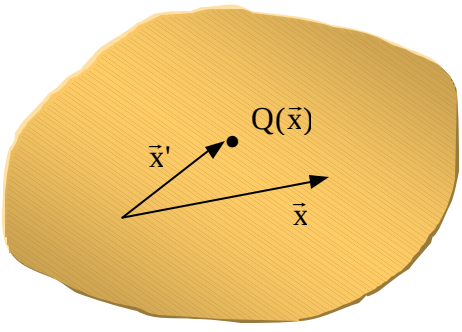

Figure 3.11. Three-dimensional body with internal heat generation.

3.3.3 Green's Function Solution Equation for the Heat Conduction Problem.

For the steady state heat conduction problem the temperature $T(\vec{x})$ at any position $\vec{x}$ in a body of constant thermal conductivity k with thermal heat generation rate $Q(\vec{x})$ per unit volume (W/m^3) satisfies the heat conduction equation. Equation (3.12).

Analogous to the concepts of positive and negative electrostatic charges in electrodynamics, we can introduce the concept of a heat sources and heat sinks. Then we define the temperature Green's function $G(\vec{x},\vec{x}')$ as the temperature at the field point $\vec{x}$ due to unit heat source at the source point $\vec{x}'$ (Figure 3.11)

Therefore $G(\vec{x},\vec{x}')$ must satisfy the heat conduction equation.

Then:

$$\nabla^2 G(\vec{x},\vec{x}') = -\frac{Q(\vec{x})}{k} \quad \ldots\ldots\ldots\ldots\ldots\ldots\ldots\ldots\ldots\ldots\ldots\ldots\ldots\ldots \quad (3.17)$$

Where $Q(\vec{x})$, is the heat generation intensity of a unit heat source.

$$Q(\vec{x}) = \delta(\vec{x} - \vec{x}')$$

So that $\iiint_V Q(\vec{x})dV = 1$

Substituting the equation (3.16) in (3.17) to obtain (remember Q_T=1, since heat source is of unit strength):

$$\nabla^2 G(\vec{x},\vec{x}') = -\frac{\delta(\vec{x} - \vec{x}')}{k} \quad \ldots\ldots\ldots\ldots\ldots\ldots\ldots\ldots\ldots\ldots\ldots\ldots\ldots\ldots \quad (3.18)$$

Using the corollary of divergence theorem equation (3.7) and by setting $\phi = G$ and $\psi = T$ where x is the observation point and x' is the integration variable, the following expression is obtained:

$$\iiint_V \left\{G(\vec{x},\vec{x}')\nabla^2 T(\vec{x}') - T(\vec{x}')\nabla^2 G(\vec{x},\vec{x}')\right\}dV' = \iint_S \left\{G(\vec{x},\vec{x}')\frac{\partial T(\vec{x}')}{\partial n'} - T(\vec{x}')\frac{\partial G(\vec{x},\vec{x}')}{\partial n'}\right\}dS'$$

Substituting the equations (3.12) and (3.18) in the previous expression to obtained:

$$-\iiint_V G(\vec{x},\vec{x}')\frac{Q(\vec{x})}{k}dV' + \iiint_V T(\vec{x}')\frac{\delta(\vec{x}-\vec{x}')}{k}dV' = \iint_S \left(G(\vec{x},\vec{x}')\frac{\partial T(\vec{x}')}{\partial n'} - T(\vec{x}')\frac{\partial G(\vec{x},\vec{x}')}{\partial n'}\right)dS'$$

By applying first property for Dirac-Delta function on the second term in the left hand side:

$$-\iiint_V G(\vec{x},\vec{x}')\frac{Q(\vec{x})}{k}dV' + \frac{T(\vec{x})}{k} = \iint_S \left(G(\vec{x},\vec{x}')\frac{\partial T(\vec{x}')}{\partial n'} - T(\vec{x}')\frac{\partial G(\vec{x},\vec{x}')}{\partial n'}\right)dS'$$

Solving for temperature T:

$$T(\vec{x}) = \iiint_{V'} G(\vec{x},\vec{x}')Q(\vec{x}')dV' + k\iint_{S'} \left(G(\vec{x},\vec{x}')\frac{\partial T(\vec{x}')}{\partial n'} - T(\vec{x}')\frac{\partial G(\vec{x},\vec{x}')}{\partial n'}\right)dS' \quad \ldots. \quad (3.19)$$

The primes indicate that the integration is done around the source point $\vec{x}'$

The source contribution is represented by the first term on the right hand side, boundary condition contributions are represented by other two terms.

The equation (3.19) is valid for any shape, any heat source and any boundary condition.

The temperature $T(\vec{x})$ at any point $\vec{x}$ can be determined if Green's function $G(\vec{x},\vec{x}')$ is known.

Green's function must satisfy equation (3.18) but cannot be uniquely determined until G is specified on the boundary. The purpose of the present work is to solve the heat conduction problem for Dirichlet boundary conditions (i.e. temperature specified on surface). In this case the best choice is to make $G(\vec{x},\vec{x}')=0$ on the boundary such that the first term in the surface integral of equation (3.19) vanishes. Then we have:

$$T(\vec{x}) = \iiint_{V'} G(\vec{x},\vec{x}')Q(\vec{x}')dV' - k\iint_{S'} T(\vec{x}')\frac{\partial G(\vec{x},\vec{x}')}{\partial n'}dS' \quad \ldots\ldots\ldots\ldots\ldots\ldots \quad (3.20)$$

This is the fundamental solution equation using Green's function for the heat conduction problem with Dirichlet boundary conditions.

It should be reemphasized that once the Green's function is obtained for a body, it can be used for any type of source.

3.4 Problem analysis

With equation (3.20) the problem for the determination of the temperature profile has been reduced to finding the Green's function. There are two general ways to obtain Green's functions:

3.4.1. Orthogonal Expansion:

It must be said that Green's functions depend on the geometry of the body; there are several ways to find them.

The first one is the general method, which consists in expanding $G(\vec{x},\vec{x}')$ in orthogonal eigenfunctions, obtaining the Green's function in terms of:

- Sine and cosine functions for rectangular coordinates system.
- Sine, cosine and Bessel functions for cylindrical coordinates system.
- Legendre polynomials and associated Legendre polynomials, for spherical coordinates system.

3.4.2. Physical Approach:

The second is a physical approach: known as method of images, this method is useful for infinite and semi-infinite geometries, circular plates and spheres, when temperature is specified on the boundaries.

This method consists in replacing the boundary by virtual image sources or sinks. The method of images is the method used in the development of the present research.

3.5. Method of Images

In this part of the present work, Green's functions for two and three dimensional semi-infinite spaces and infinite quadrant are found. Before the development is done it is necessary to introduce the following relationships:

3.5.1 $\tilde{N}^2$(lnr) in Cylindrical Coordinates

Recalling equation (3.14) for the steady state temperature distribution in a medium with a two-dimensional line source of strength Λ(W/m):

$$T(r) = \frac{-\Lambda}{2\pi k} \ln r$$

After applying the operator ∇^2 to both sides in the previous equation, and since Λ, k and I are constants, the following expression is obtained:

$$\nabla^2 T(r) = \frac{-\Lambda}{2\pi k} \nabla^2 \ln r \quad \ldots\ldots\ldots\ldots\ldots\ldots\ldots\ldots\ldots\ldots\ldots\ldots\ldots\ldots\ldots\ldots\ldots\ldots \quad (3.21)$$

Since the temperature distribution in this case is only function of radius, then in cylindrical coordinates ∇^2 can be expressed as follows:

$$\nabla^2 = \frac{1}{r}\frac{\partial}{\partial r}\left(r \frac{\partial}{\partial r} \right)$$

Therefore (∇^2 lnr) in equation (3.21) becomes:

$$\nabla^2 (\ln r) = \frac{1}{r}\frac{\partial}{\partial r}\left(r \frac{\partial}{\partial r} (\ln r) \right) = \begin{cases} 0 & \text{if} \quad r \neq 0 \\ \rightarrow \infty & \text{if} \quad r = 0 \end{cases} \ldots\ldots\ldots\ldots\ldots\ldots\ldots\ldots \quad (3.22)$$

Applying divergence theorem to equation (3.22), using the cylindrical volume enclosing the point r = 0 shown in figure 3.21, results in:

$$\iiint_V \nabla^2 (\ln r) dV = \iint_S \frac{\partial (\ln r)}{\partial r} dS$$

In cylindrical coordinates the differential surface dS is equal to rdθdz; solving the right hand side term in the previous expression and integrating the following is obtained:

$$\int_0^{\ell}\int_0^{2\pi}\frac{\partial(\ln r)}{\partial r}\,r\,d\theta dz=\int_0^{\ell}\int_0^{2\pi}d\theta dz=2\pi\ell$$

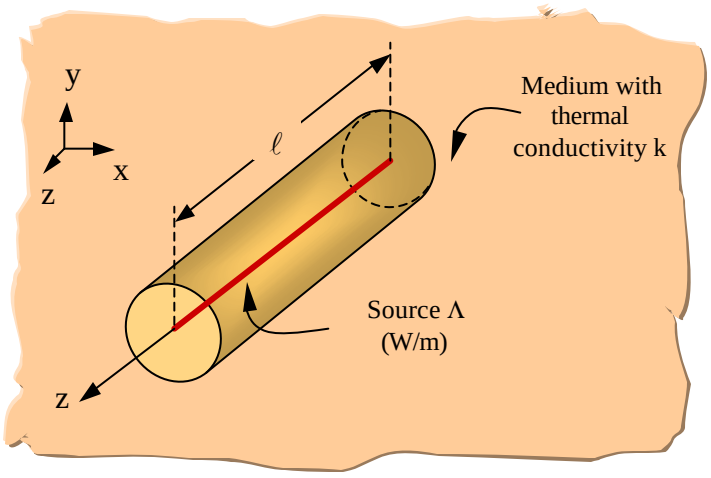

Figure 3.12. (a) Line source in an infinite medium of constant conductivity k.

Therefore:

$$\iiint_V \nabla^2(\ln r)\,dV=2\pi\ell$$

The last expression is valid for the volume including the point r = 0

Dividing both sides in this last expression by $2\pi l$ and doing the same in equation (3.22), the following is obtained:

$$\left.\begin{aligned}&\frac{1}{2\pi\ell}\nabla^2(\ln r)=\begin{cases}0 & \text{if} \quad r\neq 0\\ \to\infty & \text{if} \quad r=0\end{cases}\\[2ex]&\iiint_V\frac{1}{2\pi\ell}\nabla^2(\ln r)\,dV=1\end{aligned}\right\} \quad \ldots\ldots\ldots\ldots\ldots\ldots\ldots\ldots \quad (3.23)$$

Where volume V encloses point $r = 0$.

Equation (3.23) behaves as a Dirac-Delta function and satisfies its conditions, therefore it can be said that:

$$\frac{1}{2\pi\ell}\nabla^2(\ln r) = \delta(r)$$

Or

$$\nabla^2(\ln r) = 2\pi\ell\delta(r) \quad \ldots\ldots\ldots\ldots\ldots\ldots\ldots\ldots\ldots\ldots\ldots\ldots\ldots\ldots\ldots\ldots \quad (3.24)$$

3.5.2. $\nabla^2\left(\frac{1}{r}\right)$ in Spherical Coordinates

By a similar procedure, a relationship between $\nabla^2(1/r)$ and Dirac-Delta function in spherical coordinates can be found.

Recalling equation (3.13) for the steady state temperature distribution for a spherical source of strength Q_T watts:

$$T(r) = \frac{Q_T}{4\pi kr}$$

After applying the operator ∇^2 to both sides in previous equation, and since Q_T and k are constants, the following expression is obtained:

$$\nabla^2 T(r) = \frac{Q_T}{4\pi k}\nabla^2\left(\frac{1}{r}\right) \quad \ldots\ldots\ldots\ldots\ldots\ldots\ldots\ldots\ldots\ldots\ldots\ldots\ldots\ldots\ldots\ldots \quad (3.25)$$

As in the previous case, temperature distribution is only function of radius, therefore ∇^2 for spherical coordinates can be expressed as follows:

$$\nabla^2 = \frac{1}{r^2}\frac{\partial}{\partial r}\left(r^2\frac{\partial}{\partial r}\right)$$

Therefore $[\nabla^2 (1/r)]$ in equation (3.25) becomes:

$$\nabla^2\left(\frac{1}{r}\right)=\frac{1}{r^2}\frac{\partial}{\partial r}\left(r^2\frac{\partial}{\partial r}\left(\frac{1}{r}\right)\right)=\begin{cases}0 & \text{if} \quad r\neq 0\\ \to\infty & \text{if} \quad r=0\end{cases} \qquad \text{(3.26)}$$

Applying divergence theorem to a spherical volume enclosing the point r = 0 as shown in figure 3.16.

$$\iiint_V \nabla^2\left(\frac{1}{r}\right)dV=\iint_S \frac{\partial}{\partial r}\left(\frac{1}{r}\right)dS$$

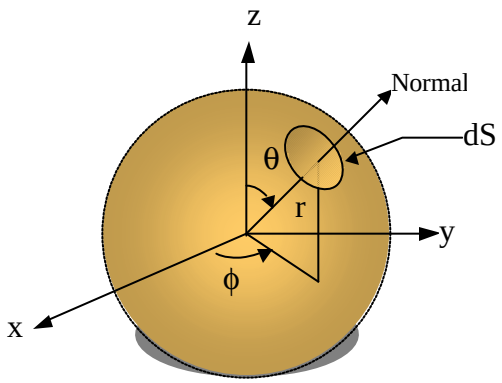

Figure 3.13. Spherical volume enclosing the point r = 0.

In spherical coordinates the differential surface dS is equal to $r^2 \sin\theta d\theta d\phi$; solving the right hand side term in previous expression and integrating:

$$\int_0^{2\pi}\int_0^{\pi}\left\{\frac{\partial}{\partial r}\left(\frac{1}{r}\right)\right\}r^2\sin\theta d\theta d\phi=\int_0^{2\pi}\int_0^{\pi}-\frac{1}{r^2}r^2\sin\theta d\theta d\phi=-4\pi$$

Therefore:

$$\iiint_V \nabla^2\left(\frac{1}{r}\right)dV = -4\pi$$

This is valid for the volume including the point r = 0

Dividing both sides in previous the equation by -4π and doing the same as we did for equation (3.24), the following is obtained:

$$\left.\begin{aligned} &\frac{-1}{4\pi}\nabla^2\left(\frac{1}{r}\right) = \begin{cases} 0 & \text{if} \quad r \neq 0 \\ \to \infty & \text{if} \quad r = 0 \end{cases} \\ &\iiint_V \frac{-1}{4\pi}\nabla^2\left(\frac{1}{r}\right)dV = 1 \end{aligned}\right\} \quad \ldots\ldots\ldots\ldots\ldots\ldots\ldots\ldots\ldots\ldots \quad (3.27)$$

Where volume V enclosing the point r = 0

Equation (3.21) behaves as a Dirac-Delta function and satisfies its conditions; therefore the following expression is valid too:

$$\frac{-1}{4\pi}\nabla^2\left(\frac{1}{r}\right) = \delta(r)$$

Or

$$\nabla^2\left(\frac{1}{r}\right) = -4\pi\delta(r) \quad \ldots\ldots\ldots\ldots\ldots\ldots\ldots\ldots\ldots\ldots\ldots\ldots\ldots\ldots\ldots\ldots \quad (3.28)$$

3.5.3 Green's Function for a Two-Dimensional Semi-Infinite Space

Consider the two-dimensional semi-infinite space with constant thermal conductivity k, a heat source of unit strength is applied at P as shown in figure 3.14.

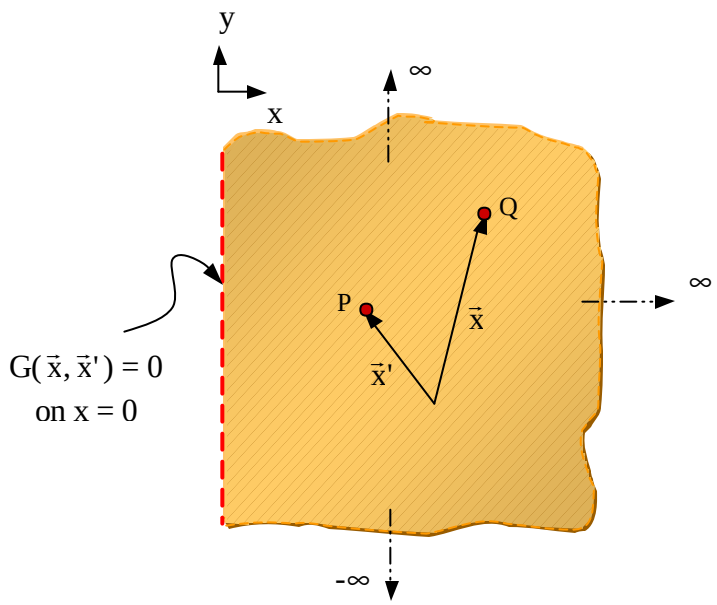

Figure 3.14. Green's function for a two-Dimensional semi-infinite space.

$Q(\vec{x})$ is the field point.

$G(P,Q) = G(\vec{x},\vec{x}')$ = Temperature at $\vec{x}$ due to unit source at $\vec{x}'$.

G must satisfy equation (3.18), i.e, $\nabla^2 G(\vec{x},\vec{x}') = \dfrac{-\delta(x-x')}{k}$

and:

$G(\vec{x},\vec{x}') = 0$ on $x = 0$ ..... (3.29)

Consider now an infinite space of thermal conductivity k. Put an equal and opposite heat source at P′, the image of the point P through the boundary of the semi-infinite space as shown in figure 3.15.

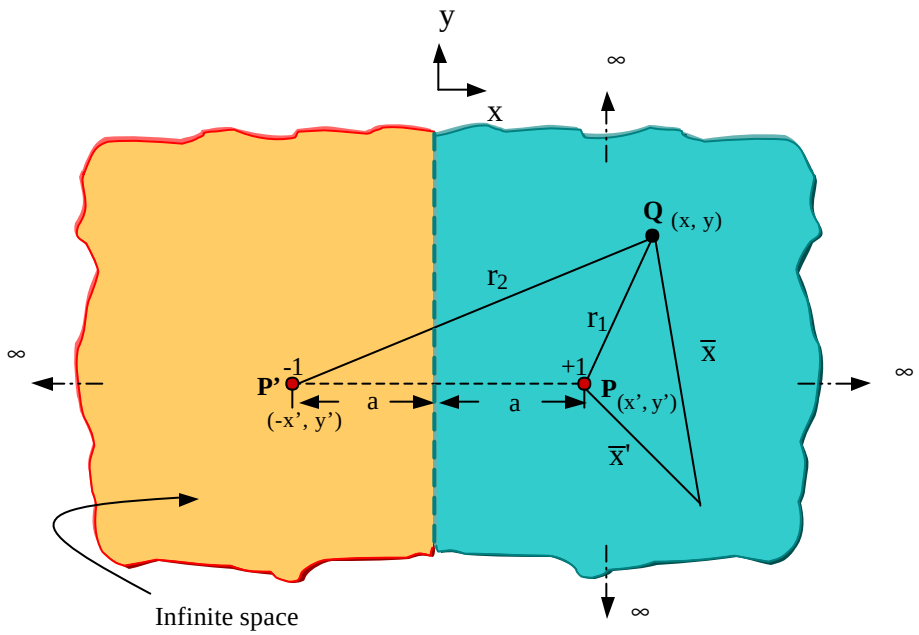

Figure 3.15. Image for a unit heat source for a two-dimensional space with thermal conductivity k.

Since the source and the sink are of unit strength, then $|Q_T| = 1$ for both the source and sink.

Equation (3.15) gives the temperature distribution for a two dimensional space due to a heat source (the same expression but with opposite sign is valid for the temperature distribution due to a sink), then, for this case, the temperature profile can be expressed as follows:

$$T(r) = \frac{-1}{2\pi k \ell} \ln r_1 + \frac{1}{2\pi k \ell} \ln r_2$$

Applying the operator ∇^2 to both left and right hand side in previous equation:

$$\nabla^2 T = \frac{-1}{2\pi k \ell}\left[\nabla^2 \ln r_1 - \nabla^2 \ln r_2\right]$$

Since r_2 is in the imaginary region it never can be zero (actually $r_2 \geq a$ to be able to interact in the real two-dimensional body - i.e. $x > 0$ in figure 3.15), therefore according to equations (3.23) and (3.24) for the region of interest, $x > 0$, the following is accomplished:

$$r_2 > 0 \quad \Rightarrow \quad \nabla^2 \ln r_2 = 0$$

$$\nabla^2 \ln r_1 = 2\pi \ell \delta(r_1)$$

Substituting these values in the previous equation the following relationship is obtained:

$$\nabla^2 T = -\frac{\delta(r_1)}{k} \quad \text{Or:}$$

$$\nabla^2 T = -\frac{\delta(\vec{x} - \vec{x}')}{k}$$

On boundary $r_1 = r_2$ (see figure 3.16)

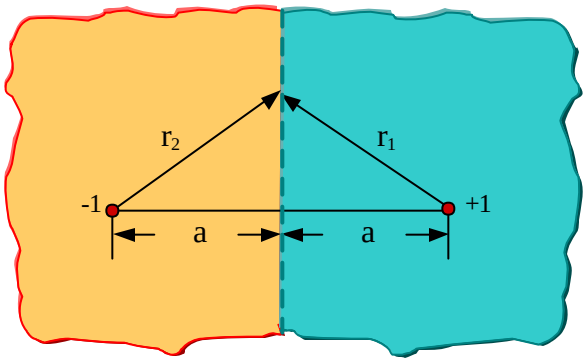

Figure 3.16. Effect of heat source and sink on boundary.

When $r_1 = r_2$ then T = 0 (temperature on boundary), then T satisfies equations (3.18) and (3.29) (G=0 on boundary) therefore $T(\vec{x}, \vec{x}')$ is the Green's function:

$$G(\vec{x}, \vec{x}') = \frac{-1}{2\pi k\ell} \ln r_1 + \frac{1}{2\pi k\ell} \ln r_2$$

$$G(\vec{x}, \vec{x}') = \frac{1}{2\pi k\ell} \ln\left[\frac{r_2}{r_1}\right] \text{.....(3.30)}$$

The distances r_1 y r_2 are obtain of figure 3.15

$$r_1 = \sqrt{(x - x')^2 + (y - y')^2}$$

$$r_2 = \sqrt{(x + x')^2 + (y - y')^2}$$

Substituting in the equation 3.30 to obtain:

$$G(\vec{x}, \vec{x}') = \frac{1}{2\pi k\ell} \ln\left[\frac{\sqrt{(x + x')^2 + (y - y')^2}}{\sqrt{(x - x')^2 + (y - y')^2}}\right]$$

$$G(\vec{x}, \vec{x}') = \frac{1}{4\pi k\ell} \ln\left[\frac{(x + x')^2 + (y - y')^2}{(x - x')^2 + (y - y')^2}\right] \text{.....(3.31)}$$

Finally, for this case, it can be said that finding the Green's function for a semi-infinite space x>0, is equivalent to solving the problem of a source and its image (a sink) in an infinite space as shown in figure 3.17

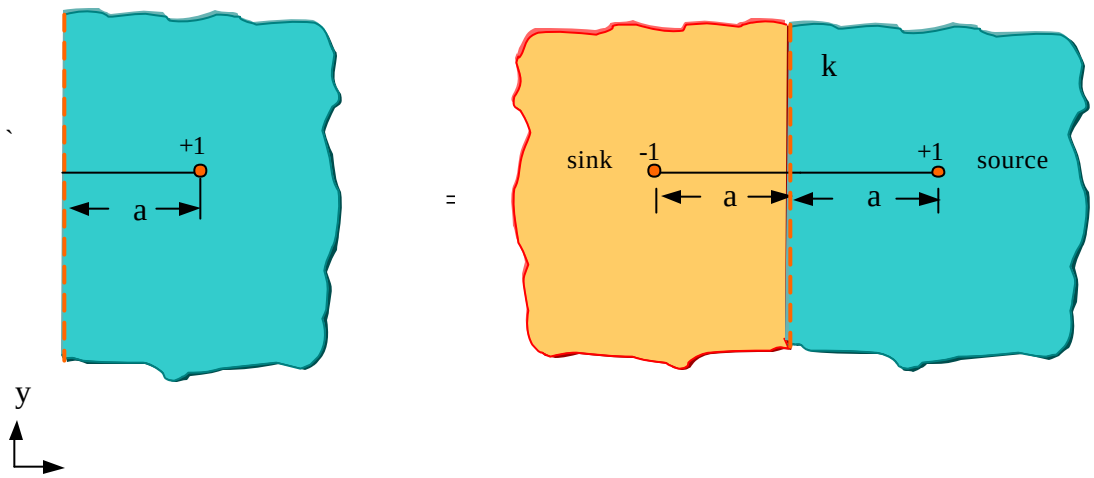

Figure 3.17. Semi-infinite two-dimensional space with a unit heat source and its equivalent image through the boundary.

3.5.4 Green's Function for a Three-Dimensional Semi-Infinite Space

Consider the three-dimensional semi-infinite space with constant thermal conductivity k similarly to point 35.3; a heat source of unitary strength is applied at P as shown in figure 3.18

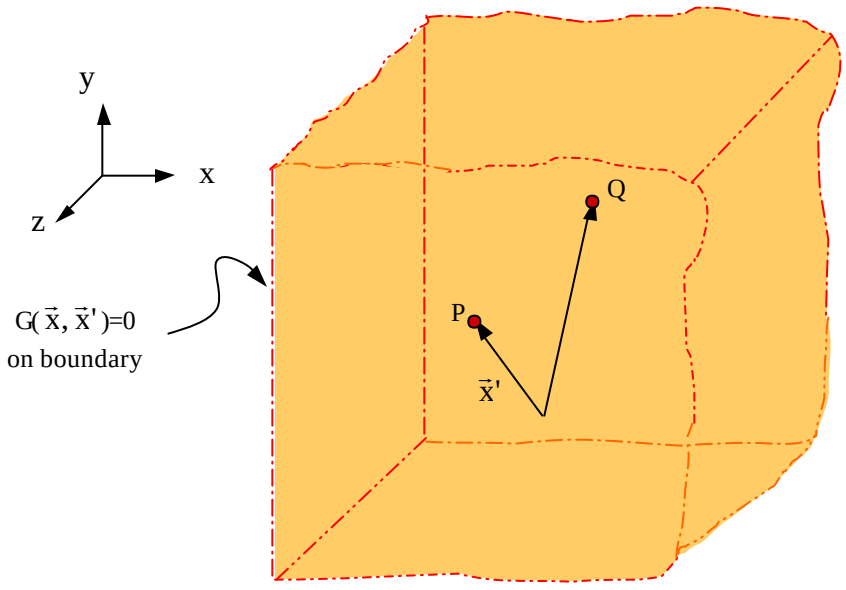

Figure 3.18. Green's function for a three-dimensional semi-infinite space.

Once again:

G(P,Q) = $G(\vec{x}, \vec{x}')$ = Temperature at $\vec{x}$ due to unit source at $\vec{x}'$ and must satisfy:

$$\nabla^2 G = \frac{-\delta(\vec{x} - \vec{x}')}{k} \quad \ldots\ldots\ldots\ldots\ldots\ldots\ldots\ldots\ldots\ldots\ldots\ldots\ldots\ldots\ldots\ldots \quad (3.32)$$

G(x,x') = 0 on boundary (x = 0) ……. (3.33)

Consider now an infinite space of thermal conductivity k. Put an equal and opposite heat source at P′, the image of the point P through the plane x = 0 as shown in figure 3.19.

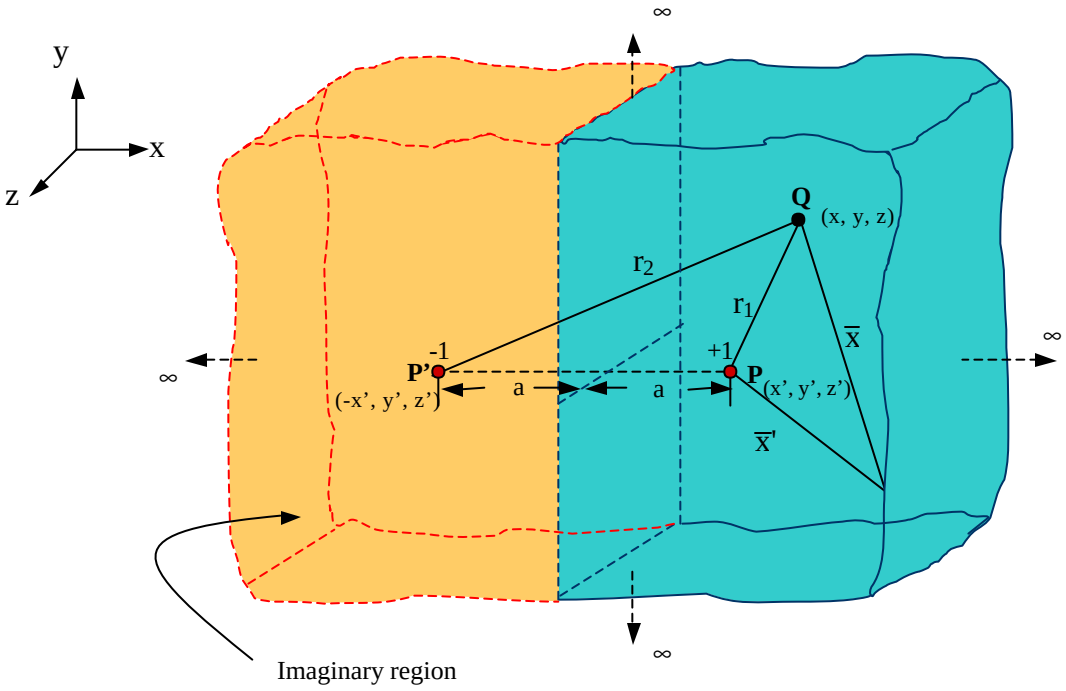

Figure 3.19. Image for a unit heat source for a three-dimensional space with thermal conductivity k.

Source and the sink are of unit strength ($|Q_T| = 1$ for both the source and sink)

Equation (3.13) gives the temperature distribution for a three dimensional space due to a heat source (the same expression but with opposite sign is valid for the temperature distribution due to a sink), then the temperature profile can be expressed as:

$$T(r) = \frac{1}{4\pi k r_1} - \frac{1}{4\pi k r_2}$$

Applying the operator ∇^2 to both left and right hand side terms:

$$\nabla^2 T = \frac{1}{4\pi k}\left[\nabla^2 \frac{1}{r_1} - \nabla^2 \frac{1}{r_2}\right]$$

The value of r_2 can never be zero since this is in the imaginary region ($r_2 \geq a$; i.e. $x > 0$ in figure 3.19), therefore according to equations (3.27) and (3.28) for the region of interest, $x > 0$, the following is accomplished:

$$r_2 > 0 \quad \Rightarrow \quad \nabla^2\left(\frac{1}{r_2}\right) = 0$$

$$\nabla^2\left(\frac{1}{r_1}\right) = -4.\pi.\delta(r_1)$$

Substitute these last values in the previous equation to obtain:

$$\nabla^2 T = -\frac{\delta(r_1)}{k}$$

Or:

$$\nabla^2 T = -\frac{\delta(\vec{x} - \vec{x}')}{k}$$

In consequence, since T satisfies equations (3.32) and (3.33), the Green's function for a three-dimensional space of thermal conductivity k is:

$$G(\vec{x},\vec{x}') = \frac{1}{4\pi k r_1} - \frac{1}{4\pi k r_2}$$

$$G(\vec{x},\vec{x}') = \frac{1}{4\pi k}\left[\frac{1}{r_1} - \frac{1}{r_2}\right] \quad \text{..... (3.34)}$$

The distances r_1 y r_2 are obtain of figure 3.19

$$r_1 = \sqrt{(x-x')^2 + (y-y')^2 + (z-z')^2}$$

$$r_2 = \sqrt{(x+x')^2 + (y-y')^2 + (z-z')^2}$$

Substituting in the equation 3.33 to obtain general equation of Green's function for a three-dimensional space of thermal conductivity k:

$$G(\vec{x},\vec{x}') = \frac{1}{4\pi k}\left[\frac{1}{\sqrt{(x-x')^2 + (y-y')^2 + (z-z')^2}} - \frac{1}{\sqrt{(x+x')^2 + (y-y')^2 + (z-z')^2}}\right] \quad \text{.....(3.35)}$$

3.5.5 Green's Function for a Two-Dimensional Infinite Quadrant

Consider the two-dimensional infinite quadrant with constant thermal conductivity k, a heat source of unitary strength is applied at P as shown in figure 3.20.

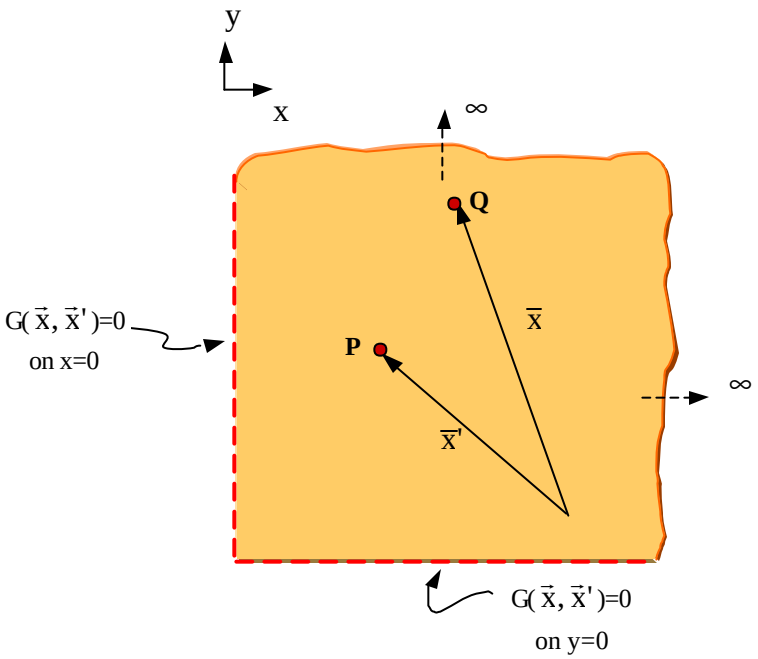

Figure 3.20. Green's function for a two-dimensional infinite quadrant.

$G(P,Q) = G(\vec{x},\vec{x}')$ = Temperature at $\vec{x}$ due to unit source at $\vec{x}'$.

G must satisfy equation (3.12)

and:

$$G(\vec{x},\vec{x}') = 0 \text{ on } x = 0 \quad \ldots\ldots\ldots\ldots\ldots\ldots\ldots\ldots\ldots\ldots\ldots\ldots\ldots\ldots \quad (3.36)$$

$$G(\vec{x},\vec{x}') = 0 \text{ on } y = 0 \quad \ldots\ldots\ldots\ldots\ldots\ldots\ldots\ldots\ldots\ldots\ldots\ldots\ldots\ldots \quad (3.37)$$

Consider now an infinite quadrant of thermal conductivity k. Put three heat source, two of opposite sign at P′ and P’’’ and a third of the same sing at P’’, the images of the point P through the plane x = 0 and y = 0 as shown in figure 3.21.

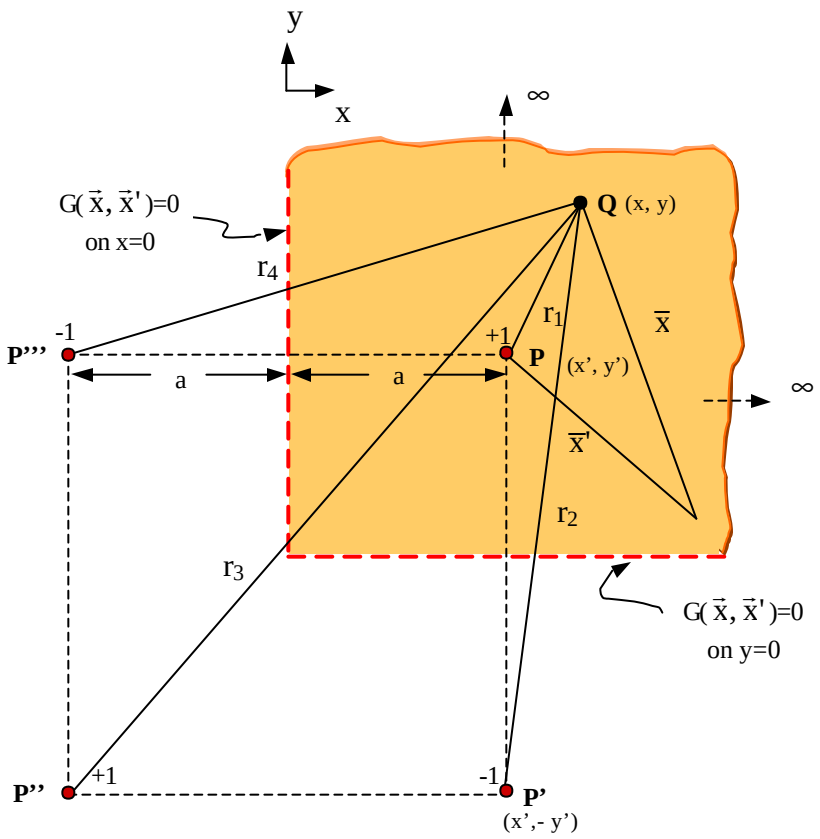

Figure 3.21. Image for a unit heat source for a two-dimensional infinite quadrant with thermal conductivity k.

Since the source and the sink are of unitary strength, then $|Q_T| = 1$ for the sources and sinks.

Equation (3.15) gives the temperature distribution for a two-dimensional infinite quadrant due to a heat source (the same expression but with opposite sign is valid for the

temperature distribution due to a sink), then, for this case, the temperature profile can be expressed as follows:

$$T(r) = \frac{-1}{2\pi k\ell} \ln r_1 + \frac{1}{2\pi k\ell} \ln r_2 \frac{-1}{2\pi k\ell} \ln r_3 + \frac{1}{2\pi k\ell} \ln r_4$$

Applying the operator ∇^2 to both left and right hand side in previous equation:

$$\nabla^2 T = \frac{-1}{2\pi k\ell} \left[\nabla^2 \ln r_1 - \nabla^2 \ln r_2 + \nabla^2 \ln r_3 - \nabla^2 \ln r_4 \right]$$

Since r_2, r_3 and r_4 are in the imaginary region, these never can be zero (actually r_2, r_3 and $r_4 \geq a$, to be able to interact in the real two-dimensional body - i.e. $x > 0$ and $y>0$ in figure 3.21), therefore according to equations (3.23) and (3.24) for the region of interest, $x > 0$, $y>0$ the following is accomplished:

$r_2 > 0 \quad \Rightarrow \quad \nabla^2 \ln r_2 = 0$

$r_3 > 0 \quad \Rightarrow \quad \nabla^2 \ln r_3 = 0$

$r_4 > 0 \quad \Rightarrow \quad \nabla^2 \ln r_4 = 0$

$$\nabla^2 \ln r_1 = 2\pi\ell\delta(r_1)$$

Substituting these values in the previous equation the following relationship is obtained:

$$\nabla^2 T = -\frac{\delta(r_1)}{k} \quad \text{Or:}$$

$$\nabla^2 T = -\frac{\delta(\vec{x} - \vec{x}')}{k}$$

On boundary $r_1 = r_4$ (see figure 3.22 (a))

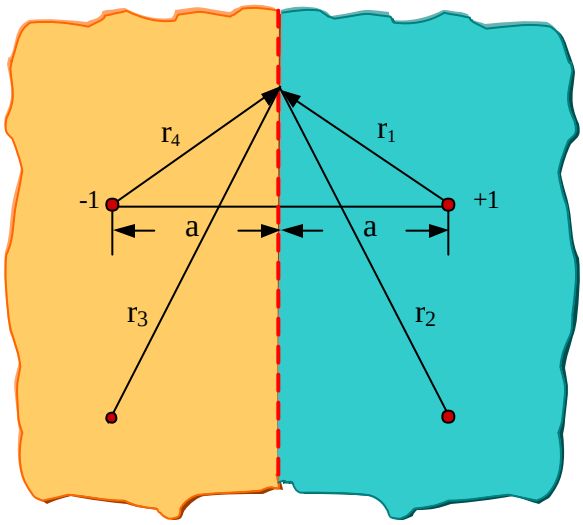

Figure 3.22 (a). Effect of heat source and sink on boundary x = 0.

On boundary $r_1 = r_2$ (see figure 3.22 (b))

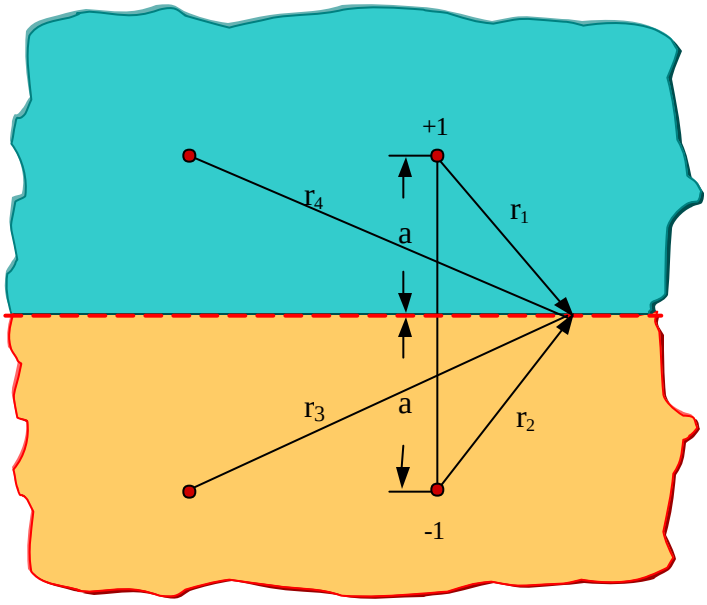

Figure 3.22.(b). Effect of heat source and sink on boundary y = 0.

When $r_1 = r_4$, $r_1 = r_2$, then T = 0 (temperature on boundary), then T satisfies equations (3.18), (3.36) and (3.37), (G = 0 on boundary) therefore $T(\vec{x},\vec{x}')$ is the Green's function:

$$G(\vec{x},\vec{x}') = \frac{-1}{2\pi k\ell}\ln r_1 + \frac{1}{2\pi k\ell}\ln r_2 - \frac{1}{2\pi k\ell}\ln r_3 + \frac{1}{2\pi k\ell}\ln r_4$$

$$G(\vec{x},\vec{x}') = \frac{1}{2\pi k\ell}\ln\left[\frac{r_2.r_4}{r_1.r_3}\right] \ldots\ldots\ldots\ldots\ldots\ldots\ldots\ldots \quad (3.38)$$

The distances r_1, r_2, r_3 and r_4 are obtain of figure 3.15

$$r_1 = \sqrt{(x-x')^2 + (y-y')^2}$$

$$r_2 = \sqrt{(x-x')^2 + (y+y')^2}$$

$$r_3 = \sqrt{(x+x')^2 + (y+y')^2}$$

$$r_4 = \sqrt{(x+x')^2 + (y-y')^2}$$

Substituting in the equation 3.38 to obtain the general equation of Green's function for a two-dimensional infinite quadrant of thermal conductivity k:

$$G(\vec{x},\vec{x}') = \frac{1}{2\pi k\ell}\ln\left[\frac{\sqrt{(x-x')^2 + (y+y')^2}.\sqrt{(x+x')^2 + (y-y')^2}}{\sqrt{(x-x')^2 + (y-y')^2}.\sqrt{(x+x')^2 + (y+y')^2}}\right]$$

$$G(\vec{x},\vec{x}') = \frac{1}{4\pi k\ell}\ln\left[\frac{\left[(x-x')^2 + (y+y')^2\right]}{\left[(x-x')^2 + (y-y')^2\right]}\frac{\left[(x+x')^2 + (y-y')^2\right]}{\left[(x+x')^2 + (y+y')^2\right]}\right] \ldots\ldots\ldots\ldots \quad (3.39)$$

IV. RESULTS AND DISCUSSION

The main objective of this thesis, was to find and apply Green's functions solution equation to the solution of conduction heat transfer with Dirichlet boundary conditions for specific geometries of semi-infinite slabs and infinite quadrants with various types of discrete heat generation source and determine the temperature profile. The objective was also to show that for the cases considered here Green's function integral techniques yield an elegant analytical or almost analytical solution, with far less effort compared to numerical solutions.

The solutions for semi-infinite slabs with thin plate heating source, the hollow box heating source, a square prismatic heating source, thin cylindrical heating source and infinite quadrant with square line heating source are compared with numerical solutions of finite elements using ANSYS 6.0.

The six cases solved are those with Dirichlet boundary conditions (temperature specified on boundary), this means, if T_B is the temperature of the boundary (assumed constant), then at $x = 0 \Rightarrow T = T_B$. For the case of semi-infinite quadrant at $x = 0 \Rightarrow T = T_B$, $y = 0 \Rightarrow T = T_B$. It should be noted that the method is equally applicable if T_B is a function of position. Using the method of superposition, the temperature profile can be expressed as follows:

$$T(x,y,z) = T_B + T_1(x,y,z) \qquad \ldots\ldots\ldots\ldots\ldots\ldots\ldots\ldots\ldots\ldots\ldots\ldots\ldots\ldots \quad (4.1)$$

From equation (4.1) clearly can be seen that T_1 must satisfy the following differential equation and the boundary condition:

$$\nabla^2 T_1(x,y,z) = -\frac{Q(\vec{x},\vec{y},\vec{z})}{k}$$

With the boundary condition:

$T_1(0,y,z) = 0$ …… (4.2)

T_1 can be solved using equation (3.19):

$$T_1(x,y,z) = \iiint_{V'} G(x,y,z,x',y',z')Q(x',y',z')dV' - k\iint_{S'} T_1(0,y,z)\frac{\partial G(x,y,z,x',y',z')}{\partial n'}dS' \quad \text{……..……} \quad (4.3)$$

By substituting boundary condition (4.2), the second term in the equation above vanishes (remember this is the contribution due to temperature on the boundary, which is zero for this case). Therefore, the expression for the temperature profile becomes:

$$T(x,y,z) = T_B + \iiint_{V'} G(x,y,z,x',y',z')\cdot Q(x',y',z')dV' \quad \text{……} \quad (4.4)$$

Since G has been already obtained for two-dimensional semi-infinite space, three-dimensional semi-infinite space and two-dimensional infinite quadrant (equations (3.31), (3.35) and (3.39)), the only unknown is the heat generation per unit volume along the heat source (W/m^3) Q(x',y',z') which depends on its geometry, strength and the geometry of the body. Then the problem of finding the temperature distribution has been reduced to specifying the heat generation per unit volume and integrating it in equation (4.4).

Is very important to emphasize that equation (4.3) was derived with no constrains on the geometry, therefore this expression is valid to solve temperature profiles for any body of any shape with the only constraint that temperature must be known on the boundary.

4.1. Semi-Infinite Slab (Two-dimensional cases)

4.1.1. Semi-Infinite Slab with a Thin Plate Heating Source

A thin plate carrying current is embedded, as a heat-generating element, in a semi-infinite slab $x > 0$, $-\infty < y < \infty$, $-\infty < z < \infty$, and constant thermal conductivity k. The plate can be assumed as an infinitesimally thin heat source; with large depth ℓ ($\ell \to \infty$) and width L; the heat generation per unit length per unit depth is constant and the boundary in $x = 0$ is maintained at constant temperature T_B as shown in figure 4.1.(a)

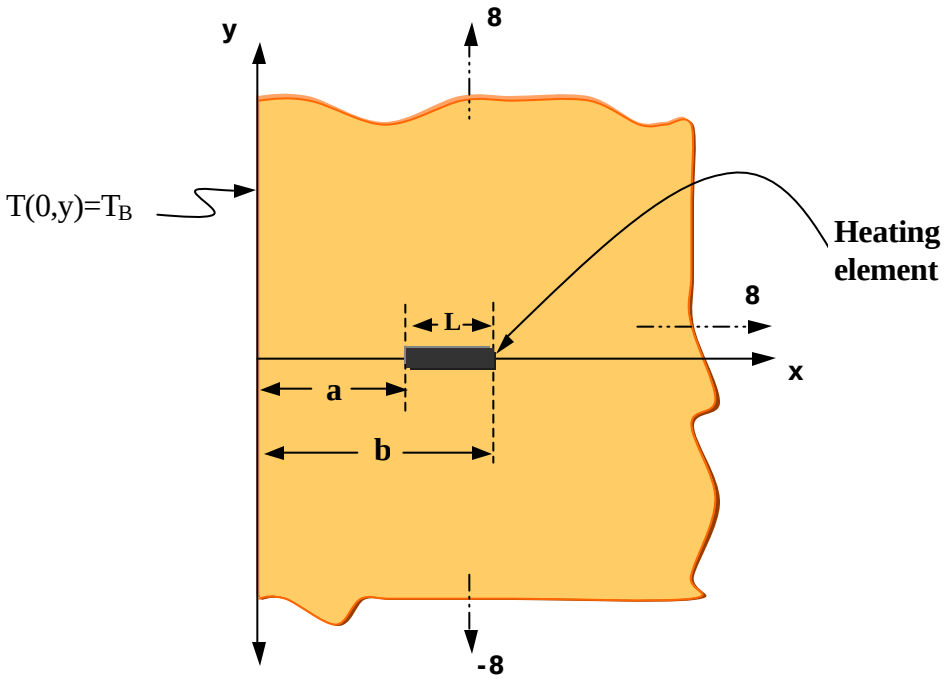

Figure 4.1(a) Semi-Infinite Slab of constant thermal conductivity k with a thin plate heating source element.

Let:

$Q_T \equiv$ Total heat generation (W) $= \lambda.\ell.L$

$\lambda \equiv$ Strength of the heat source per unit depth per unit length (W/m^2).

$Q(x,y) \equiv$ Heat generation intensity per unit volume (W/m^3)

Q(x,y) when integrated over the whole volume must be equal to the total heat generation inside the semi-infinite slab, i.e. $\iiint_V Q(x,y).dv = Q_T$

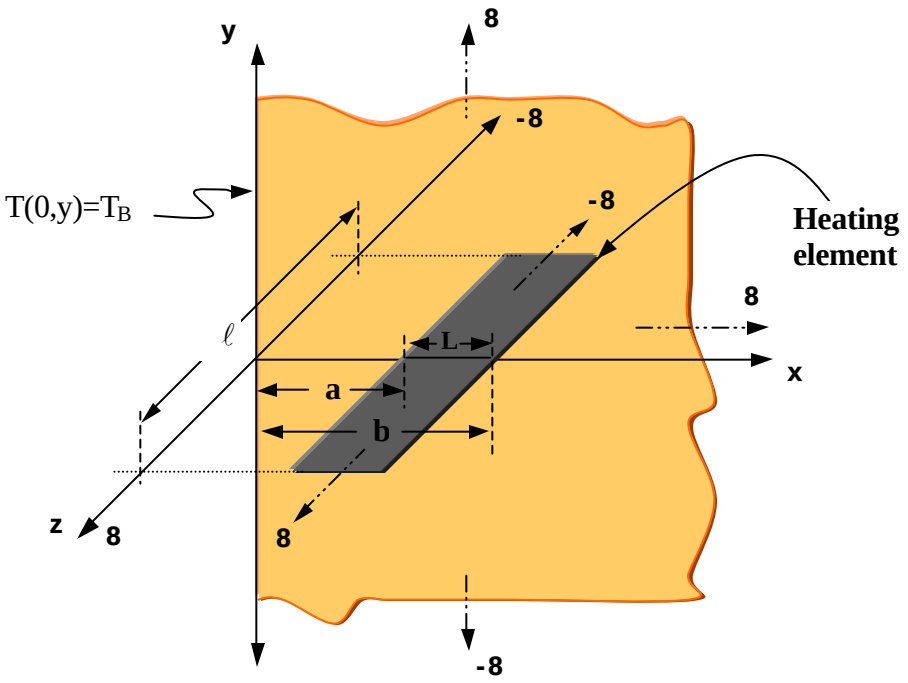

Figure 4.1(b) Semi-Infinite Slab of constant thermal conductivity k with a thin plate heating source element.

For cartesian coordinates this condition becomes:

$$\int_{-\frac{\ell}{2}}^{\frac{\ell}{2}}\int_{-\infty}^{\infty}\int_{0}^{\infty} Q(x,y).dx.dy.dz = Q_T = \lambda.\ell.(b-a) = \lambda.\ell.L \qquad \ldots\ldots\ldots\ldots\ldots\ldots\ldots\ldots \quad (4.5)$$

The heat generation Q(x,y) is then expressed of the following form:

$$Q(x,y) = \lambda \cdot \delta(y) \cdot \{H[x-a] - H[x-b]\} \qquad \ldots\ldots\ldots\ldots\ldots\ldots\ldots\ldots \quad (4.6)$$

The equation (4.6) satisfy to equation (4.5), where H(x) is the Heaviside function that was explained in the equation (3.2) in the chapter III.

Integrate the right hand side of expression (4.6) as indicated in equation (4.5)

$$\int_{-\frac{\ell}{2}}^{\frac{\ell}{2}}\int_{-\infty}^{\infty}\int_{0}^{\infty} \lambda \cdot \delta(y) \cdot \{H[x-a] - H[x-b]\}.dx.dy.dz = \lambda \int_{-\frac{\ell}{2}}^{\frac{\ell}{2}} dz. \int_{-\infty}^{\infty} \delta(y).dy \cdot \int_{0}^{\infty} \{H[x-a] - H[x-b]\}.dx$$

Using the properties for Dirac-Delta and Heaviside function we get:

$$\lambda \cdot \ell \cdot 1. \int_{a}^{b} dx = \lambda \cdot \ell \cdot (b-a) = \lambda \cdot \ell.L$$

Equation (4.6) after integration becomes:

$$\iiint_V Q(x,y).dv = Q_T = \lambda \cdot \ell \cdot (b-a) = \lambda \cdot \ell .L$$

Substitute equations (3.31) and (4.6) in equation (4.4):

$$T(x,y) = T_B + \frac{\lambda}{4\pi k\ell} \int_{-\frac{\ell}{2}}^{\frac{\ell}{2}} \int_{-\infty}^{0} \int_{0}^{\infty} \delta(y') \cdot \{H[x-a] - H[x-b]\} . \ln \left\{ \frac{(x+x')^2 + y^2}{(x-x')^2 + y^2} \right\} dx'\, dy'\, dz'$$

Integration on z is easily performed, for x and y the properties for Dirac Delta and Heaviside functions mentioned in chapter III are applied obtaining:

$$T(x,y) = T_B + \frac{\lambda}{4\pi k} \int_a^b \ln \left\{ \frac{(x+x')^2 + y^2}{(x-x')^2 + y^2} \right\} .dx'$$

In order to express results in non-dimensional form, the following non-dimensional quantities are defined:

$\overline{T}(\overline{x},\overline{y}) = \dfrac{T(x,y)}{T_B}$ Non-dimensional temperature

$\overline{\lambda} = \dfrac{\lambda.(b-a)}{kT_B}$ Non-dimensional heat generation

$\overline{x} = \dfrac{x}{L}$, $\overline{y} = \dfrac{y}{L}$ Non-dimensional field point location

$\overline{x}' = \dfrac{x'}{L}$ Non-dimensional source point location

$\overline{a} = \dfrac{a}{L}$, $\overline{b} = \dfrac{b}{L}$ Non-dimensional distances

Finally, substitute all these quantities in the previous equation and the following relationship is obtained:

$$\overline{T}(\overline{x},\overline{y}) = 1 + \frac{\overline{\lambda}}{4\pi}\int_{\overline{a}}^{\overline{b}} \ln\left\{\frac{(\overline{x}+\overline{x}')^2+\overline{y}^2}{(\overline{x}-\overline{x}')^2+\overline{y}^2}\right\}.d\overline{x}'$$

$$\overline{T}(\overline{x},\overline{y}) = 1 + \frac{\overline{\lambda}}{4\pi}\left[\begin{array}{l}(\overline{x}+\overline{b}).\left[\ln\left[(\overline{x}+\overline{b})^2+\overline{y}^2\right]-2\right]-(\overline{x}+\overline{a}).\left[\ln\left[(\overline{x}+\overline{a})^2+\overline{y}^2\right]-2\right]+\\ (\overline{x}-\overline{b}).\left[\ln\left[(\overline{x}-\overline{b})^2+\overline{y}^2\right]-2\right]-(\overline{x}-\overline{a}).\left[\ln\left[(\overline{x}-\overline{a})^2+\overline{y}^2\right]-2\right]\\ +2\overline{y}.\left[\begin{array}{l}\mathrm{Arctg}\left(\frac{\overline{x}+\overline{b}}{\overline{y}}\right)-\mathrm{Arctg}\left(\frac{\overline{x}+\overline{a}}{\overline{y}}\right)+\\ \mathrm{Arctg}\left(\frac{\overline{x}-\overline{b}}{\overline{y}}\right)-\mathrm{Arctg}\left(\frac{\overline{x}-\overline{a}}{\overline{y}}\right)\end{array}\right]\end{array}\right] \quad ..(4.8)$$

Equation (4.8) is the temperature profile for a semi-infinite slab with constant temperature on boundary heated by very thin plate carrying a current and embedded in the slab. Thus a closed form expression for the temperature distribution has been obtained.

Equation (4.8) can be easily evaluated for example with Mathcad obtaining highly accurate plots for the temperature profiles. In contrast with numerical solution, the analytical solution permits extensive parametric studies with minimal computational time. Some of the results for different values of $\overline{?},\overline{a},\overline{b},$ are presented in the figures 4.2 to 4.16.

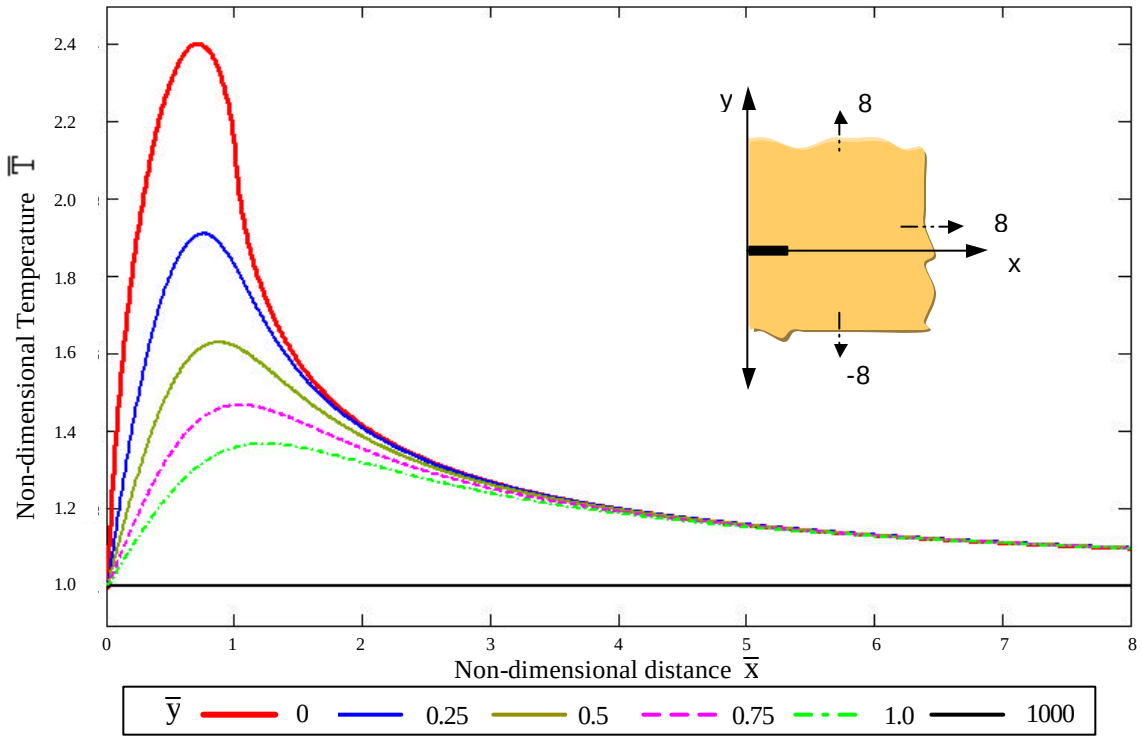

Figure 4.2. Dimensionless temperature distribution, line plate heating source $\overline{\lambda}=5,\ \overline{a}=0,\ \overline{b}=1$.

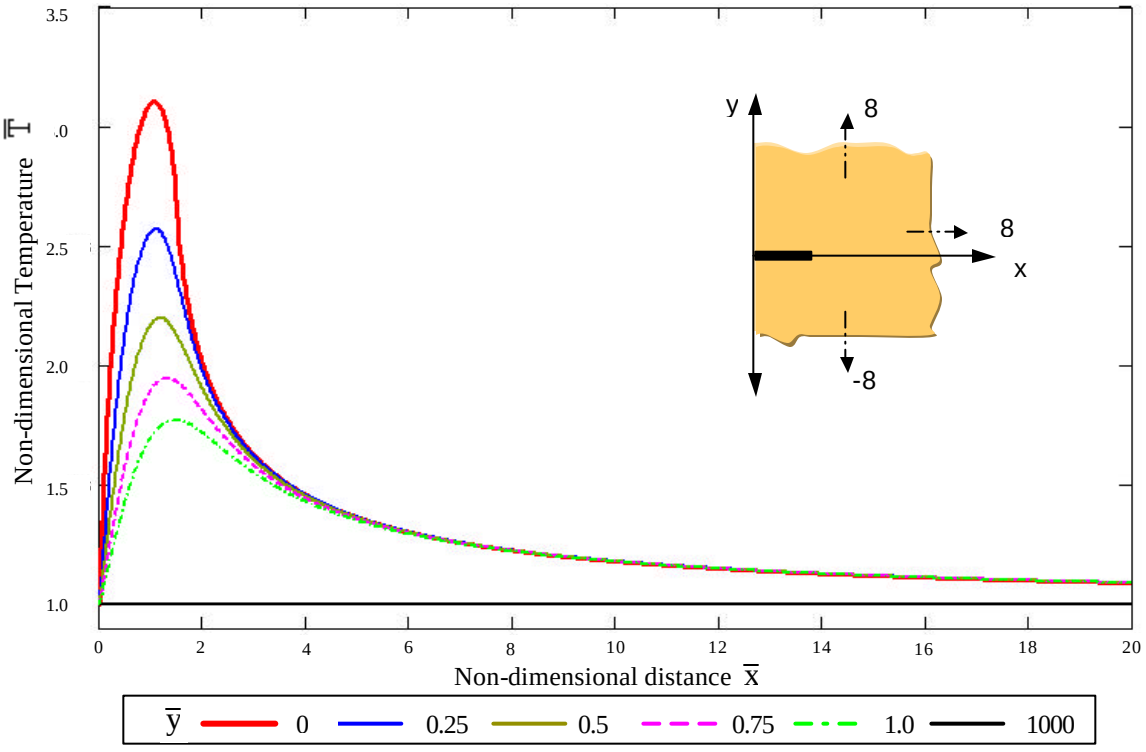

Figure 4.3. Dimensionless temperature distribution, line plate heating source $\overline{\lambda}=5,\ \overline{a}=0,\ \overline{b}=1.5$

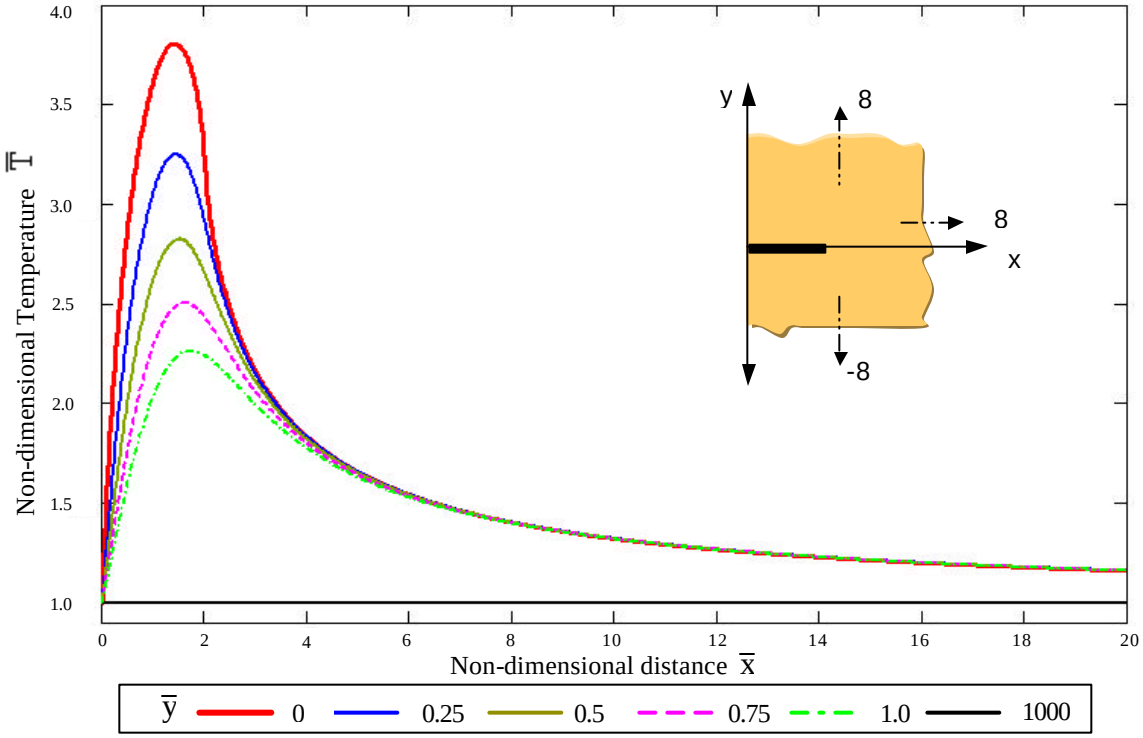

Figure 4.4. Dimensionless temperature distribution, line plate heating source $\overline{\lambda} = 5,\ \overline{a} = 0,\ \overline{b} = 2$

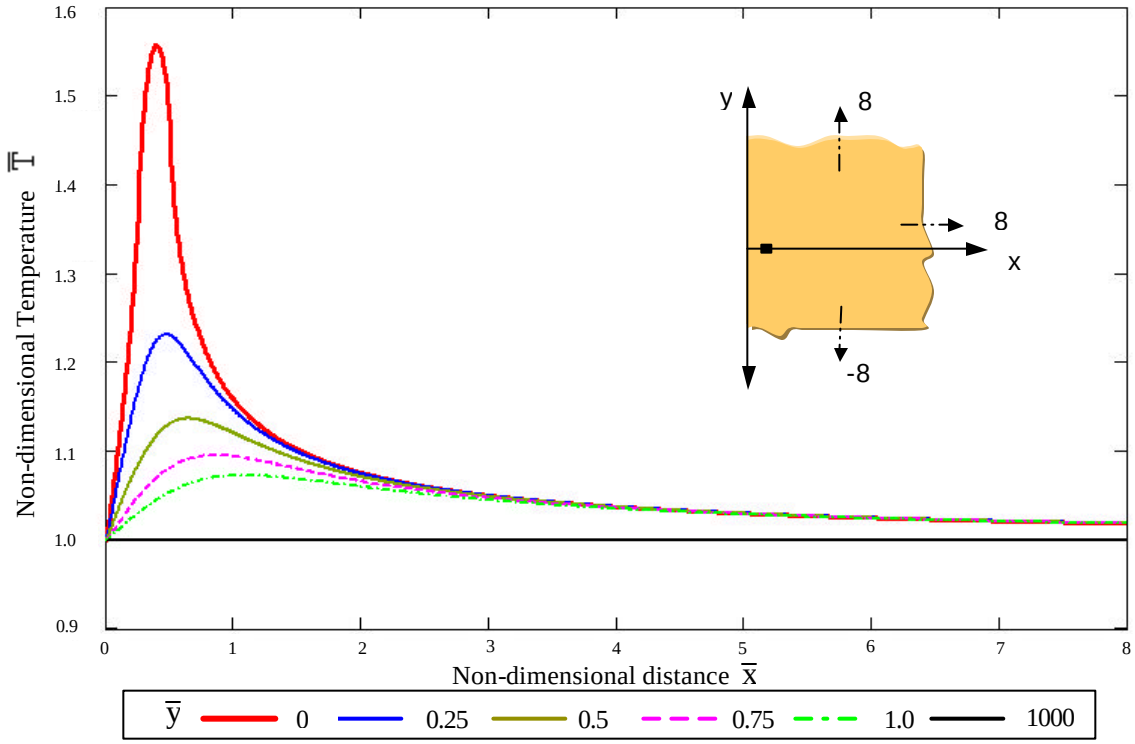

Figure 4.5. Dimensionless temperature distribution, line plate heating source $\overline{\lambda} = 5,\ \overline{a} = 0.25,\ \overline{b} = 0.5$

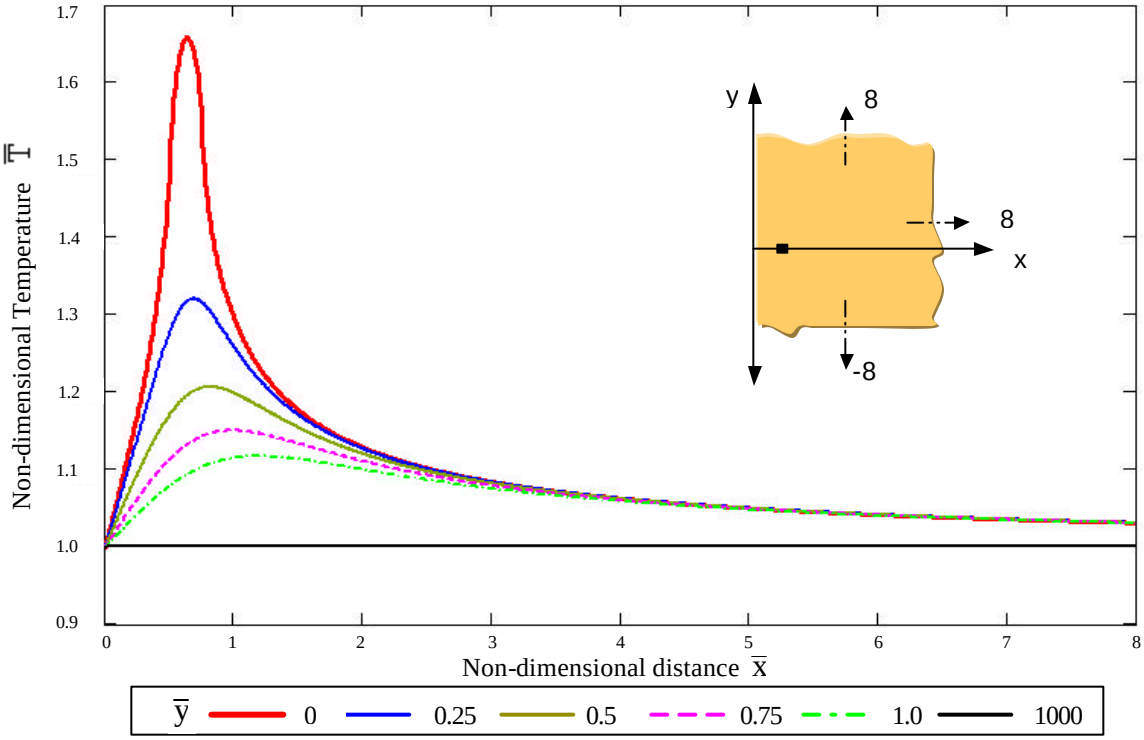

Figure 4.6. Dimensionless temperature distribution, line plate heating source $\overline{\lambda}=5,\ \overline{a}=0.5,\ \overline{b}=0.75$

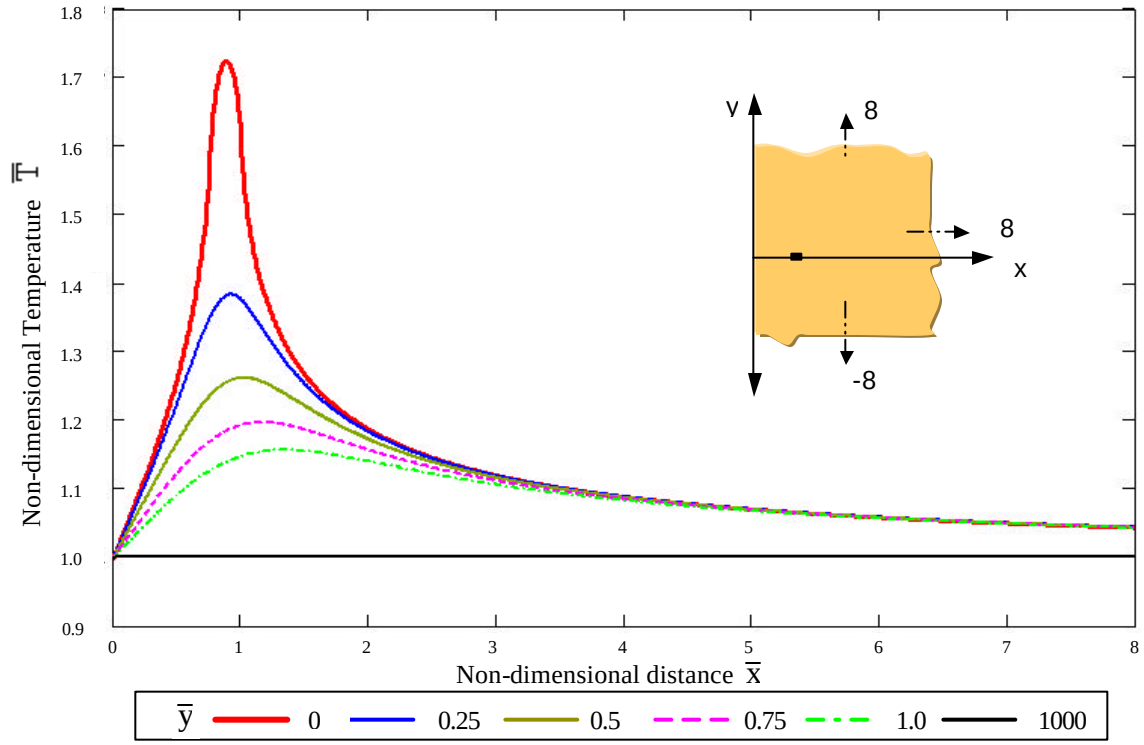

Figure 4.7. Dimensionless temperature distribution, line plate heating source $\overline{\lambda}=5,\ \overline{a}=0.75,\ \overline{b}=1.$

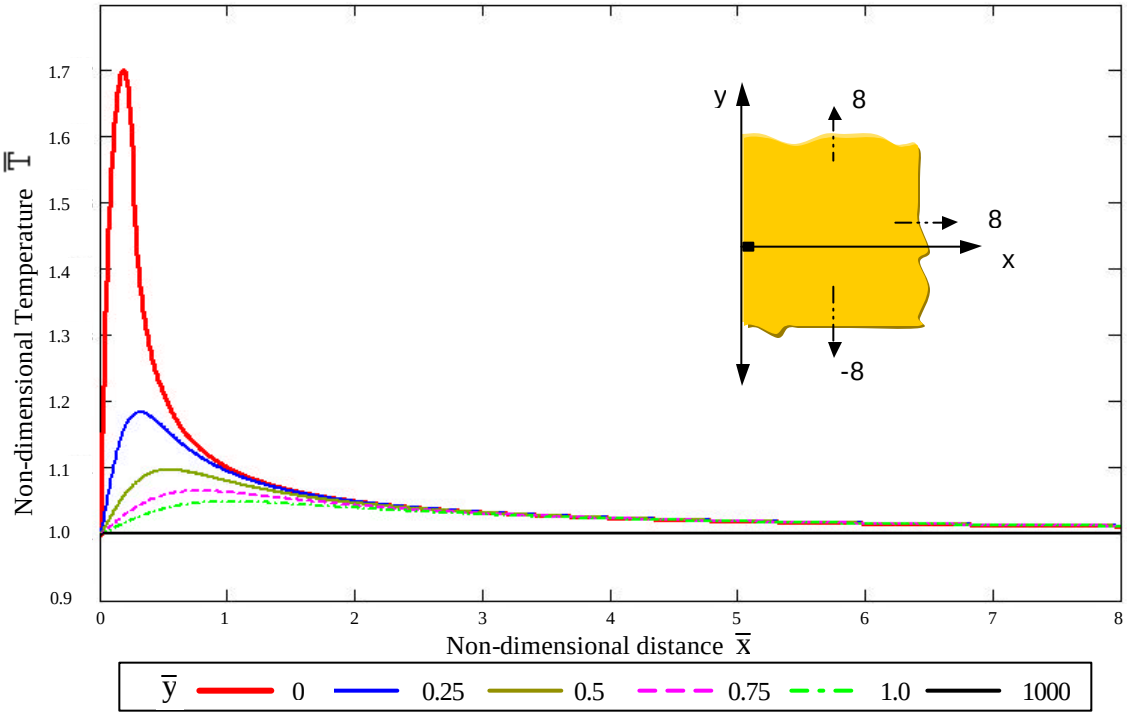

Figure 4.8. Dimensionless temperature distribution, line plate heating source $\overline{\lambda} = 10,\ \overline{a} = 0,\ \overline{b} = 0.25$.

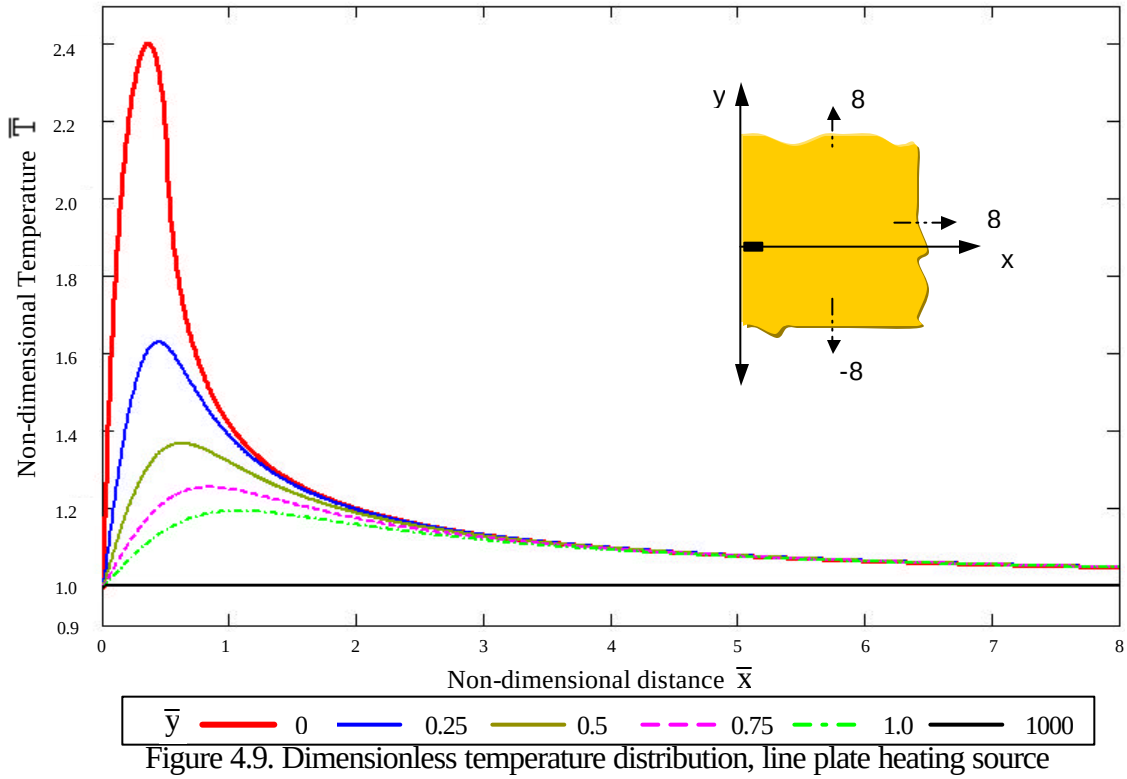

Figure 4.9. Dimensionless temperature distribution, line plate heating source $\overline{\lambda} = 10,\ \overline{a} = 0,\ \overline{b} = 0.50$

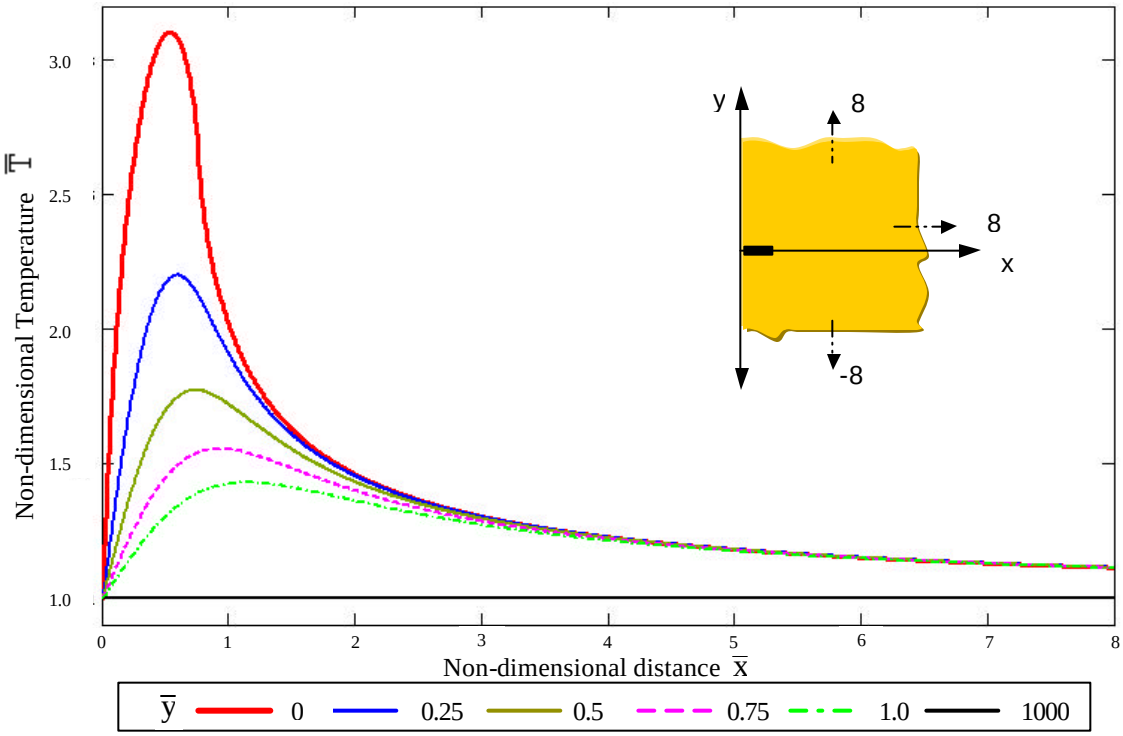

Figure 4.10. Dimensionless temperature distribution, line plate heating source $\overline{\lambda} = 10,\ \overline{a} = 0,\ \overline{b} = 0.75$

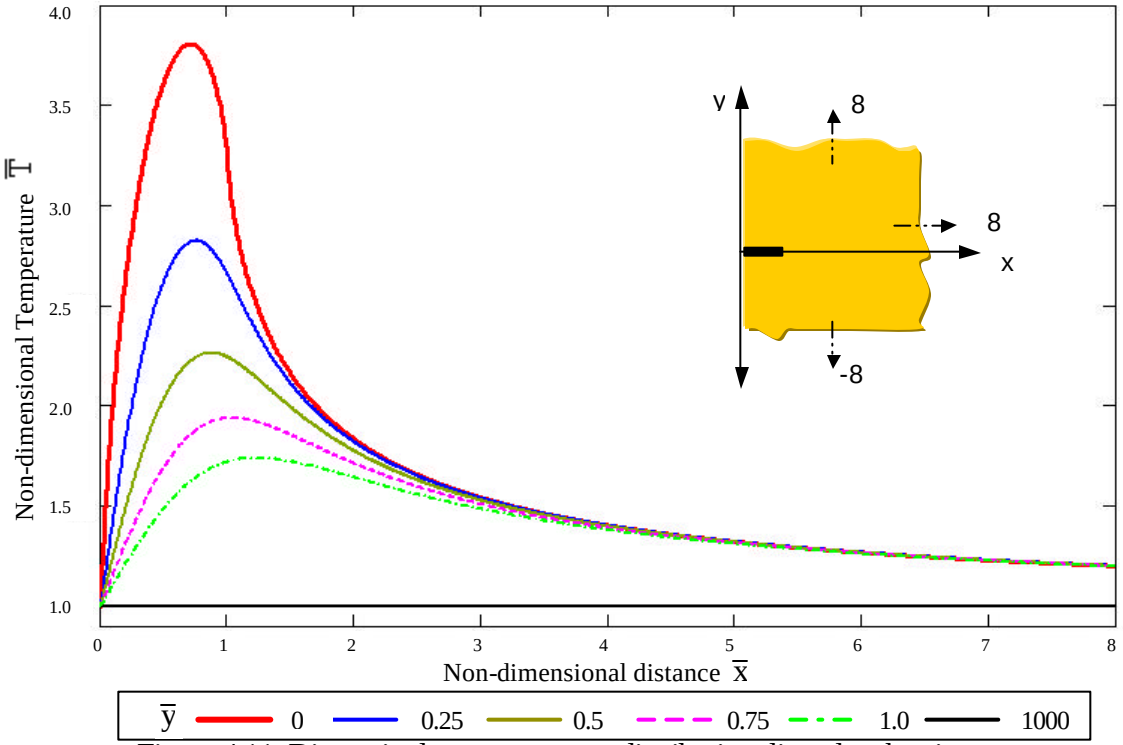

Figure 4.11. Dimensionless temperature distribution, line plate heating source $\overline{\lambda} = 10,\ \overline{a} = 0,\ \overline{b} = 1.0$

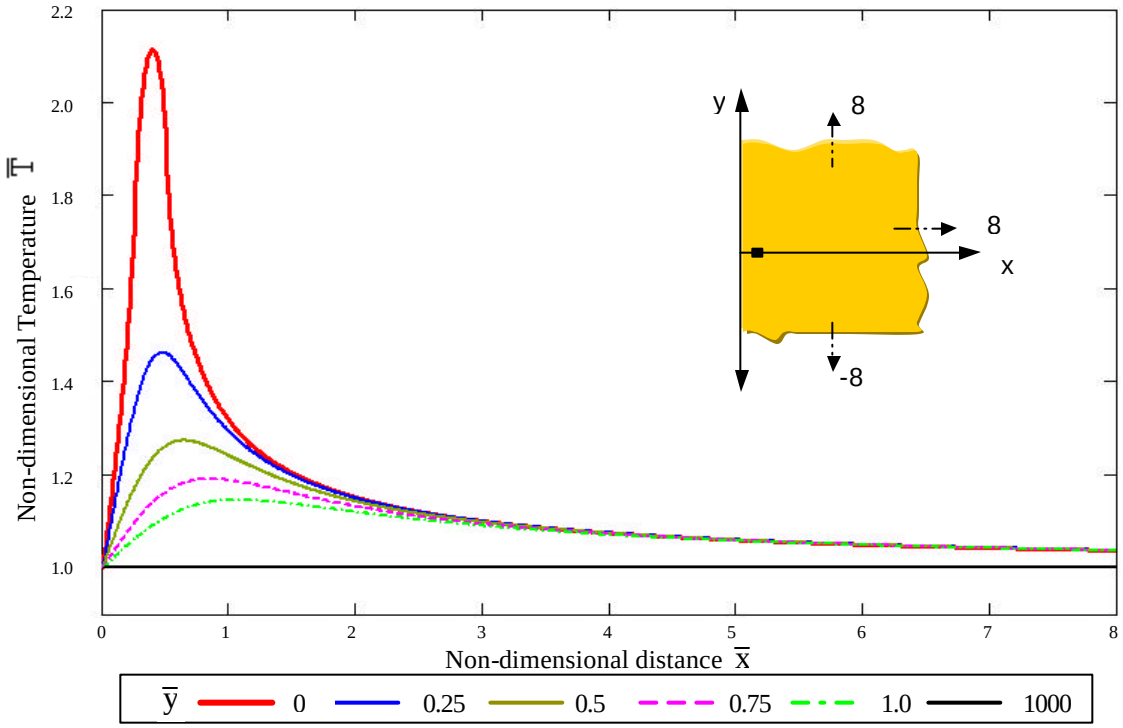

Figure 4.12. Dimensionless temperature distribution, line plate heating source $\overline{\lambda} = 10,\ \overline{a} = 0.25,\ \overline{b} = 0.50$.

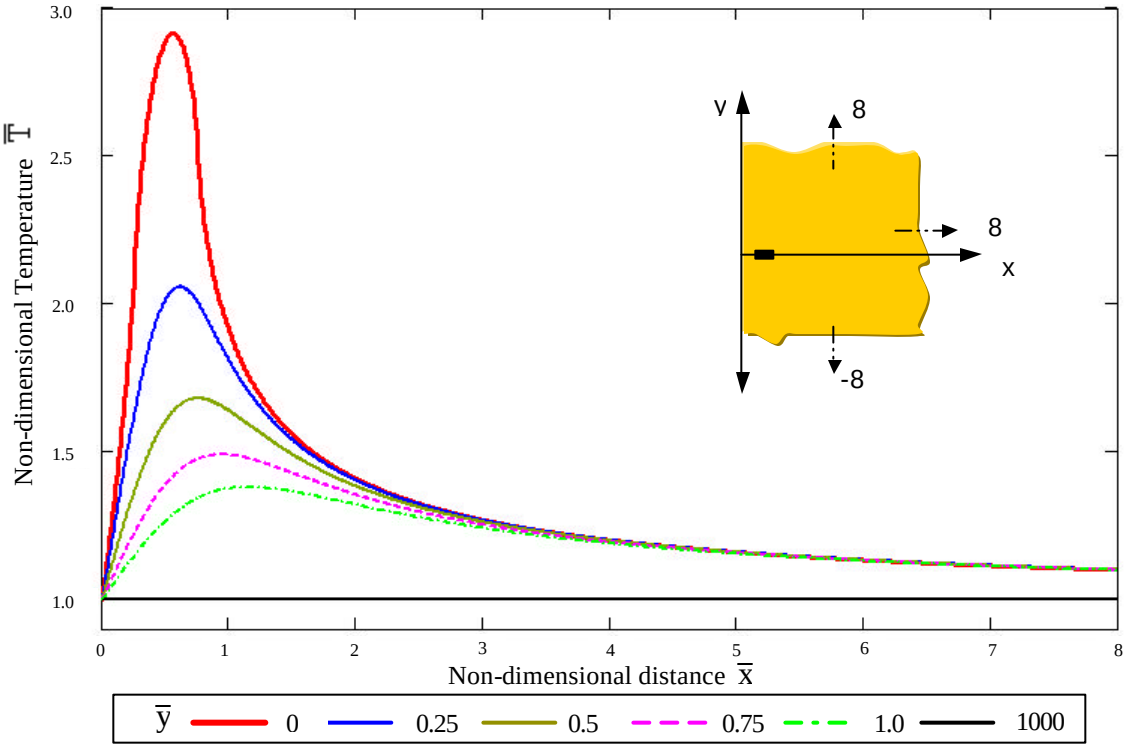

Figure 4.13. Dimensionless temperature distribution, line plate heating source $\overline{\lambda} = 10,\ \overline{a} = 0.25,\ \overline{b} = 0.75$

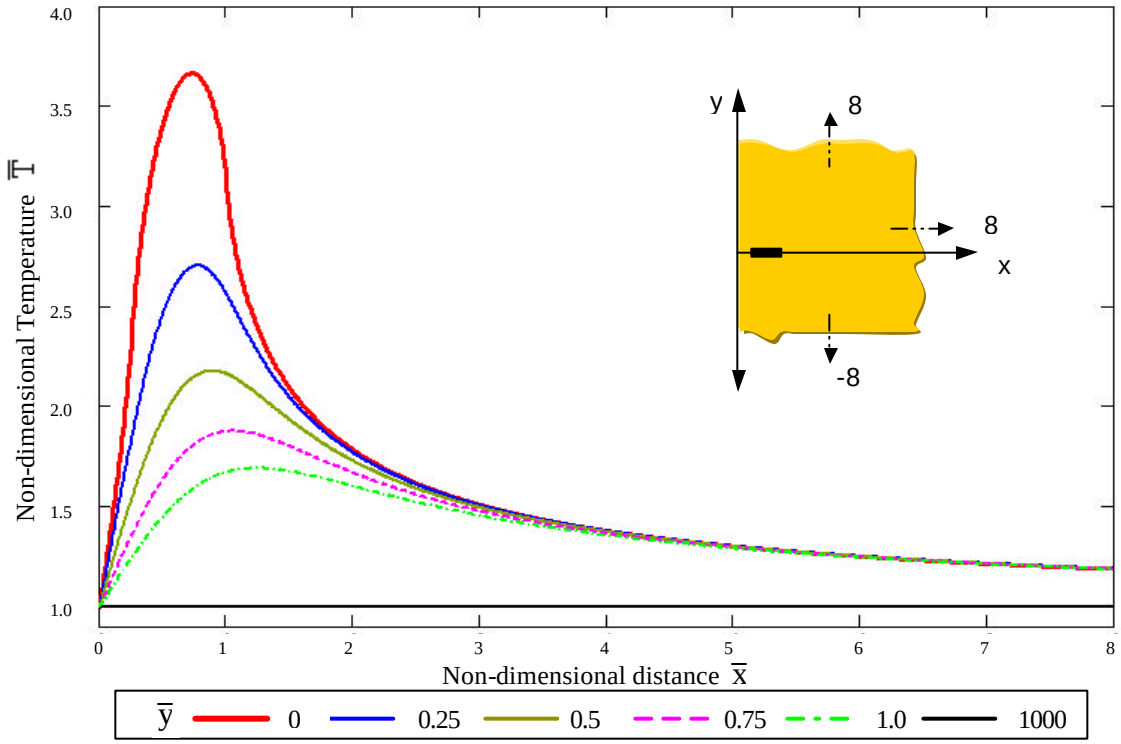

Figure 4.14. Dimensionless temperature distribution, line plate heating source $\overline{\lambda}=10,\ \overline{a}=0.25,\ \overline{b}=1.0$.

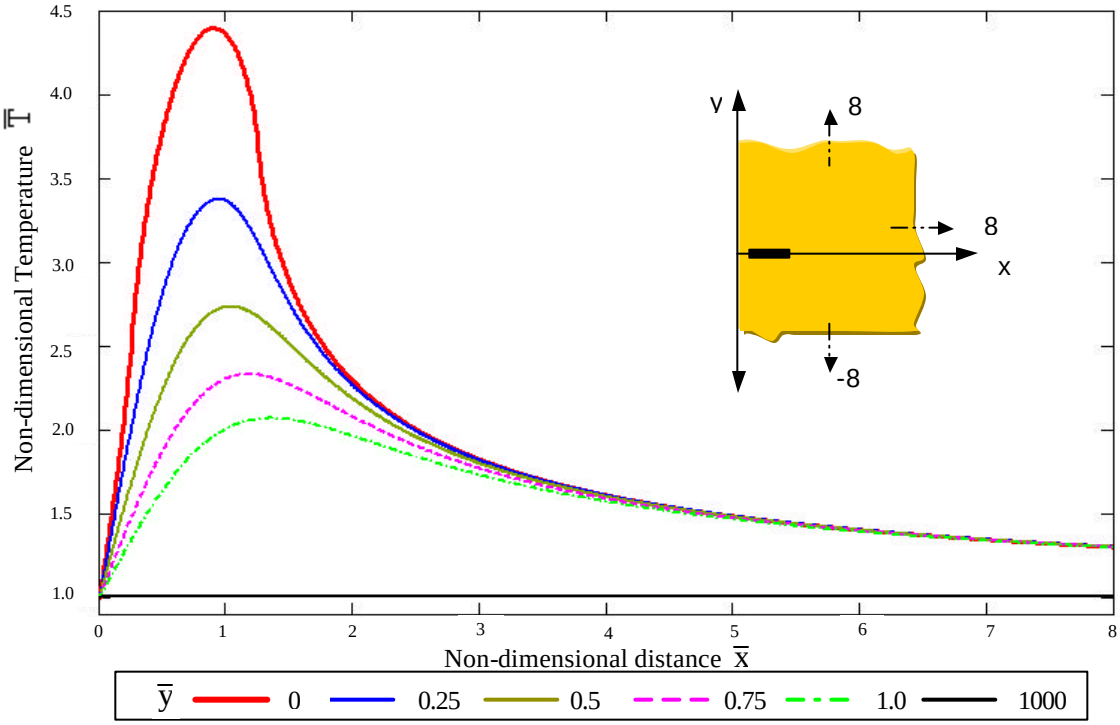

Figure 4.15. Dimensionless temperature distribution, line plate heating source $\overline{\lambda}=10,\ \overline{a}=0.25,\ \overline{b}=1.25$

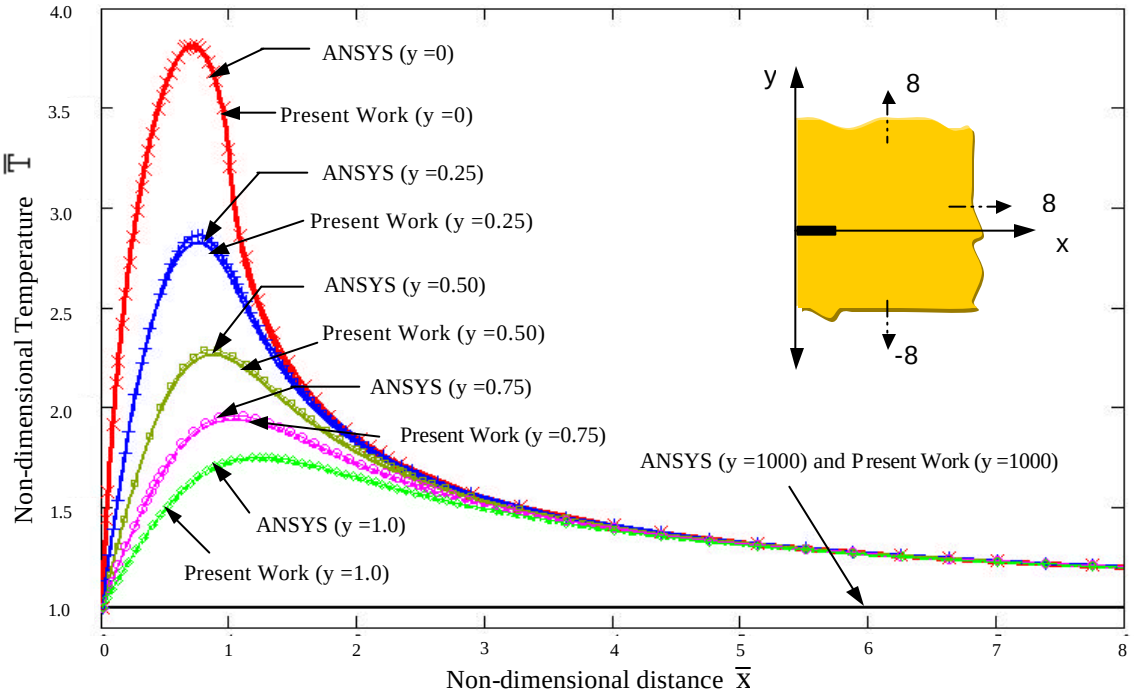

Figure 4.16. Dimensionless temperature distribution, thin plate heating source $\bar{\lambda}=10,\ \bar{a}=0,\ \bar{b}=1.0$. Comparison with results from ANSYS.

Figures 4.2 to 4.4 show the non-dimensional temperature profiles along of axis "$\bar{x}$" at different values of "$\bar{y}$" for $\bar{\lambda}=5$, $\bar{a}=0$, and $\bar{b}=(1, 1.5\ y\ 2.0)$.

For a given $\bar{y}$, the non-dimensional temperature obtains maximum value while passing over the source and then falls off to 1 for large $\bar{x}$.

Similar behavior obtained for a given $\bar{x}$ with varying $\bar{y}$. This result is expected physically. Same is true for values non-dimensional distances of $(\bar{a},\bar{b})=(0.25,0.5),(0.5,0.75),(0.75,1.0)$, as shown in figures 4.5 to 4.7, where the same behavior as the previous curves, displaced according to the new positions of the sources of heat, is observed.

Figures 4.8 to 4.15 show the case for a higher value of the non-dimensional strength of the source ($\bar{\lambda}=10$), for different sizes and different localizations of the source of heat. Observe that the curves present the same behavior as the previous cases.

This problem has also been solved by using the commercial computer software package ANSYS and results were plotted for comparison and validation purposes with the analytical results obtained here for a source of dimensionless strength ($\bar{\lambda}=10$) and $\bar{a}=0;\bar{b}=1.0$. The result in the figure 4.16 shows excellent agreement among the curves. It must be said that, for this case, ANSYS presents problems to simulate the semi-infinite slab, because the numbers of elements exceeds the capacity allowed by the version of this software used in the development of present work, ANSYS university version 6.0.

Figure 4.17. Results from Solution Analytical using TECPLOT 7.5. Dimensionless temperature distribution, thin plate heating source $\bar{\lambda}=10$, $\bar{a}=0$, $\bar{b}=1.0$.

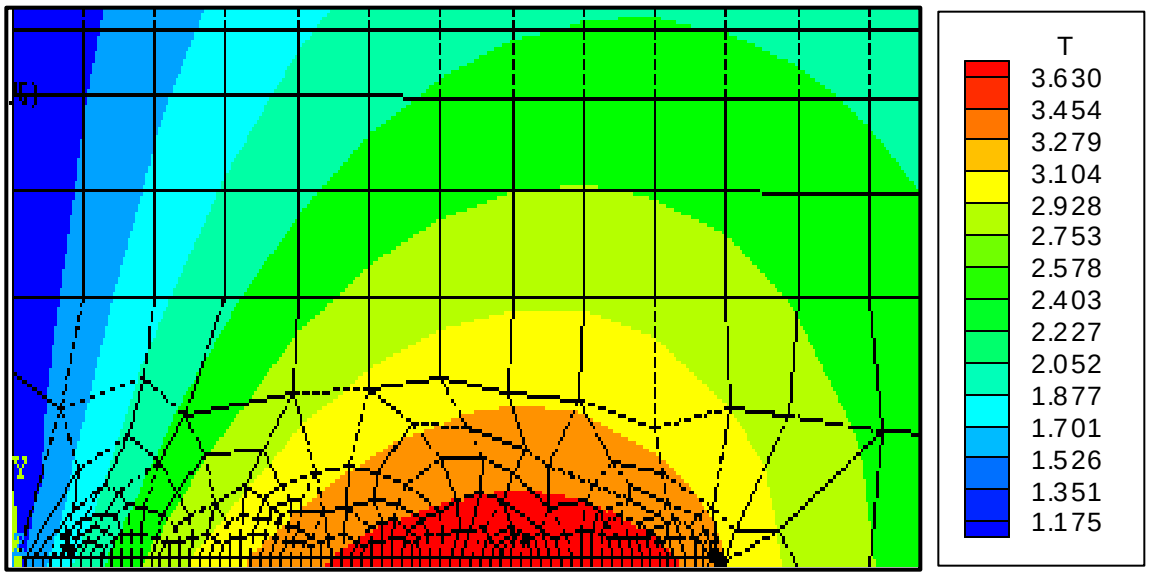

Figure 4.18. Results from ANSYS. Dimensionless temperature distribution, thin plate heating source $\bar{\lambda} = 10,\ \bar{a} = 0,\ \bar{b} = 1.0$.

Figures 4.17 and 4.18 shows the same results in a contour plot. The two figures agree very closely.

Appendix [A] shows ANSYS element and results. We conclude that the present method provides, for this case, an analytical solution and is superior to the numerical solutions in elegance and computational effort. Further, for parameter studies or when temperature is derived only at specific points or when it is required to calculate heat flux at any point, the present solution is ideally suited compared to numerical solutions.

Studies were made to examine results of varying the ratio plate length / length of the "infinite" region. This is a measure of the fineness of the mesh size. The results are show in figures 4.19 and 4.20. When this ratio is less that 1/1000 the agreement between numerical and exact results are not good. Above this value the non-convergence shows near to the source. Appendix [B] shows ANSYS results with different ratio plate length / length of the "infinite" region.

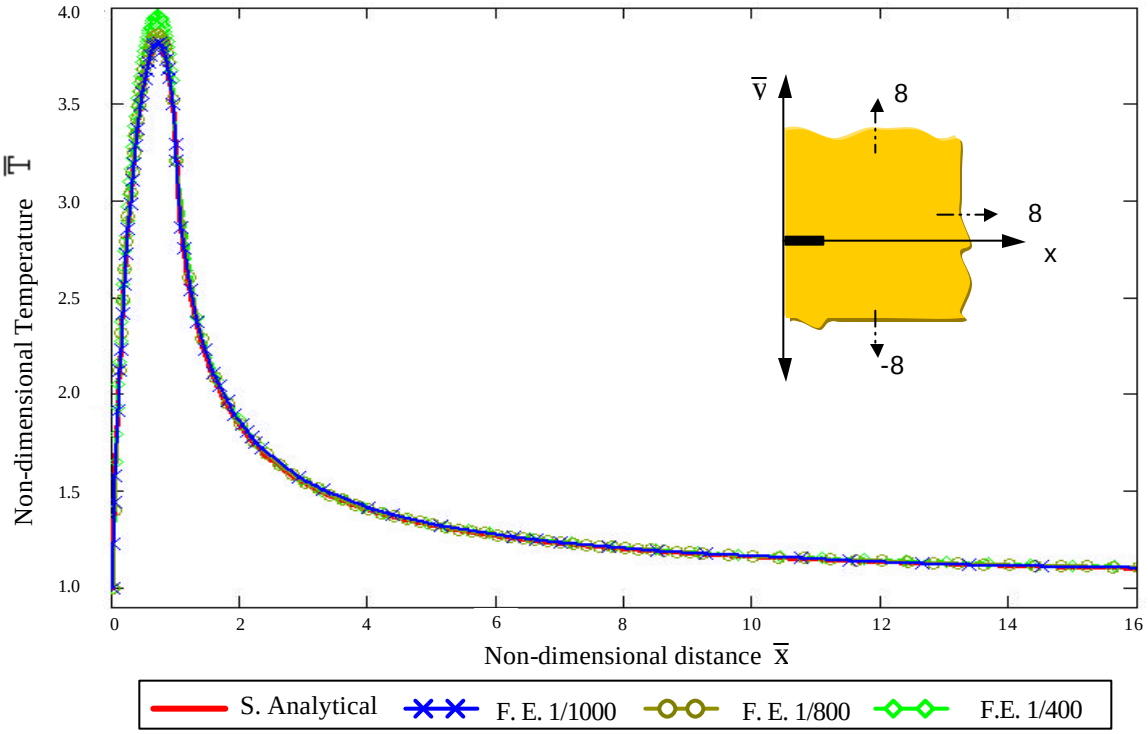

Figure 4.19. Dimensionless temperature distribution with different ratio plate length / length of the "infinite" region, line plate heating source. $\overline{\lambda}=10,\ \overline{a}=0,\ \overline{b}=1.0$.

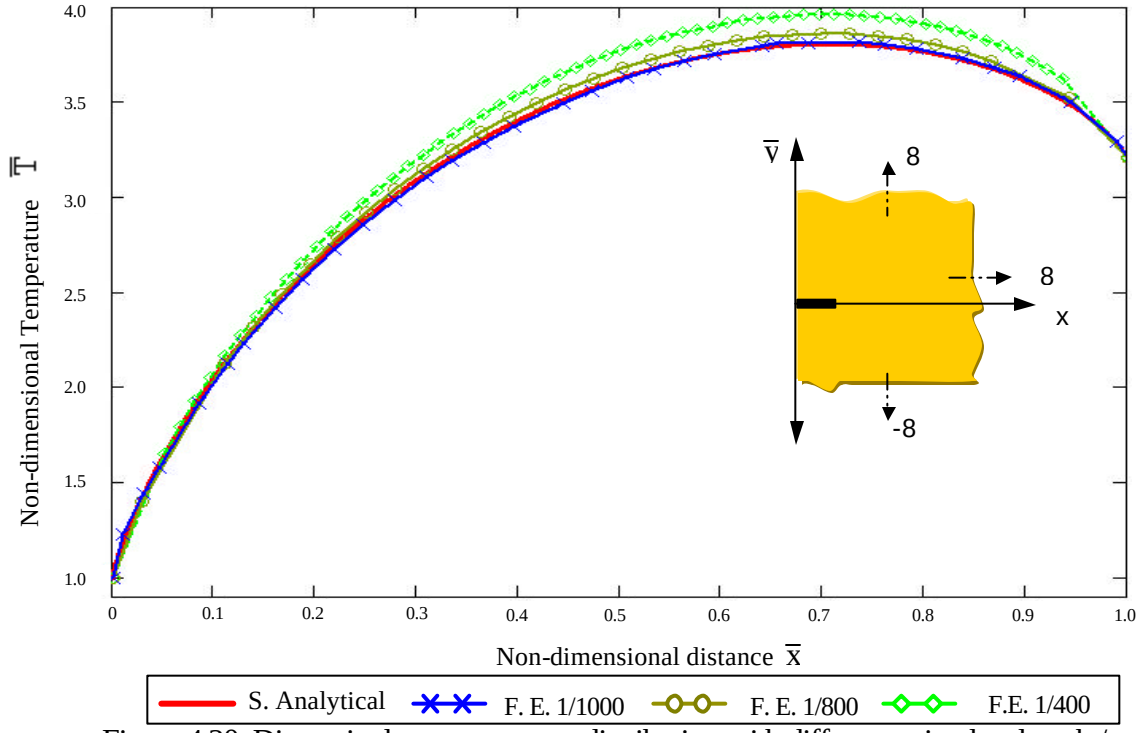

Figure 4.20. Dimensionless temperature distribution with different ratio plate length / length of the "infinite" region, line plate heating source. $\overline{\lambda}=10,\ \overline{a}=0,\ \overline{b}=1.0$.

4.1.2 Semi-Infinite Slab with a Hollow Box- Heating Source

A thin current carrying wire bent in the form of a square forming a hollow box-heating source is embedded, as a heat-generating element, in a semi-infinite two dimensional slab $x > 0$, $-\infty < y < \infty$, $-\infty < z < \infty$, and constant thermal conductivity k. The heating element can be assumed as a hollow box heat source with walls infinitesimally thin; with large depth ℓ and side L. The heat generation per unit length along the source per unit depth is constant and the boundary $x = 0$ is maintained at constant temperature T_B as shown in figure 4.21 (a).

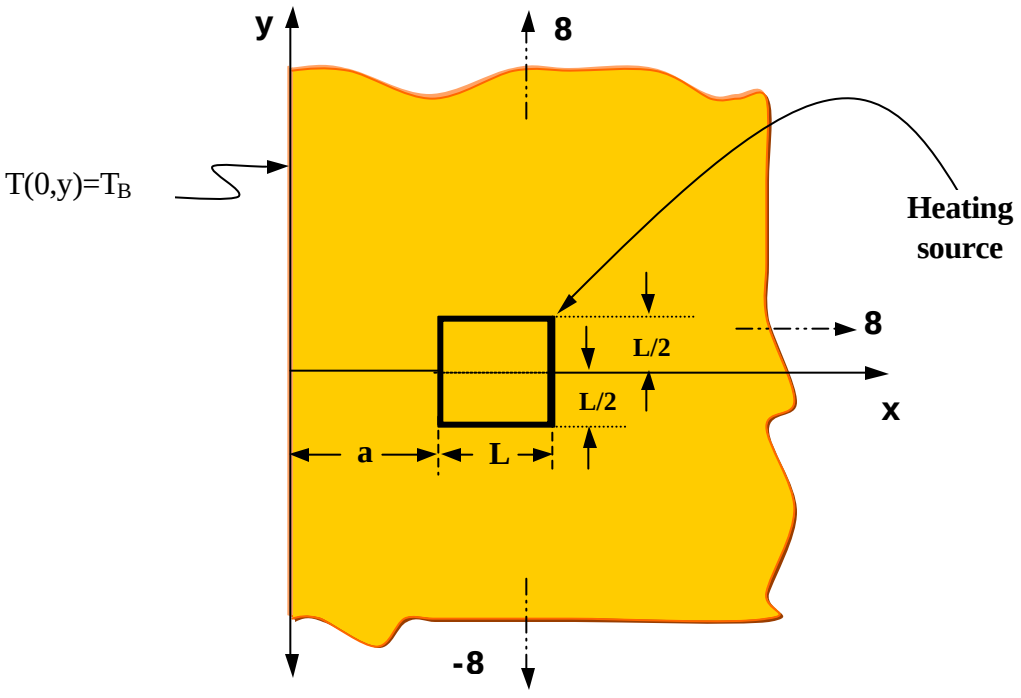

Figure 4.21 (a). Semi-infinite slab with a square hollow box-heating source

Let:

$Q_T \equiv$ Total heat generation (W) = $4.\lambda \cdot \ell \cdot L$

$\lambda \equiv$ Strength of the heat source per unit depth per unit length (W/m^2)

$Q(x,y) \equiv$ Heat generation intensity per unit volume (W/m^3).

Q(x,y) when integrated over the whole volume must be equal to the total heat generation inside the semi-infinite slab, i.e. $\iiint_V Q(x,y).dx.dy.dz = Q_T$

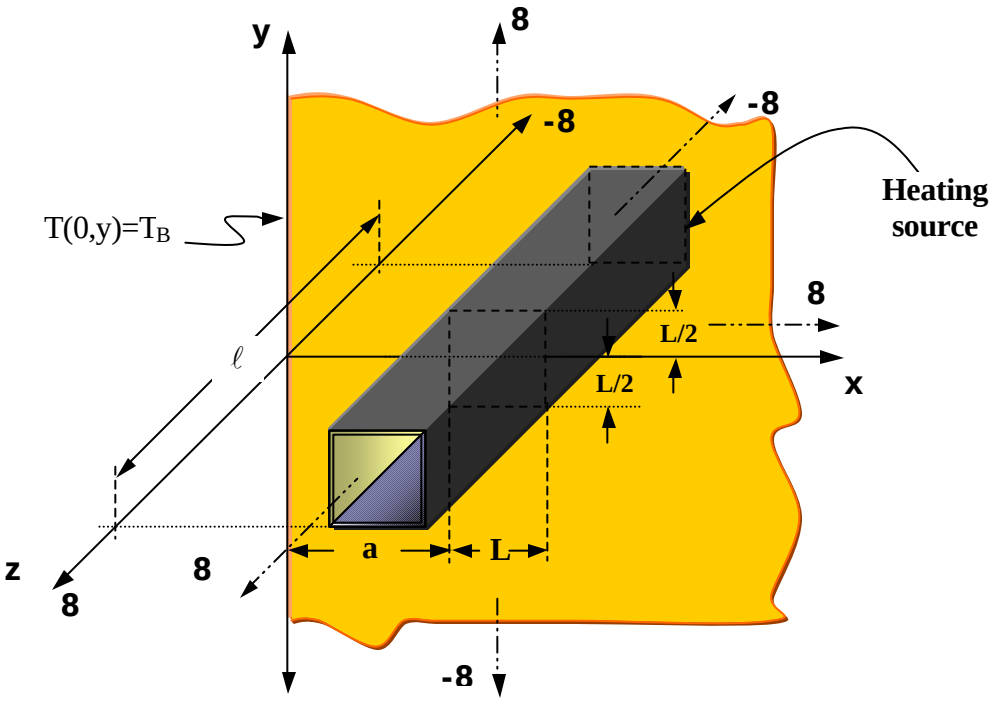

Figure 4.21 (b). Semi-infinite slab with a square hollow box-heating source

For cartesian coordinates this condition becomes:

$$\int_{-\frac{\ell}{2}}^{\frac{\ell}{2}}\int_{-\infty}^{\infty}\int_{0}^{\infty} Q(x,y).dx.dy.dz = Q_T = \lambda.\ell.(L+L+L+L) = 4.\lambda.\ell.L \ldots\ldots\ldots\ldots\ldots\ldots\ldots\ldots\ldots\ldots (4.9)$$

Similarly to the previous case, an expression was derived for the generation of heat for unit of volume using the same principle, but with the assumption that the hollow box this formed by 4 plates infinitesimally thin. They were calculated in an independent way adding the results, obtaining the following expression for the heat generation Q(x,y):

$$Q(x,y) = \begin{Bmatrix} \lambda\cdot\delta(y+L/2)\cdot\{H[x-a]-H[x-(L+a)]\}+ \\ \lambda\cdot\delta(x-(L+a))\cdot\{H[y+L/2]-H[y-L/2]\}+ \\ \lambda\cdot\delta(y-L/2)\cdot\{H[x-a]-H[x-(L+a)]\}+ \\ \lambda\cdot\delta(x-a)\cdot\{H[y+L/2]-H[y-L/2]\} \end{Bmatrix} \ldots\ldots\ldots\ldots\ldots\ldots\ldots\ldots (4.10)$$

The equation (4.10) satisfy to equation (4.9), Now integrate the right hand side of expression (4.10) as indicated in equation (4.9):

$$\int_{-\frac{\ell}{2}}^{\frac{\ell}{2}}\int_{-\infty}^{\infty}\int_{0}^{\infty} \begin{Bmatrix} \lambda\cdot\delta(y+L/2)\cdot\{H[x-a]-H[x-(L+a)]\}+ \\ \lambda\cdot\delta(x-(L+a))\cdot\{H[y+L/2]-H[y-L/2]\}+ \\ \lambda\cdot\delta(y-L/2)\cdot\{H[x-a]-H[x-(L+a)]\}+ \\ \lambda\cdot\delta(x-a)\cdot\{H[y+L/2]-H[y-L/2]\} \end{Bmatrix} .dx.dy.dz =$$

$$\lambda\int_{-\frac{\ell}{2}}^{\frac{\ell}{2}} dz.\int_{-\infty}^{\infty}\delta(y+L/2).dy\cdot\int_{0}^{\infty}\{H[x-a]-H[x-(L+a)]\}.dx + \lambda\int_{-\frac{\ell}{2}}^{\frac{\ell}{2}} dz.\int_{0}^{\infty}\delta(x-(L+a)).dx\cdot\int_{-\infty}^{\infty}\{H[y+L/2]-H[y-L/2]\}.dy +$$

$$\lambda\int_{-\frac{\ell}{2}}^{\frac{\ell}{2}} dz.\int_{-\infty}^{\infty}\delta(y-L/2).dy\cdot\int_{0}^{\infty}\{H[x-a]-H[x-(L+a)]\}.dx + \lambda\int_{-\frac{\ell}{2}}^{\frac{\ell}{2}} dz.\int_{0}^{\infty}\delta(x-a).dx\cdot\int_{-\infty}^{\infty}\{H[y+L/2]-H[y-L/2]\}.dy$$

Using the properties for Dirac-Delta and Heaviside function is obtained:

$$\lambda\cdot\ell\cdot 1.\int_{a}^{L+a} dx+\lambda\cdot\ell\cdot 1.\int_{-L/2}^{L/2} dy+\lambda\cdot\ell\cdot 1.\int_{a}^{L+a} dx+\lambda\cdot\ell\cdot 1.\int_{-L/2}^{L/2} dy=\begin{Bmatrix}\lambda\cdot\ell\cdot L+\lambda\cdot\ell\cdot L+\\ \lambda\cdot\ell\cdot L+\lambda\cdot\ell\cdot L\end{Bmatrix}$$

Equation (4.9) after integration becomes:

$$\iiint_{V} Q(x,y)=Q_T=4.\lambda\cdot\ell\cdot L$$

Substitute equations (3.31) and (4.10) in equation (4.4):

$$T(x,y)=T_B+\frac{\lambda}{4\pi k\ell}\int_{-\frac{\ell}{2}}^{\frac{\ell}{2}}\int_{-\infty}^{\infty}\int_{0}^{\infty}\begin{Bmatrix}\delta(y'+L/2)\cdot\{H[x-a]-H[x-(L+a)]\}.\ln\left\{\frac{(x+x')^2+(y+L/2)^2}{(x-x')^2+(y+L/2)^2}\right\}+\\ \delta(x'-(L+a))\cdot\{H[y+L/2]-H[y-L/2]\}.\ln\left\{\frac{(x+(L+a))^2+(y-y')^2}{(x-L+a))^2+(y-y')^2}\right\}+\\ \delta(y'-L/2)\cdot\{H[x-a]-H[x-(L+a)]\}.\ln\left\{\frac{(x+x')^2+(y-L/2)^2}{(x-x')^2+(y-L/2)^2}\right\}+\\ \delta(x'-a)\cdot\{H[y+L/2]-H[y-L/2]\}.\ln\left\{\frac{(x+a)^2+(y-y')^2}{(x-a)^2+(y-y')^2}\right\}\end{Bmatrix}.dx'dy'dz'$$

Integration on z is easily performed, then applying again the properties for Dirac Delta and Heaviside functions for x and y, we get:

$$T(x,y)=T_B+\frac{\lambda}{4\pi k}\begin{Bmatrix}\int_{a}^{L+a}\left\{\ln\left\{\frac{(x+x')^2+(y+L/2)^2}{(x-x')^2+(y+L/2)^2}\right\}+\ln\left\{\frac{(x+x')^2+(y-L/2)^2}{(x-x')^2+(y-L/2)^2}\right\}\right\}dx'+\\ \int_{-L/2}^{L/2}\left\{\ln\left\{\frac{(x+a)^2+(y-y')^2}{(x-a)^2+(y-y')^2}\right\}+\ln\left\{\frac{(x+(L+a))^2+(y-y')^2}{(x-(L+a))^2+(y-y')^2}\right\}\right\}dy'\end{Bmatrix}$$

In order to express results in non-dimensional form, the following non-dimensional quantities are defined:

$\overline{T}(\overline{x},\overline{y}) = \dfrac{T(x,y)}{T_B}$ Non-dimensional temperature

$\overline{\lambda} = \dfrac{\lambda.L}{kT_B}$ Non-dimensional heat generation

$\overline{x} = \dfrac{x}{L}, \ \overline{y} = \dfrac{y}{L}$ Non-dimensional field point location

$\overline{x}' = \dfrac{x'}{L}, \ \overline{y}' = \dfrac{y'}{L}$ Non-dimensional source point location

$\overline{a} = \dfrac{a}{L}$ Non-dimensional distances

Finally, substitute all these quantities in the previous equation and the following relationship is obtained:

$$\overline{T}(\overline{x},\overline{y}) = 1 + \frac{\overline{\lambda}}{4.\pi}\left\{\begin{array}{l}\displaystyle\int_{\overline{a}}^{1+\overline{a}}\left\{\ln\left\{\frac{(\overline{x}+\overline{x}')^2+(\overline{y}+1/2)^2}{(\overline{x}-\overline{x}')^2+(\overline{y}+1/2)^2}\right\}+\ln\left\{\frac{(\overline{x}+\overline{x}')^2+(\overline{y}-1/2)^2}{(\overline{x}-\overline{x}')^2+(\overline{y}-1/2)^2}\right\}\right\}d\overline{x}'+ \\ \displaystyle\int_{-1/2}^{1/2}\left\{\ln\left\{\frac{(\overline{x}+\overline{a})^2+(\overline{y}-\overline{y}')^2}{(\overline{x}-\overline{a})^2+(\overline{y}-\overline{y}')^2}\right\}+\ln\left\{\frac{(\overline{x}+(1+\overline{a}))^2+(\overline{y}-\overline{y}')^2}{(\overline{x}-(1+\overline{a}))^2+(\overline{y}-\overline{y}')^2}\right\}\right\}d\overline{y}'\end{array}\right\}$$

$$\overline{T}(\overline{x},\overline{y}) = 1+\frac{\overline{\lambda}}{4.\pi}\left[\begin{array}{l}
(\overline{x}+(1+\overline{a})).\left\{\begin{array}{l}\ln\left[\left[(\overline{x}+1+\overline{a})^2+(\overline{y}+0.5)^2\right],\left[(\overline{x}+1+\overline{a})^2+(\overline{y}-0.5)^2\right]\right]-\\ 2.\mathrm{Arctg}\left(\dfrac{\overline{y}-0.5}{\overline{x}+1+\overline{a}}\right)+2.\mathrm{Arctg}\left(\dfrac{\overline{y}+0.5}{\overline{x}+1+\overline{a}}\right)\end{array}\right\}-\\
(\overline{x}+\overline{a}).\left\{\begin{array}{l}\ln\left[\left[(\overline{x}+\overline{a})^2+(\overline{y}+0.5)^2\right],\left[(\overline{x}+\overline{a})^2+(\overline{y}-0.5)^2\right]\right]+\\ 2.\mathrm{Arctg}\left(\dfrac{\overline{y}-0.5}{\overline{x}+\overline{a}}\right)-2.\mathrm{Arctg}\left(\dfrac{\overline{y}+0.5}{\overline{x}+\overline{a}}\right)\end{array}\right\}+\\
(\overline{x}-1-\overline{a}).\left\{\begin{array}{l}\ln\left[\left[(\overline{x}-1-\overline{a})^2+(\overline{y}+0.5)^2\right],\left[(\overline{x}-1-\overline{a})^2+(\overline{y}-0.5)^2\right]\right]+\\ 2.\mathrm{Arctg}\left(\dfrac{\overline{y}-0.5}{\overline{x}-1-\overline{a}}\right)-2.\mathrm{Arctg}\left(\dfrac{\overline{y}+0.5}{\overline{x}-1-\overline{a}}\right)\end{array}\right\}-\\
(\overline{x}-\overline{a}).\left\{\begin{array}{l}\ln\left[\left[(\overline{x}-\overline{a})^2+(\overline{y}+0.5)^2\right],\left[(\overline{x}-\overline{a})^2+(\overline{y}-0.5)^2\right]\right]-\\ 2.\mathrm{Arctg}\left(\dfrac{\overline{y}-0.5}{\overline{x}-\overline{a}}\right)+2.\mathrm{Arctg}\left(\dfrac{\overline{y}+0.5}{\overline{x}-\overline{a}}\right)\end{array}\right\}+\\
(\overline{y}-0.5).\left\{\begin{array}{l}\ln\left[\dfrac{\left[(\overline{y}-0.5)^2+(\overline{x}-1-\overline{a})^2\right],\left[(\overline{y}-0.5)^2+(\overline{x}-\overline{a})^2\right]}{\left[(\overline{y}-0.5)^2+(\overline{x}+1+\overline{a})^2\right],\left[(\overline{y}-0.5)^2+(\overline{x}+\overline{a})^2\right]}\right]+\\ 2.\mathrm{Arctg}\left(\dfrac{\overline{x}+1+\overline{a}}{\overline{y}-0.5}\right)-2.\mathrm{Arctg}\left(\dfrac{\overline{x}+\overline{a}}{\overline{y}-0.5}\right)+\\ 2.\mathrm{Arctg}\left(\dfrac{\overline{x}-1-\overline{a}}{\overline{y}-0.5}\right)-2.\mathrm{Arctg}\left(\dfrac{\overline{x}-\overline{a}}{\overline{y}-0.5}\right)\end{array}\right\}+\\
(\overline{y}+0.5).\left\{\begin{array}{l}\ln\left[\dfrac{\left[(\overline{y}+0.5)^2+(\overline{x}+1+\overline{a})^2\right],\left[(\overline{y}+0.5)^2+(\overline{x}+\overline{a})^2\right]}{\left[(\overline{y}+0.5)^2+(\overline{x}-1-\overline{a})^2\right],\left[(\overline{y}+0.5)^2+(\overline{x}-\overline{a})^2\right]}\right]+\\ 2.\mathrm{Arctg}\left(\dfrac{\overline{x}+1+\overline{a}}{\overline{y}+0.5}\right)-2.\mathrm{Arctg}\left(\dfrac{\overline{x}+\overline{a}}{\overline{y}+0.5}\right)+\\ 2.\mathrm{Arctg}\left(\dfrac{\overline{x}-1-\overline{a}}{\overline{y}+0.5}\right)-2.\mathrm{Arctg}\left(\dfrac{\overline{x}-\overline{a}}{\overline{y}+0.5}\right)\end{array}\right\}
\end{array}\right] \quad \ldots \quad (4.11)$$

Equation 4.11 is the temperature profile for a semi-infinite slab with constant temperature on boundary heated by a wire in the form of a square hollow box carrying a current and embedded in the slab. Thus an “analytical solution” for the temperature distribution has been obtained.

Equation 4.11 is algebraic expression, which can be easily evaluated. Some of the results for different values of $\overline{\lambda}$ and $\overline{a}$ are presented in the figures 4.22 to 4.30.

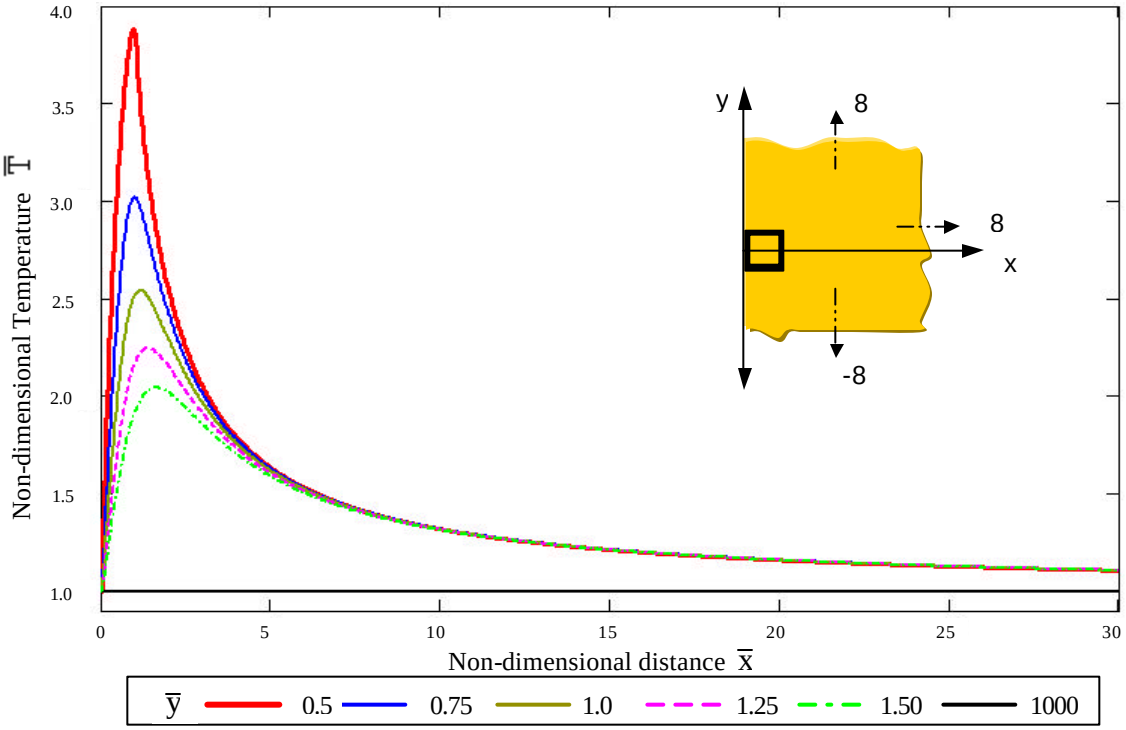

Figure 4.22. Dimensionless temperature distribution, hollow box-heating source $\overline{\lambda} = 5,\ \overline{a} = 0$.

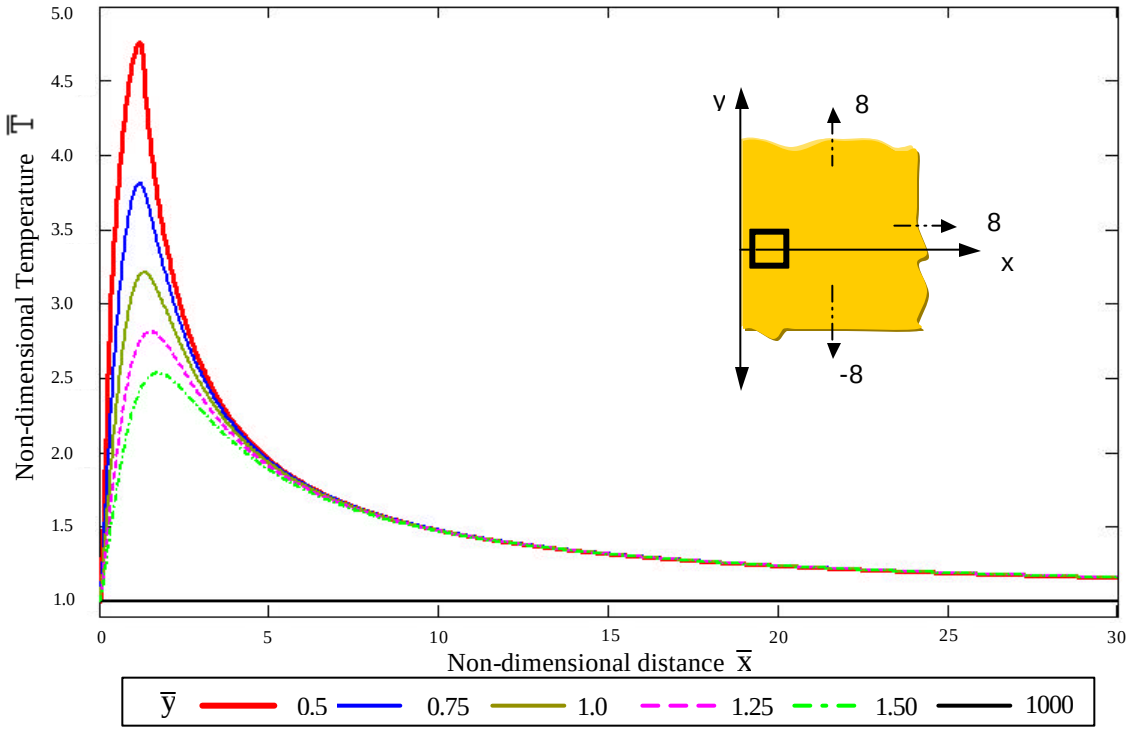

Figure 4.23. Dimensionless temperature distribution, hollow box-heating source $\overline{\lambda} = 5,\ \overline{a} = 0.25$

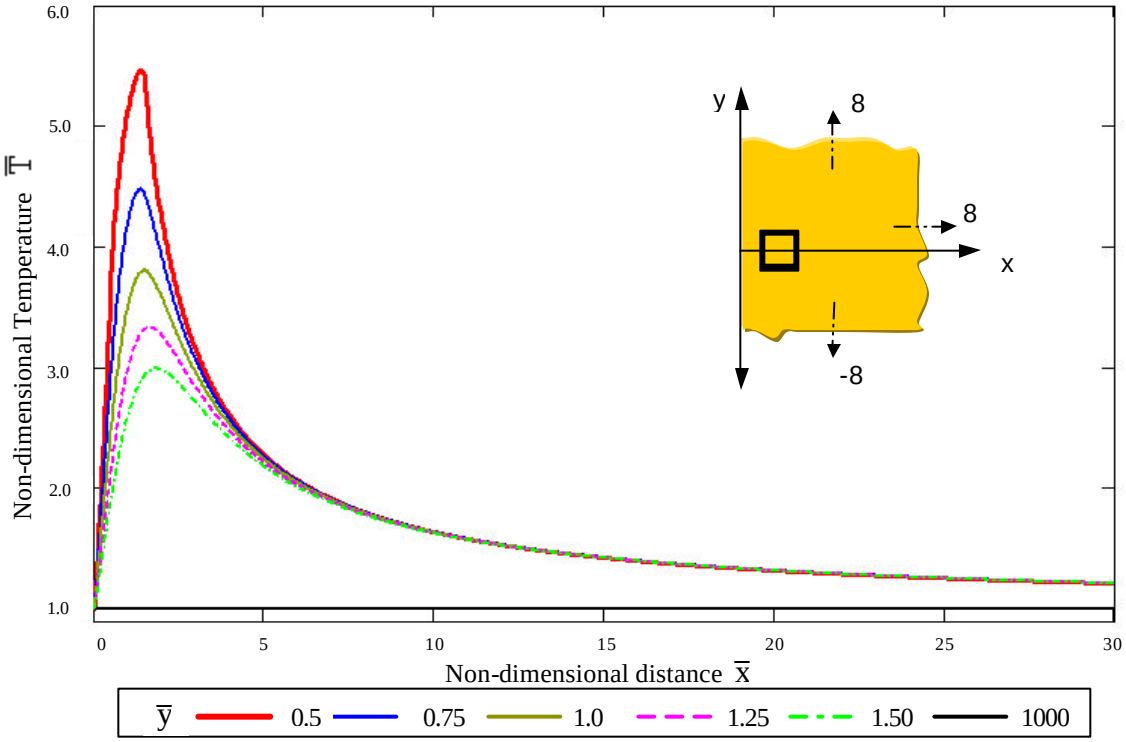

Figure 4.24. Dimensionless temperature distribution, hollow box-heating source $\overline{\lambda} = 5,\ \overline{a} = 0.5$.

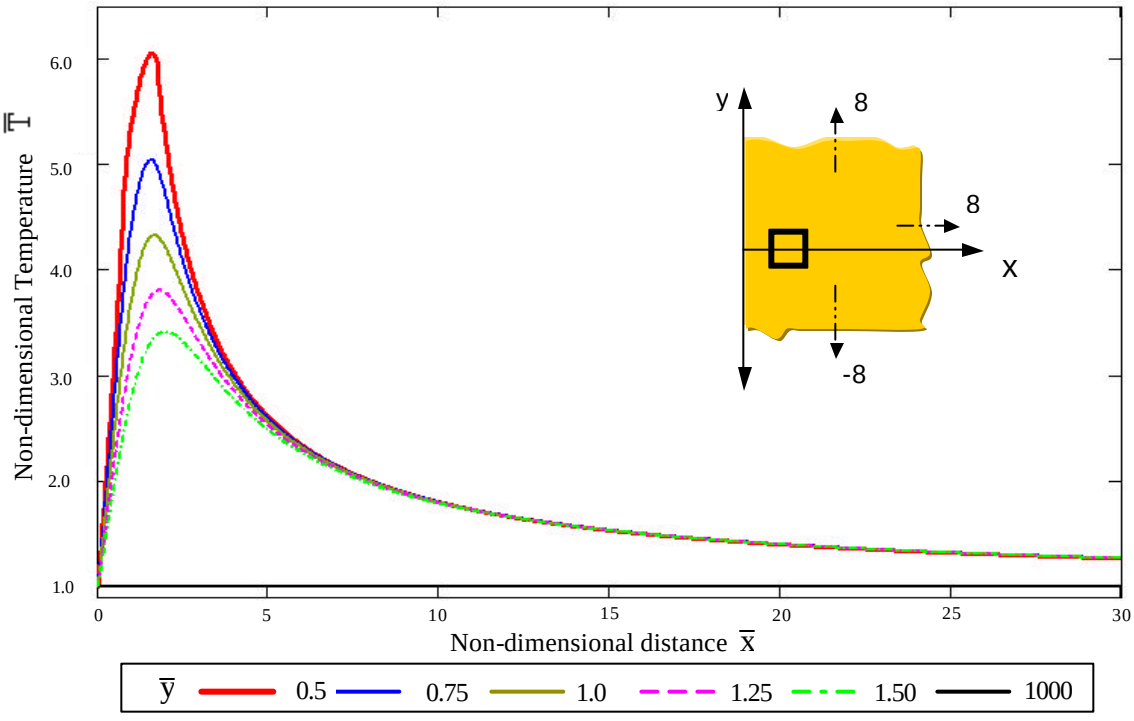

Figure 4.25. Dimensionless temperature distribution, hollow box-heating source $\overline{\lambda} = 5,\ \overline{a} = 0.75$

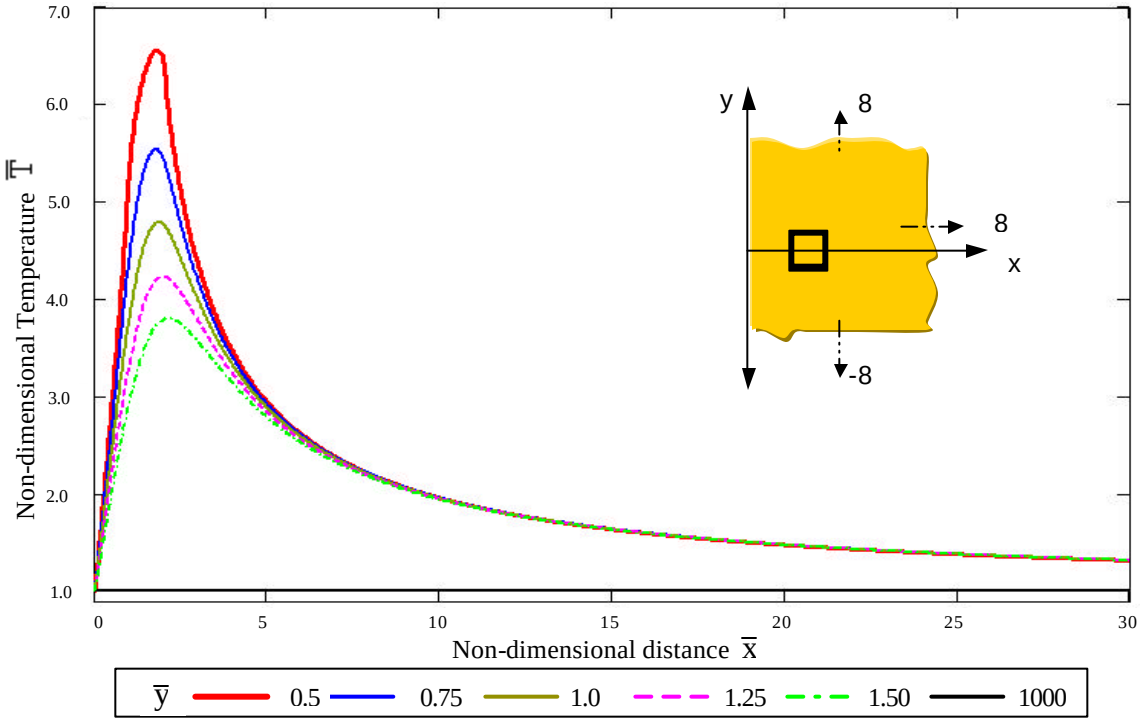

Figure 4.26. Dimensionless temperature distribution, hollow box-heating source $\overline{\lambda}=5,\ \overline{a}=1$.

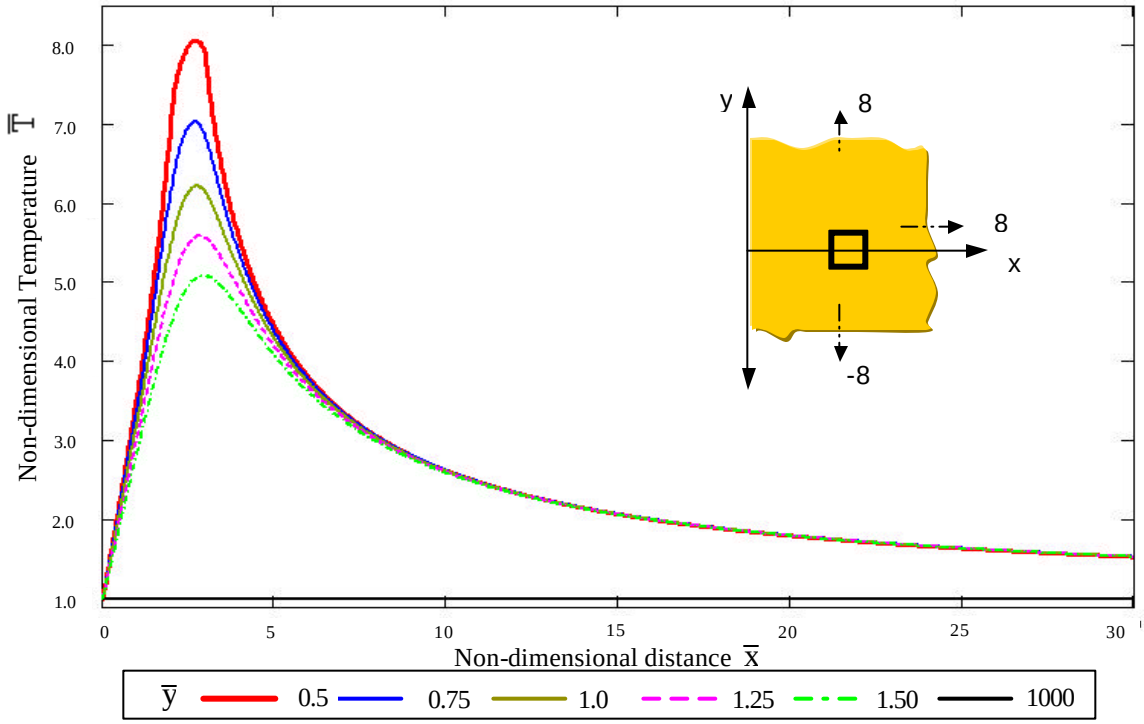

Figure 4.27. Dimensionless temperature distribution, hollow box-heating source $\overline{\lambda}=5,\ \overline{a}=2$.

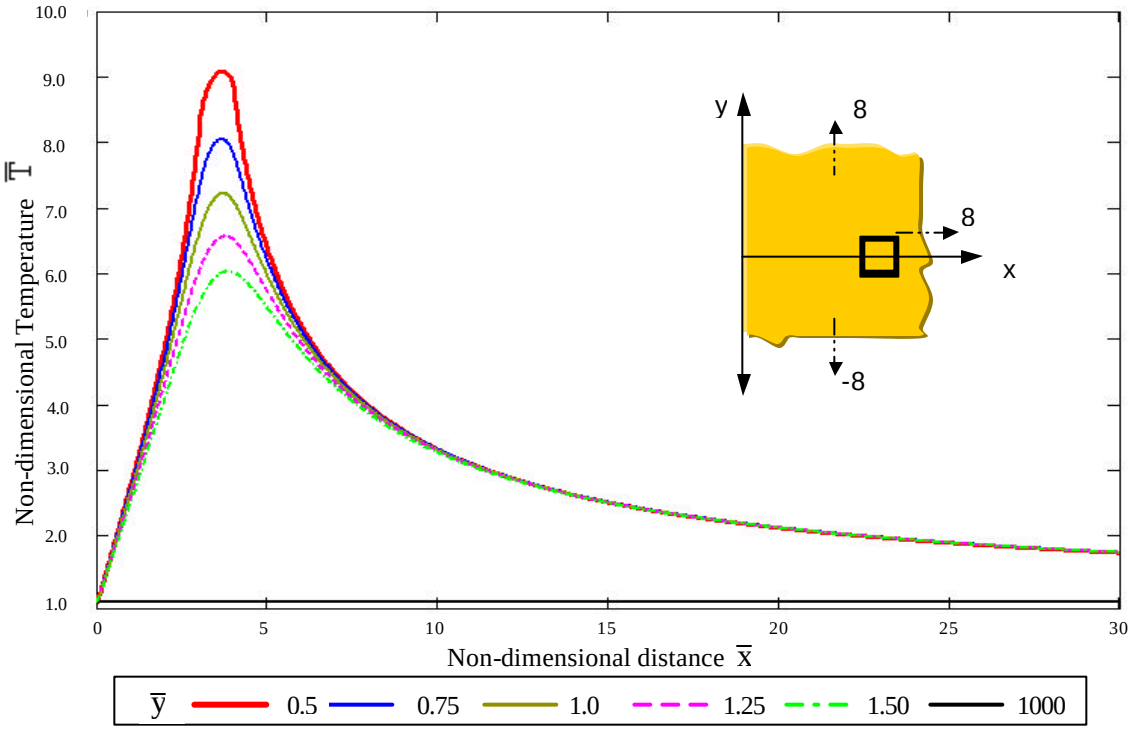

Figure 4.28. Dimensionless temperature distribution, hollow box-heating source $\overline{\lambda} = 5,\ \overline{a} = 3$.

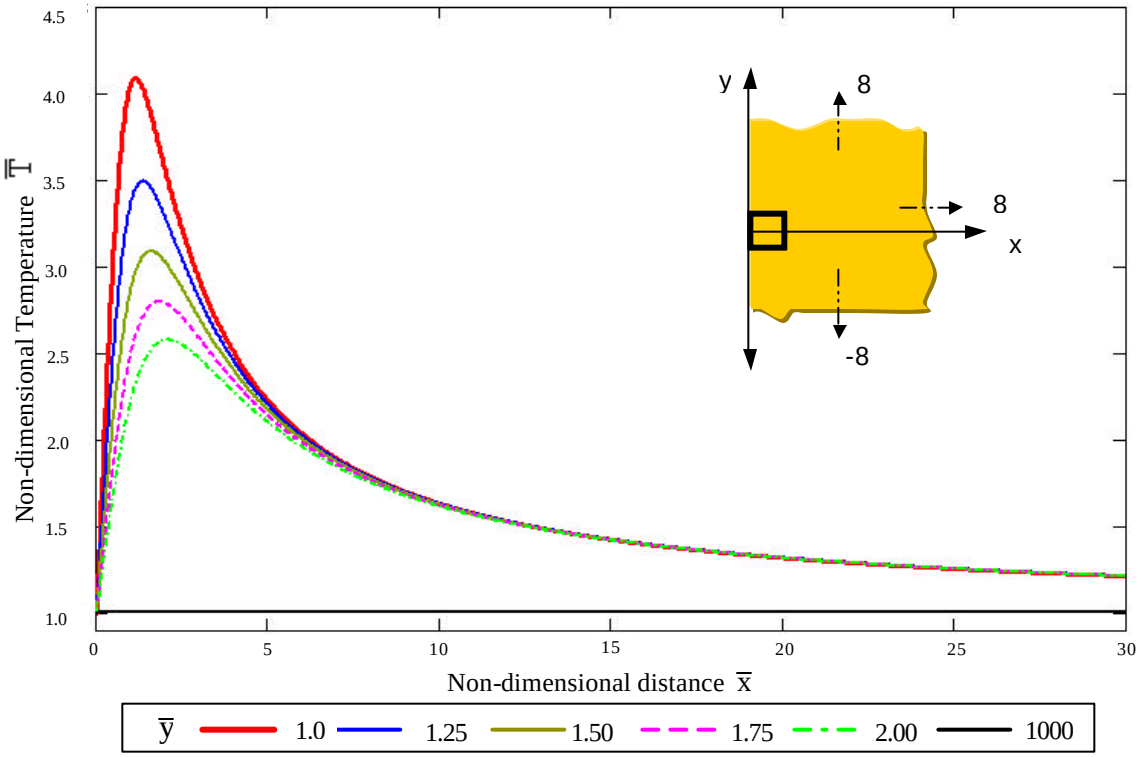

Figure 4.29. Dimensionless temperature distribution, hollow box-heating source $\overline{\lambda} = 10,\ \overline{a} = 0$.

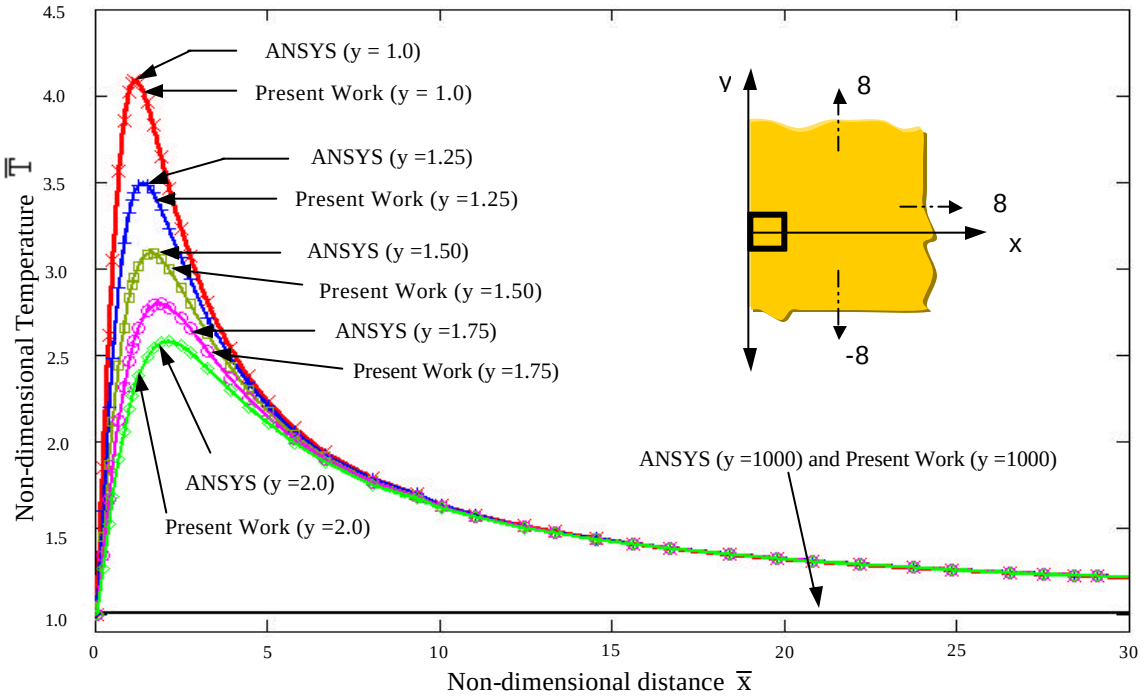

Figure 4.30. Dimensionless temperature distribution, hollow box-heating source $\bar{\lambda} = 10,\ \bar{a} = 0$. Comparison with the results from ANSYS.

The obtained solution is an analytical, even though long can be easily evaluated.

Figures 4.22 to 4.28 show the profiles of dimensionless temperature along “x” axis for different values of "y" for $\bar{\lambda}$ and $\bar{a}$, with different locations of the source of heat. We observe that the curves begin in $\bar{T} = 1$ for $\bar{x} = 0$, obtaining the maximum value when passing over the source of heat generation. Then $\bar{T}$ slowly decreases to 1 for very high values of “x” and “y”.

The maximum value of the temperature is obtained, when the lines cross $\bar{y} = \pm L/2$ over the source of heat generation.

Finally the figure 4.29 shows the result for a constant value source dimensionless strength of $\overline{\lambda} = 10$ and $\bar{a} = 0$. The figure has the same behavior of the previous curves, but these are displaced according to the location of the source of heat generation.

In the figure 4.30 the results obtained by our method is compared to numerical solutions obtained from software ANSYS specifically for the case of $\overline{\lambda} = 10$ and $\bar{a} = 1$, we observe a very high agreement between both methods. The small differences are due to the difficulty of simulating in ANSYS the semi-infinite slab with a very small discrete heat generation source; because the number of mesh elements required to get good agreement with our analytical method exceeds the number of elements allowed by the version 6.0 of ANSYS. Appendix [C] shows ANSYS element and results. We conclude that the present method provides, for this case, an analytical solution and is superior and simpler to the numerical solutions in term of labor and cost. The method is even more advantageous where parametric studies have to be performed.

Appendix [D] also shows the results for a rectangular hollow box-heating element. The result show for inside the box the temperature distribution shows two kinds in contrast to one peak for outside the box.

4.1.3 Semi-Infinite Slab with a Square Prismatic Heating Source

A body in the form of a square prismatic bar carrying current is embedded as a heat-generating element in a semi-infinite two dimensional slab $x > 0$, $-\infty < y < \infty$, $-\infty < z < \infty$, and constant thermal conductivity k. The square prismatic bar heat source has side L and infinite large depth ℓ; the heat generation per unit area of plate per unit depth λ (W/m^3) is constant. The boundary at $x = 0$ is maintained at constant temperature T_B as shown in figure 4.31 (a).

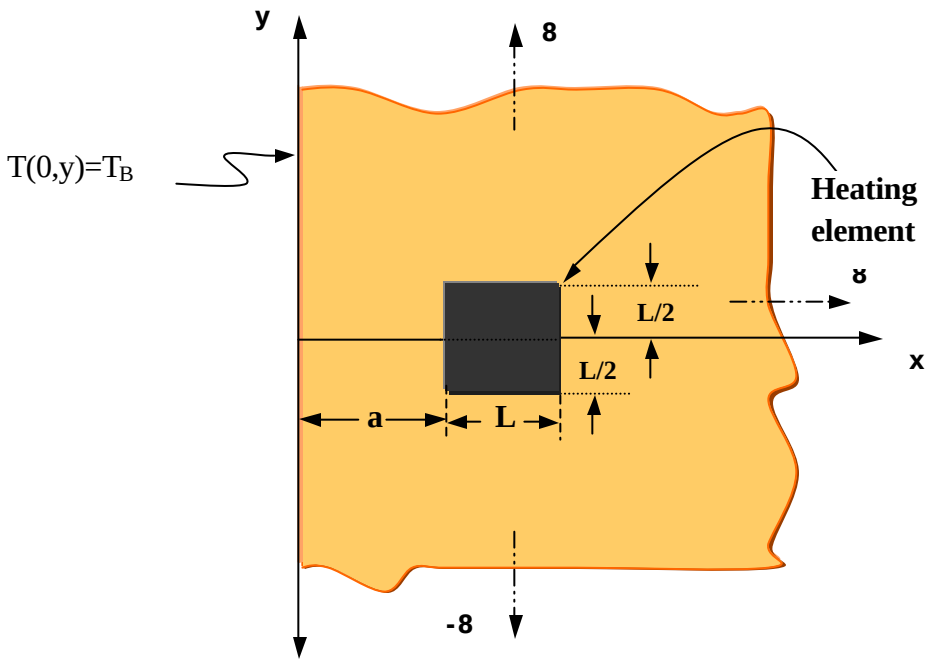

Figure 4.31. (a) Semi-infinite slab with a square prismatic-heating source

Let:

$Q_T \equiv$ Total heat generation (W) = $\lambda.\ell.L^2$

$\lambda \equiv$ Strength of the heat source per unit area per unit depth (W/m^3)

$Q(x,y) \equiv$ Heat generation per unit volume (W/m^3)

Q(x,y) when integrated over the whole volume must be equal to the total heat generation inside the semi-infinite slab, i.e. $\iiint_V Q(x,y).dv = Q_T$

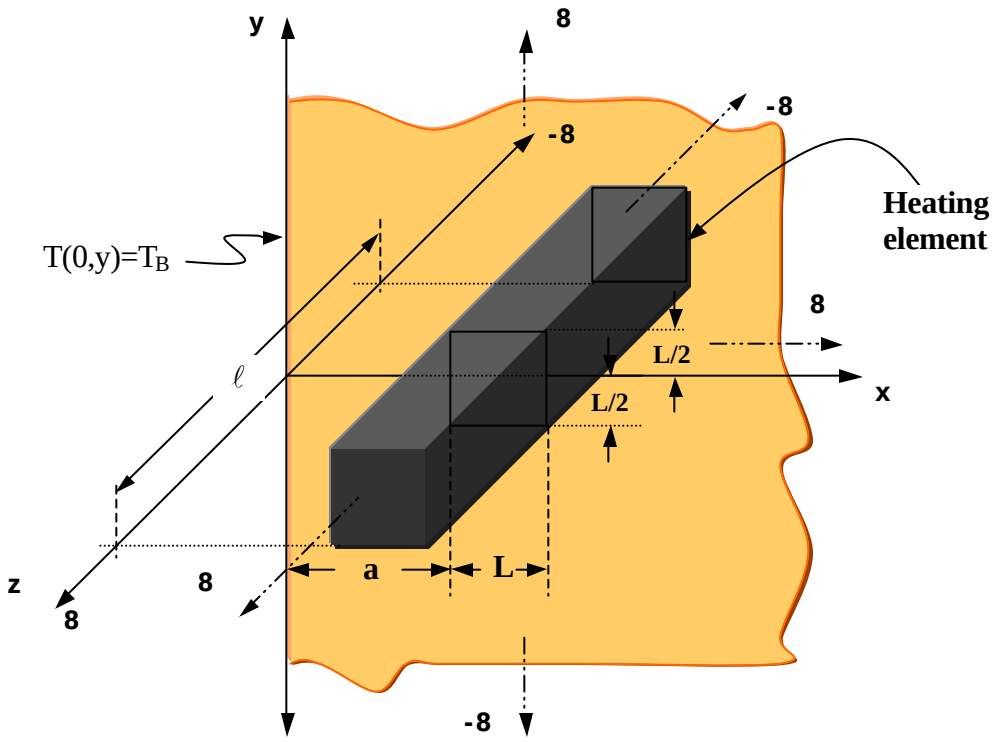

Figure 4.31. (b). Semi-infinite slab with a square prismatic-heating source

From figure 4.31.(b) the total heat generation Q_T, inside the volume can be expressed in Cartesian coordinates:

$$\int_{-\frac{\ell}{2}}^{\frac{\ell}{2}}\int_{-\infty}^{\infty}\int_{0}^{\infty} Q(x,y).dx.dy.dz = Q_T = \lambda.\ell.L^2 \quad \ldots\ldots\ldots\ldots\ldots\ldots\ldots\ldots\ldots\ldots \quad (4.12)$$

The heat generation Q(x,y) per unit volume is expresses of the following form:

$$Q(x,y) = \lambda \cdot \{H[x-a] - H[x-(L+a)]\}.\{H[y+L/2] - H[y-L/2]\} \ldots\ldots\ldots\ldots\ldots \quad (4.13)$$

The equation (4.13) satisfies to equation (4.12). Taking the right hand side term and integrating over the semi-infinite slab.

$$\int_{-\frac{\ell}{2}}^{\frac{\ell}{2}}\int_{-\infty}^{\infty}\int_{-\infty}^{\infty} \{\lambda \cdot \{H[x-a] - H[x-(L+a)]\}.\{H[y+L/2] - H[y-L/2]\}\}.dx.dy.dz =$$

$$\lambda \int_{-\frac{\ell}{2}}^{\frac{\ell}{2}} dz. \int_{-\infty}^{\infty} \{H[y+L/2] - H[y-L/2]\}.dy \cdot \int_{0}^{\infty} \{H[x-a] - H[x-(L+a)]\}.dx$$

Applying properties for Heaviside function and integrating obtained:

$$\lambda \cdot \ell . \int_{-L/2}^{L/2} dy . \int_{a}^{L+a} dx = \lambda \cdot \ell \cdot L^2$$

Equation (4.12) after integration becomes:

$$\iiint_V Q(x,y).dv = Q_T = \lambda \cdot \ell \cdot L^2$$

Substituting equations (3.31) and (4.13) in equation (4.4) the following expression is obtained:

$$T(x,y) = T_B + \frac{\lambda}{4\pi k \ell} \int_{-\frac{\ell}{2}}^{\frac{\ell}{2}} \int_{-\infty}^{\infty} \int_{0}^{\infty} \left\{ \begin{bmatrix} H[x-a] - \\ H[x-(L+a)] \end{bmatrix} . \begin{bmatrix} H[y+L/2] - \\ H[y-L/2] \end{bmatrix} . \ln \left\{ \frac{(x+x')^2 + (y-y')^2}{(x-x')^2 + (y-y')^2} \right\} \right\} . dx'\, dy'\, dz'$$

After applying properties of the Heaviside as before and simplifying, we get:

$$T(x,y) = T_B + \frac{\lambda}{4\pi k} \left\{ \int_{-L/2}^{L/2} \int_{a}^{L+a} \ln \left\{ \frac{(x+x')^2 + (y-y')^2}{(x-x')^2 + (y-y')^2} \right\} . dx' . dy' \right\}$$

In order to express results in non-dimensional form, the following non-dimensional quantities are defined:

$\overline{T}(\overline{x},\overline{y}) = \dfrac{T(x,y)}{T_B}$ Non-dimensional temperature

$\overline{\lambda} = \dfrac{\lambda.L^2}{kT_B}$ Non-dimensional heat generation

$\overline{x} = \dfrac{x}{L}, \ \overline{y} = \dfrac{y}{L}$ Non-dimensional field point location

$\overline{x}' = \dfrac{x'}{L}, \ \overline{y}' = \dfrac{y'}{L}$ Non-dimensional source point location

$\overline{a} = \dfrac{a}{L}$ Non-dimensional distances

Finally, substitute all these quantities in the previous equation and the following relationship is obtained:

$$\overline{T}(\overline{x},\overline{y}) = 1 + \frac{\overline{\lambda}}{4.\pi}\left\{\int_{-1/2}^{1/2}\int_{\overline{a}}^{1+\overline{a}} \ln\left\{\frac{(\overline{x}+\overline{x}')^2 + (\overline{y}-\overline{y}')^2}{(\overline{x}-\overline{x}')^2 + (\overline{y}-\overline{y}')^2}\right\} d\overline{x}' d\overline{y}'\right\} \quad \text{..... (4.14)}$$

$$\overline{T}(\overline{x},\overline{y}) = 1+\frac{\overline{\lambda}}{4.\pi}\left[\begin{array}{l}
\left\{\begin{array}{l}(\overline{x}+\overline{a}).\left\{\begin{array}{l}(\overline{y}-0.5).\ln\left[(\overline{x}+\overline{a})^2+(\overline{y}-0.5)^2\right]-\\(\overline{y}+0.5).\ln\left[(\overline{x}+\overline{a})^2+(\overline{y}+0.5)^2\right]\end{array}\right\}+\\4(\overline{x}+\overline{a})+2.(\overline{x}+\overline{a})^2.\left[\mathrm{Arctg}\left(\frac{\overline{y}-0.5}{\overline{x}+\overline{a}}\right)-\mathrm{Arctg}\left(\frac{\overline{y}+0.5}{\overline{x}+\overline{a}}\right)\right]\end{array}\right\}+\\
\left\{\begin{array}{l}(\overline{x}+1+\overline{a}).\left\{\begin{array}{l}(\overline{y}+0.5).\ln\left[(\overline{x}+1+\overline{a})^2+(\overline{y}+0.5)^2\right]-\\(\overline{y}-0.5).\ln\left[(\overline{x}+1+\overline{a})^2+(\overline{y}-0.5)^2\right]\end{array}\right\}-\\4(\overline{x}+1+\overline{a})+2.(\overline{x}+1+\overline{a})^2.\left[\mathrm{Arctg}\left(\frac{\overline{y}+0.5}{\overline{x}+1+\overline{a}}\right)-\mathrm{Arctg}\left(\frac{\overline{y}-0.5}{\overline{x}+1+\overline{a}}\right)\right]\end{array}\right\}+\\
\left\{\begin{array}{l}(\overline{x}-\overline{a}).\left\{\begin{array}{l}(\overline{y}-0.5).\ln\left[(\overline{x}-\overline{a})^2+(\overline{y}-0.5)^2\right]-\\(\overline{y}+0.5).\ln\left[(\overline{x}-\overline{a})^2+(\overline{y}+0.5)^2\right]\end{array}\right\}+\\4(\overline{x}-\overline{a})+2.(\overline{x}-\overline{a})^2.\left[\mathrm{Arctg}\left(\frac{\overline{y}-0.5}{\overline{x}-\overline{a}}\right)-\mathrm{Arctg}\left(\frac{\overline{y}+0.5}{\overline{x}-\overline{a}}\right)\right]\end{array}\right\}+\\
\left\{\begin{array}{l}(\overline{x}-1-\overline{a})).\left\{\begin{array}{l}(\overline{y}+0.5).\ln\left[(\overline{x}-1-\overline{a}))^2+(\overline{y}+0.5)^2\right]-\\(\overline{y}-0.5).\ln\left[(\overline{x}-1-\overline{a})^2+(\overline{y}-0.5)^2\right]\end{array}\right\}-\\4(\overline{x}-\overline{b})+2.(\overline{x}-1+\overline{a})^2.\left[\mathrm{Arctg}\left(\frac{\overline{y}+0.5}{\overline{x}-1-\overline{a}}\right)-\mathrm{Arctg}\left(\frac{\overline{y}-0.5}{\overline{x}-1-\overline{a}}\right)\right]\end{array}\right\}+\\
\left\{\begin{array}{l}(\overline{y}-0.5)^2.\mathrm{Arctg}\left(\frac{\overline{x}+\overline{a}}{\overline{y}-0.5}\right)+(\overline{x}+\overline{a}).(\overline{y}-0.5)-(\overline{x}+\overline{a})^2.\mathrm{Arctg}\left(\frac{\overline{y}-0.5}{\overline{x}+\overline{a}}\right)-\\(\overline{y}+0.5)^2.\mathrm{Arctg}\left(\frac{\overline{x}+\overline{a}}{\overline{y}+0.5}\right)-(\overline{x}+\overline{a}).(\overline{y}+0.5)+(\overline{x}+\overline{a})^2.\mathrm{Arctg}\left(\frac{\overline{y}+0.5}{\overline{x}+\overline{a}}\right)\end{array}\right\}-\\
\left\{\begin{array}{l}(\overline{y}-0.5)^2.\mathrm{Arctg}\left(\frac{\overline{x}+1+\overline{a}}{\overline{y}-0.5}\right)+(\overline{x}+1+\overline{a}).(\overline{y}-0.5)-(\overline{x}+1+\overline{a})^2.\mathrm{Arctg}\left(\frac{\overline{y}-0.5}{\overline{x}+1+\overline{a}}\right)-\\(\overline{y}+0.5)^2.\mathrm{Arctg}\left(\frac{\overline{x}+1+\overline{a}}{\overline{y}+0.5}\right)-(\overline{x}+1+\overline{a}).(\overline{y}+0.5)+(\overline{x}+1+\overline{a})^2.\mathrm{Arctg}\left(\frac{\overline{y}+0.5}{\overline{x}+1+\overline{a}}\right)\end{array}\right\}+\\
\left\{\begin{array}{l}(\overline{y}-0.5)^2.\mathrm{Arctg}\left(\frac{\overline{x}-\overline{a}}{\overline{y}-0.5}\right)+(\overline{x}-\overline{a}).(\overline{y}-0.5)-(\overline{x}-\overline{a})^2.\mathrm{Arctg}\left(\frac{\overline{y}-0.5}{\overline{x}-\overline{a}}\right)-\\(\overline{y}+0.5)^2.\mathrm{Arctg}\left(\frac{\overline{x}-\overline{a}}{\overline{y}+0.5}\right)-(\overline{x}-\overline{a}).(\overline{y}+0.5)+(\overline{x}-\overline{a})^2.\mathrm{Arctg}\left(\frac{\overline{y}+0.5}{\overline{x}-\overline{a}}\right)\end{array}\right\}-\\
\left\{\begin{array}{l}(\overline{y}-0.5)^2.\mathrm{Arctg}\left(\frac{\overline{x}-1-\overline{a}}{\overline{y}-0.5}\right)+(x-1-\overline{a}).(\overline{y}-0.5)-(x-1-\overline{a})^2.\mathrm{Arctg}\left(\frac{\overline{y}-0.5}{\overline{x}-1-\overline{a}}\right)-\\(\overline{y}+0.5)^2.\mathrm{Arctg}\left(\frac{\overline{x}-1-\overline{a}}{\overline{y}+0.5}\right)-(\overline{x}-1-\overline{a}).(\overline{y}+0.5)+(\overline{x}-1-\overline{a})^2.\mathrm{Arctg}\left(\frac{\overline{y}+0.5}{\overline{x}-1-\overline{a}}\right)\end{array}\right\}
\end{array}\right] \quad \ldots(4.15)$$

Equation (4.15) is the temperature profile for a semi-infinite slab with constant temperature on boundary heated by a square prismatic bar carrying a current and embedded in the slab. Thus an "analytical solution" for the temperature distribution has been obtained.

Equation (4.15) can be easily evaluated. Some of the results for different values of $\bar{\lambda}$ and $\bar{a}$ are presented in the figures 4.32 to 4.41.

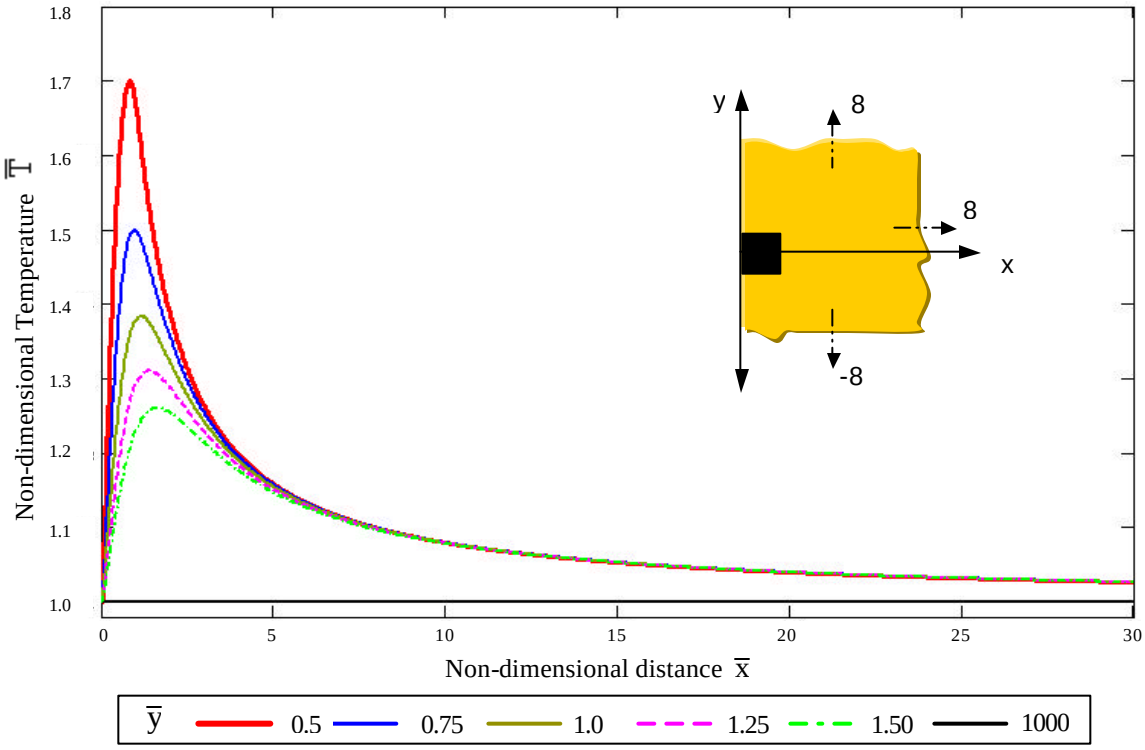

Figure 4.32. Dimensionless temperature distribution, square prismatic-heating source $\bar{\lambda} = 5,\ \bar{a} = 0$.

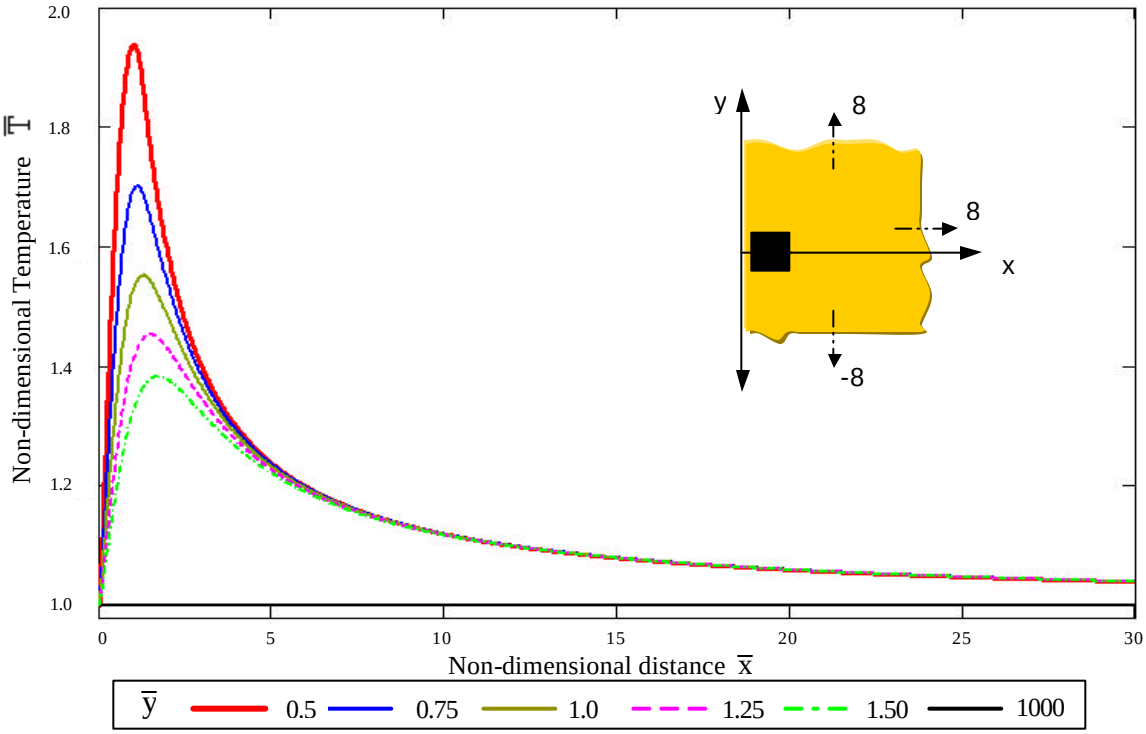

Figure 4.33. Dimensionless temperature distribution, square prismatic-heating source $\overline{\lambda} = 5,\ \overline{a} = 0.25$.

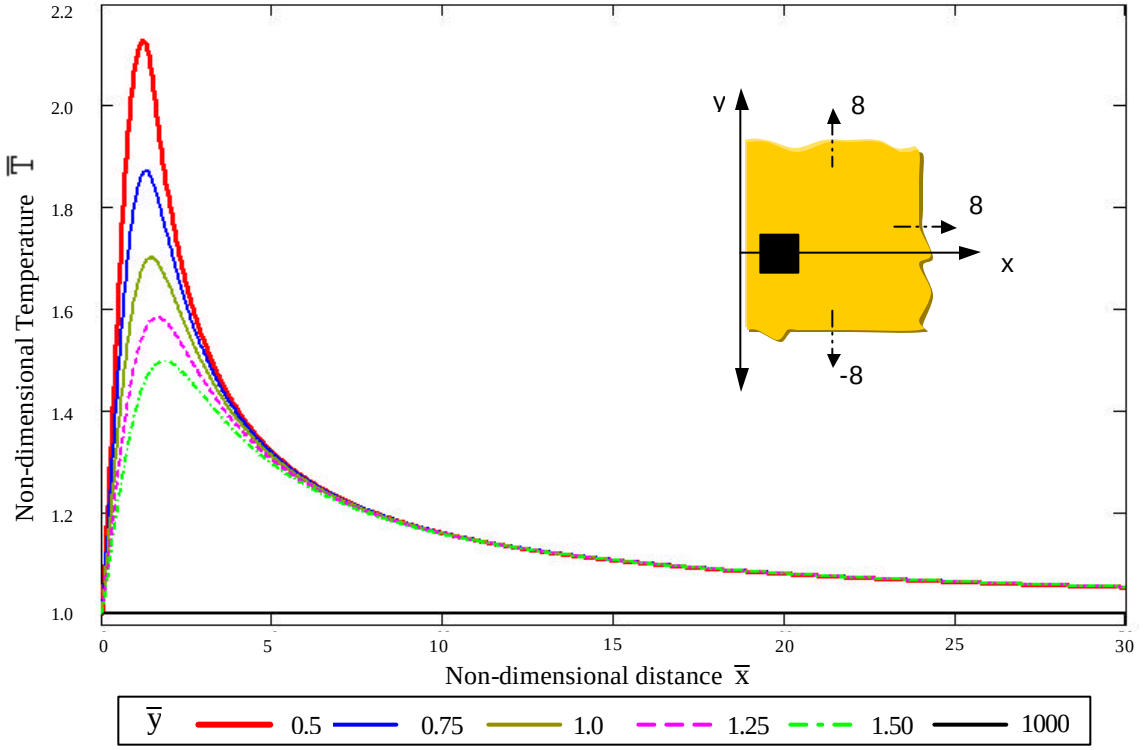

Figure 4.34. Dimensionless temperature distribution, square prismatic-heating source $\overline{\lambda} = 5,\ \overline{a} = 0.5$.

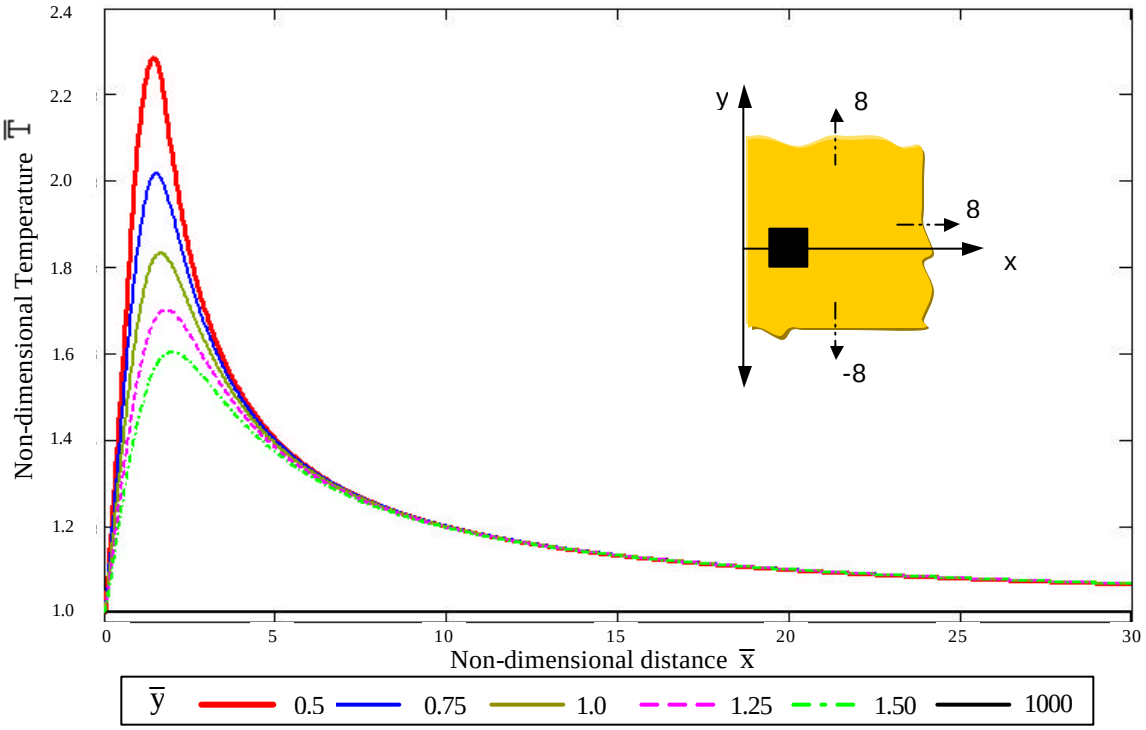

Figure 4.35. Dimensionless temperature distribution, square prismatic-heating source $\lambda = 5,\ a = 0.75$.

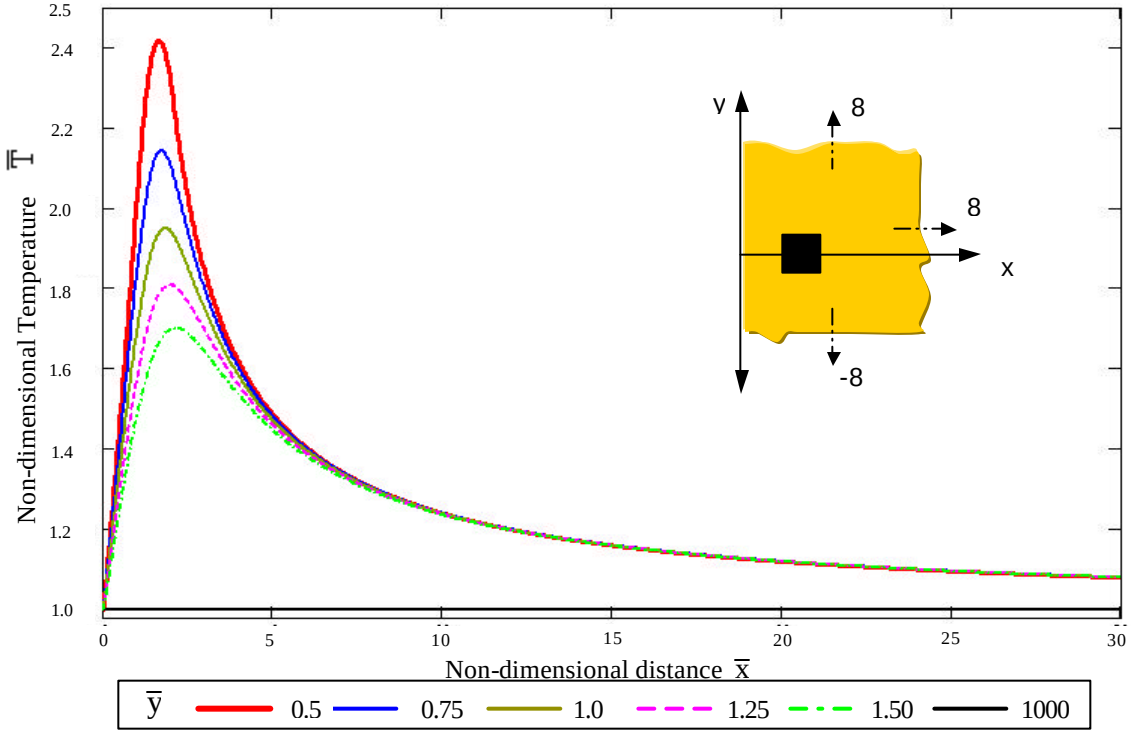

Figure 4.36. Dimensionless temperature distribution, square prismatic-heating source $\overline{\lambda} = 5,\ \overline{a} = 1$.

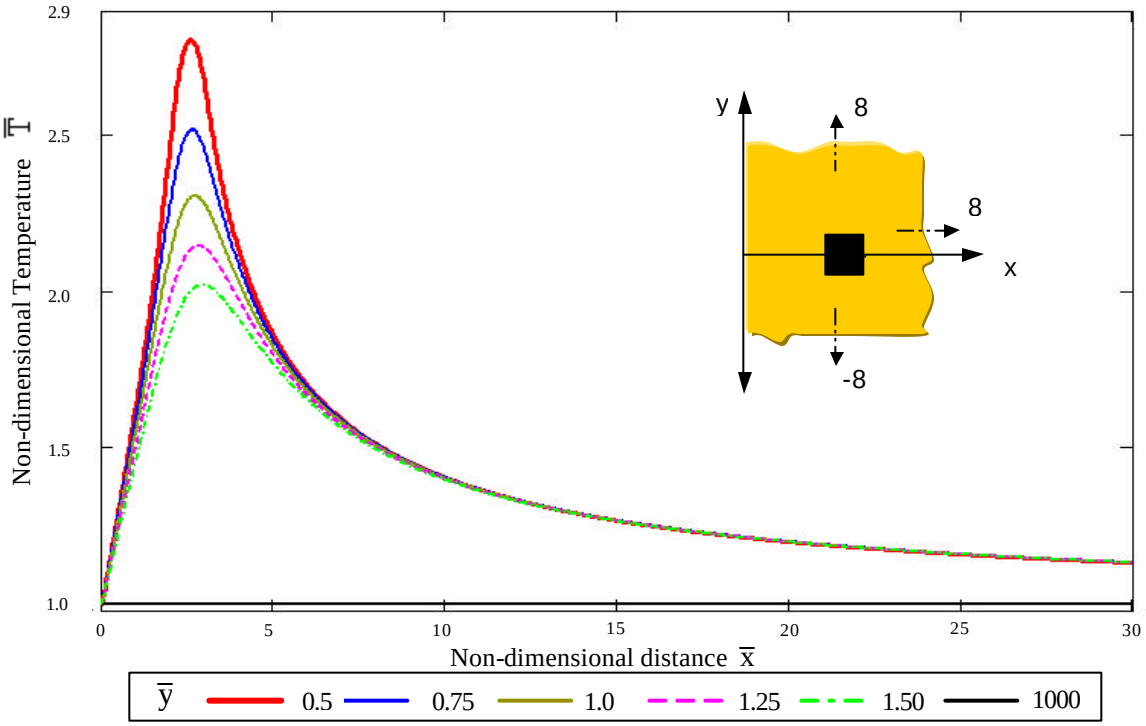

Figure 4.37. Dimensionless temperature distribution, square prismatic-heating source $\overline{\lambda} = 5,\ \overline{a} = 2$.

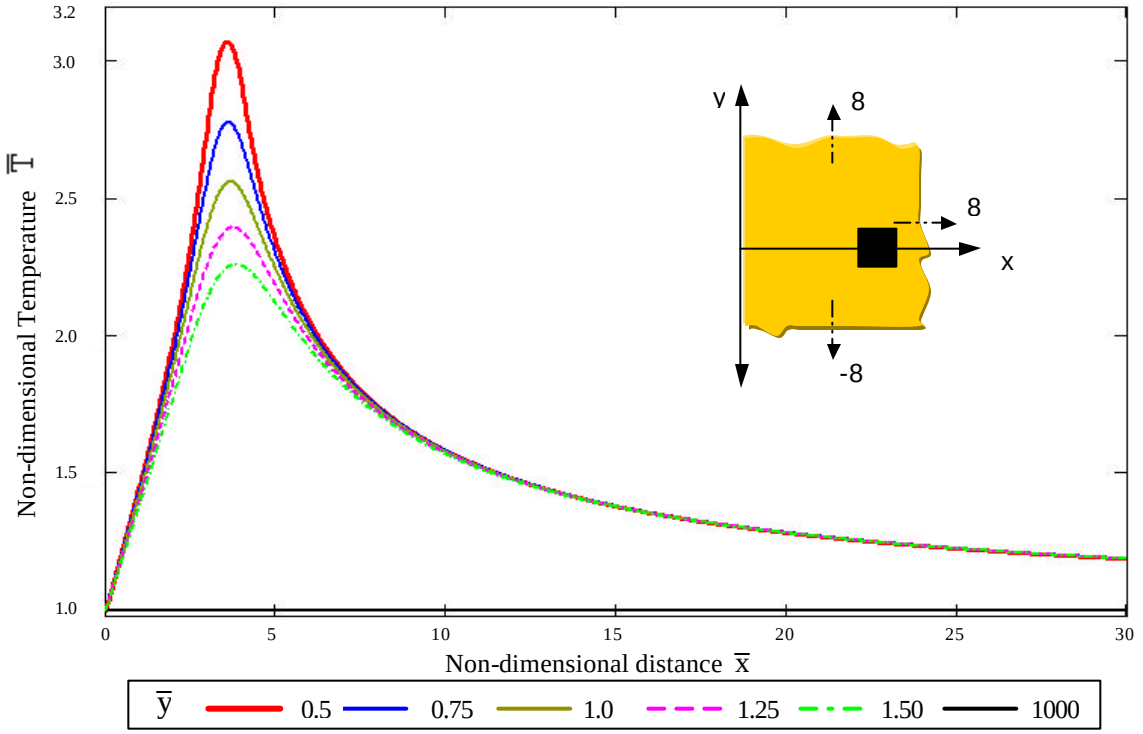

Figure 4.38. Dimensionless temperature distribution, square prismatic-heating source $\overline{\lambda} = 5,\ \overline{a} = 3$.

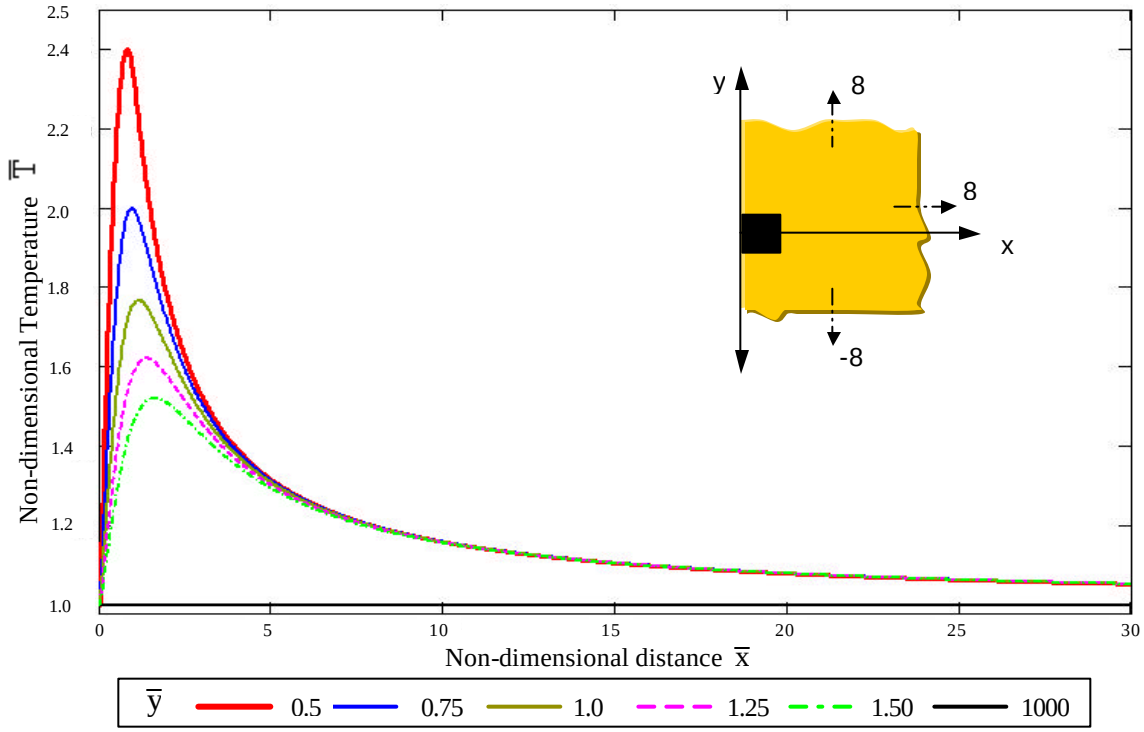

Figure 4.39. Dimensionless temperature distribution, square prismatic-heating source $\bar{\lambda}=10,\ \bar{a}=0$.

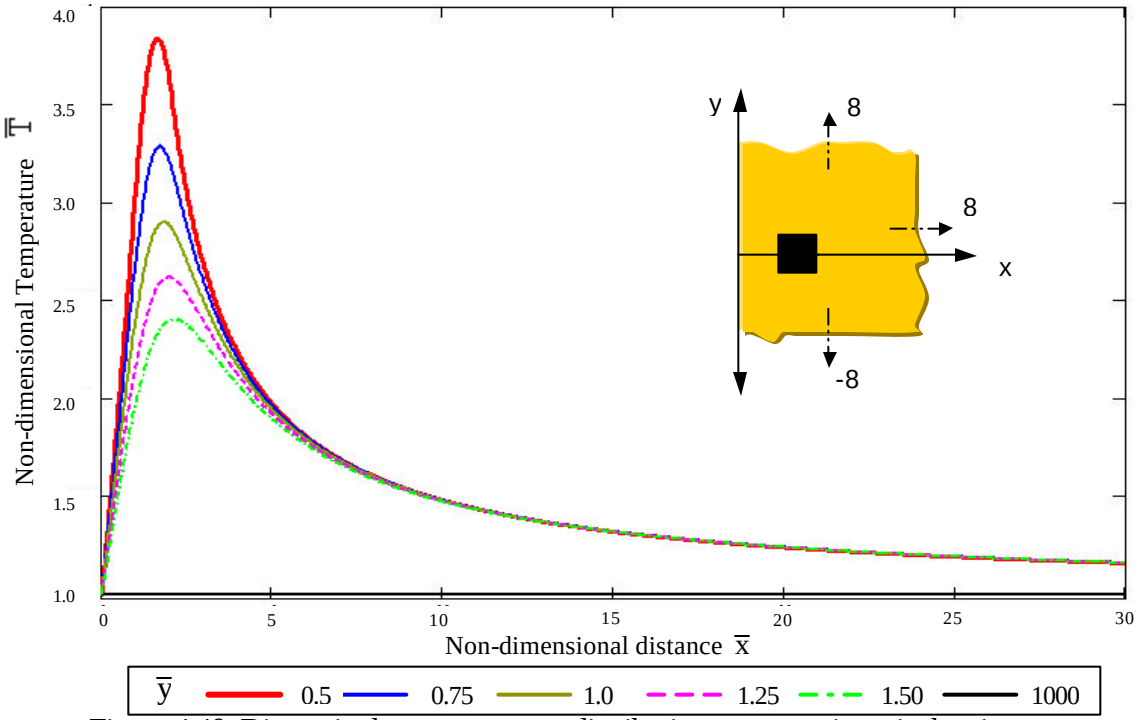

Figure 4.40. Dimensionless temperature distribution, square prismatic-heating source $\bar{\lambda}=10,\ \bar{a}=1$.

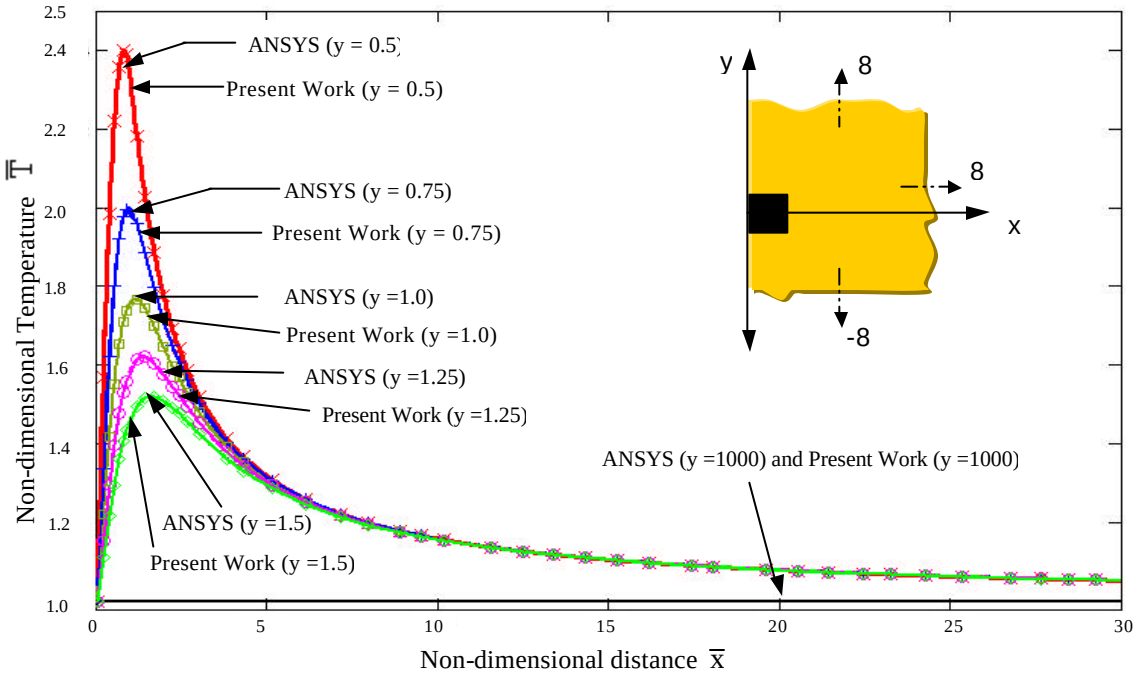

Figure 4.41. Dimensionless temperature distribution, square prismatic-heating source. $\bar{\lambda} = 10,\ \bar{a} = 0$. Comparison with results from ANSYS.

Figures 4.32 to 4.41 show the non-dimensional temperature profiles along the "x" axis for different values of "$\bar{y}$", $\bar{\lambda}$ and $\bar{a}$. From these results it can be seen that the behavior is similar to that observed in the cases of thin plate heating source and square hollow box heating source.

For a given $\bar{x}$ lying on the source of heat generation, the maximum temperature is obtained when the lines cross $\bar{y} = \pm L/2$ and then fall off to 1, all the curves have the same behavior as in the previous cases, They begin with $\bar{T} = 1$ for $\bar{x} = 0$, obtaining the maximum value when passing over the source of heat generation, then falls slowly to $\bar{T} = 1$ for high values of "x" and "y".

Figures 4.32 to 4.38 show the profiles of non-dimensional temperature along the axis "x", to different values of "y", for $\overline{\lambda} = 5$ and to different location of the source of heat generation. We observe that the maximum points of the curves are displaced according to the location of the source of heat generation.

Figures 4.39 to 4.40 show the case for a higher value of the non-dimensional strength of the source ($\overline{\lambda} = 10$) and different locations of source. It observed that curves keep the same behavior that the previous curves.

Again for comparison purposes this case was resolved using ANSYS (which uses analysis of finite element to solve the problems), the results for both the present work and ANSYS are shown in the figure 4.41. The figure 4.41 shows the profiles of dimensionless temperature for $\overline{\lambda} = 10$ and $\bar{a} = 0$. The analytical solution obtained here and the results of ANSYS are plotted. It observed that the results agree very well. Appendix [E] shows ANSYS element and results. Once again the figure 4.41 validates the results obtained with the method used in this work, which is much simpler and easier to evaluate.

4.1.4 Semi-Infinite Slab with a Thin Cylindrical - Heating Source

A thin wire in the form of a thin cylindrical heating source is embedded, as a heat-generating element, in a semi-infinite two-dimensional slab $x > 0$, $-\infty < y < \infty$, $-\infty < z < \infty$, and constant thermal conductivity k. The source can be assumed as a thin cylindrical heat source with walls infinitesimally thin; with large depth ℓ and radius "a"; the heat generation per unit length along the source per unit depth is constant and the boundary in $x = 0$ is maintained at constant temperature T_B as shown in figure 4.42 (a).

Let:

$Q_T \equiv$ Total heat generation (W) = $2.\pi.a.\lambda.\ell$

$\lambda \equiv$ Strength of the heat source per unit depth per unit length (W/m^2)

$Q(r,\theta) \equiv$ Heat generation intensity per unit volume (W/m^3) at position (r,θ).

$Q(r,\theta)$ when integrated over the whole volume must be equal to the total heat generation inside semi-infinite slab, i.e. $\iiint_V Q(r,\theta).dv = Q_T$

For cylindrical coordinates the total heat generation of the heat source Q_T can be expressed as follows:

$$\int_{-\frac{\ell}{2}}^{\frac{\ell}{2}} \int_0^{2\pi} \int_0^{\infty} Q(r,\theta).r.dr.d\theta.dz = Q_T = 2.\pi.a.\lambda.\ell \qquad \text{.....} \quad (4.16)$$

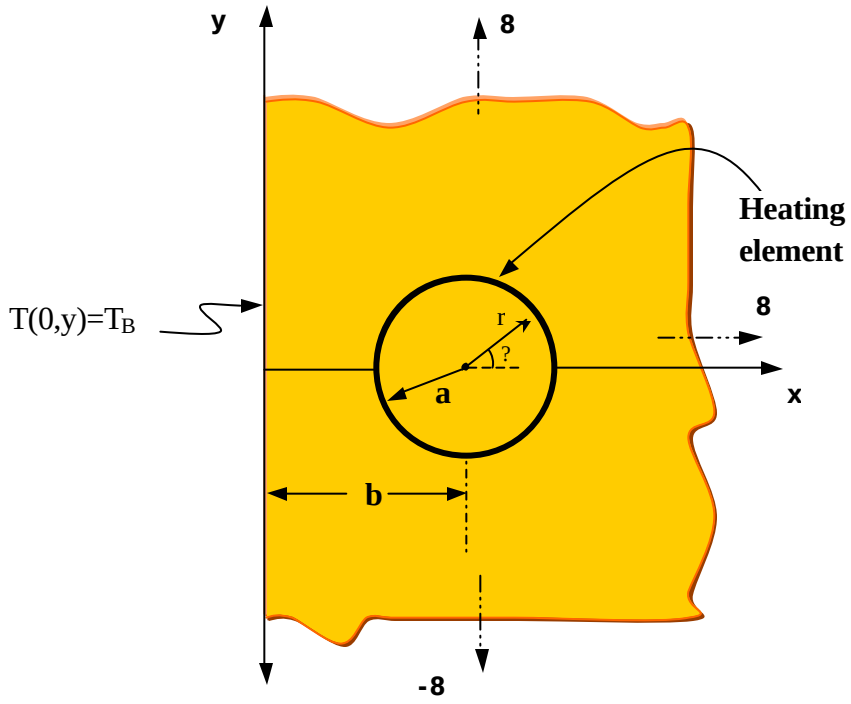

Figure 4.42. (a). Semi-infinite slab with a thin cylindrical-heating source

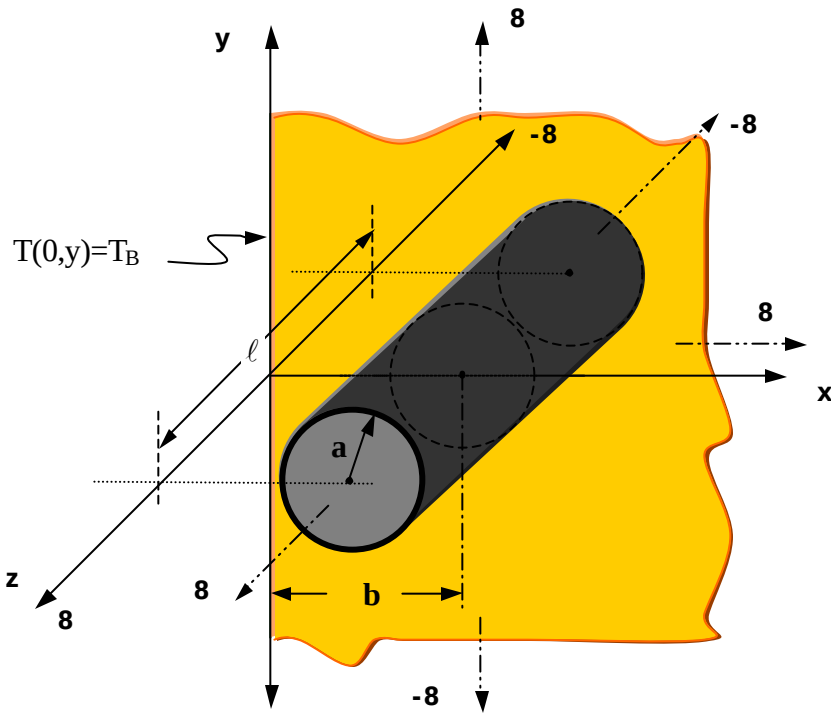

Figure 4.42. (b) Semi-infinite slab with a thin cylindrical-heating source

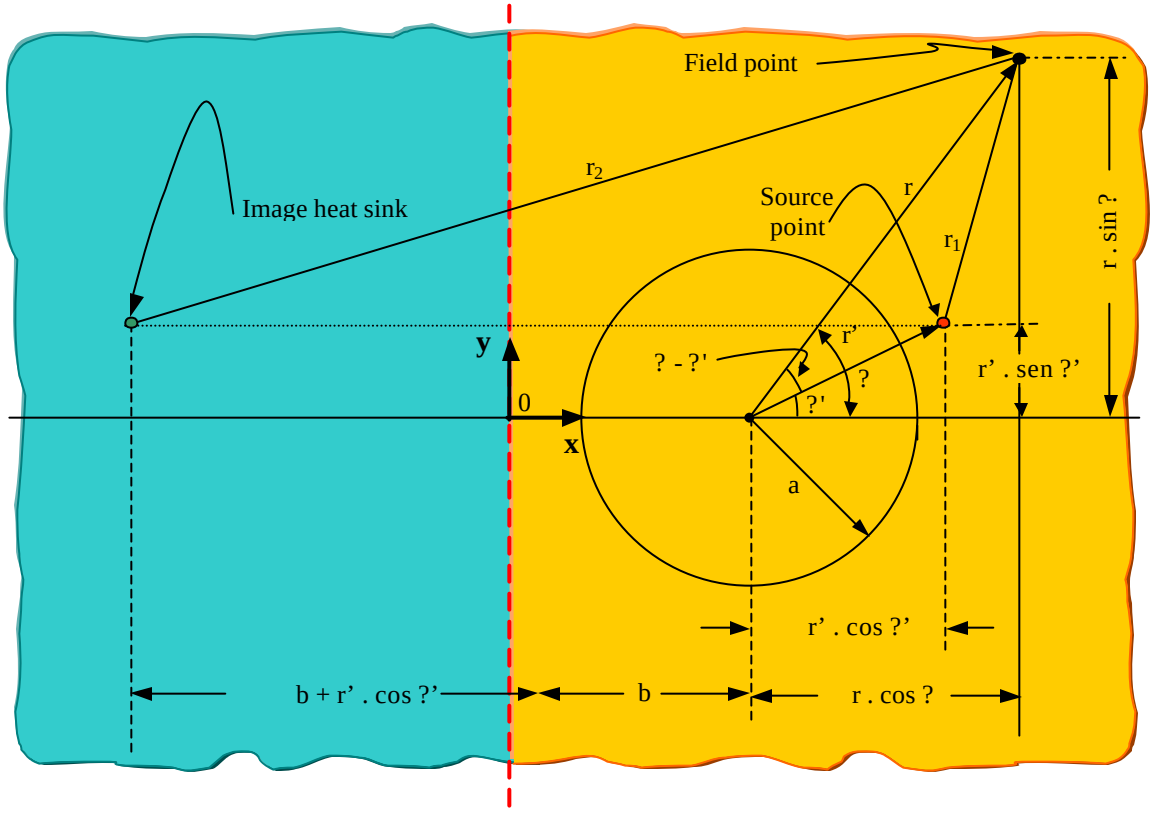

Figure 4.42. (c) Image for a unit heat source for a thin cylindrical-heating source

The procedure to solve this problem is similar to that followed for the previous cases, using the same equation of Green's function, developed for the previous cases. The only difference is cylindrical coordinates are used to represent the expression of the generation of heat, as they are more convenient.

According the geometry show in the figure 4.42. (c) the heat generation Q(x,y) is expresses of the following form:

$$Q(x,y) = Q(r,\theta) = \lambda.\delta(r-a) \quad \ldots\ldots (4.17)$$

The equation (4.16) satisfy to equation (4.17), integrating over the volume of semi-infinite slab obtained:

$$\int_{-\frac{\ell}{2}}^{\frac{\ell}{2}}\int_{0}^{2\pi}\int_{0}^{\infty}\lambda.\delta(r-a).r.dr.d\theta.dz = \lambda.\int_{-\frac{\ell}{2}}^{\frac{\ell}{2}}dz.\int_{0}^{2\pi}d\theta.\int_{0}^{\infty}r.\delta(r-a).dr$$

Using the properties for Dirac-Delta function we get:

$$\lambda\cdot\ell\cdot a.\int_{0}^{2\pi}d\theta = 2.\pi.a.\lambda.\ell$$

Equation (4.17) after integration becomes:

$$\iiint_{V} Q(r,\theta) = Q_T = 2.\pi.a.\lambda.\ell$$

Substitute equations (3.31) and (4.17) in equation (4.4):

$$T(x,y) = T_B + \frac{\lambda}{4\pi k\ell}\int_{-\frac{\ell}{2}}^{\frac{\ell}{2}}\int_{0}^{2\pi}\int_{0}^{\infty}\delta(r'-a).\ln\left\{\frac{(r_2)^2}{(r_1)^2}\right\}.r'dr'd\theta'dz' \quad \ldots\ldots (4.18)$$

Using the figure 4.45. (c) one can get:

$$(r_1)^2 = (r)^2 + (r')^2 - 2.r'.r.\cos(\theta - \theta')$$

$$(r_2)^2 = [r.\sin\theta - r'.\sin\theta']^2 + [2b + r'.\cos\theta' + r.\cos\theta]^2$$

Where: $r' = a$ localization of ring heat source

$$(r_1)^2 = r^2 + a^2 - 2.a.r.\cos(\theta - \theta') \quad \text{(4.19)}$$

$$(r_2)^2 = [r.\sin\theta - a.\sin\theta']^2 + [2b + r.\cos\theta + a.\cos\theta']^2 \quad \text{(4.20)}$$

Substituting the values of r_1, and r_2 in the equation 4.18, equation 4.21 is obtained as:

$$T(x,y) = T_B + \frac{\lambda}{4\pi k\ell}\int_{-\frac{\ell}{2}}^{\frac{\ell}{2}}\int_0^{2\pi}\int_0^{\infty}\delta(r'-a).\ln\left\{\frac{[r.\sin\theta - a.\sin\theta']^2 + [2b + r.\cos\theta + a.\cos\theta']^2}{r^2 + a^2 - 2.a.r.\cos(\theta - \theta')}\right\}.r'.dr'\,d\theta'\,dz' \quad \text{(4.21)}$$

Applying again properties for Dirac Delta function and after integrating along of z-axis, obtaining:

$$T(x,y) = T_B + \frac{\lambda.a}{4\pi k}\int_0^{2\pi}\ln\left\{\frac{[r.\sin\theta - a.\sin\theta']^2 + [2b + r.\cos\theta + a.\cos\theta']^2}{r^2 + a^2 - 2.a.r.\cos(\theta - \theta')}\right\}.d\theta' \quad \text{(4.22)}$$

In order to express results in non-dimensional form, the following non-dimensional quantities are defined:

$\overline{T}(\overline{r},\theta) = \frac{T(r,\theta)}{T_B}$ Non-dimensional temperature

$\overline{\lambda} = \frac{2.\lambda.a.\pi}{kT_B}$ Non-dimensional heat generation

$\overline{r} = \frac{r}{a}$ Non-dimensional radius

$\overline{b} = \frac{b}{a}$ Non-dimensional source point location

Finally, substitute all these quantities in the previous equation and the following relationship is obtained:

$$\overline{T}(\overline{x},\overline{y}) = \overline{T}(\overline{r},\theta) = 1 + \frac{\overline{\lambda}}{8.\pi^2}\int_0^{2\pi} \ln\left\{\frac{\left[2.\overline{b} + \overline{r}.\cos\theta + \cos\theta'\right] + \left[\overline{r}.\sin\theta - \sin\theta'\right]^2}{1 + \overline{r}^2 - 2.\overline{r}.\cos(\theta - \theta')}\right\}.d\theta' \quad \text{.....(4.23)}$$

Equation (4.23) is the temperature profile for a semi-infinite slab with constant temperature on boundary heated by a wire in the form of a thin circle carrying a current and embedded in the slab. Thus an "almost analytical" solution" for the temperature distribution has been obtained. Using the software Mathcad this solution in the form of an integral can be easily evaluated. Some of the results for different values of $\overline{\lambda}$, y $\overline{b}$ are presented in the figures 4.43 to 4.50.

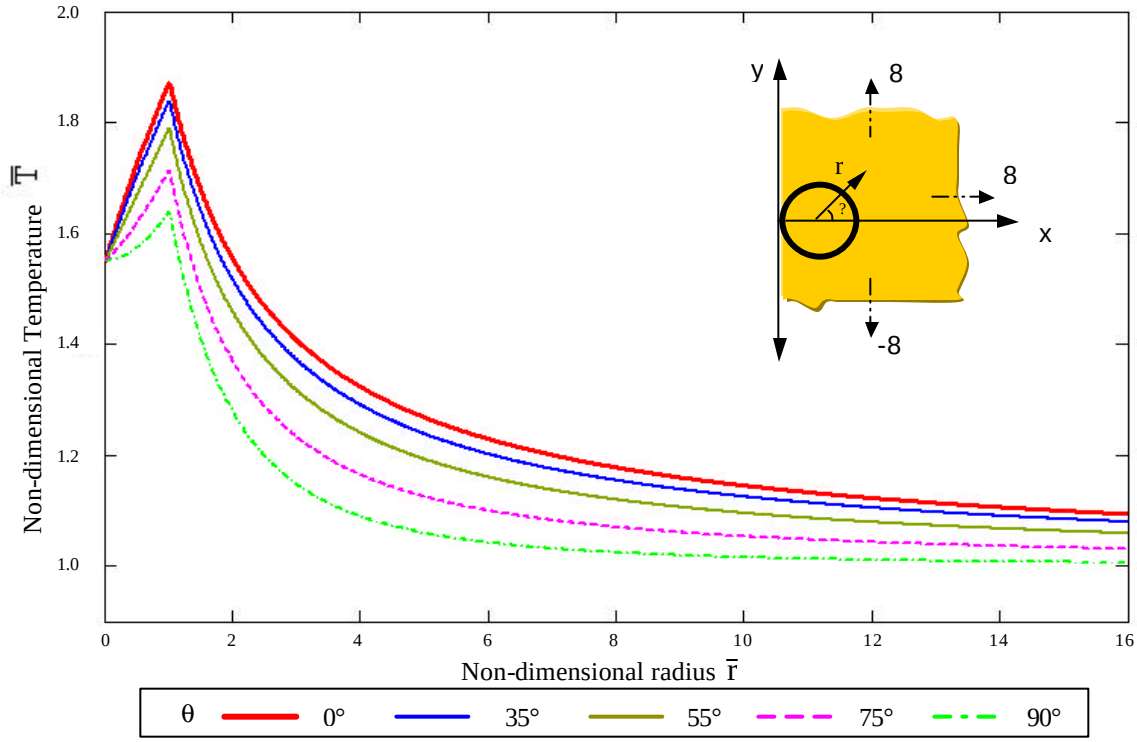

Figure 4.43. Dimensionless temperature distribution, thin cylindrical-heating source $\bar{\lambda} = 5,\ \bar{b} = 1$

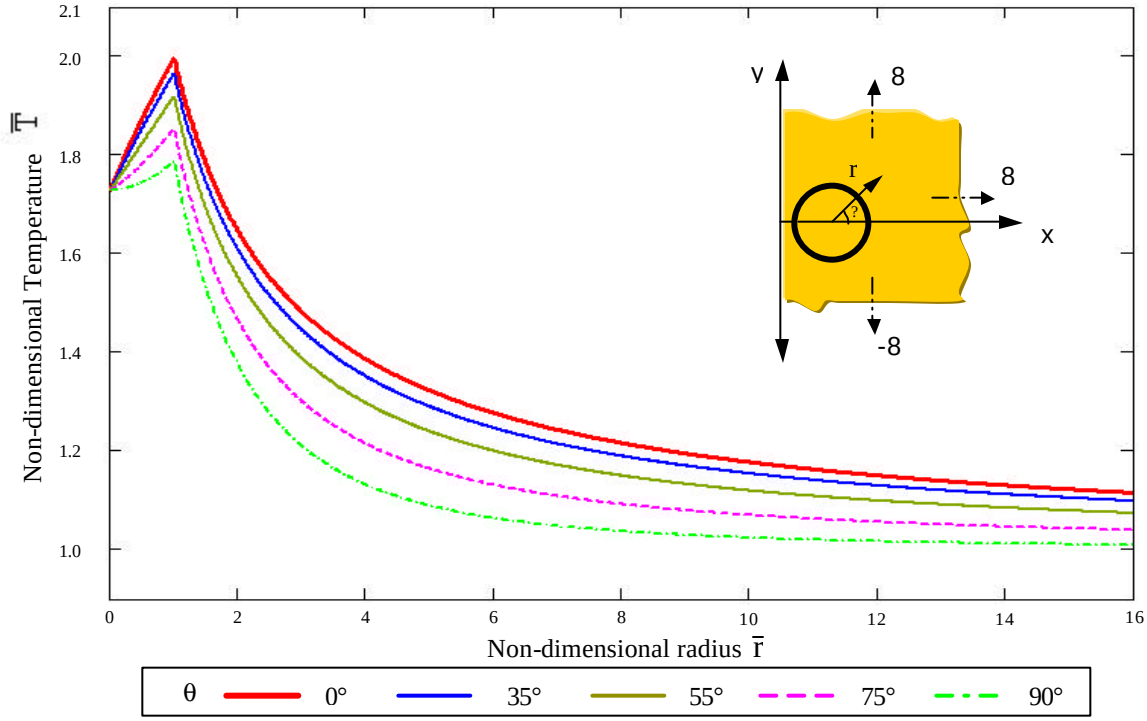

Figure 4.44. Dimensionless temperature distribution, thin cylindrical-heating source $\bar{\lambda} = 5,\ \bar{b} = 1.25$

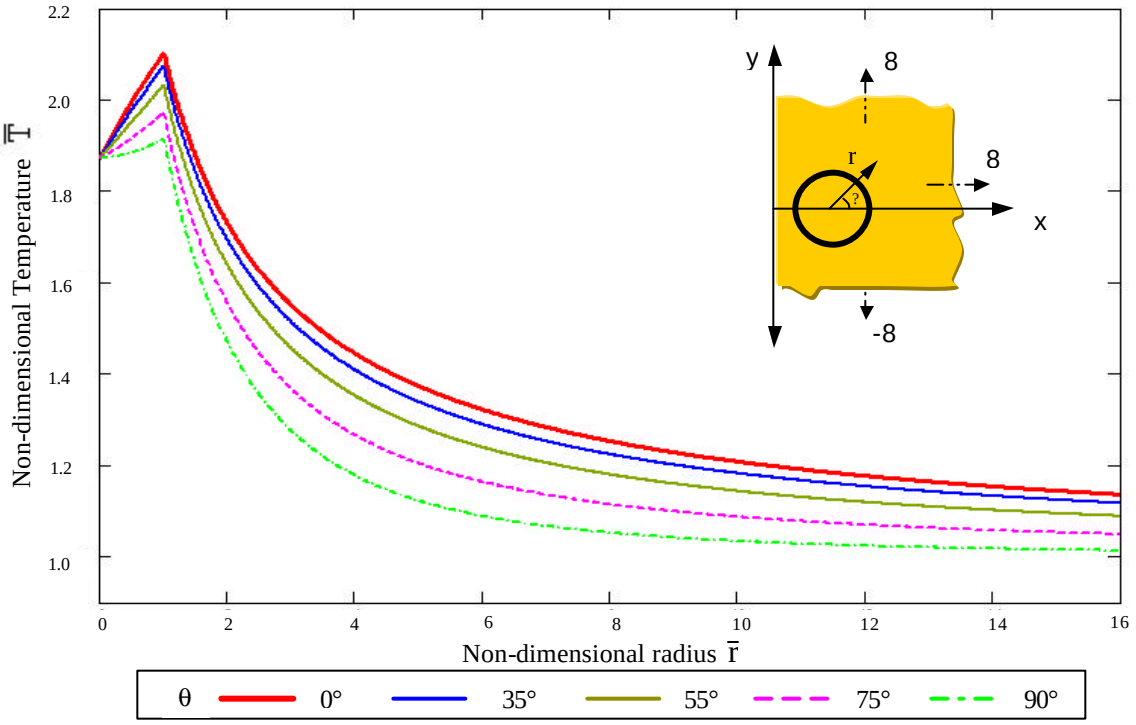

Figure 4.45. Dimensionless temperature distribution, thin cylindrical-heating source $\overline{\lambda} = 5,\ \overline{b} = 1.5$

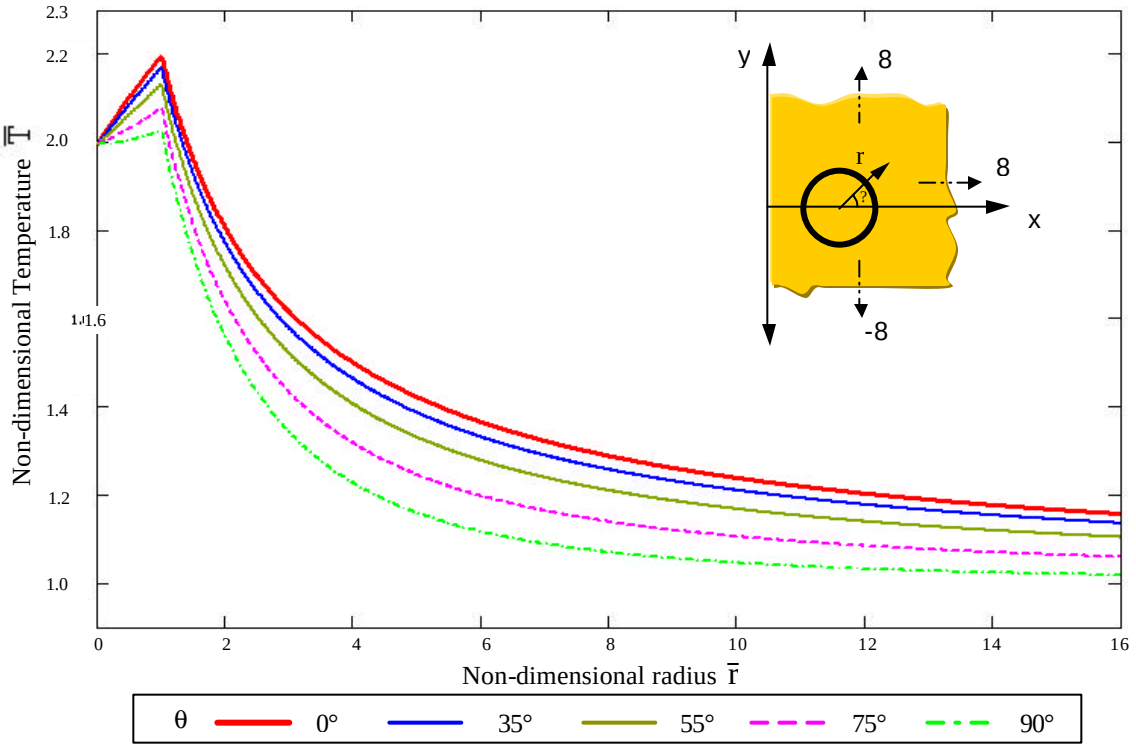

Figure 4.46. Dimensionless temperature distribution, thin cylindrical-heating source $\overline{\lambda} = 5,\ \overline{b} = 1.75$

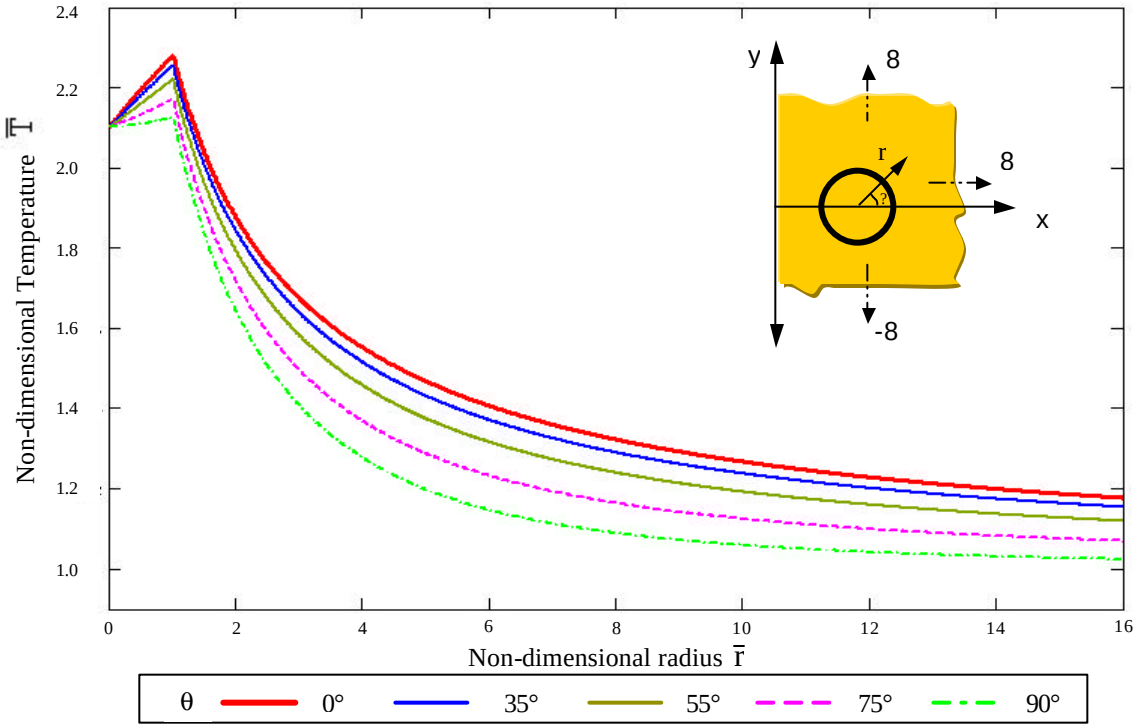

Figure 4.47. Dimensionless temperature distribution, thin cylindrical-heating source $\overline{\lambda}=5,\ \overline{b}=2$

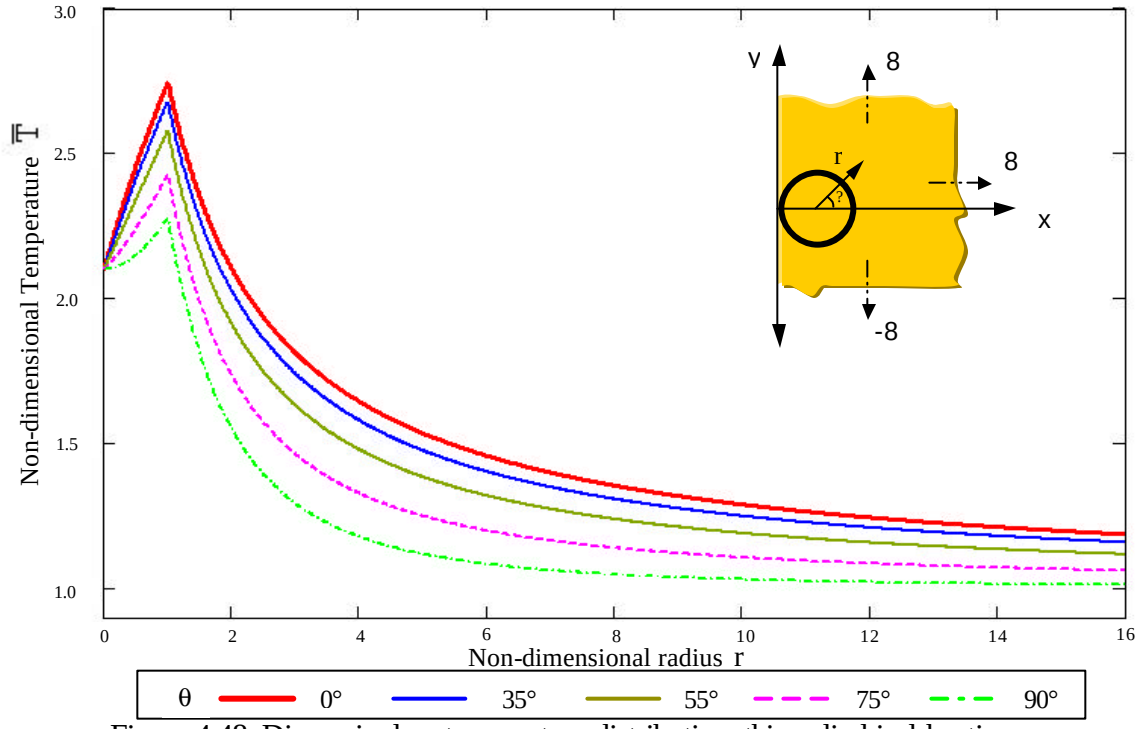

Figure 4.48. Dimensionless temperature distribution, thin cylindrical-heating source $\overline{\lambda}=10,\ \overline{b}=1$

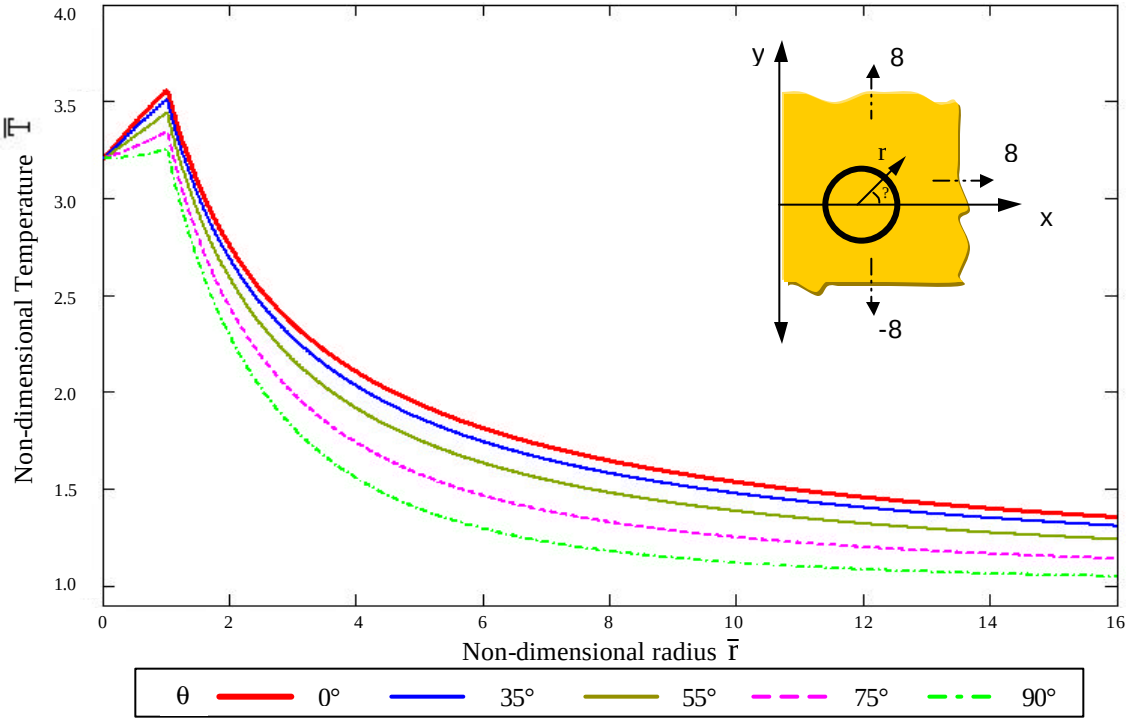

Figure 4.49.(a) Dimensionless temperature distribution, thin cylindrical-heating source $\overline{\lambda}=10,\ \overline{b}=2$

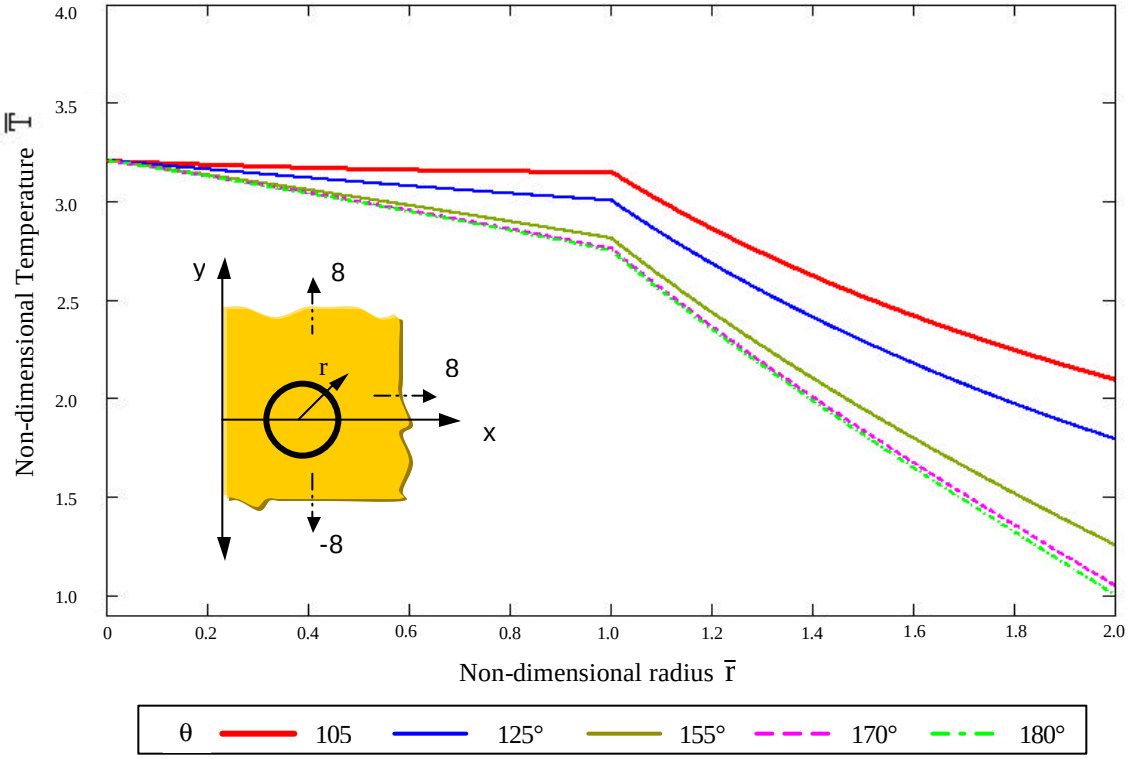

Figure 4.49.(b) Dimensionless temperature distribution, thin cylindrical-heating source $\overline{\lambda}=10,\ \overline{b}=2$

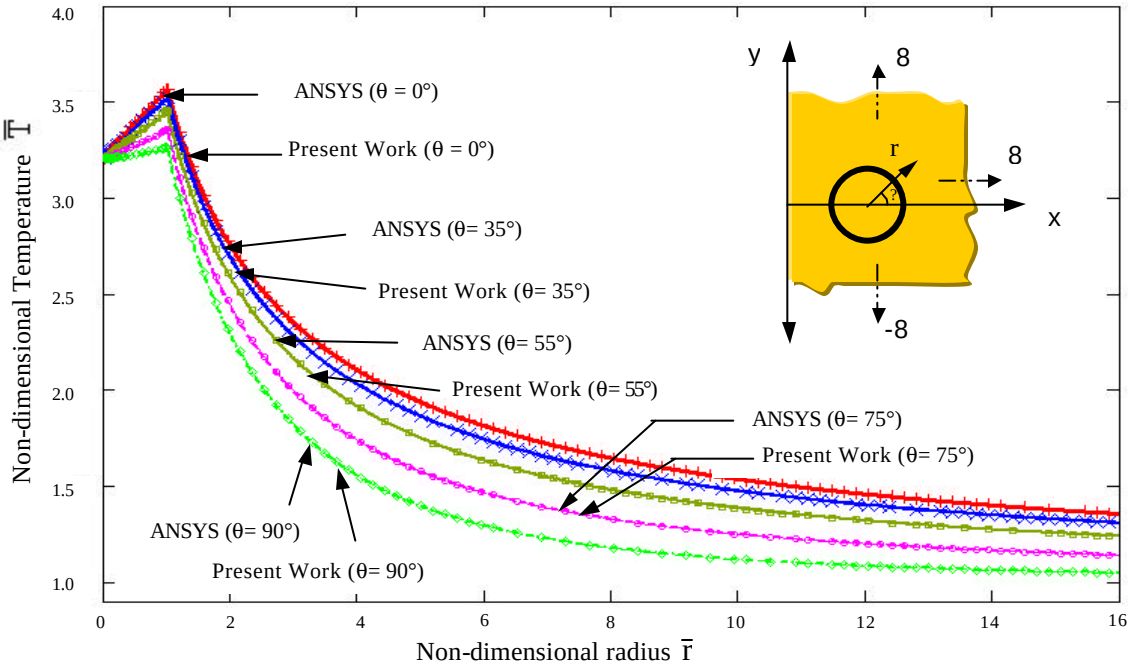

Figure 4.50. Dimensionless temperature distribution, thin cylindrical-heating source $\overline{\lambda}=10,\ \overline{b}=2$. Comparison with result from ANSYS.

Figures 4.43 at 4.50 show the non-dimensional temperature profiles along radial lines for various angles θ and $\overline{b}$. The non-dimensional temperature increases along any radial line increases from the origin to a maximum value when the radial line cuts the source and then drops off monotonically to $\overline{T}=1$ at large distances.

The highest value of the temperature is obtained at point where radial line cuts the source of heat with the angle $\theta=0°$. Figures 4.43 to 4.47 shown result for $\overline{\lambda}=5$ and different values of $\overline{b}$. This result is as expected physically. Same is case for a higher value of the non-dimensional strength of the source $\overline{\lambda}=10$, $\overline{b}=1$ and $\overline{b}=2$. The results

are plotted in the Figures 4.48 to 4.49.(b). Similar behavior as that of the previous curves are observed.

Figure 4.49.(b) shows the behavior of temperature profile near the boundary x = 0, along radial lines for various angles θ, between 90^o and 180^o. The non-dimensional temperature decreases to $\overline{T} = 1$.

For comparison and validation purposes the "almost analytical solution" obtained from Green's function equation is compared with a numerical solution using ANSYS and the results agree closely as shown in figure 4.50 for $\overline{\lambda} = 10$ and $\overline{b} = 2$.

To obtain good precisions computation using ANSYS needed a very fine mesh size with high memory and time requirements. Appendix [F] shows ANSYS element and results. Again our method is almost analytical and superior for parametric studies.

4.2. Semi-Infinite Slab (Three-dimensional case)

4.2.1 Semi-Infinite Slab with a Finite Line Heating Source

A current carrying wire of finite length L $(L = 2b)$ is embedded as a heat-generating element. In a semi-infinite three-dimensional slab $x > 0$, $-\infty < y < \infty$, $-\infty < z < \infty$, and constant thermal conductivity k. The finite line can be assumed as a finite line heat source with finite length L; the heat generation per unit length is constant and the boundary in $x = 0$ is maintained at constant temperature T_B as shown in figure 4.51 (a).

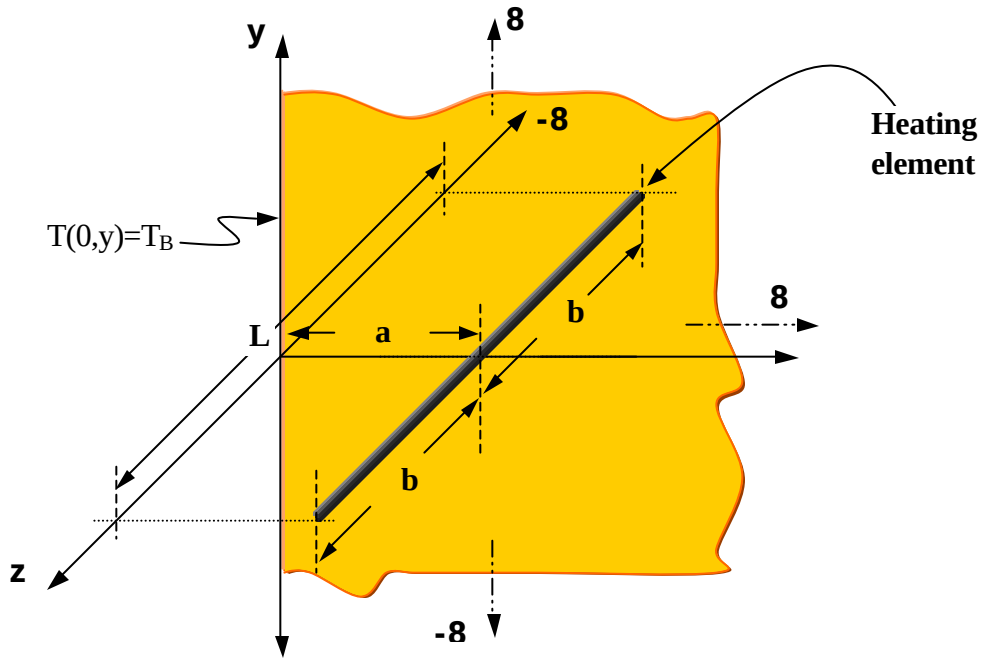

Figure 4.51. (a) Semi-infinite slab with a finite line-heating source

Let:

$Q_T \equiv$ Total heat generation (W) = $\lambda.L$

$\lambda \equiv$ Strength of the heat source per unit length of source (W/m)

$Q(x,y,z) \equiv$ Heat generation intensity per unit volume (W/m^3)

Q(x,y,z) when integrated over the whole volume must be equal to the total heat generation inside the semi-infinite slab, i.e. $\iiint_V Q(x,y,z).dv = Q_T$

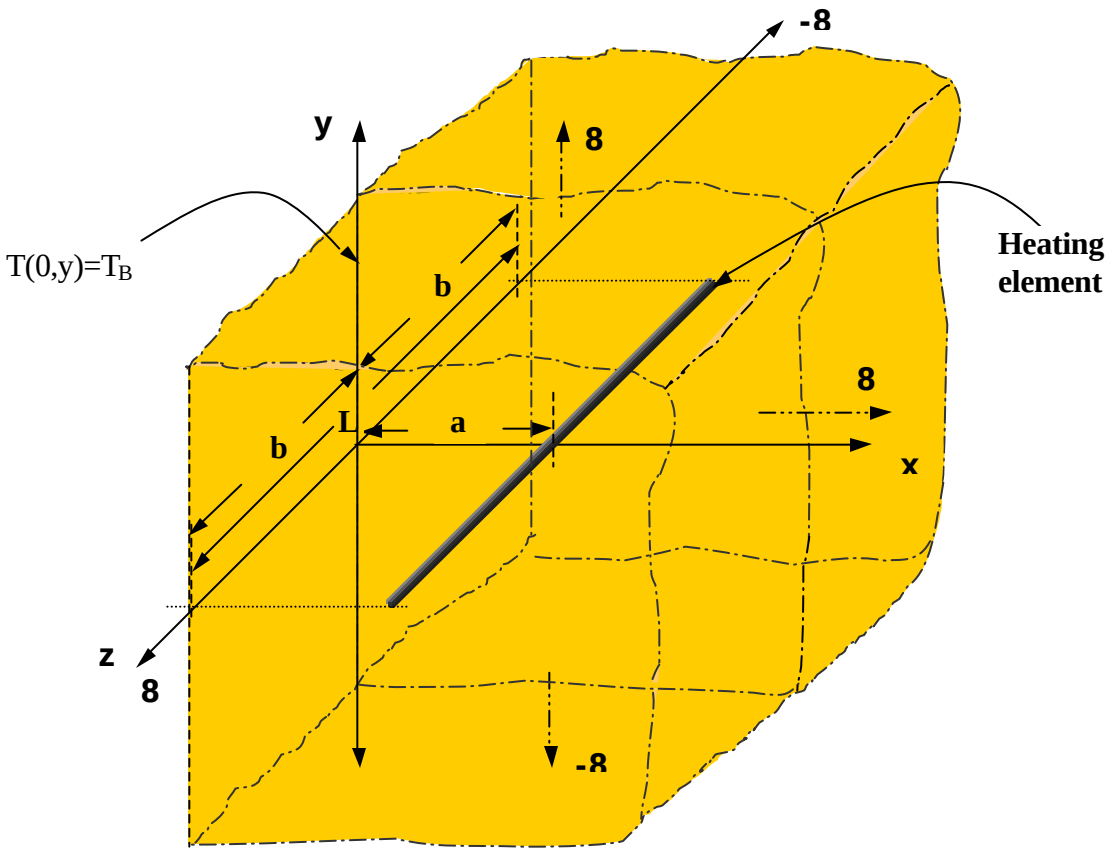

Figure 4.51. (b) Semi-infinite slab with a finite line-heating source

For cartesian coordinates this condition becomes:

$$\int_{-\frac{\ell}{2}}^{\frac{\ell}{2}}\int_{-\infty}^{\infty}\int_{0}^{\infty} Q(x,y,z).dx.dy.dz = Q_T = \lambda.L \quad \ldots\ldots\ldots\ldots\ldots\ldots\ldots\ldots\ldots\ldots\ldots\ldots\ldots\ldots\ldots\ldots \quad (4.24)$$

The heat generation Q(x,y) is expresses of the following form:

$$Q(x,y,z) = \lambda.\delta(x-a).\delta(y).\{H[z+b]-H[z-b]\} \ldots\ldots\ldots\ldots\ldots\ldots\ldots\ldots\ldots\ldots\ldots\ldots\ldots\ldots\ldots\ldots \quad (4.25)$$

The equation (4.25) satisfy to equation (4.24), Now integrate the right hand side of expression (4.25) as indicated in equation (4.24)

$$\int_{-\infty}^{\infty}\int_{-\infty}^{\infty}\int_{0}^{\infty}\{\lambda.\delta(x-a).\delta(y).\{H[z+b]-H[z-b]\}\}.dx.dy.dz = \lambda \int_{-b=-\frac{L}{2}}^{b=\frac{L}{2}} dz.\int_{-\infty}^{\infty}\delta(y).dy\cdot\int_{0}^{\infty}\delta(x-a).dx$$

Using the properties for Dirac-Delta and Heaviside function is obtained:

$$\lambda \int_{-b=-\frac{L}{2}}^{b=\frac{L}{2}} dz.1.1 = \lambda.L$$

Equation (4.24) after integration becomes:

$$\iiint_V Q(x,y,z) = Q_T = \lambda.L$$

Substitute equations (3.35) and (4.25) in equation (4.4):

$$T(x,y,z) = T_B + \frac{\lambda}{4.\pi.k}\int_{-\frac{\ell}{2}}^{\frac{\ell}{2}}\int_{-\infty}^{0}\int_{0}^{\infty}\left\{\begin{array}{l}\{\delta(x-a).\delta(y).\{H[z+b]-H[z-b]\}\}.\\ \left[\dfrac{1}{\sqrt{(x-x')^2+(y-y')^2+(z-z')^2}}-\dfrac{1}{\sqrt{(x+x')^2+(y-y')^2+(z-z')^2}}\right]\end{array}\right\}.dx'dy'dz'$$

Integration on z is easily performed, for x and y the properties for Dirac Delta and Heaviside functions obtaining the following:

$$T(x,y,z) = T_B + \frac{\lambda}{4\pi k}\left\{\int_{-b}^{b}\left[\frac{1}{\sqrt{(x-x')^2+(y-y')^2+(z-z')^2}}-\frac{1}{\sqrt{(x+x')^2+(y-y')^2+(z-z')^2}}\right]dz'\right\}$$

In order to express results in non-dimensional form, the following non-dimensional quantities are defined:

$\overline{T}(\overline{x},\overline{y}) = \dfrac{T(x,y)}{T_B}$ Non-dimensional temperature

$\overline{\lambda} = \dfrac{\lambda}{kT_B}$ Non-dimensional heat generation

$\overline{x} = \dfrac{x}{L},\ \overline{y} = \dfrac{y}{L},\ \overline{z} = \dfrac{z}{L}$ Non-dimensional field point location

$\overline{x}' = \dfrac{x'}{L},\ \overline{y}' = \dfrac{y'}{L}, \overline{z}' = \dfrac{z'}{L}$ Non-dimensional source point location

$\overline{a} = \dfrac{a}{L}$ Non-dimensional distance

Finally, substitute all these quantities in the previous equation and the following relationship is obtained:

$$\overline{T}(\overline{x},\overline{y},\overline{z}) = 1 + \frac{\overline{\lambda}}{4.\pi}\left\{\int_{-1/2}^{1/2}\left[\frac{1}{\sqrt{(\overline{x}-\overline{a}')^2 + (\overline{y})^2 + (\overline{z}-\overline{z}')^2}} - \frac{1}{\sqrt{(\overline{x}+\overline{a}')^2 + (\overline{y})^2 + (\overline{z}-\overline{z}')^2}}\right] dz'\right\}$$

$$\overline{T}(\overline{x},\overline{y},\overline{z}) = 1 + \frac{\overline{\lambda}}{4.\pi}.\ln\left\{\frac{\left[(z+0.5)+\sqrt{(x-a)^2 + y^2 + (z+0.5)^2}\right]}{\left[(z-0.5)+\sqrt{(x-a)^2 + y^2 + (z-0.5)^2}\right]}.\frac{\left[(z-0.5)+\sqrt{(x+a)^2 + y^2 + (z-0.5)^2}\right]}{\left[(z+0.5)+\sqrt{(x+a)^2 + y^2 + (z+0.5)^2}\right]}\right\} \quad \text{..... (4.26)}$$

Where: $\bar{x}' = \bar{a}$, $\bar{y}' = 0$ locates the finite line-heating source

Equation (4.26) is the temperature profile for a semi-infinite slab with constant temperature on boundary heated by a wire in the form of a finite line carrying a current and embedded in the slab. Thus an "analytical solution" for the temperature distribution has been obtained.

Equation (4.26) can be easily evaluated. Some of the results for different values of $\bar{\lambda}$, and $\bar{a}$ are presented in the figures 4.52. (a) to 4.59.

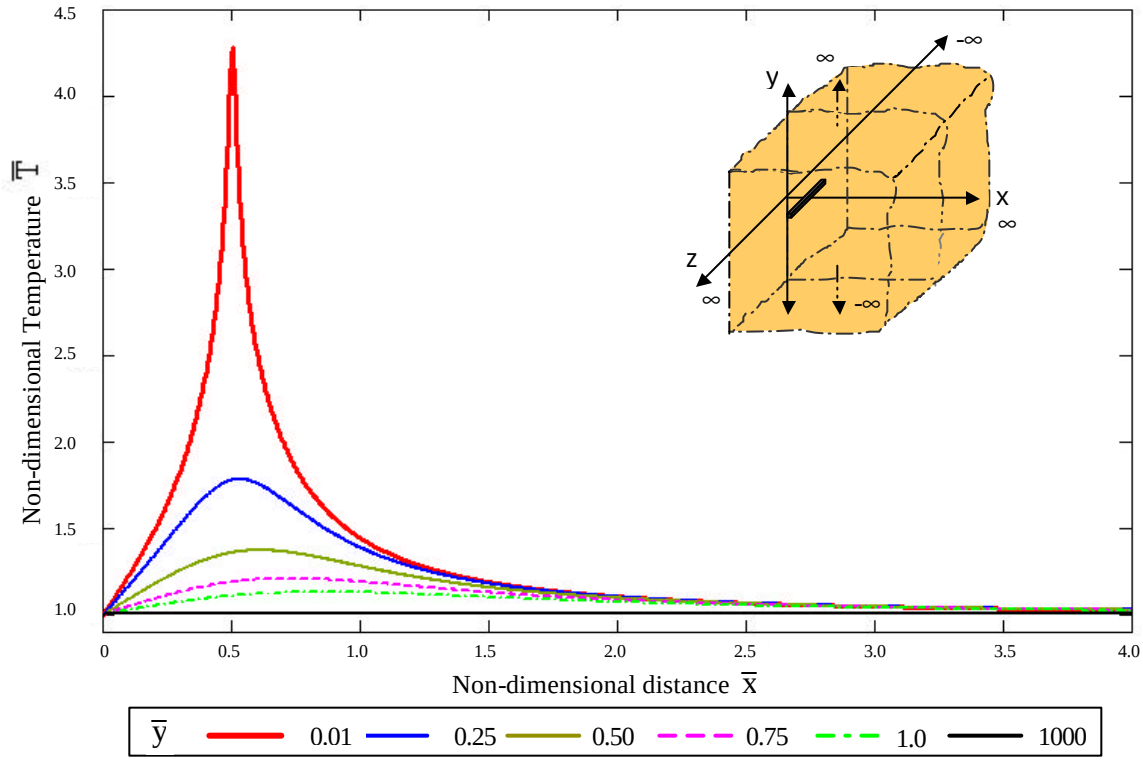

Figure 4.52. (a) Dimensionless temperature distribution, finite line-heating source $\bar{\lambda} = 5,\ \bar{a} = 0.5,\ \bar{z} = 0$.

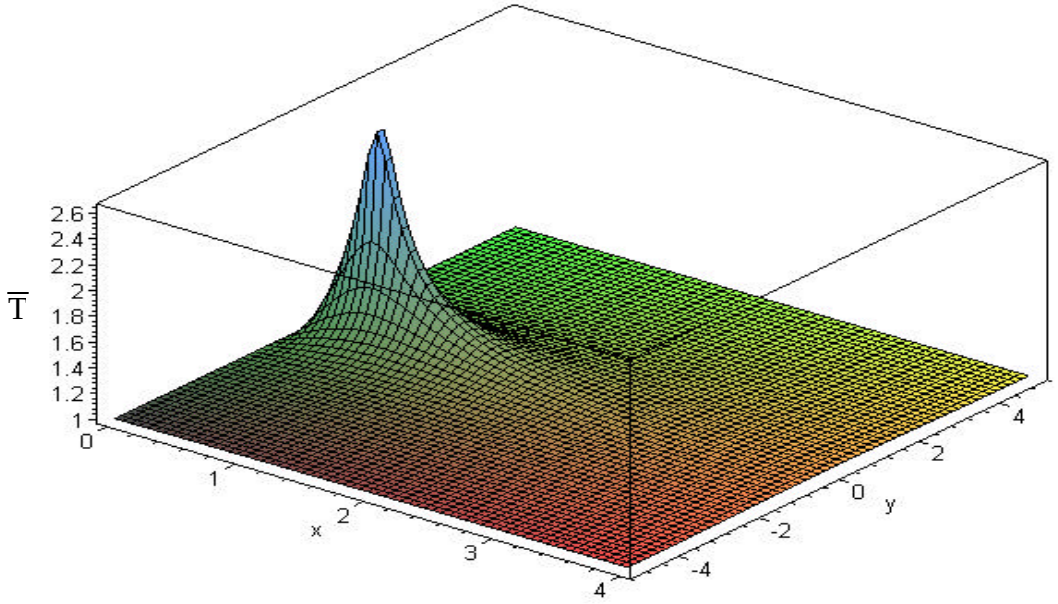

Figure 4.52. (b) Dimensionless temperature distribution, finite line-heating source $\overline{\lambda} = 5,\ \overline{a} = 0.5,\ \overline{z} = 0$.

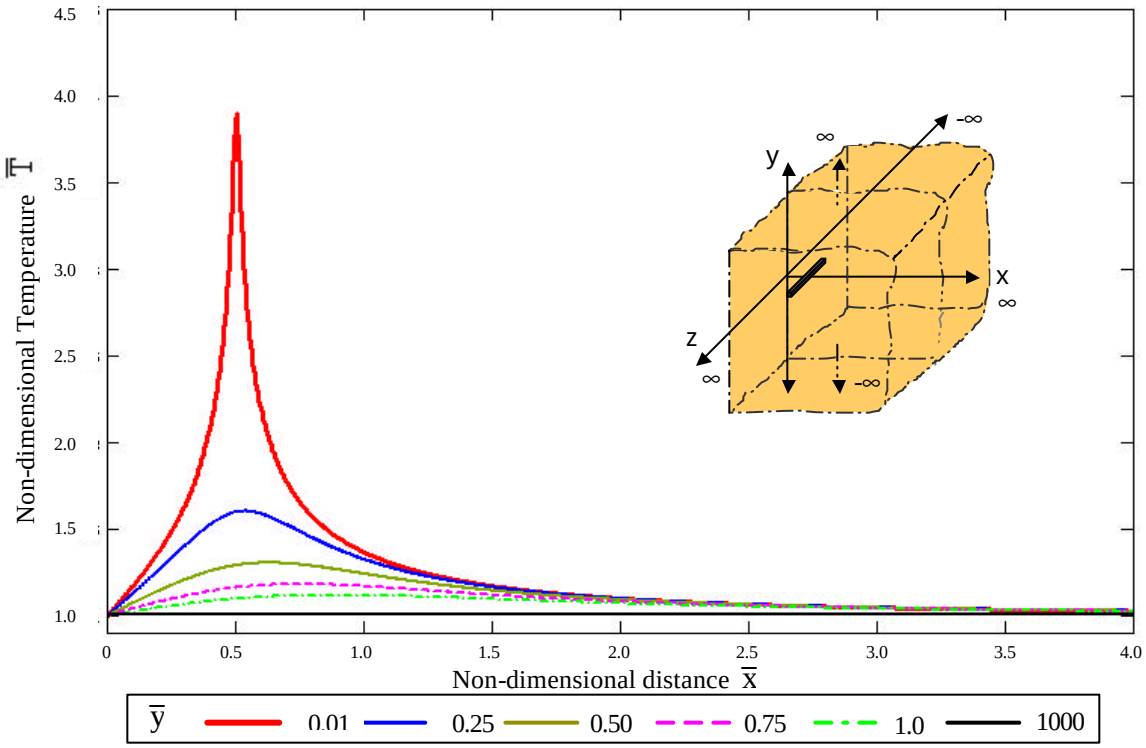

Figure 4.53. (a) Dimensionless temperature distribution, finite line-heating source $\overline{\lambda} = 5,\ \overline{a} = 0.5,\ \overline{z} = \pm 0.4$.

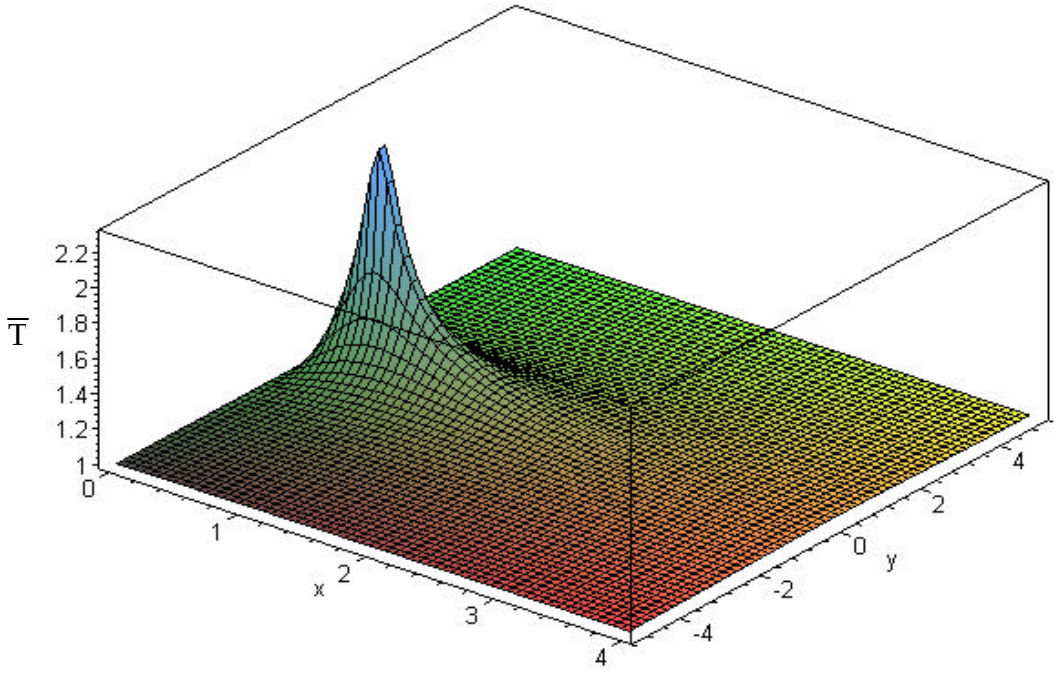

Figure 4.53. (b) Dimensionless temperature distribution, finite line-heating source $\overline{\lambda} = 5,\ \overline{a} = 0.5,\ \overline{z} = \pm 0.4$

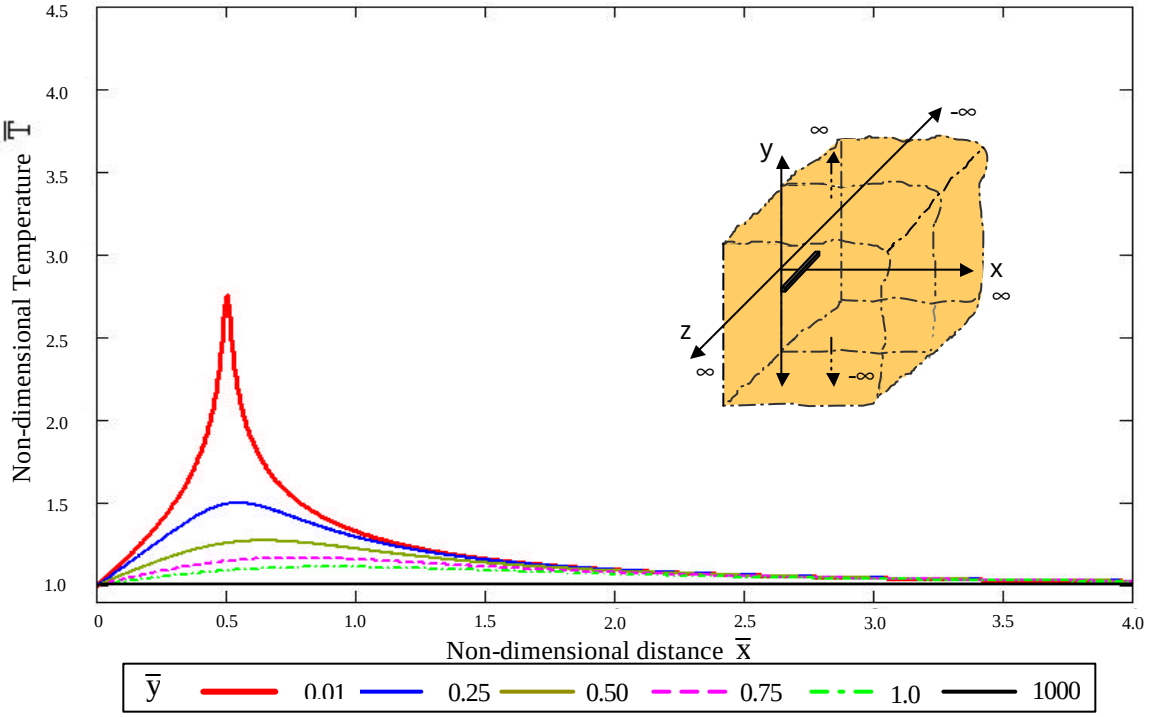

Figure 4.54. (a). Dimensionless temperature distribution, finite line-heating source $\overline{\lambda} = 5,\ \overline{a} = 0.5,\ \overline{z} = \pm 0.5$

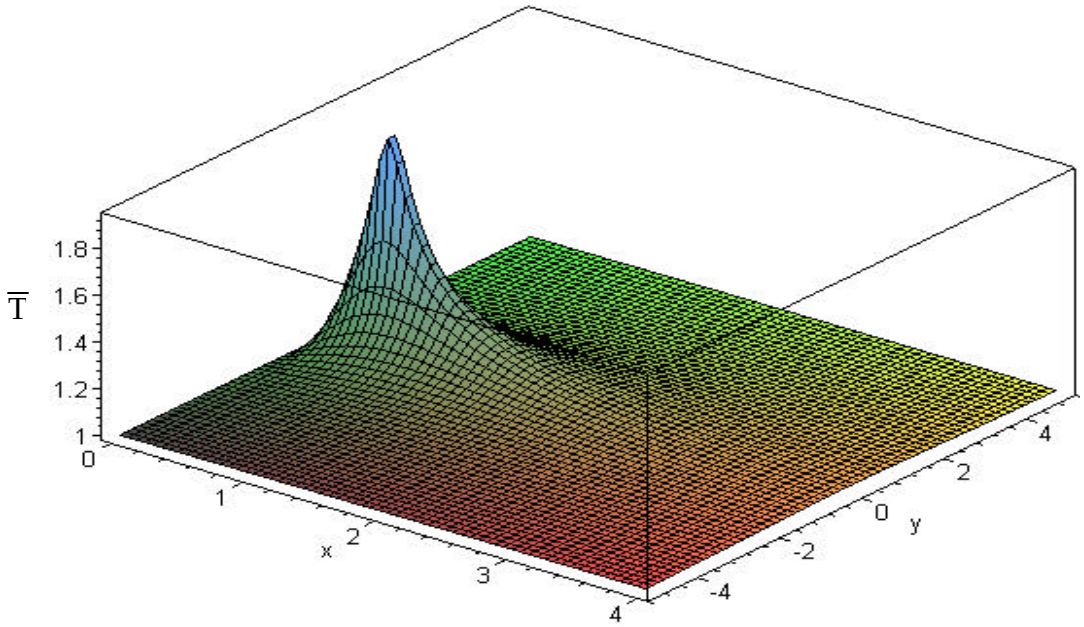

Figure 4.54. (b). Dimensionless temperature distribution, finite line-heating source $\overline{\lambda} = 5,\ \overline{a} = 0.5,\ \overline{z} = \pm 0.5$

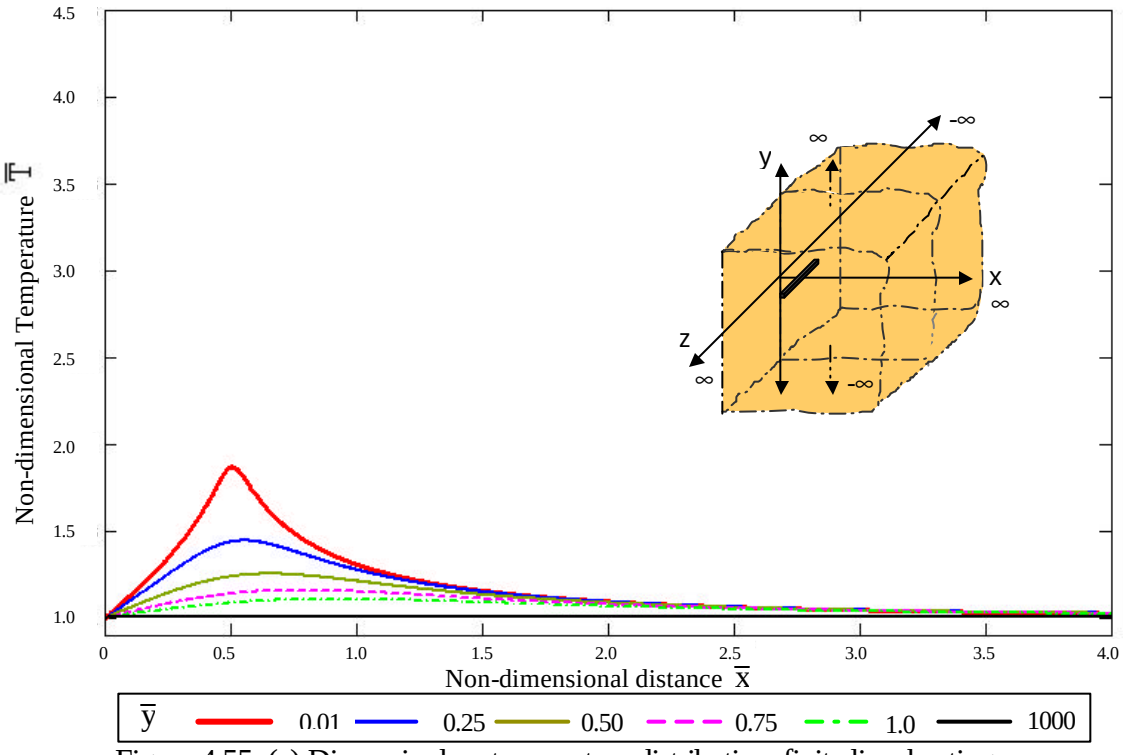

Figure 4.55. (a) Dimensionless temperature distribution, finite line-heating source $\overline{\lambda} = 5,\ \overline{a} = 0.5,\ \overline{z} = \pm 0.55$.

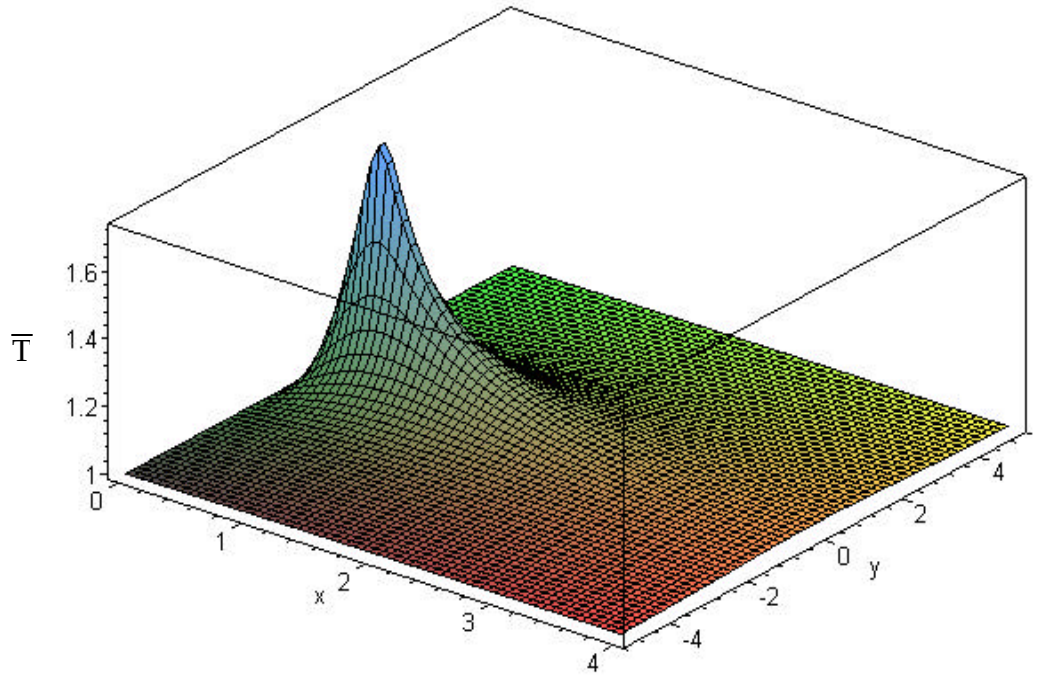

Figure 4.55. (b). Dimensionless temperature distribution, finite line-heating source $\overline{\lambda} = 5,\ \overline{a} = 0.5,\ \overline{z} = \pm 0.55$.

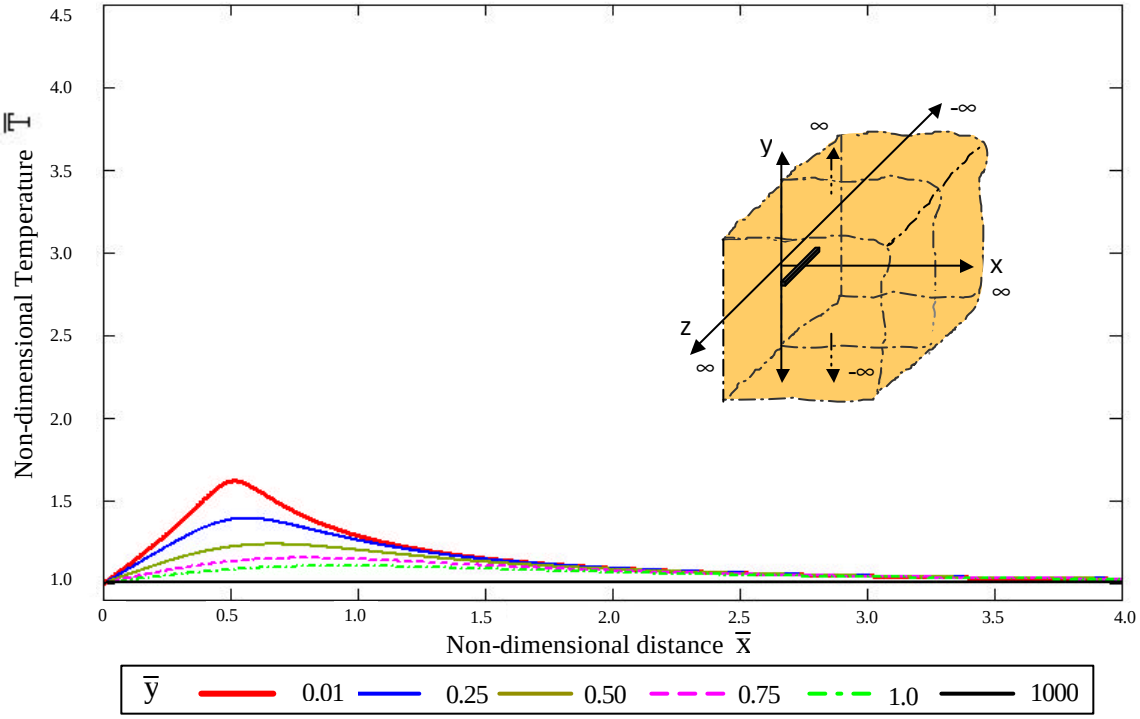

Figure 4.56. (a) Dimensionless temperature distribution, finite line-heating source $\overline{\lambda} = 5,\ \overline{a} = 0.5,\ \overline{z} = \pm 0.6$

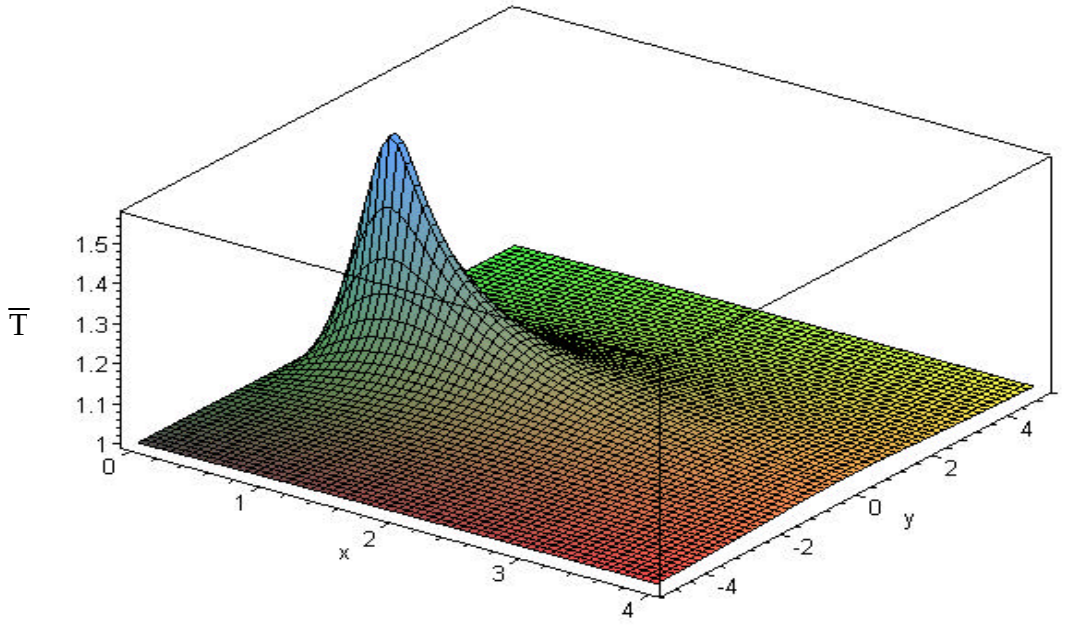

Figure 4.56. (b) Dimensionless temperature distribution, finite line-heating source $\overline{\lambda} = 5,\ \overline{a} = 0.5,\ \overline{z} = \pm 0.6$

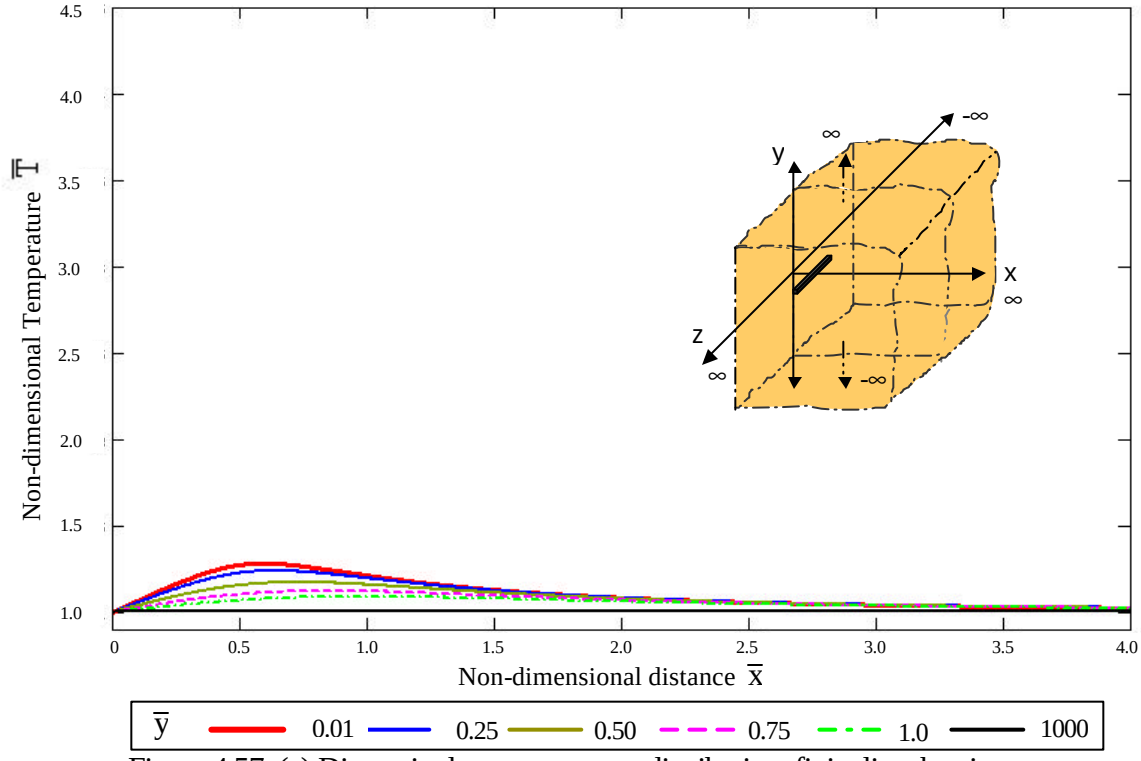

Figure 4.57. (a) Dimensionless temperature distribution, finite line-heating source $\overline{\lambda} = 5,\ \overline{a} = 0.5, \overline{z} = \pm 0.8$.

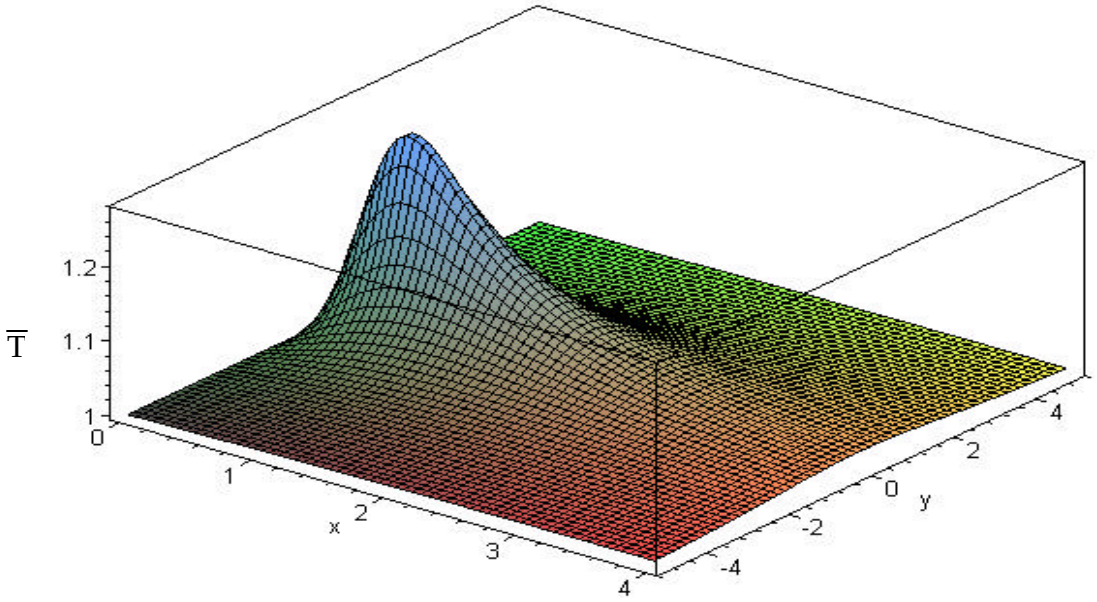

Figure 4.57. (b) Dimensionless temperature distribution, finite line-heating source $\bar{\lambda} = 5,\ \bar{a} = 0.5,\ \bar{z} = \pm 0.8$.

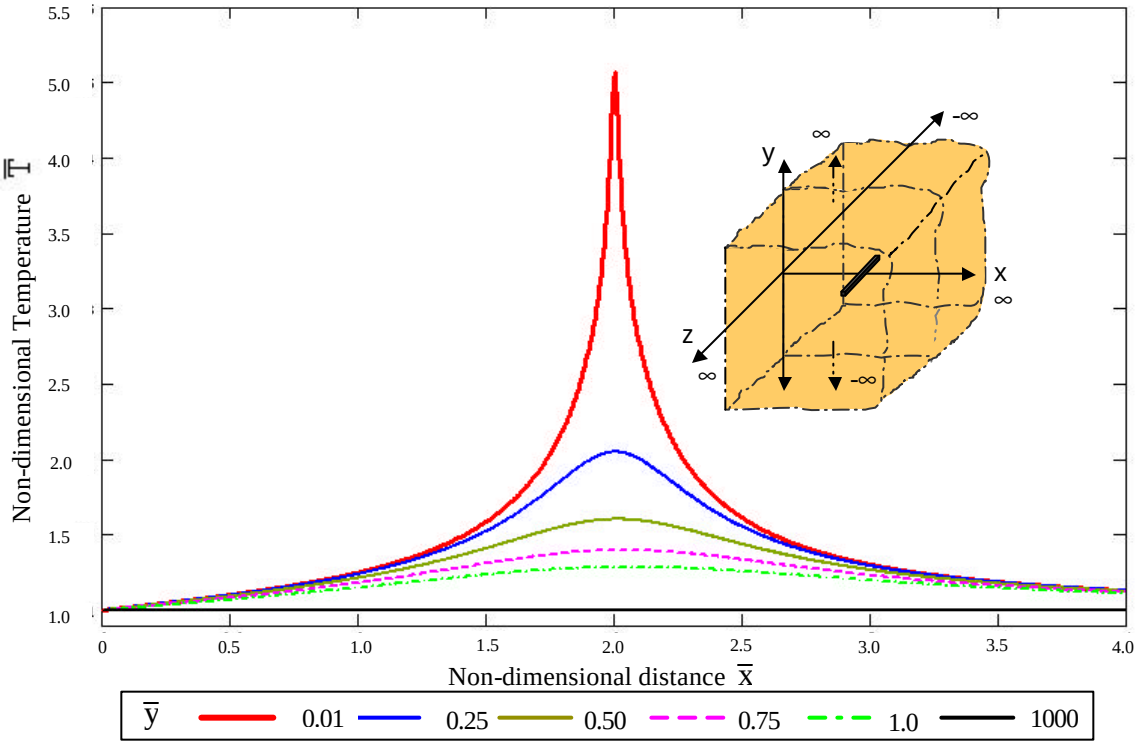

Figure 4.58. Dimensionless temperature distribution, finite line-heating source $\bar{\lambda} = 5,\ \bar{a} = 2,\ \bar{z} = 0$.

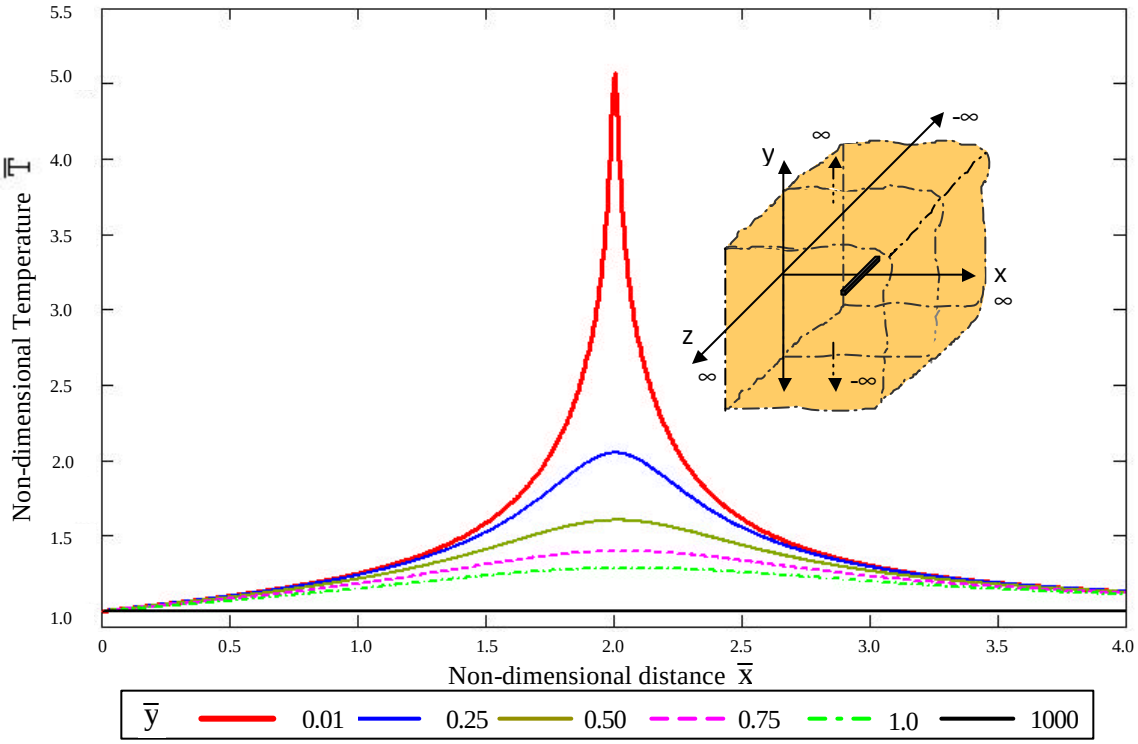

Figure 4.59. Dimensionless temperature distribution, finite line-heating source $\overline{\lambda} = 5,\ \overline{a} = 2,\ \overline{z} = 0$.

The obtained solution is an analytical expression that can be easily evaluated.

Figures 4.52.(a) to 4.59 show the profiles of dimensionless temperature along "$\overline{x}$"axis for different values of "$\overline{y}$" and "$\overline{z}$", with different values of $\overline{\lambda}$ and $\overline{a}$. The figures are in two dimensions, maintaining constant z. We observe that the curves begin in $\overline{T} = 1$ for $\overline{x} = 0$, obtaining the maximum value when cross very close by the source of heat generation, then slowly decrease to $\overline{T} = 1$ for very high values of "x" and "y".

For a given $\overline{y}$, the maximum temperature is obtained when $\overline{x} = \overline{a}$ on the source. Figures 4.52. (a) to 4.57. (b) shown the cases for the constant value of the non-

dimensional strength of the source $\bar{\lambda} = 5$, $\bar{a} = 0.5$, at different values of $\bar{z}$. The same behavior of the previous curves is observed, but the peaks fall to $\bar{T} = 1$ when z>0.

Finally the figures 4.58 to 4.59 shown the cases for the non-dimensional strength of the source $\bar{\lambda} = 5$, $\bar{b} = 0.5$, but different values $\bar{a} = 1$ and $\bar{a} = 2$, maintaining constant the value of $\bar{z} = 0$. The figures have the same behavior of the previous curves. But these are displaced according to the location of the source of heat generation.

Thus we have a closed form analytical solution for temperature distribution in this case, which is easy to evaluate. This problem was not solved numerically by using ANSYS because the problem is fully three-dimensional and is extremely difficult to solve by ANSYS.

4.3. Infinite Quadrant

4.3.1 Infinite Quadrant with a Square Line Heating Source

A thin wire in the form of square line-heating source is embedded, as a heat-generating element in an infinite two-dimensional quadrant $x > 0$, $y > 0$, $-\infty < z < \infty$, and constant thermal conductivity k. The square line can be assumed as a square line source with walls infinitesimally thin, side L and large depth ℓ; the heat generation per unit length per unit depth is constant and the boundary in $x = 0$ and $y = 0$ is maintained at constant temperature T_B as shown in figure 4.60. (a)

Let:

$Q_T \equiv$ Total heat generation (W) = $4.\lambda.\ell.L$

$\lambda \equiv$ Strength of the heat source per unit depth per unit length (W/m^2)

$Q(x,y) \equiv$ Heat generation per unit volume (W/m^3)

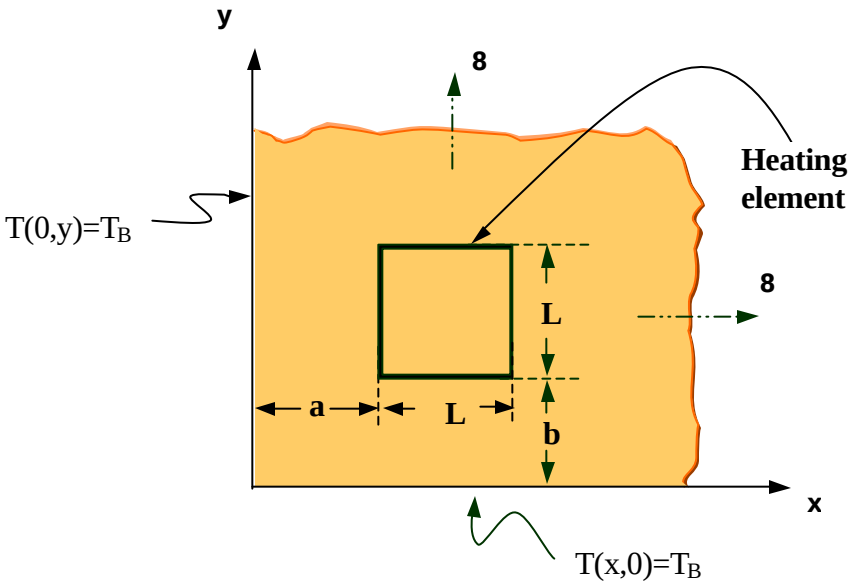

Figure 4.60. (a) Infinite quadrant with a square line-heating source

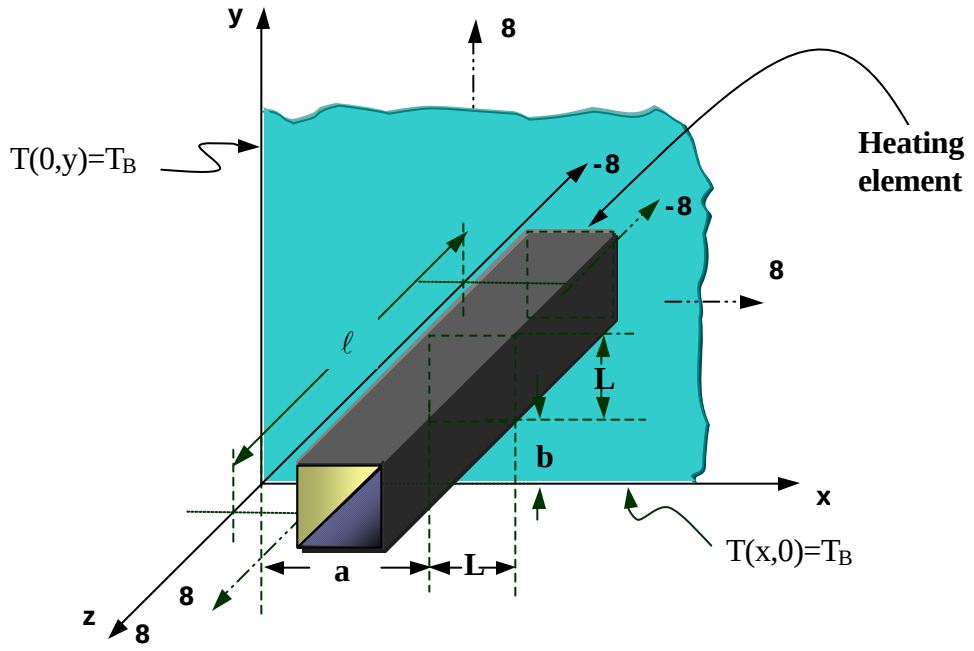

Figure 4.60. (b) Infinite quadrant with a square line heating source

Q(x,y) when integrated over the whole volume must be equal to the total heat generation inside the hollow box, i.e. $\iiint_V Q(x,y).dv = Q_T$

For cartesian coordinates this condition becomes:

$$\int_{-\frac{\ell}{2}}^{\frac{\ell}{2}}\int_{0}^{\infty}\int_{0}^{\infty} Q(x,y).dx.dy.dz = Q_T = \lambda.\ell.[L+L+L+L] = 4.\lambda.\ell.L \ldots\ldots\ldots\ldots\ldots\ldots \quad (4.27)$$

The heat generation Q(x,y) is expresses of the following form:

$$Q(x,y) = \begin{Bmatrix} \lambda\cdot\delta(y-b)\cdot\{H[x-a]-H[x-(L+a)]\}+ \\ \lambda\cdot\delta(x-(L+a))\cdot\{H[y-b]-H[y-(L+b)]\}+ \\ \lambda\cdot\delta(y-(L+b))\cdot\{H[x-a]-H[x-(L+a)]\}+ \\ \lambda\cdot\delta(x-a)\cdot\{H[y-b]-H[y-(L+b)]\} \end{Bmatrix} \ldots\ldots\ldots\ldots\ldots\ldots \quad (4.28)$$

The equation (4.28) satisfy to equation (4.27), Now integrate the right hand side of expression (4.28) as indicated in equation (4.27)

$$\int_{-\frac{\ell}{2}}^{\frac{\ell}{2}}\int_{0}^{\infty}\int_{0}^{\infty}\begin{Bmatrix}\lambda\cdot\delta(y-b)\cdot\{H[x-a]-H[x-(L+a)]\}+\\ \lambda\cdot\delta(x-(L+a))\cdot\{H[y-b]-H[y-(L+b)]\}+\\ \lambda\cdot\delta(y-(L+b))\cdot\{H[x-a]-H[x-(L+a)]\}+\\ \lambda\cdot\delta(x-a)\cdot\{H[y-b]-H[y-(L+b)]\}\end{Bmatrix}.dx.dy.dz =$$

$$\lambda\int_{-\frac{\ell}{2}}^{\frac{\ell}{2}}dz.\int_{0}^{\infty}\delta(y-b).dy\cdot\int_{0}^{\infty}\{H[x-a]-H[x-(L+a)]\}.dx +$$

$$\lambda\int_{-\frac{\ell}{2}}^{\frac{\ell}{2}}dz.\int_{0}^{\infty}\delta(x-(L+a)).dx\cdot\int_{0}^{\infty}\{H[y-b]-H[y-(L+b)]\}.dy +$$

$$\lambda\int_{-\frac{\ell}{2}}^{\frac{\ell}{2}}dz.\int_{0}^{\infty}\delta(y-(L+b)).dy\cdot\int_{0}^{\infty}\{H[x-a]-H[x-(L+a)]\}.dx +$$

$$\lambda\int_{-\frac{\ell}{2}}^{\frac{\ell}{2}}dz.\int_{0}^{\infty}\delta(x-a).dx\cdot\int_{0}^{\infty}\{H[y-b]-H[y-(L+b)]\}.dy$$

Using the properties for Dirac-Delta and Heaviside function is obtained:

$$\lambda\cdot\ell\cdot 1.\int_{a}^{L+a}dx+\lambda\cdot\ell\cdot 1.\int_{b}^{L+b}dy+\lambda\cdot\ell\cdot 1.\int_{a}^{L+a}dx+\lambda\cdot\ell\cdot 1.\int_{b}^{L+b}dy=\begin{Bmatrix}\lambda\cdot\ell\cdot L+\lambda\cdot\ell\cdot L+\\ \lambda\cdot\ell\cdot L+\lambda\cdot\ell\cdot L\end{Bmatrix}$$

Equation (4.27) after integration becomes:

$$\iiint_{V}Q(x,y)=Q_{T}=\lambda\cdot\ell\cdot[L+L+L+L]=4.\lambda.\ell.L$$

Substitute equations (3.39) and (4.28) in equation (4.4):

$$T(x,y)=T_B+\frac{\lambda}{4\pi k\ell}\int_{-\frac{\ell}{2}}^{\frac{\ell}{2}}\int_0^\infty\int_0^\infty\left\{\begin{array}{l}\delta(y'-b)\cdot\{H[x-a]-H[x-L-a]\}\cdot\\ \ln\left\{\dfrac{\left[(x-x')^2+(y+b)^2\right]\cdot\left[(x+x')^2+(y-b)^2\right]}{\left[(x-x')^2+(y-b)^2\right]\cdot\left[(x+x')^2+(y+b)^2\right]}\right\}+\\ \delta(x'-L-a)\cdot\{H[y+L+b]-H[y-L-b]\}\cdot\\ \ln\left\{\dfrac{\left[(x-L-a)^2+(y+y')^2\right]\cdot\left[(x+L+a)^2+(y-y')^2\right]}{\left[(x-L-a)^2+(y-y')^2\right]\cdot\left[(x+L+a)^2+(y+y')^2\right]}\right\}+\\ \delta(y-L-b)\cdot\{H[x-a]-H[x-L-a]\}\cdot\\ \ln\left\{\dfrac{\left[(x-x')^2+(y+L+b)^2\right]\cdot\left[(x+x')^2+(y-L-b)^2\right]}{\left[(x-x')^2+(y-L-b)^2\right]\cdot\left[(x+x')^2+(y+L+b)^2\right]}\right\}+\\ \delta(x'-a)\cdot\{H[y+L+b]-H[y-L-b]\}\cdot\\ \ln\left\{\dfrac{\left[(x-a)^2+(y+y')^2\right]\cdot\left[(x+a)^2+(y-y')^2\right]}{\left[(x-a)^2+(y-y')^2\right]\cdot\left[(x+a)^2+(y+y')^2\right]}\right\}\end{array}\right\}\cdot dx'\,dy'\,dz'$$

Integration on z is easily performed, for x and y the properties for Dirac Delta and Heaviside functions obtaining the following expression:

$$T(x,y)=T_B+\frac{\lambda}{4\pi k}\cdot\left\{\begin{array}{l}\displaystyle\int_a^{L+a}\left\{\begin{array}{l}\ln\left\{\dfrac{\left[(x-x')^2+(y+b)^2\right]\cdot\left[(x+x')^2+(y-b)^2\right]}{\left[(x-x')^2+(y-b)^2\right]\cdot\left[(x+x')^2+(y+b)^2\right]}\right\}+\\ \ln\left\{\dfrac{\left[(x-x')^2+(y+L+b)^2\right]\cdot\left[(x+x')^2+(y-L-b)^2\right]}{\left[(x-x')^2+(y-L-b)^2\right]\cdot\left[(x+x')^2+(y+L+b)^2\right]}\right\}\end{array}\right\}\cdot dx+\\ \displaystyle\int_b^{L+b}\left\{\begin{array}{l}\ln\left\{\dfrac{\left[(x-L-a)^2+(y+y')^2\right]\cdot\left[(x+L+a)^2+(y-y')^2\right]}{\left[(x-L-a)^2+(y-y')^2\right]\cdot\left[(x+L+a)^2+(y+y')^2\right]}\right\}+\\ \ln\left\{\dfrac{\left[(x-a)^2+(y+y')^2\right]\cdot\left[(x+a)^2+(y-y')^2\right]}{\left[(x-a)^2+(y-y')^2\right]\cdot\left[(x+a)^2+(y+y')^2\right]}\right\}\end{array}\right\}\cdot dy\end{array}\right\}$$

In order to express results in non-dimensional form the following non-dimensional quantities are defined:

$\overline{T}(\overline{x},\overline{y}) = \dfrac{T(x,y)}{T_B}$ Non-dimensional temperature

$\overline{\lambda} = \dfrac{\lambda L}{kT_B}$ Non-dimensional heat generation

$\overline{x} = \dfrac{x}{L}, \overline{y} = \dfrac{y}{L}$ Non-dimensional field point location

$\overline{x}' = \dfrac{x'}{L}, \overline{y}' = \dfrac{y'}{L}$ Non-dimensional source point location

$\overline{a} = \dfrac{a}{L}, \overline{b} = \dfrac{b}{L}$ Non-dimensional distances

Finally, substitute all these quantities in the previous equation and the following relationship is obtained:

$$\overline{T}(\overline{x},\overline{y}) = 1 + \frac{\overline{\lambda}}{4.\pi}.\left\{\begin{array}{l}\displaystyle\int_{\overline{a}}^{1+\overline{a}} \left\{\begin{array}{l}\ln\left\{\dfrac{\left[(\overline{x}-\overline{x}')^2+(\overline{y}+\overline{b})^2\right]\left[(\overline{x}+\overline{x}')^2+(\overline{y}-\overline{b})^2\right]}{\left[(\overline{x}-\overline{x}')^2+(\overline{y}-\overline{b})^2\right]\left[(\overline{x}+\overline{x}')^2+(\overline{y}+\overline{b})^2\right]}\right\}+ \\ \ln\left\{\dfrac{\left[(\overline{x}-\overline{x}')^2+(\overline{y}+1+\overline{b})^2\right]\left[(\overline{x}+\overline{x}')^2+(\overline{y}-1-\overline{b})^2\right]}{\left[(\overline{x}-\overline{x}')^2+(\overline{y}-1-\overline{b})^2\right]\left[(\overline{x}+\overline{x}')^2+(\overline{y}+1+\overline{b})^2\right]}\right\}\end{array}\right\}.d\overline{x}+ \\ \displaystyle\int_{\overline{b}}^{1+\overline{b}} \left\{\begin{array}{l}\ln\left\{\dfrac{\left[(\overline{x}-1-\overline{a})^2+(\overline{y}+\overline{y}')^2\right]\left[(\overline{x}+1+\overline{a})^2+(\overline{y}-\overline{y}')^2\right]}{\left[(\overline{x}-1-\overline{a})^2+(\overline{y}-\overline{y}')^2\right]\left[(\overline{x}+1+\overline{a})^2+(\overline{y}+\overline{y}')^2\right]}\right\}+ \\ \ln\left\{\dfrac{\left[(\overline{x}-\overline{a})^2+(\overline{y}+\overline{y}')^2\right]\left[(\overline{x}+\overline{a})^2+(\overline{y}-\overline{y}')^2\right]}{\left[(\overline{x}-\overline{a})^2+(\overline{y}-\overline{y}')^2\right]\left[(\overline{x}+\overline{a})^2+(\overline{y}+y')^2\right]}\right\}\end{array}\right\}.d\overline{y}\end{array}\right\}$$

$$\overline{T}(\overline{x},\overline{y}) = 1+\frac{\overline{\lambda}}{4.\pi}\left[\begin{array}{l}
(\overline{x}+\overline{a}).\left\{\begin{array}{l}\ln\left[\dfrac{\left[(\overline{x}+\overline{a})^2+(\overline{y}+\overline{b})^2\right]\left[(\overline{x}+\overline{a})^2+(\overline{y}+1+\overline{b})^2\right]}{\left[(\overline{x}+\overline{a})^2+(\overline{y}-\overline{b})^2\right]\left[(\overline{\overline{x}}+\overline{a})^2+(\overline{y}-1-\overline{b})^2\right]}\right]+2.\mathrm{Arctg}\left(\dfrac{\overline{y}-\overline{b}}{\overline{x}+\overline{a}}\right)-\\ 2.\mathrm{Arctg}\left(\dfrac{\overline{y}-1-\overline{b}}{\overline{x}+\overline{a}}\right)+2.\mathrm{Arctg}\left(\dfrac{\overline{y}+\overline{b}}{\overline{x}+a}\right)-2.\mathrm{Arctg}\left(\dfrac{\overline{y}+1+\overline{b}}{\overline{x}+\overline{a}}\right)\end{array}\right\}+\\
(\overline{x}+1+\overline{a}).\left\{\begin{array}{l}\ln\left[\dfrac{\left[(\overline{x}+1+\overline{a})^2+(\overline{y}-\overline{b})^2\right]\left[(\overline{x}+1+\overline{a})^2+(\overline{y}-1-\overline{b})^2\right]}{\left[(\overline{x}+1+\overline{a})^2+(\overline{y}+\overline{b})^2\right]\left[(\overline{\overline{x}}+1+\overline{a})^2+(\overline{y}+1+\overline{b})^2\right]}\right]+2.\mathrm{Arctg}\left(\dfrac{\overline{y}-\overline{b}}{\overline{x}+1+\overline{a}}\right)-\\ 2.\mathrm{Arctg}\left(\dfrac{\overline{y}-1-\overline{b}}{\overline{x}+1+\overline{a}}\right)+2.\mathrm{Arctg}\left(\dfrac{\overline{y}+\overline{b}}{\overline{x}+1+\overline{a}}\right)-2.\mathrm{Arctg}\left(\dfrac{\overline{y}+1+\overline{b}}{\overline{x}+1+\overline{a}}\right)\end{array}\right\}+\\
(\overline{x}-\overline{a}).\left\{\begin{array}{l}\ln\left[\dfrac{\left[(\overline{x}-\overline{a})^2+(\overline{y}+\overline{b})^2\right]\left[(\overline{x}-\overline{a})^2+(\overline{y}+1+\overline{b})^2\right]}{\left[(\overline{x}-\overline{a})^2+(\overline{y}-\overline{b})^2\right]\left[(\overline{\overline{x}}-\overline{a})^2+(\overline{y}-1-\overline{b})^2\right]}\right]+2.\mathrm{Arctg}\left(\dfrac{\overline{y}+1+\overline{b}}{\overline{x}-\overline{a}}\right)-\\ 2.\mathrm{Arctg}\left(\dfrac{\overline{y}+\overline{b}}{\overline{x}-a}\right)+2.\mathrm{Arctg}\left(\dfrac{\overline{y}-1-\overline{b}}{\overline{x}-\overline{a}}\right)-2.\mathrm{Arctg}\left(\dfrac{\overline{y}-\overline{b}}{\overline{x}-\overline{a}}\right)\end{array}\right\}+\\
(\overline{x}-1-\overline{a}).\left\{\begin{array}{l}\ln\left[\dfrac{\left[(\overline{x}-1-\overline{a})^2+(\overline{y}-\overline{b})^2\right]\left[(\overline{x}-1-\overline{a})^2+(\overline{y}-1-\overline{b})^2\right]}{\left[(\overline{x}-1-\overline{a})^2+(\overline{y}+\overline{b})^2\right]\left[(\overline{\overline{x}}-1-\overline{a})^2+(\overline{y}+1+\overline{b})^2\right]}\right]+2.\mathrm{Arctg}\left(\dfrac{\overline{y}+1+\overline{b}}{\overline{x}-1-\overline{a}}\right)-\\ 2.\mathrm{Arctg}\left(\dfrac{\overline{y}+\overline{b}}{\overline{x}-1-\overline{a}}\right)+2.\mathrm{Arctg}\left(\dfrac{\overline{y}-1-\overline{b}}{\overline{x}-1-\overline{a}}\right)-2.\mathrm{Arctg}\left(\dfrac{\overline{y}-\overline{b}}{\overline{x}-1-\overline{a}}\right)\end{array}\right\}+\\
(\overline{y}+\overline{b}).\left\{\begin{array}{l}\ln\left[\dfrac{\left[\left(\overline{y}+\overline{b}\right)^2+(\overline{x}+1+\overline{a})^2\right].\left[(\overline{y}+\overline{b})^2+(\overline{x}+\overline{a})^2\right]}{\left[\left(\overline{y}+\overline{b}\right)^2+(\overline{x}-1-\overline{a})^2\right].\left[(\overline{y}+\overline{b})^2+(\overline{x}-\overline{a})^2\right]}\right]+2.\mathrm{Arctg}\left(\dfrac{\overline{x}+\overline{a}}{\overline{y}+\overline{b}}\right)-\\ 2.\mathrm{Arctg}\left(\dfrac{\overline{x}+1+\overline{a}}{\overline{y}+\overline{b}}\right)+2.\mathrm{Arctg}\left(\dfrac{\overline{x}-\overline{a}}{\overline{y}+\overline{\overline{b}}}\right)-2.\mathrm{Arctg}\left(\dfrac{\overline{x}-1-\overline{a}}{\overline{y}+\overline{b}}\right)\end{array}\right\}+\\
(\overline{y}+1+\overline{b}).\left\{\begin{array}{l}\ln\left[\dfrac{\left[\left(\overline{y}+1+\overline{b}\right)^2+(\overline{x}-1-\overline{a})^2\right].\left[(\overline{y}+1+\overline{b})^2+(\overline{x}-\overline{a})^2\right]}{\left[\left(\overline{y}+1+\overline{b}\right)^2+(\overline{x}+1+\overline{a})^2\right].\left[(\overline{y}+1+\overline{b})^2+(\overline{x}+\overline{a})^2\right]}\right]+2.\mathrm{Arctg}\left(\dfrac{\overline{x}-\overline{a}}{\overline{y}+1+\overline{b}}\right)-\\ 2.\mathrm{Arctg}\left(\dfrac{\overline{x}-1-\overline{a}}{\overline{y}+1+\overline{b}}\right)+2.\mathrm{Arctg}\left(\dfrac{\overline{x}+\overline{a}}{\overline{y}+1+\overline{\overline{b}}}\right)-2.\mathrm{Arctg}\left(\dfrac{\overline{x}+1+\overline{a}}{\overline{y}+1+\overline{\overline{b}}}\right)\end{array}\right\}+\\
(\overline{y}-\overline{b}).\left\{\begin{array}{l}\ln\left[\dfrac{\left[\left(\overline{y}-\overline{b}\right)^2+(\overline{x}+1+\overline{a})^2\right].\left[(\overline{y}-\overline{b})^2+(\overline{x}+\overline{a})^2\right]}{\left[\left(\overline{y}-\overline{b}\right)^2+(\overline{x}-1-\overline{a})^2\right].\left[(\overline{y}-\overline{b})^2+(\overline{x}-\overline{a})^2\right]}\right]+2.\mathrm{Arctg}\left(\dfrac{\overline{x}-1-\overline{a}}{\overline{y}-\overline{b}}\right)-\\ 2.\mathrm{Arctg}\left(\dfrac{\overline{x}-\overline{a}}{\overline{y}-\overline{\overline{b}}}\right)+2.\mathrm{Arctg}\left(\dfrac{\overline{x}+1+\overline{a}}{\overline{y}-\overline{b}}\right)-2.\mathrm{Arctg}\left(\dfrac{\overline{x}+\overline{a}}{\overline{y}-\overline{\overline{b}}}\right)\end{array}\right\}+\\
(\overline{y}-1-\overline{b}).\left\{\begin{array}{l}\ln\left[\dfrac{\left[\left(\overline{y}-1-\overline{b}\right)^2+(\overline{x}-1-\overline{a})^2\right].\left[(\overline{y}-1-\overline{b})^2+(\overline{x}-\overline{a})^2\right]}{\left[\left(\overline{y}-1-\overline{b}\right)^2+(\overline{x}+1+\overline{a})^2\right].\left[(\overline{y}-1-\overline{b})^2+(\overline{x}+\overline{a})^2\right]}\right]+2.\mathrm{Arctg}\left(\dfrac{\overline{x}+1+\overline{a}}{\overline{y}-1-\overline{b}}\right)-\\ 2.\mathrm{Arctg}\left(\dfrac{\overline{x}+\overline{a}}{\overline{y}-1-\overline{\overline{b}}}\right)+2.\mathrm{Arctg}\left(\dfrac{\overline{x}-1-\overline{a}}{\overline{y}-1-\overline{\overline{b}}}\right)-2.\mathrm{Arctg}\left(\dfrac{\overline{x}-\overline{a}}{\overline{y}-1-\overline{\overline{b}}}\right)\end{array}\right\}
\end{array}\right]. \quad (4.29)$$

Equation (4.29) is the temperature profile for an infinite quadrant with constant temperature on boundary heated by a wire in the form of a thin line square, carrying a current and embedded in the slab. Thus an exact solution for the temperature distribution has been obtained.

Equation (4.29), even though is long, can be easily evaluated. Some of the results for different values of $\bar{\lambda}$, $\bar{a}$ and $\bar{b}$ are presented in the figures 4.61 to 4.71.

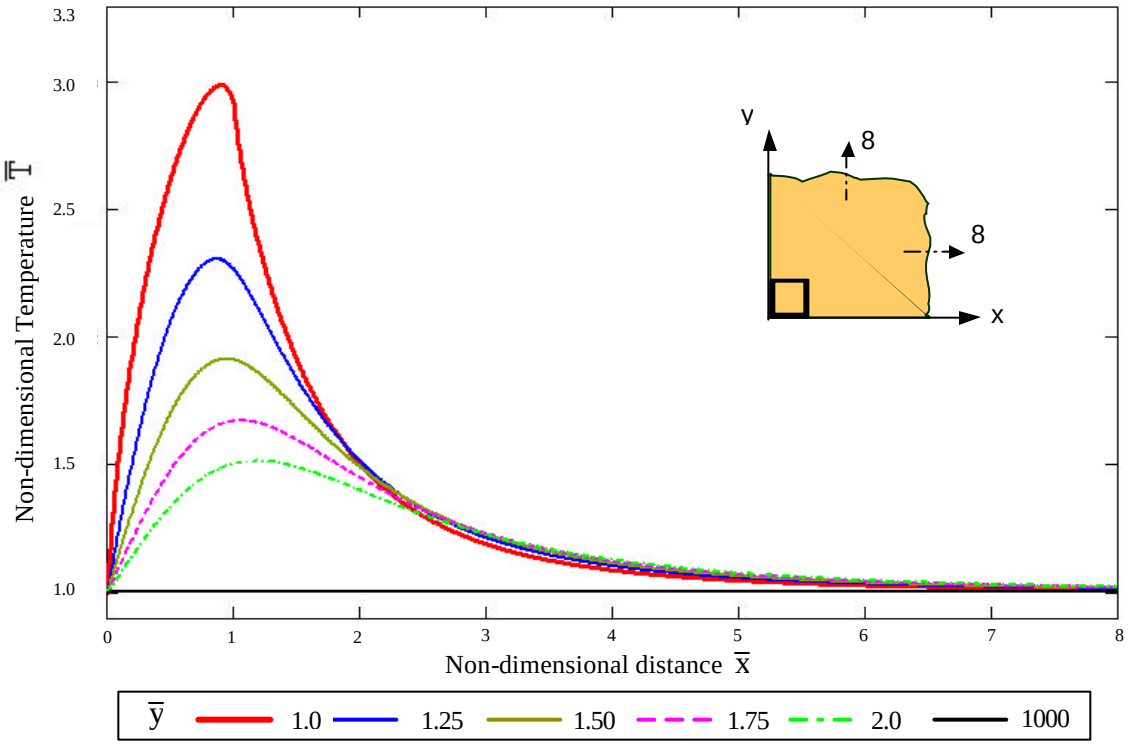

Figure 4.61. Dimensionless temperature distribution, square line-heating source $\bar{\lambda} = 5,\ \bar{a} = 0,\ \bar{b} = 0$.

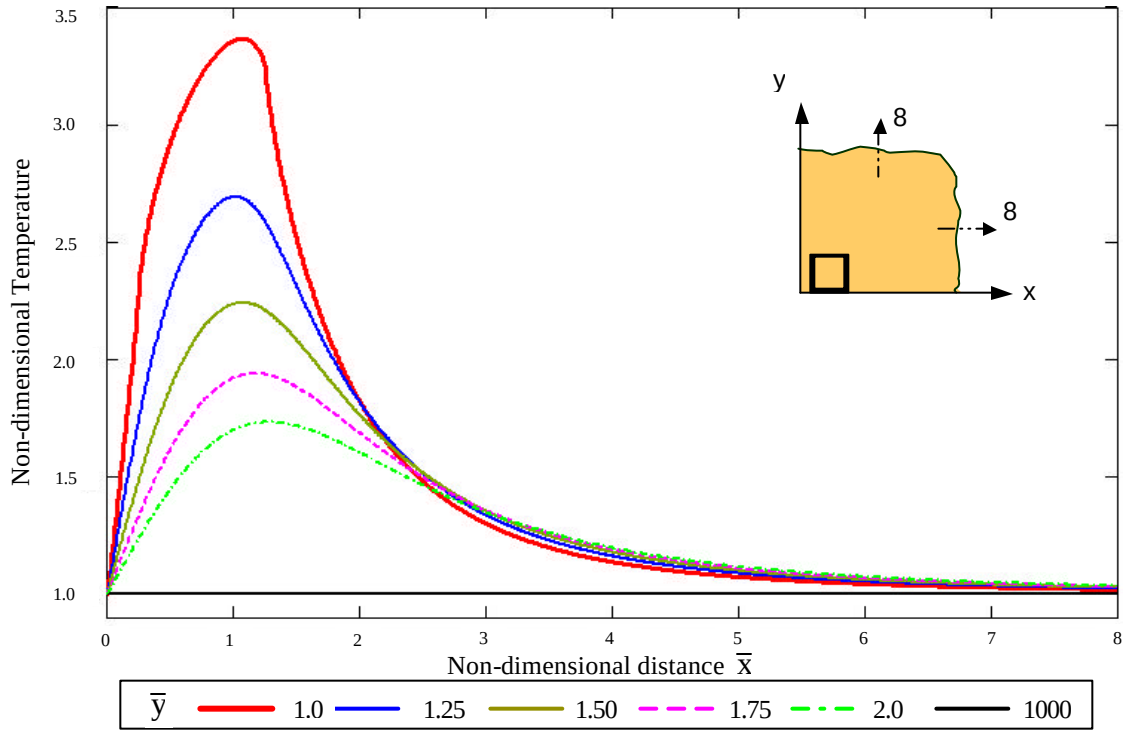

Figure 4.62. Dimensionless temperature distribution, square line-heating source $\bar{\lambda} = 5,\ \bar{a} = 0.25,\ \bar{b} = 0$.

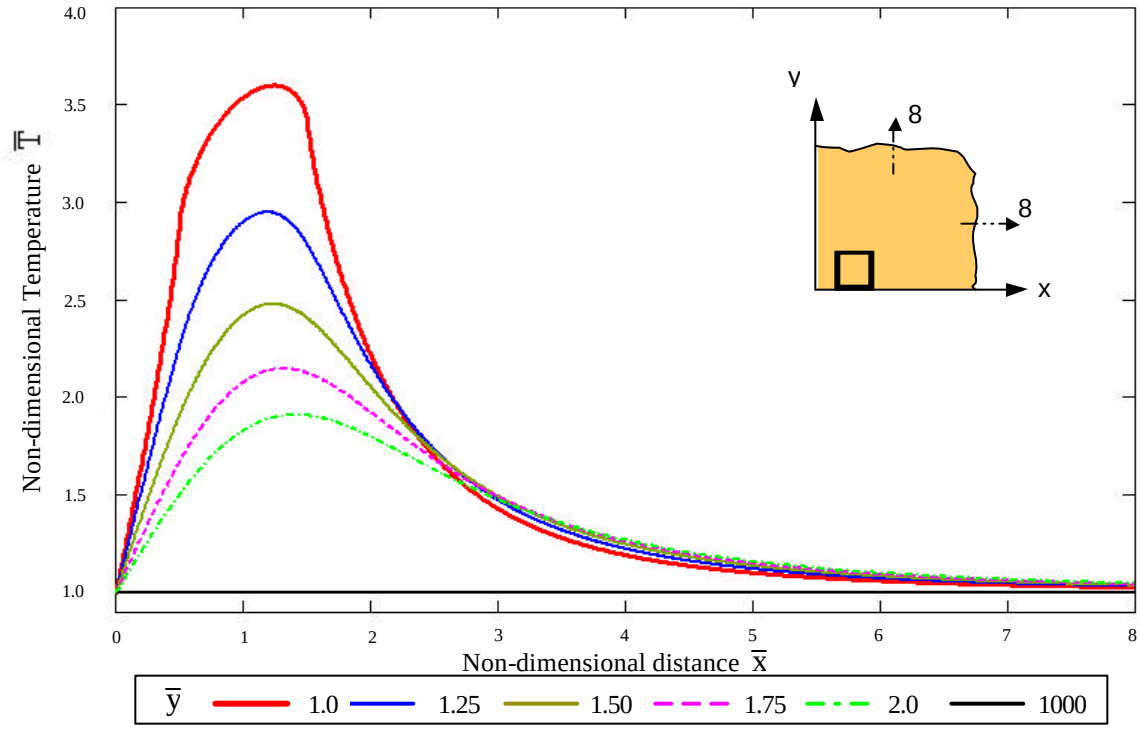

Figure 4.63. Dimensionless temperature distribution, square line-heating source $\bar{\lambda} = 5,\ \bar{a} = 0.5,\ \bar{b} = 0$.

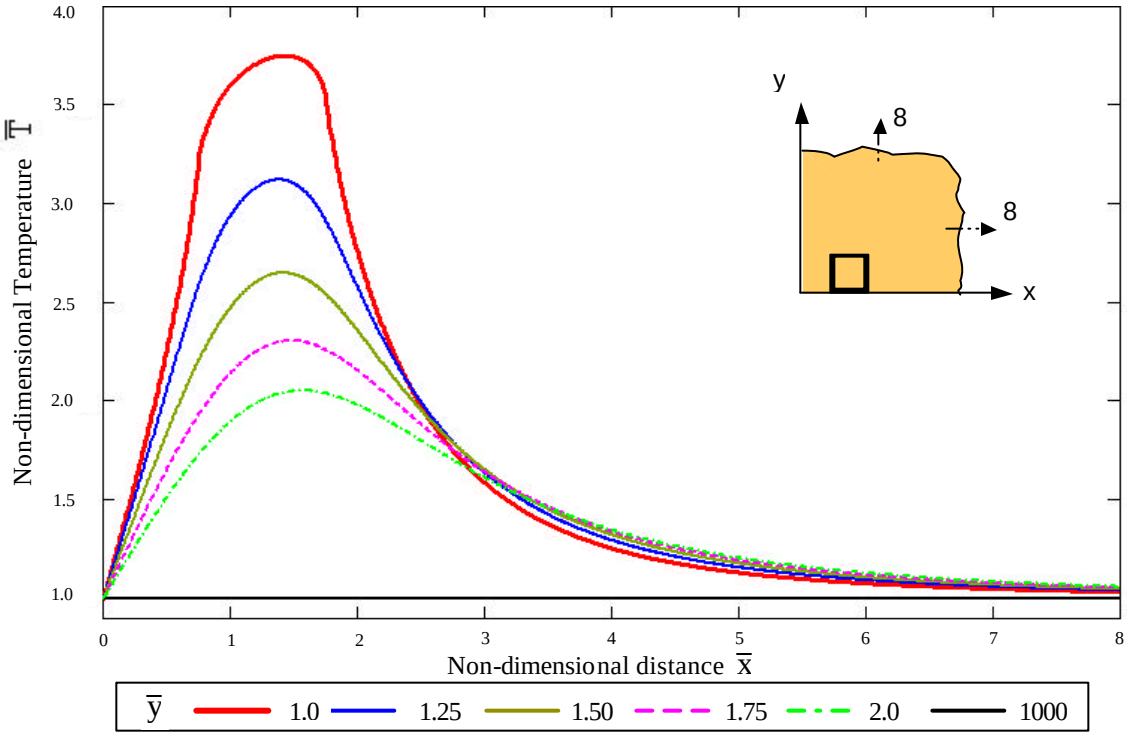

Figure 4.64. Dimensionless temperature distribution, square line-heating source $\overline{\lambda} = 5,\ \overline{a} = 0.75,\ \overline{b} = 0$.

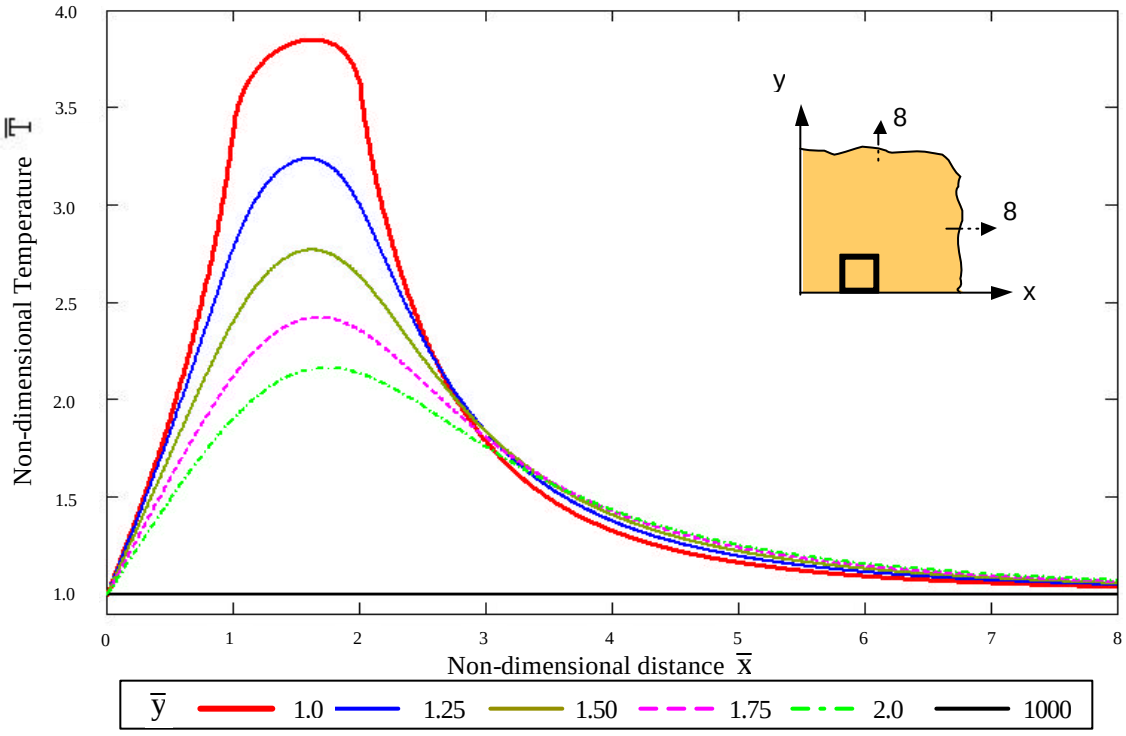

Figure 4.65. Dimensionless temperature distribution, square line-heating source $\overline{\lambda} = 5,\ \overline{a} = 1\ \overline{b} = 0$.

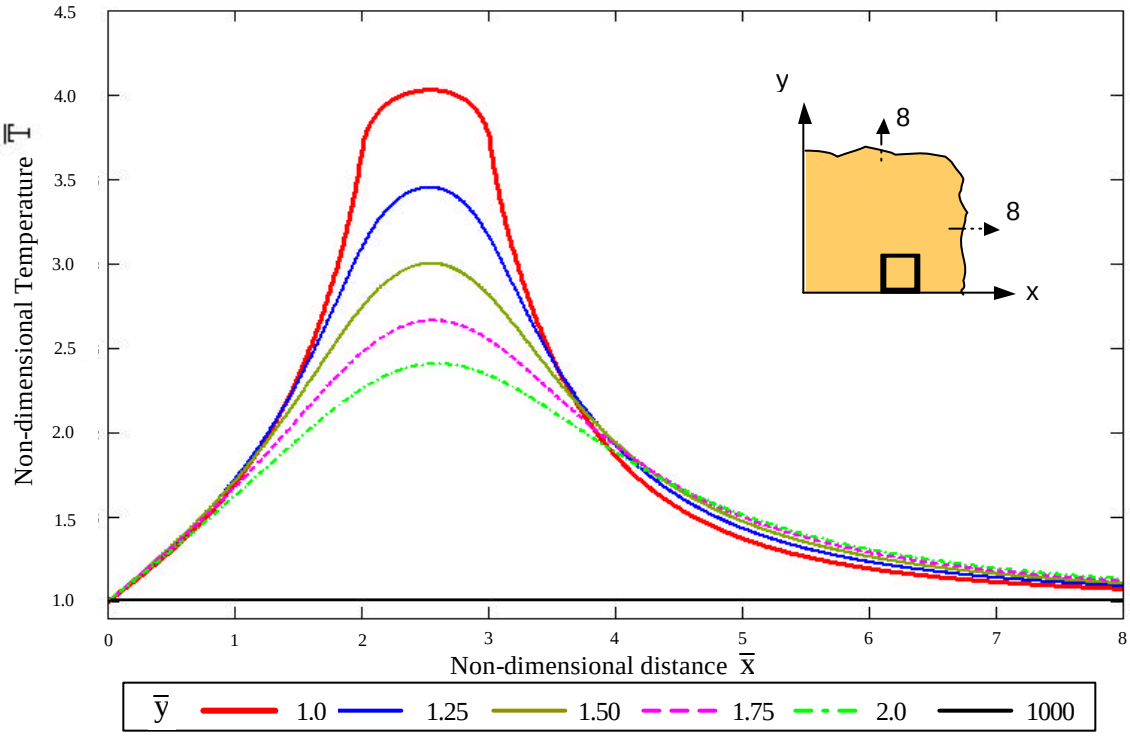

Figure 4.66. Dimensionless temperature distribution, square line-heating source $\overline{\lambda}=5,\ \overline{a}=2,\ \overline{b}=0$.

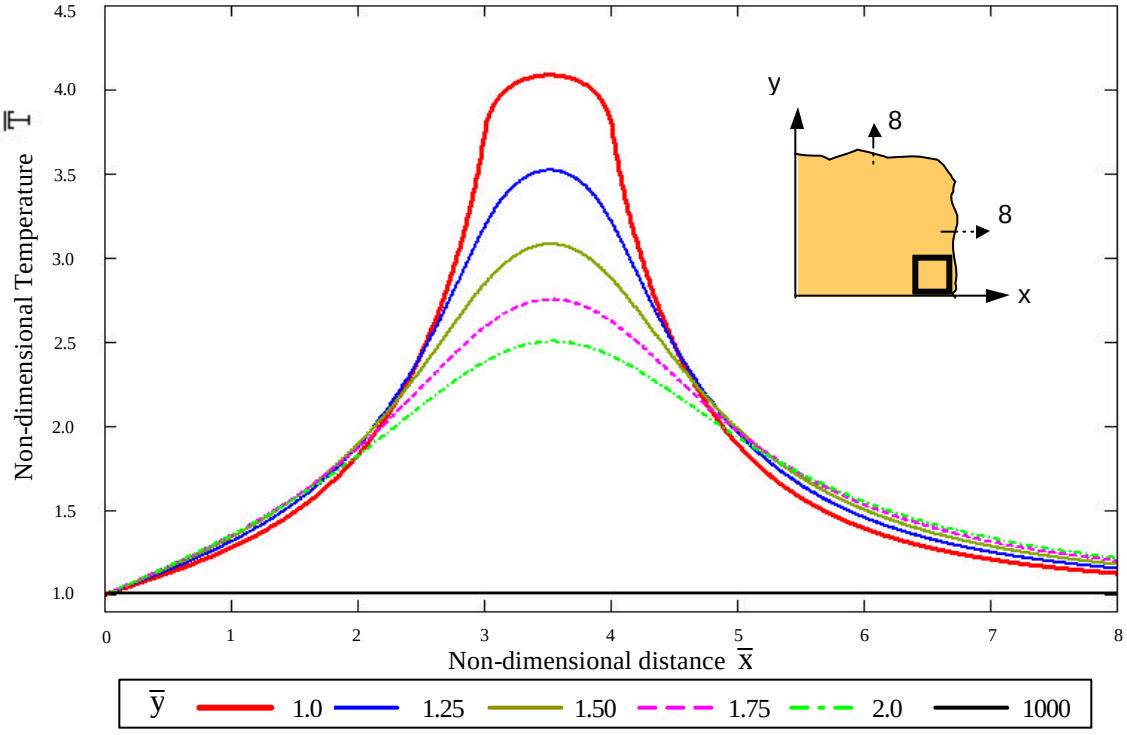

Figure 4.67. Dimensionless temperature distribution, square line-heating source $\overline{\lambda}=5,\ \overline{a}=3,\ \overline{b}=0$.

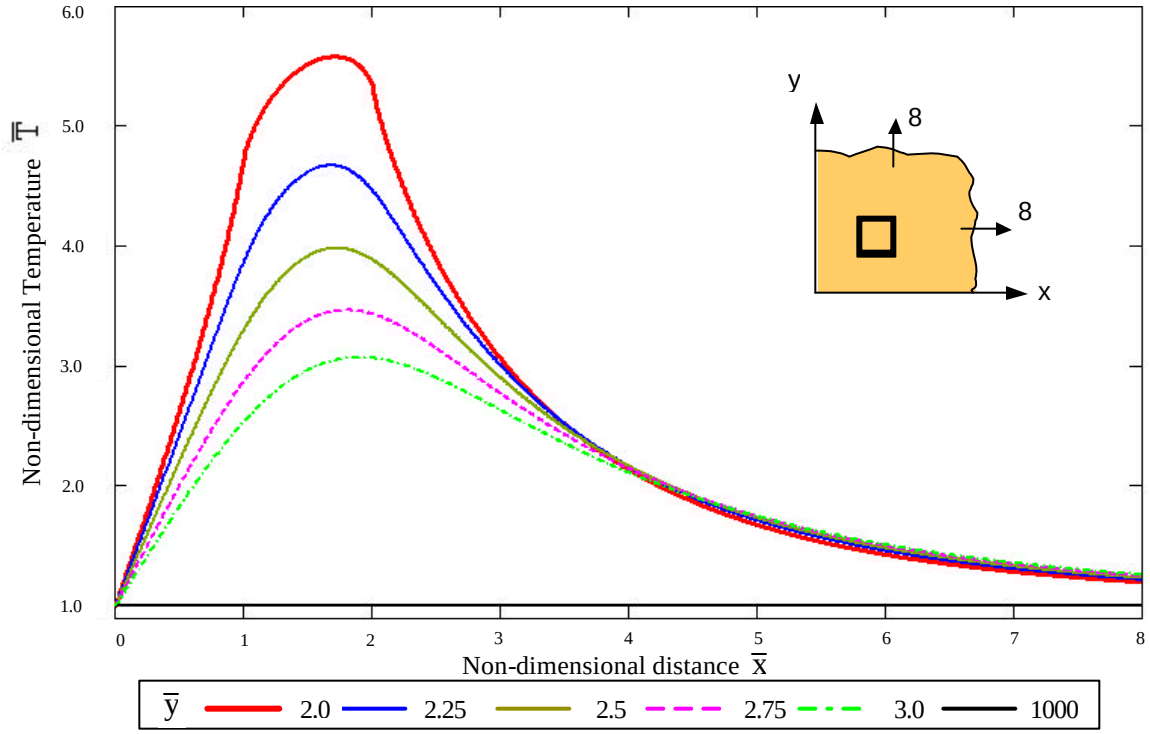

Figure 4.68. Dimensionless temperature distribution, square line-heating source $\overline{\lambda}=5,\ \overline{a}=1,\ \overline{b}=1$.

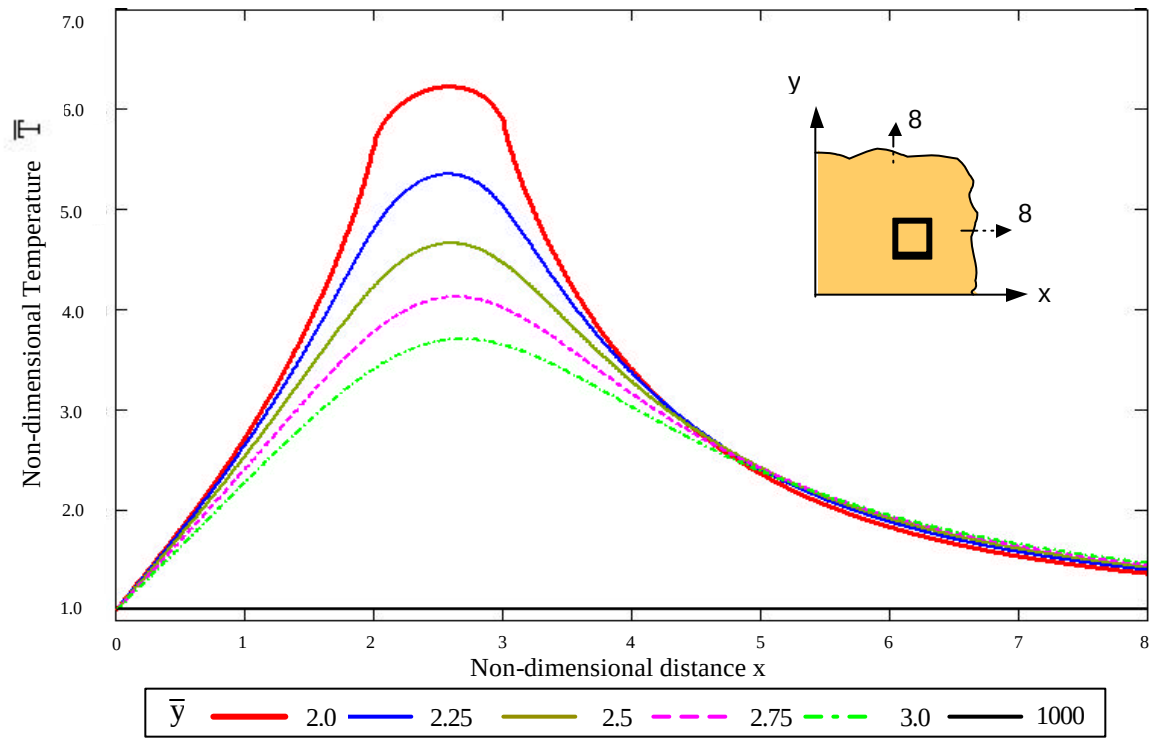

Figure 4.69. Dimensionless temperature distribution, square line-heating source $\overline{\lambda}=5,\ \overline{a}=2,\ \overline{b}=1$.

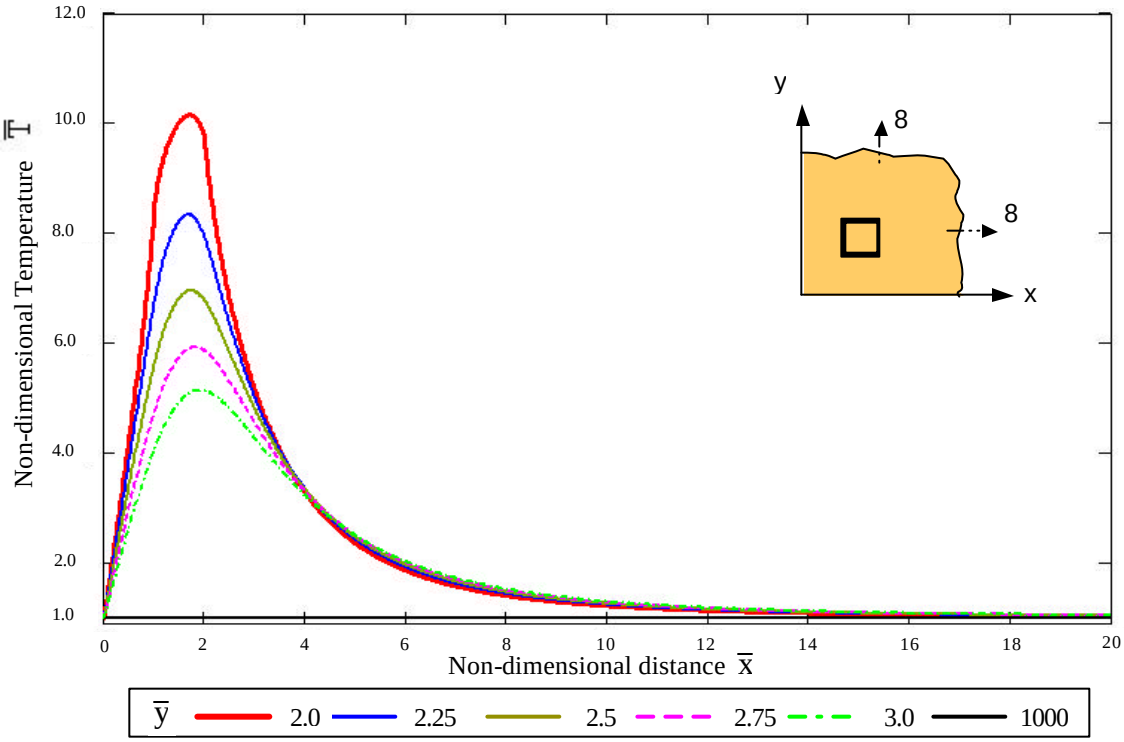

Figure 4.70. Dimensionless temperature distribution, square line-heating source $\overline{\lambda}=10,\ \overline{a}=1,\ \overline{b}=1$.

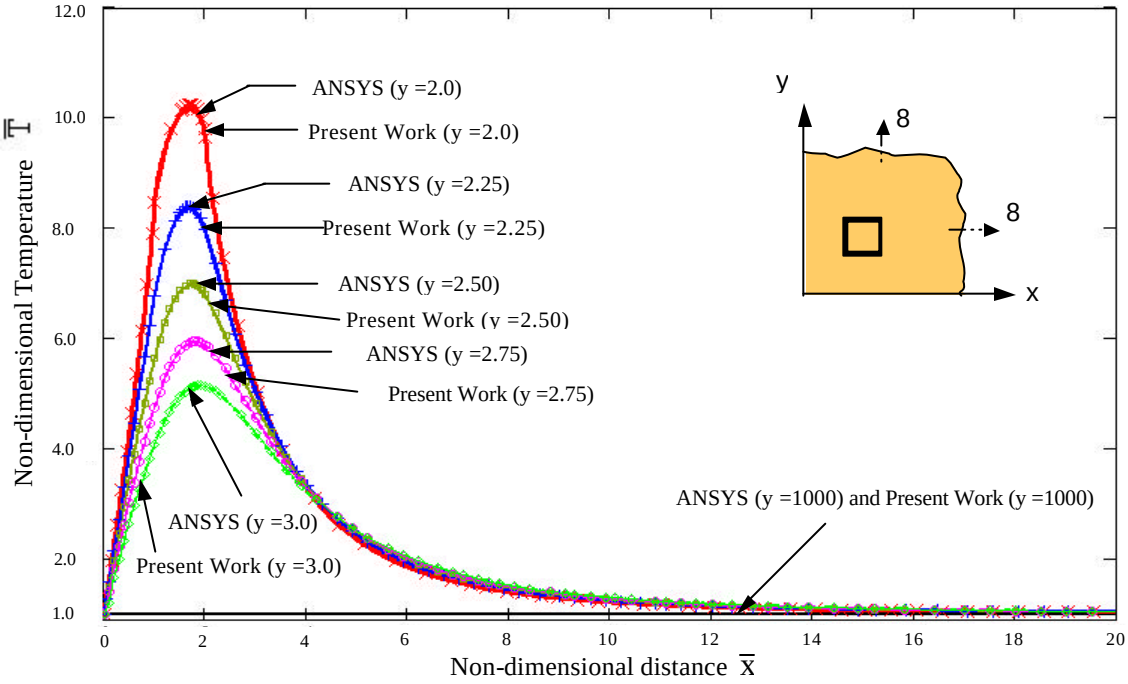

Figure 4.71. Dimensionless temperature distribution, square line-heating source $\overline{\lambda}=10,\ \overline{a}=1,\ \overline{b}=1$. Comparison whit results from ANSYS.

For this case the solution is in -the form of an exact algebraic expression. Which can be easily evaluated for the temperature profiles.

Figures 4.61 to 4.69 show the cases for the constant value of the non-dimensional strength of the source ($\bar{\lambda} = 5$), for different $\bar{a}$ and $\bar{b}$. The heating generating elements are moved to different locations. The same behavior of the previous curves is observed, but the peaks are displaced according to the source location.

Figures 4.70 shows the non-dimensional temperature profiles for the particular case with $\bar{\lambda} = 10$, with $\bar{a} = 1$ and $\bar{b} = 1$. The behavior is similar to previous case, the temperature is maximum when $\bar{x}$ or $\bar{y}$ = constant line cuts through the source.

Thus, once again we get a closed-form elegant solution. Figure 4.71 compares the results obtained with the analytic solution and the result from ANSYS, both results agree closely. Appendix [G] shows ANSYS element and results. While the present method needs a “simple calculator” ANSYS required tremendous computational effort and time which gets multiplied by factors if we have to make parametric studies.

V. CONCLUSIONS

The temperature distribution in semi-infinite slabs and infinite quadrants with various form of discrete heat generation source has been calculated, using Green's function techniques. The Green's function itself was calculated using the method of images. Six cases of heat generation were considered. For the cases considered here, we get an exact solution or an almost analytical solution in the form of a simple integral. These solutions are elegant, easy to evaluate and highly suitable for parametric studies and for accurate heat flux calculations. In all cases the solution by present method has been shown to be superior to numerical solution in terms of computational requirements.

We considered two and three-dimensional geometries with Dirichlet boundary conditions (temperature specified on boundary). It should be noted that the method of images when applied to more complex geometries would result in difficulties similar that encountered in other methods.

Classical solutions by separation of variables method (or any other method involving orthogonal eigenfunction expansions), results are usually in terms of infinite series. Infinite series solutions are sensitive to the number of terms of the series and sometime have convergence problems. Numerical solutions when used with discrete heat sources can produce inaccuracies near source region especially for calculating heat flux. For discrete sources the method of separation of variables fails.

The commercial computer software package ANSYS (university version 6.0. which uses Finite Element Analysis to solve the problems) is a very important tool to solve problems of conduction heat transfer with complex geometry for the discrete heat generation sources. The analytical or almost analytical solutions obtained here have been compared with the numerical solutions obtained by ANSYS.

For the case of semi-infinite slab with finite line heating source, it was not possible to obtain a numerical solution by ANSYS, because of the fully three dimensionality of the problem. The present method yields and elegant algebraic expression.

The installation of the complete version of software is necessary and to make tests with the purpose of determining if this solves the problems.

In contrast, the method used in the present work proved to be a good alternative to solve heat conduction problems with discrete heat generation sources, the solution is an elegant analytical expression yielding algebraic expression in all cases, except for the case of thin cylindrical heating source where it is in the form of an integral which can be easily evaluated. These methods are extremely convenient for parametric studies and heat flux calculations. Another advantage in complex solutions can be obtained as superposition of simpler solutions.

The limitation of the method is it is applicable to semi-infinite regions, thin and infinitely long cylinders and spheres. For other geometries the image system will become very complex.

The solutions obtained with the method of images are applicable to similar problems (with the same boundary conditions) in other areas of the science and engineering such as electrodynamics, fluids mechanics, elasticity and potential theory.

Future work could be directed on problems with variable thermal conductivity k, in bodies such as cylinders, spheres as well as semi-infinite slabs and infinite quadrants. Studies should also include the effect of temperature varying along the boundaries.

BIBLIOGRAPHY

1. Barton Györgi 1989, Elements of Green's Functions and Propagation, Oxford University Press, New York USA, pg 7-69.
2. Beck J.V. 1984. Green's Function Solution for Transient Heat Conduction Problems. International Journal of Heat and Mass Transfer. Vol 27, pg 1235-1244.
3. Beck J.V. 1986. Green's Functions and Numbering System for Transient Heat Conduction. AIAA Journal. Vol 24, pg 327-333.
4. Beck J.V., Cole K.D., Haji A. and Litkouhi B. 1992. Heat Conduction Using Green's Functions. Hemisphere Publishing Corporation, New York, USA.
5. Berger John R. 2001 Green's Functions and Applications for Steady-State Heat Transfer in Functionally Graded Materials National Institute of Standards and Technology Boulder Colorado USA.
6. Bradley G.L. and Smith K.J. 1999. Calculus Second Edition. Prentice Hall International, London, United Kingdom, pg 1011-1017.
7. Carslaw H.S. and Jaeger J.C. 1959. Conduction of Heat in Solids. Oxford University Press, London, England, pg 353-386.
8. Carrier G.F. and Pearson C.E. 1976. Partial Differential Equations-Theory and Technique. Academic Press Editors, New York, USA, pg 139-158.
9. Chang Y.P. and Tsou R.C. 1977. Heat Conduction in an Anisotropic Medium Homogeneous in Cylindrical Regions-Unsteady State. Journal of Heat Transfer, Transactions ASME. Vol 99, Ser. C, pg 41-46.
10. Cole Kevin D. 2001 Steady Heat Conduction in Cartesian coordinates and a Library of Green's Functions, 35th National Heat Transfer Conference, Anaheim, California USA, June 10-12-2001
11. Courant R. and Hilbert D. 1953. Methods of Mathematical Physics. Vol I, Interscience Publishers, Inc. New York USA, pg 351-387.

12. Erich Zauderer 1983, Partial Differential Equations of Applied Mathematics, Jhon Whyle & Sons, Inc., New York USA, pg 353-449.
13. Ghandour E. 1974. Initial Value Problem for Boundary Values of a Green's Function. Journal of Applied Mathematics. Vol. 27, pg 649-654.
14. Greenberg M.D. 1971. Application of Green's Functions in Science and Engineering. Prentice-Hall Inc. Editors, New Jersey, USA.
15. Haji-Sheikh and Beck J.V. 1994. Green's Function Solution for Thermal Wave Equation in Finite Bodies. International Journal of Heat and Mass Transfer. Vol 37, pg 2615-2626.
16. Hayek S. I. 2001. Advanced Mathematical Methods in Science and Engineering. Marcel Deckker, Inc. New York, USA, pg 453 – 536.
17. Jackson J.D. 1999. Classical Electrodynamics. John Wiley & Sons, Inc. New York, USA.
18. James M. Hill & Jeffrey N. Dewynne 1987. Heat Conduction, Blackwell Scientific Publications, Oxford, USA, pg 64-153.
19. Larry C. Andrews 1986, Elementary Partial Differential Equations with Boundary Value Problems, Academic Press, Inc., Orlando, Florida, USA, pg 77-109.
20. Mackie A. G. 1965 Boundary Value Problems, Oliver & Boyd Ltd, Edinburgh Great Britain, pg 158-203.
21. Morse P.M. and Feshbach H. 1953. Methods of Theoretical Physics. Vol I, McGraw-Hill Book Company, Inc., New York USA, pg 791-895.
22. Ozisik M.N. 1993. "Heat Conduction". John Wiley & Sons, Inc. New York, USA, pg 214-251.
23. Perez Diaz Eduardo G. 2002 "Analysis of Conduction Heat Transfer in two and three dimensional geometries using Green's function integral Method" Thesis M.S. University of Puerto Rico – Mayagüez, Campus
24. Publication in Internet -Biographical Notes on George Green http://www.nottingham.ac.uk/~ppzwww/green/homepage.htm. Created: 21st August 1997.

25. Pinsky Mark A. 1991 Partial Differential Equations and Boundary-Value Problems with Applications, McGraw-Hill, Inc. New York USA, pg 343-377.
26. Roach G. F. 1970. Green's Functions Introductory Theory with Applications, The New University Mathematics Series, Van Nostrand Reinhold Company, London, Great Britain, pg 213-256.
27. Sadri Hasani 1999. Mathematical Physics A Modern Introduction to Its Foundations, Springer-Verlag New York, Inc. New York, USA, pg 551 – 648.
28. Shendeleva M.L., Molloy J.A., and Ljepojevic N.N. 2002. Modeling of interfacial temperature effects due to an impulsive line heat source, American Institute of Physics Vol 80, Number, pg 1486-1488.
29. Stakgold Ivar 1979. Green's Functions and Boundary Value Problems, Jhon Whyle & Sons, Inc., New York USA, pg 42-85.
30. Tewary V.K. 1996. Elastic Green's Functions for Anisotropic Solids NIST Special Publication SP 910, Boulder Colorado, USA.
31. Venkataraman N.S. and Oliveira C.E. 1988. Temperature Distribution in Satellite Mounting Plates Due to Conductive Heat Transfer. Acta Astronáutica. Vol. 17, pg 1127-1135.
32. Venkataraman N.S. and Sepulveda D.G. 1991. Thermal Resistance in Satellite Mounting Plates Due to Conductive Heat Transfer. Acta Astronautica. Vol 25, pg 757-764.
33. Venkataraman N.S., Pérez E. and Delgado I. 2003. Temperature Distribution in Spacecraft Mounting Plates with Discrete Heat Generation Sources Due Conductive Heat Transfer.Accepted for publication in Acta Astronáutica. Vol 1, N^{o} 10, May 2003.
34. Weast Robert. 1972. Handbook of Chemistry and Physics. The Chemical Rubber Co. Ohio. USA.

APPENDICES

APPENDIX A

ANSYS RESULTS, LINE PLATE HEAT SOURCE

ANSYS RESULTS FOR A LINE PLATE HEAT SOURCE $\bar{\lambda} = 10$, $\bar{a} = 0$ AND $\bar{b} = 1.0$

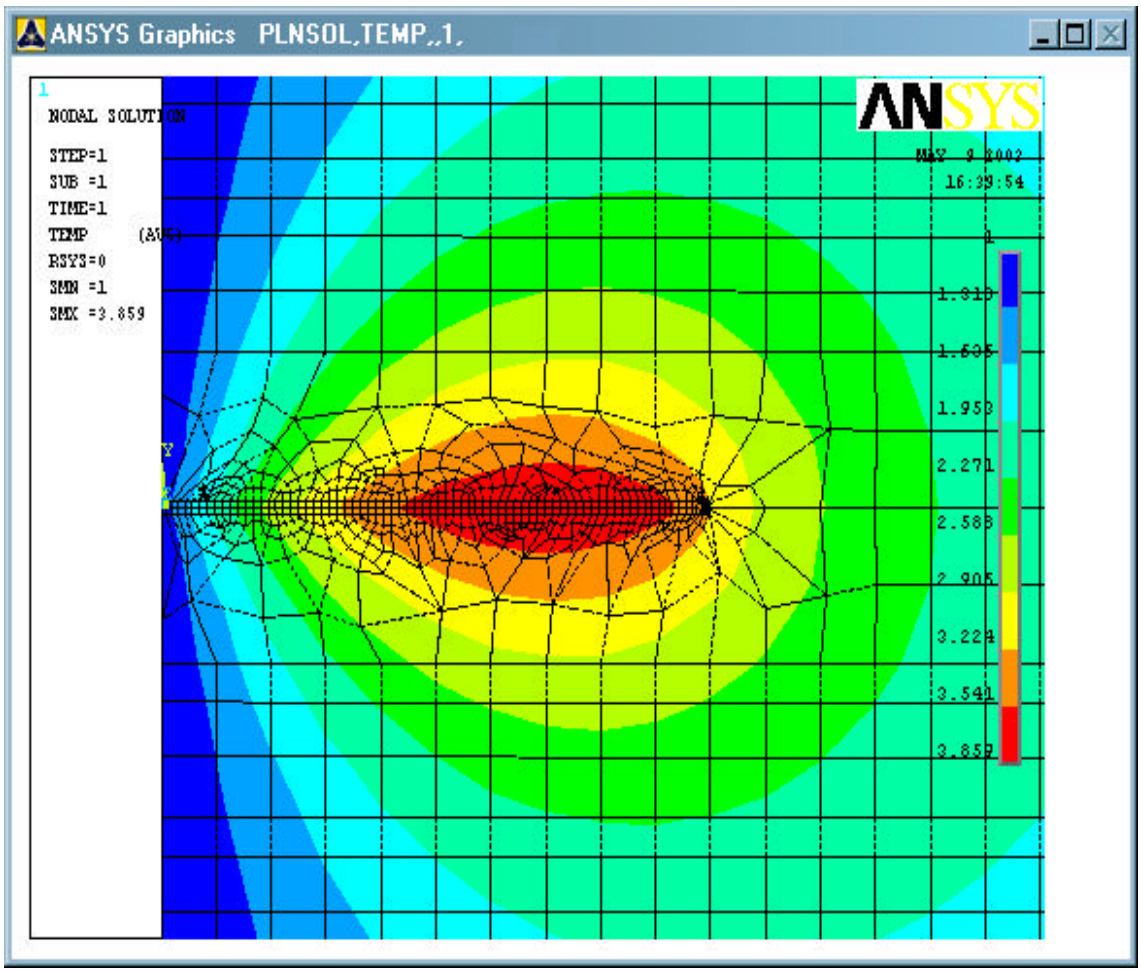

APPENDIX B

ANSYS RESULTS WITH DIFFERENT RATIO PLATE LENGTH / LENGTH OF THE "INFINITE" REGION, LINE PLATE HEAT SOURCE. $\bar{\lambda} = 10$ AND $\bar{a} = 0$.

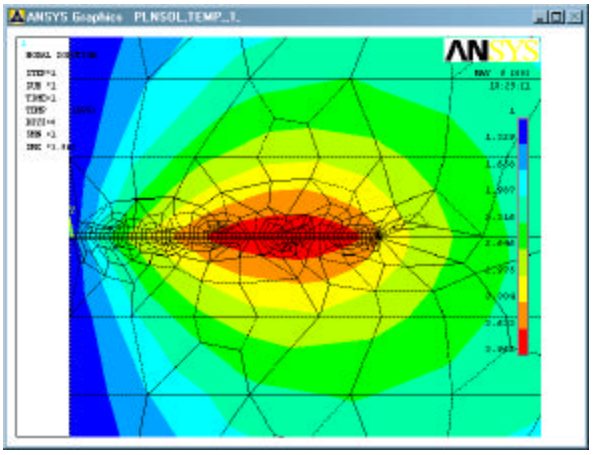

Ratio 1/400

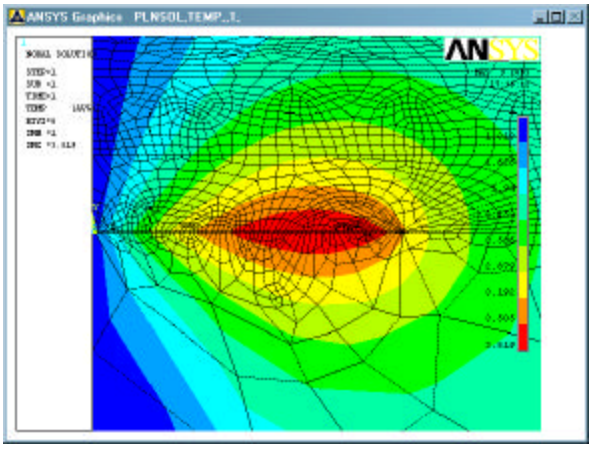

Ratio 1/800

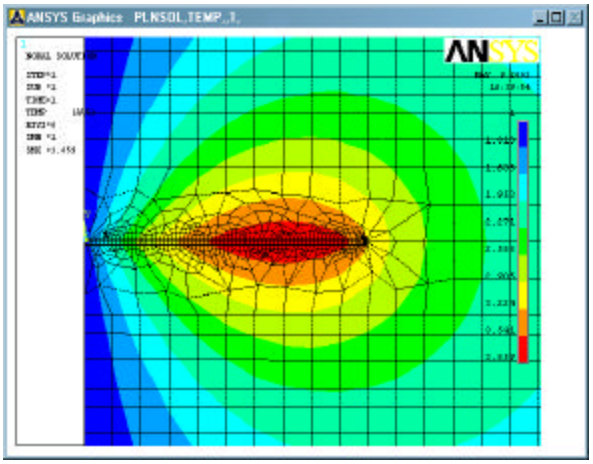

Ratio 1/1000

APPENDIX C

ANSYS RESULTS, HOLLOW BOX HEAT SOURCE (SQUARE)

ANSYS RESULTS FOR A HOLLOW BOX HEAT SOURCE $\bar{\lambda} = 10$ AND $\bar{a} = 0$.

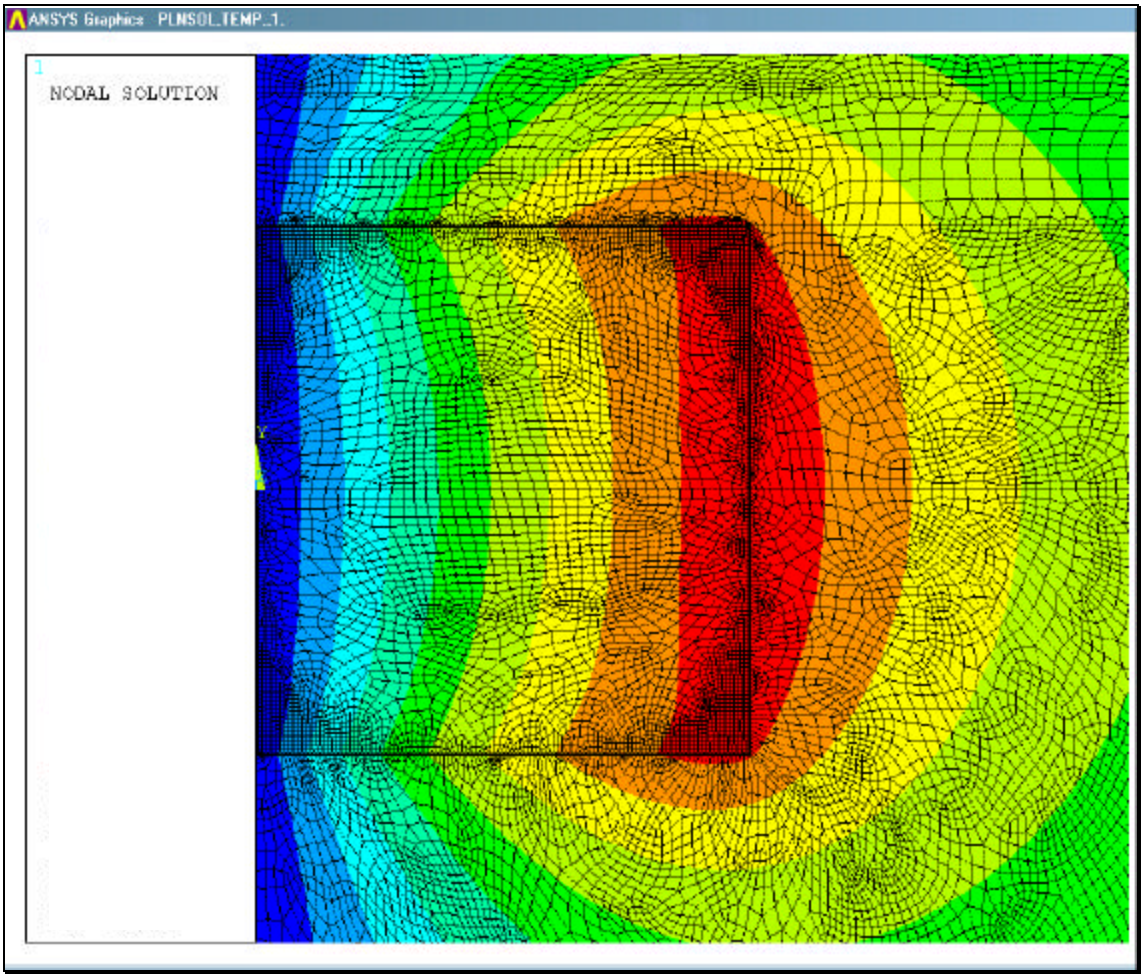

APPENDIX D

RESULTS FOR A RECTANGULAR HOLLOW BOX HEAT SOURCE

A thin current carrying plate bent in the form of a rectangle forming a rectangle hollow box-heating source is embedded, as a heat-generating element, in a semi-infinite two dimensional slab $x > 0$, $-\infty < y < \infty$, $\infty < z < \infty$, and constant thermal conductivity k. The heating element can be assumed as a hollow box heat source with walls infinitesimally thin; with large depth ℓ and side L. The heat generation per unit length along the source per unit depth is constant and the boundary $x = 0$ is maintained at constant temperature T_B as shown in figure (a).

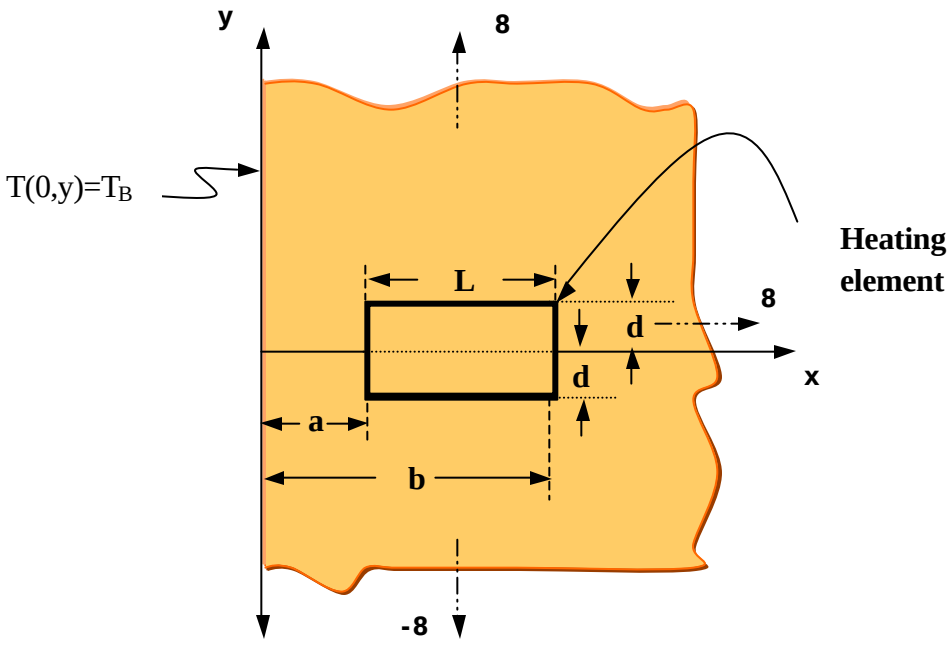

Figure (a). Semi-infinite slab with a rectangular hollow box-heating source

Let:

$Q_T \equiv$ Total heat generation (W) =

$\lambda \equiv$ Strength of the heat source per unit depth per unit length (W/m^2)

$Q(x,y) \equiv$ Heat generation intensity per unit volume (W/m^3)

Q(x,y) when integrated over the whole volume must be equal to the total heat generation inside the semi-infinite slab, i.e. $\iiint_V Q(x,y).dx.dy.dz = Q_T$

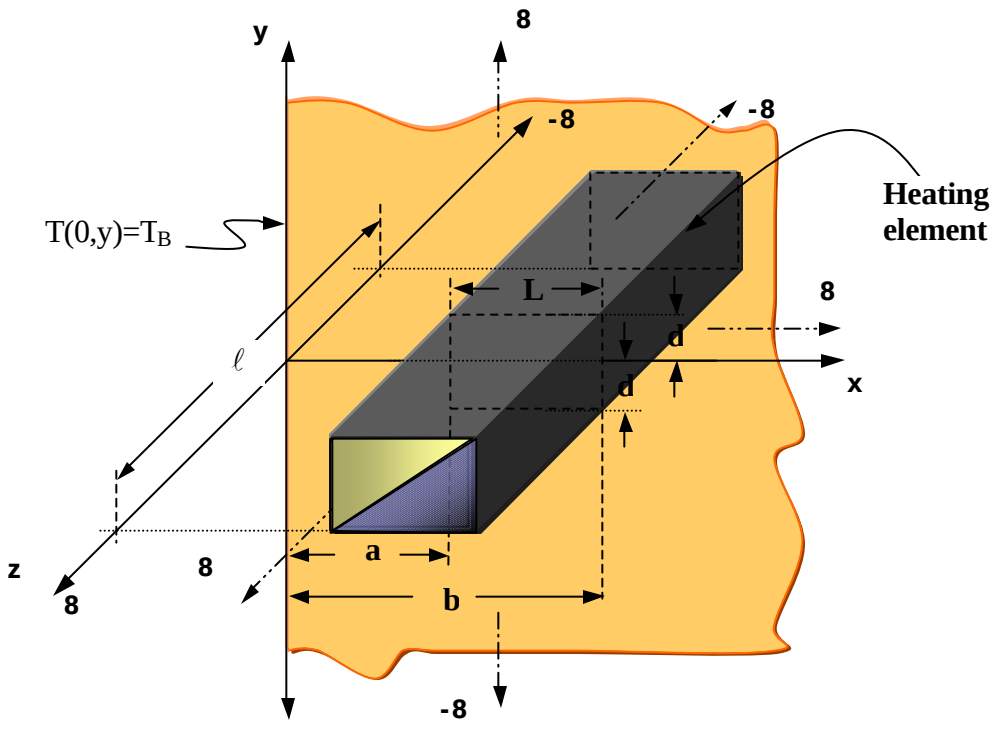

Figure (b). Semi-infinite slab with a rectangular hollow box-heating source

For cartesian coordinates this condition becomes:

$$\int_{-\frac{\ell}{2}}^{\frac{\ell}{2}}\int_{\ell-\infty}^{\infty}\int_{0}^{\infty} Q(x,y).dx.dy.dz = Q_T = \lambda.\ell.\left[(b-a)+d+(b-a)+d\right] \quad \text{.....} \quad \text{(A)}$$

Similarly to the previous case, an expression was derived for the generation of heat for unit of volume using the same principle, but with the assumption that the hollow box this formed by 4 plates infinitesimally thin. They were calculated in an independent way adding the results, obtaining the following expression for the heat generation Q(x,y):

$$Q(x,y) = \begin{Bmatrix} \lambda\cdot\delta(y+d)\cdot\{H[x-a]-H[x-b]\}+ \\ \lambda\cdot\delta(x-b)\cdot\{H[y+d]-H[y-d]\}+ \\ \lambda\cdot\delta(y-d)\cdot\{H[x-a]-H[x-b]\}+ \\ \lambda\cdot\delta(x-a)\cdot\{H[y+d]-H[y-d]\} \end{Bmatrix} \quad \text{.....} \quad \text{(B)}$$

The equation (B) satisfy to equation (A), Now integrate the right hand side of expression (B) as indicated in equation (A):

$$\int_{-\frac{\ell}{2}}^{\frac{\ell}{2}}\int_{\ell-\infty}^{\infty}\int_{0}^{\infty} \begin{Bmatrix} \lambda\cdot\delta(y+d)\cdot\{H[x-a]-H[x-b]\}+ \\ \lambda\cdot\delta(x-b)\cdot\{H[y+d]-H[y-d]\}+ \\ \lambda\cdot\delta(y-d)\cdot\{H[x-a]-H[x-b]\}+ \\ \lambda\cdot\delta(x-a)\cdot\{H[y+d]-H[y-d]\} \end{Bmatrix} .dx.dy.dz$$

$$\lambda\int_{-\frac{\ell}{2}}^{\frac{\ell}{2}}dz.\int_{-\infty}^{\infty}\delta(y+d).dy\cdot\int_{0}^{\infty}\{H[x-a]-H[x-b]\}.dx+\lambda\int_{-\frac{\ell}{2}}^{\frac{\ell}{2}}dz.\int_{-\infty}^{\infty}\delta(x-b).dx\cdot\int_{0}^{\infty}\{H[y+d]-H[y-d]\}.dy+$$

$$\lambda\int_{-\frac{\ell}{2}}^{\frac{\ell}{2}}dz.\int_{-\infty}^{\infty}\delta(y-d).dy\cdot\int_{0}^{\infty}\{H[x-a]-H[x-b]\}.dx+\lambda\int_{-\frac{\ell}{2}}^{\frac{\ell}{2}}dz.\int_{-\infty}^{\infty}\delta(x-a).dx\cdot\int_{0}^{\infty}\{H[y+d]-H[y-d]\}.dy$$

Using the properties for Dirac-Delta and Heaviside function is obtained:

$$\lambda\cdot\ell\cdot1.\int_{a}^{b}dx+\lambda\cdot\ell\cdot1.\int_{-d}^{d}dy+\lambda\cdot\ell\cdot1.\int_{a}^{b}dx+\lambda\cdot\ell\cdot1.\int_{-d}^{d}dy=\begin{Bmatrix}\lambda\cdot\ell\cdot(b-a)+\lambda\cdot\ell\cdot d+\\ \lambda\cdot\ell\cdot(b-a)+\lambda\cdot\ell\cdot d\end{Bmatrix}$$

Equation (A) after integration becomes:

$$\iiint_{V}Q(x,y)=Q_{T}=\lambda\cdot\ell\cdot[(b-a)+d+(b-a)+d]=2.\lambda.\ell.[L+d]$$

Substitute equations (3.31) and (B) in equation (4.4):

$$T(x,y)=T_{B}+\frac{\lambda}{4\pi k\ell}\int_{-\frac{\ell}{2}}^{\frac{\ell}{2}}\int_{-\infty}^{\infty}\int_{0}^{\infty}\begin{Bmatrix}\delta(y'+d)\cdot\{H[x-a]-H[x-b]\}.\ln\left\{\frac{(x+x')^2+(y+d)^2}{(x-x')^2+(y+d)^2}\right\}+\\ \delta(x'-b)\cdot\{H[y+d]-H[y-d]\}.\ln\left\{\frac{(x+b)^2+(y-y')^2}{(x-b)^2+(y-y')^2}\right\}+\\ \delta(y'-d)\cdot\{H[x-a]-H[x-b]\}.\ln\left\{\frac{(x+x')^2+(y-d)^2}{(x-x')^2+(y-d)^2}\right\}+\\ \delta(x'-a)\cdot\{H[y+d]-H[y-d]\}.\ln\left\{\frac{(x+a)^2+(y-y')^2}{(x-a)^2+(y-y')^2}\right\}\end{Bmatrix}.dx'\,dy'\,dz'$$

Integration on z is easily performed, then applying again the properties for Dirac Delta and Heaviside functions for x and y, we get:

$$T(x,y) = T_B + \frac{\lambda}{4\pi k}\left\{\begin{array}{l}\int_a^b \left\{\ln\left\{\frac{(x+x')^2+(y+d)^2}{(x-x')^2+(y+d)^2}\right\}+\ln\left\{\frac{(x+x')^2+(y-d)^2}{(x-x')^2+(y-d)^2}\right\}\right\}dx'+ \\ \int_{-d}^{d}\left\{\ln\left\{\frac{(x+a)^2+(y-y')^2}{(x-a)^2+(y-y')^2}\right\}+\ln\left\{\frac{(x+b)^2+(y-y')^2}{(x-b)^2+(y-y')^2}\right\}\right\}dy'\end{array}\right\}$$

In order to express results in non-dimensional form the following non-dimensional quantities are defined:

$\overline{T}(\overline{x},\overline{y}) = \frac{T(x,y)}{T_B}$ Non-dimensional temperature

$\overline{\lambda} = \frac{\lambda(b-a)}{kT_B} = \frac{2\lambda d}{kT_B}$ Non-dimensional heat generation

$\overline{x} = \frac{x}{L}, \overline{y} = \frac{y}{L}$ Non-dimensional temperature location

$\overline{x}' = \frac{x'}{L}, \overline{y}' = \frac{y'}{L}$ Non-dimensional source location

$\overline{a} = \frac{a}{L}, \overline{b} = \frac{b}{L}, \overline{d} = \frac{d}{L}$ Non-dimensional distances

Finally, substitute all these quantities in the previous equation and the following relationship is obtained:

$$\overline{T}(\overline{x},\overline{y}) = 1 + \frac{\lambda}{4\pi k}\left\{\begin{array}{l}\displaystyle\int_{\overline{a}}^{\overline{b}}\left\{\ln\left\{\frac{(\overline{x}+\overline{x}')^2+(\overline{y}+\overline{d})^2}{(\overline{x}-\overline{x}')^2+(\overline{y}+\overline{d})^2}\right\}+\ln\left\{\frac{(\overline{x}+\overline{x}')^2+(\overline{y}-\overline{d})^2}{(\overline{x}-\overline{x}')^2+(\overline{y}-\overline{d})^2}\right\}\right\}d\overline{x}'+\\ \displaystyle\int_{-\overline{d}}^{\overline{d}}\left\{\ln\left\{\frac{(\overline{x}+\overline{a})^2+(\overline{y}-\overline{y}')^2}{(\overline{x}-\overline{a})^2+(\overline{y}-\overline{y}')^2}\right\}+\ln\left\{\frac{(\overline{x}+\overline{b})^2+(\overline{y}-\overline{y}')^2}{(\overline{x}-\overline{b})^2+(\overline{y}-\overline{y}')^2}\right\}\right\}d\overline{y}'\end{array}\right\}$$

$$\overline{T}(\overline{x},\overline{y}) = 1 + \frac{\overline{\lambda}}{4.\pi}\left[\begin{array}{l}(\overline{x}+\overline{b}).\left\{\begin{array}{l}\ln\left[\left[(\overline{x}+\overline{b})^2+(\overline{y}+d)^2\right]\left[(\overline{x}+\overline{b})^2+(\overline{y}-d)^2\right]\right]-\\ 2.\mathrm{Arctg}\left(\frac{\overline{y}-\overline{d}}{\overline{x}+\overline{b}}\right)+2.\mathrm{Arctg}\left(\frac{\overline{y}+\overline{d}}{\overline{x}+\overline{b}}\right)\end{array}\right\}-\\ (\overline{x}+\overline{a}).\left\{\begin{array}{l}\ln\left[\left[(\overline{x}+\overline{a})^2+(\overline{y}+d)^2\right]\left[(\overline{x}+\overline{a})^2+(\overline{y}-d)^2\right]\right]+\\ 2.\mathrm{Arctg}\left(\frac{\overline{y}-\overline{d}}{\overline{x}+\overline{a}}\right)-2.\mathrm{Arctg}\left(\frac{\overline{y}+\overline{d}}{\overline{x}+\overline{a}}\right)\end{array}\right\}+\\ (\overline{x}-\overline{b}).\left\{\begin{array}{l}\ln\left[\left[(\overline{x}-\overline{b})^2+(\overline{y}+d)^2\right]\left[(\overline{x}-\overline{b})^2+(\overline{y}-d)^2\right]\right]+\\ 2.\mathrm{Arctg}\left(\frac{\overline{y}-\overline{d}}{\overline{x}-\overline{b}}\right)-2.\mathrm{Arctg}\left(\frac{\overline{y}+\overline{d}}{\overline{x}-\overline{b}}\right)\end{array}\right\}-\\ (\overline{x}-\overline{a}).\left\{\begin{array}{l}\ln\left[\left[(\overline{x}-\overline{a})^2+(\overline{y}+d)^2\right]\left[(\overline{x}-\overline{a})^2+(\overline{y}-d)^2\right]\right]-\\ 2.\mathrm{Arctg}\left(\frac{\overline{y}-\overline{d}}{\overline{x}-\overline{a}}\right)+2.\mathrm{Arctg}\left(\frac{\overline{y}+\overline{d}}{\overline{x}-\overline{a}}\right)\end{array}\right\}+\\ (\overline{y}-\overline{d}).\left\{\begin{array}{l}\ln\left[\frac{\left[(\overline{y}-\overline{d})^2+(\overline{x}-\overline{b})^2\right]\left[(\overline{y}-d)^2+(\overline{x}-\overline{a})^2\right]}{\left[(\overline{y}-\overline{d})^2+(\overline{x}+\overline{b})^2\right]\left[(\overline{y}-d)^2+(\overline{x}+\overline{a})^2\right]}\right]+\\ 2.\mathrm{Arctg}\left(\frac{\overline{x}+\overline{b}}{\overline{y}-\overline{d}}\right)-2.\mathrm{Arctg}\left(\frac{\overline{x}+\overline{a}}{\overline{y}-\overline{d}}\right)+\\ 2.\mathrm{Arctg}\left(\frac{\overline{x}-\overline{b}}{\overline{y}-\overline{d}}\right)-2.\mathrm{Arctg}\left(\frac{\overline{x}-\overline{a}}{\overline{y}-\overline{d}}\right)\end{array}\right\}+\\ (\overline{y}+\overline{d}).\left\{\begin{array}{l}\ln\left[\frac{\left[(\overline{y}+\overline{d})^2+(\overline{x}+\overline{b})^2\right]\left[(\overline{y}+d)^2+(\overline{x}+\overline{a})^2\right]}{\left[(\overline{y}+\overline{d})^2+(\overline{x}-\overline{b})^2\right]\left[(\overline{y}+d)^2+(\overline{x}-\overline{a})^2\right]}\right]+\\ 2.\mathrm{Arctg}\left(\frac{\overline{x}+\overline{b}}{\overline{y}+\overline{d}}\right)-2.\mathrm{Arctg}\left(\frac{\overline{x}+\overline{a}}{\overline{y}+\overline{d}}\right)+\\ 2.\mathrm{Arctg}\left(\frac{\overline{x}-\overline{b}}{\overline{y}+\overline{d}}\right)-2.\mathrm{Arctg}\left(\frac{\overline{x}-\overline{a}}{\overline{y}+\overline{d}}\right)\end{array}\right\}\end{array}\right] \quad \ldots\ldots(C)$$

Equation (C) is the temperature profile for a semi-infinite slab with constant temperature on boundary heated by a wire in the form of a rectangular hollow box

carrying a current and embedded in the slab. Thus an "analytical solution" for the temperature distribution has been obtained.

Equation (C), is an algebraic expression, which can be easily evaluated. Some of the results for different values of $\bar{\lambda}$, $\bar{a}$, $\bar{b}$, and d are presented in the following figures:

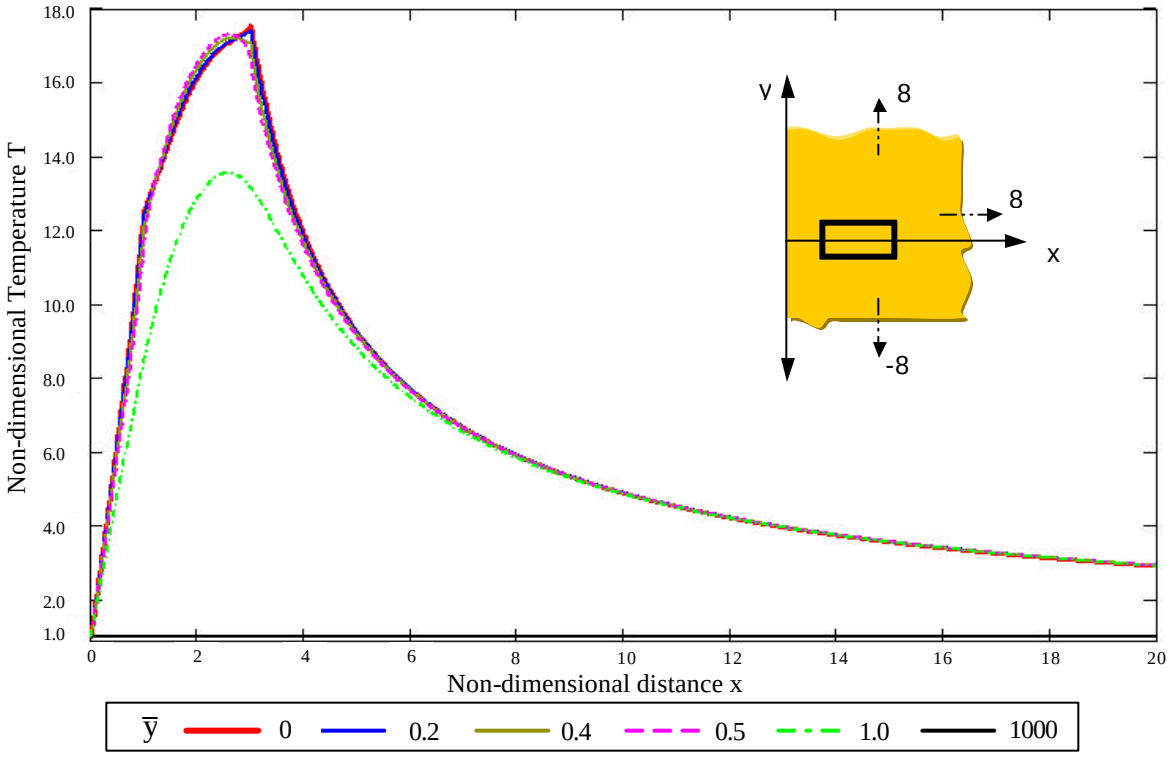

Figure (c). Dimensionless temperature distribution, rectangular hollow box-heating source. $\bar{\lambda}=10$, $\bar{a}=1$, $\bar{b}=3$, $\bar{d}=0.5$

APPENDIX E

ANSYS RESULTS, SQUARE PRISMATIC HEAT SOURCE

ANSYS RESULTS FOR A SQUARE PRISMATIC HEAT SOURCE $\bar{\lambda} = 10$ AND $\bar{a} = 0$.

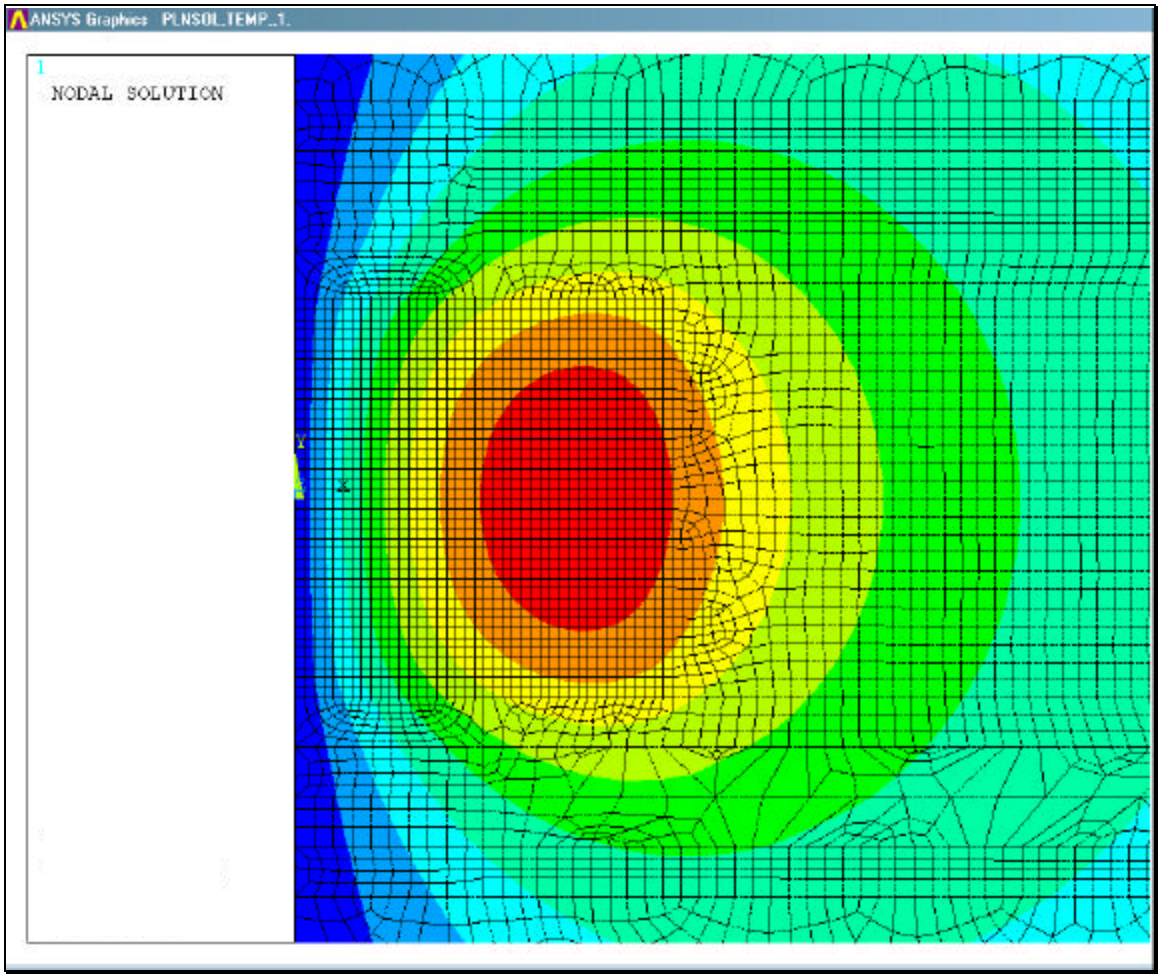

APPENDIX F

ANSYS RESULTS, THIN CYLINDRICAL HEAT SOURCE

ANSYS RESULTS FOR A THIN CYLINDRICAL HEAT SOURCE $\overline{\lambda} = 10$ AND $\overline{b} = 2.0$.

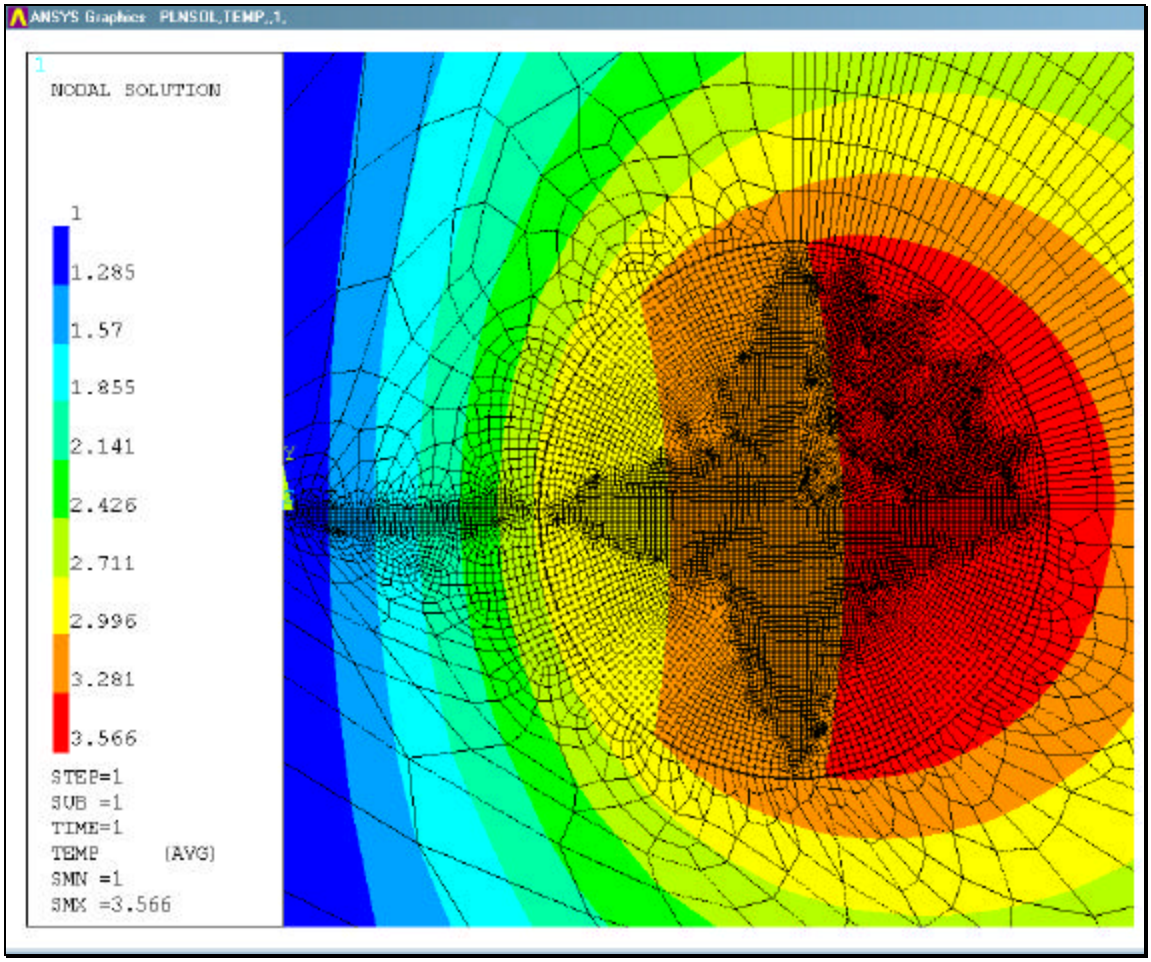

APPENDIX G

ANSYS RESULTS, SQUARE LINE HEAT SOURCE

ANSYS RESULTS FOR A SQUARE LINE HEAT SOURCE $\bar{\lambda} = 10$, $\bar{a} = 1.0$ AND $\bar{b} = 1.0$.